Investigation of Development of Pavement Roughness

PUBLICATION NO. FHWA-RD-97-147

MAY 1998

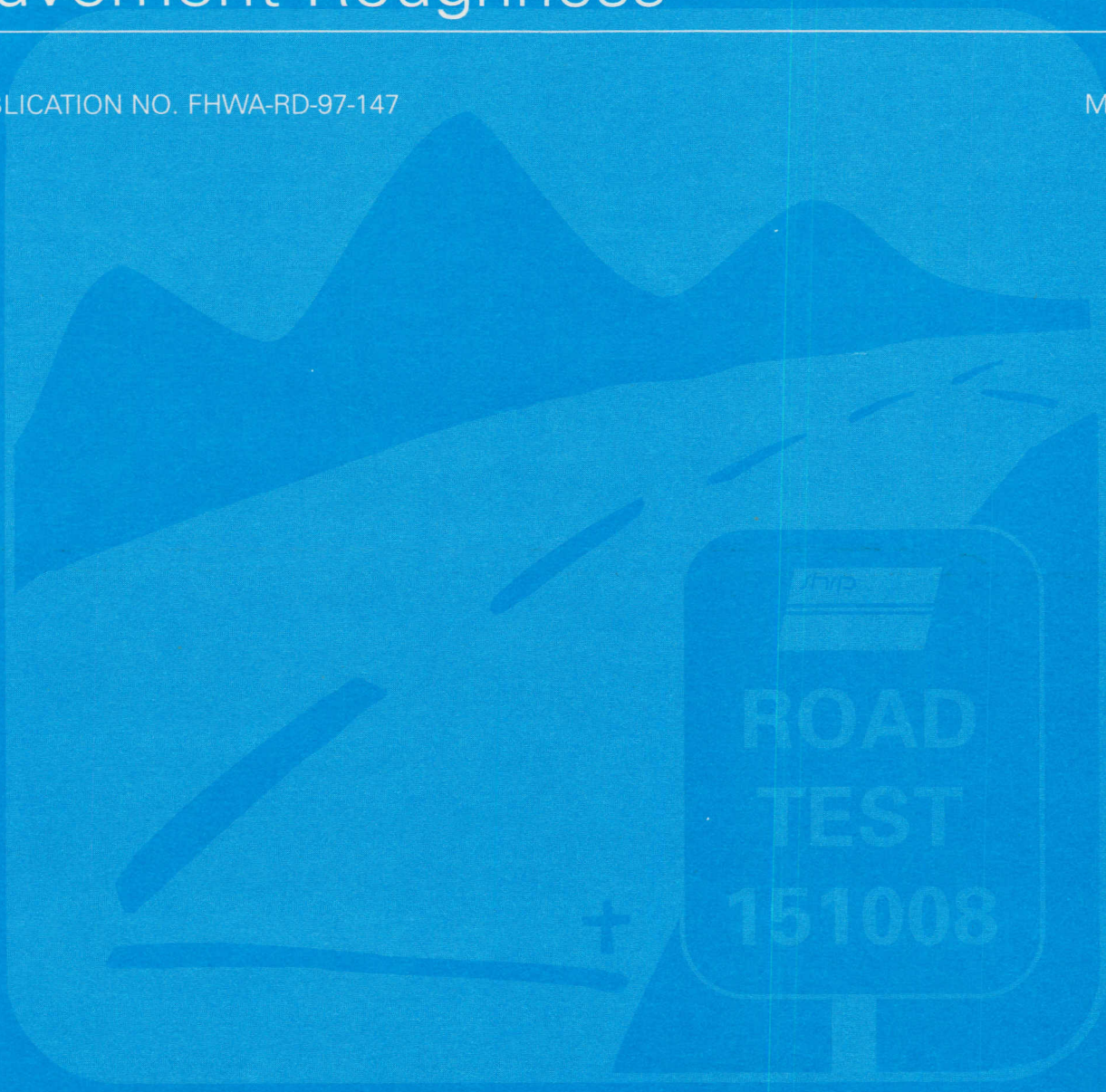

U.S. Department of Transportation
Federal Highway Administration

Research and Development
Turner-Fairbank Highway Research Center
6300 Georgetown Pike
McLean, VA 22101-2296

LTPP

FOREWORD

This report describes an analysis that was conducted to investigate the development of roughness in pavements using data collected for the Long-Term Pavement Performance (LTPP) program. The analysis included: (1) investigation of time-sequence roughness data collected at test sections to study trends in the development of roughness, (2) comparison between International Roughness Index and Ride Number, (3) development of models to predict changes in roughness, (4) investigation of roughness characteristics of new flexible and rigid pavements built for Specific Pavement Studies in the LTPP program, and (5) investigation of roughness characteristics of flexible and rigid pavements that were subjected to different rehabilitation strategies.

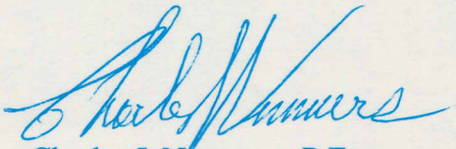

Charles J. Nemmers, P.E.
Director
Office of Engineering
Research and Development

NOTICE

Technical Report Documentation Page

1. Report No.	2. Government Accession No.	3. Recipient's Catalog No.
FHWA-RD-97-147		

4. Title and Subtitle	5. Report Date
INVESTIGATION OF DEVELOPMENT OF PAVEMENT ROUGHNESS	May 1998
	6. Performing Organization Code

7. Author(s)	8. Performing Organization Report No.
Perera, R.W., Byrum, C., and Kohn, S.D.	

9. Performing Organization Name and Address	10. Work Unit No. (TRAIS)
Soil and Materials Engineers, Inc. 43980 Plymouth Oaks Blvd. Plymouth, Michigan 48170	NCP C6B
	11. Contract or Grant No. DTFH61-95-C-00124

12. Sponsoring Agency Name and Address	13. Type of Report and Period Covered
Office of Engineering R&D Federal Highway Administration 6300 Georgetown Pike McLean, Virginia 22101-2296	Final Report June 1995 - August 1997
	14. Sponsoring Agency Code

15. Supplementary Notes
Contracting Officer's Technical Representative (COTR): Cheryl Allen Richter, HNR-30

16. Abstract
The Long-Term Pavement Performance (LTPP) program was designed as a 20-year study of pavement performance. The LTPP program consists of two programs: (1) General Pavement Studies (GPS) that use in-service test sections in either their original design phase or in their first overlay phase and (2) Specific Pavement Studies (SPS) that investigate the effect of specific design features on pavement performance. A major data collection effort at these test sections is the collection of longitudinal profile data along the wheel paths, which is performed annually. This report describes an investigation that was carried out to study the change in roughness at the test sections using the profile data. At the time this analysis was carried out, profile data were generally available for 4 years in the database. This report describes: (1) investigation of time-sequence roughness data collected at GPS test sections to study trends in development of roughness, (2) comparison between International Roughness Index and Ride Number, (3) development of models to predict changes in roughness, (4) investigation of roughness characteristics of new flexible and rigid pavements built for the SPS program, (5) investigation of roughness characteristics of flexible and rigid pavements that were subjected to different rehabilitation strategies under the SPS program, and (6) recommendations for quality assurance and profiling frequency for the test sections.

17. Key Words	18. Distribution Statement
Roughness, pavement performance, pavement profile, international roughness index, long-term pavement performance, flexible pavements, rigid pavements.	No restrictions. This document is available to the public through the National Technical Information Service, Springfield, Virginia 22161.

19. Security Classif. (of this report)	20. Security Classif. (of this page)	21. No. of Pages	22. Price
Unclassified	Unclassified	306	

Form DOT F 1700.7 (8-72) Reproduction of completed page authorized

SI* (MODERN METRIC) CONVERSION FACTORS

APPROXIMATE CONVERSIONS TO SI UNITS

Symbol	When You Know	Multiply By	To Find	Symbol
	LENGTH			
in	inches	25.4	millimeters	mm
ft	feet	0.305	meters	m
yd	yards	0.914	meters	m
mi	miles	1.61	kilometers	km
	AREA			
in^2	square inches	645.2	square millimeters	mm^2
ft^2	square feet	0.093	square meters	m^2
yd^2	square yards	0.836	square meters	m^2
ac	acres	0.405	hectares	ha
mi^2	square miles	2.59	square kilometers	km^2
	VOLUME			
fl oz	fluid ounces	29.57	milliliters	mL
gal	gallons	3.785	liters	L
ft^3	cubic feet	0.028	cubic meters	m^3
yd^3	cubic yards	0.765	cubic meters	m^3
NOTE: Volumes greater than 1000 l shall be shown in m^3.				
	MASS			
oz	ounces	28.35	grams	g
lb	pounds	0.454	kilograms	kg
T	short tons (2000 lb)	0.907	megagrams (or "metric ton")	Mg (or "t")
	TEMPERATURE (exact)			
°F	Fahrenheit temperature	5(F-32)/9 or (F-32)/1.8	Celcius temperature	°C
	ILLUMINATION			
fc	foot-candles	10.76	lux	lx
fl	foot-Lamberts	3.426	candela/m^2	cd/m^2
	FORCE and PRESSURE or STRESS			
lbf	poundforce	4.45	newtons	N
lbf/in^2	poundforce per square inch	6.89	kilopascals	kPa

APPROXIMATE CONVERSIONS FROM SI UNITS

Symbol	When You Know	Multiply By	To Find	Symbol
	LENGTH			
mm	millimeters	0.039	inches	in
m	meters	3.28	feet	ft
m	meters	1.09	yards	yd
km	kilometers	0.621	miles	mi
	AREA			
mm^2	square millimeters	0.0016	square inches	in^2
m^2	square meters	10.764	square feet	ft^2
m^2	square meters	1.195	square yards	yd^2
ha	hectares	2.47	acres	ac
km^2	square kilometers	0.386	square miles	mi^2
	VOLUME			
mL	milliliters	0.034	fluid ounces	fl oz
L	liters	0.264	gallons	gal
m^3	cubic meters	35.71	cubic feet	ft^3
m^3	cubic meters	1.307	cubic yards	yd^3
	MASS			
g	grams	0.035	ounces	oz
kg	kilograms	2.202	pounds	lb
Mg (or "t")	megagrams (or "metric ton")	1.103	short tons (2000 lb)	T
	TEMPERATURE (exact)			
°C	Celcius temperature	1.8C + 32	Fahrenheit temperature	°F
	ILLUMINATION			
lx	lux	0.0929	foot-candles	fc
cd/m^2	candela/m^2	0.2919	foot-Lamberts	fl
	FORCE and PRESSURE or STRESS			
N	newtons	0.225	poundforce	lbf
kPa	kilopascals	0.145	poundforce per square inch	lbf/in^2

* SI is the symbol for the International System of Units. Appropriate rounding should be made to comply with Section 4 of ASTM E380.

(Revised September 1993)

TABLE OF CONTENTS

TABLE OF CONTENTS (Continued)

TABLE OF CONTENTS (Continued)

TABLE OF CONTENTS (Continued)

TABLE OF CONTENTS (Continued)

LIST OF FIGURES

LIST OF FIGURES (Continued)

LIST OF FIGURES (Continued)

LIST OF FIGURES (Continued)

LIST OF FIGURES (Continued)

LIST OF FIGURES (Continued)

LIST OF FIGURES (Continued)

LIST OF FIGURES (Continued)

LIST OF TABLES

LIST OF TABLES (Continued)

LIST OF TABLES (Continued)

LIST OF TABLES (Continued)

LIST OF ACRONYMS

AASHTO	American Association of State Highway and Transportation Officials
AC	Asphalt Concrete
ACI	American Concrete Institute
ASTM	American Society of Testing and Materials
COV	Coefficient of Variation
CRCP	Continuously Reinforced Concrete Pavements
ESAL	Equivalent Single-Axle Loads
FHWA	Federal Highway Administration
GPS	General Pavement Studies
IRI	International Roughness Index
JPCP	Jointed Plain Concrete Pavements
JRCP	Jointed Reinforced Concrete Pavements
KESAL	Kilo Equivalent Single-Axle Loads
LTPP	Long-Term Pavement Performance
NCHRP	National Cooperative Highway Research Program
NIMS	National Information Management System
PCC	Portland Cement Concrete
PSI	Present Serviceability Index
RIMS	Regional Information Management System
RMSVA	Root Mean Square Vertical Acceleration
RMS	Root Mean Square
RN	Ride Number
SHRP	Strategic Highway Research Program
SN	Structural Number
SPS	Specific Pavement Studies
UMTRI	University of Michigan Transportation Research Institute
WIM	Weigh in Motion

CHAPTER 1: INTRODUCTION

It is believed that the general public perceives a good road as one that provides a smooth ride. Studies at the road test sponsored by the American Association of State Highway and Transportation Officials (AASHTO) showed that the subjective evaluation of the pavement, based on mean panel ratings, was primarily influenced by roughness. Therefore, the development of roughness in pavements is a major issue for highway agencies. This report presents the results of a study conducted to investigate the development of roughness in pavements. Data collected for the Long-Term Pavement Performance (LTPP) program, which was part of the Strategic Highway Research Program (SHRP), were used in this study.

1.1 LONG-TERM PAVEMENT PERFORMANCE PROGRAM

SHRP was a 5 year, $150 million research program that began in 1987. The research areas targeted under SHRP were asphalt, pavement performance, concrete and structures, and highway operations. One aspect of SHRP was the LTPP program. The LTPP program was designed as a 20-year study. The first 5 years of the program were administrated by SHRP, and, thereafter, the administration of the program was transferred to the Federal Highway Administration (FHWA).

The objectives of the LTPP program are to: (1) evaluate existing design methods; (2) develop improved design methods and strategies for the rehabilitation of existing pavements; (3) develop improved design equations for new and reconstructed pavements; (4) determine the effects of loading, environment, material properties and variability, construction quality, and maintenance levels on pavement distress and performance; (5) determine the effects of specific design features on pavement performance; and (6) establish a national long-term pavement database to support SHRP objectives and future needs.

To accomplish the described goals, the LTPP program was divided into two complementary programs. The first program, called General Pavement Studies (GPS), uses in-service pavement test sections in either their original design phase or in their first overlay phase. The second program, called Specific Pavement Studies (SPS), investigates the effect of specific design features on pavement performance.

1.1.1 General Pavement Studies (GPS)

Under the GPS program, more than 800 test sections were established on in-service pavements in all 50 States and in Canada. The GPS sections generally represent pavements that incorporate materials and structural designs used in standard engineering practices in the United States and in Canada. Each GPS section is 152 m (500 ft) in length and is located in the outside traffic lane. The data collected at the GPS sections include: climatic, material properties, traffic frequency, deflection, profile, distress, and friction data. The objective of the GPS program is to use the collected data to develop improved pavement design procedures. The GPS sections are categorized into different experiments based on pavement type as shown in table 1.1.1.

1.1.2 Specific Pavement Studies (SPS)

The SPS experiments are designed to study the effect of specific design features on pavement performance. Each SPS experiment consists of multiple test sections. The SPS experiments that were designed for the LTPP program are shown in table 1.1.2.

The SPS-1 and SPS-2 projects involve the construction of new asphalt concrete (AC) and portland cement concrete (PCC) pavements, respectively. Varying structural properties are used in the construction of the different test sections. SPS-3 and SPS-4 experiments study the effect of different maintenance strategies on existing AC and PCC pavements. In the SPS-5 and SPS-6 experiments, different rehabilitation techniques are used in the rehabilitation of existing AC and PCC pavements, respectively. The SPS-7 experiment studies bonded PCC overlays of PCC pavements. The SPS-8 experiment consists of AC and PCC test sections that are constructed on low-volume roads and are designed to study environmental effects on these test sections. The SPS-9 experiment consists of test sections that are constructed with the Superpave asphalt concrete mixes that were developed in the SHRP program. In this study, the SPS-1, SPS-2, SPS-5, and SPS-6 projects were analyzed.

1.1.3 Data Collection at GPS and SPS Sections

Data collection for the LTPP program is performed by four regional contractors. The data collected at the GPS and SPS sections in each region are stored in the Regional Information Management System (RIMS), which is maintained by each contractor. These data are uploaded to the National Information Management System (NIMS) after undergoing quality-control checks. The data from the NIMS are available to the research community. A major data

Table 1.1.1. GPS experiments.

GPS Number	Experiment Type
GPS-1	Asphalt Concrete Pavement on Granular Base
GPS-2	Asphalt Concrete Pavement on Stabilized Base
GPS-3	Jointed Plain Concrete Pavement
GPS-4	Jointed Reinforced Concrete Pavement
GPS-5	Continuously Reinforced Concrete Pavement
GPS-6	Asphalt Concrete Overlay of Asphalt Concrete Pavement
GPS-7	Asphalt Concrete Overlay of PCC Pavement
GPS-9	Unbonded PCC Overlay of PCC Pavement

Note: There is no GPS-8 experiment.

Table 1.1.2. SPS experiments.

SPS Number	Experiment Type
SPS-1	Strategic Study of Structural Factors for Flexible Pavements
SPS-2	Strategic Study of Structural Factors for Rigid Pavements
SPS-3	Preventive Maintenance Effectiveness for Flexible Pavements
SPS-4	Preventive Maintenance Effectiveness for Rigid Pavements
SPS-5	Rehabilitation of Asphalt Concrete Pavements
SPS-6	Rehabilitation of Jointed Portland Cement Concrete Pavements
SPS-7	Bonded PCC Overlay on PCC Pavements
SPS-8	Study of Environmental Factors in the Absence of Heavy Loads
SPS-9	Validation of SHRP Asphalt Specification and Mix Design

collection effort at the GPS and SPS sections is the collection of profile data that is performed annually. The International Roughness Index (IRI) is computed from the profile data, and the IRI, as well as the profile elevation data, are stored in the NIMS.

1.2 RESEARCH TASKS

There were six main tasks in this research study, and a brief description of the work performed for each task is presented in the following sections.

1. Investigate Development of Roughness at GPS Sections.

The collection of profile data for the GPS sections generally commenced on or after 1990. The time sequence IRI values for the GPS sections were investigated to observe the changes in IRI with time.

2. Compare International Roughness Index and Ride Number for GPS Sections.

The IRI was developed during a World Bank study. A primary requirement that was used during the development of IRI was that it should correlate well with the output from response-type roughness measuring equipment. Ride Number (RN) is a roughness index that is correlated with the subjective opinion of the road users, and procedures for computing the RN are presented by Spangler and Kelly.[1] The data from two studies that were sponsored by the National Cooperative Highway Research Program (NCHRP) and two studies funded by the Ohio Department of Transportation were used in developing RN. Relationships between IRI and RN were investigated, and, for a select group of GPS sections, changes in IRI and RN over time were compared. On the basis of results of this analysis, the IRI was selected as the roughness parameter to be used in the other tasks.

3. Develop Roughness Models for GPS Sections.

The overall trends in the change in IRI for each GPS experiment were investigated. Models were developed to predict roughness for each GPS experiment. The time-sequence IRI values at the GPS sections were related to variables associated with that section that can affect the development of roughness, such as subgrade type, traffic, and environmental parameters, to develop these models.

4. Investigate Roughness Characteristics for SPS-1 and SPS-2 Projects.

An SPS-1 project consists of AC surfaced test sections that have different layer types and thicknesses. An SPS-2 project consists of jointed PCC test sections that have different slab thicknesses, PCC strengths, and base types. The investigation of roughness characteristics at SPS-1 and SPS-2 projects provided information on roughness characteristics in newly constructed pavements.

5. Investigate Roughness Characteristics for SPS-5 and SPS-6 Projects.

In the SPS-5 and SPS-6 experiments, different rehabilitation techniques are used in the rehabilitation of existing AC and PCC pavements, respectively. An SPS-5 experiment has nine test sections, while an SPS-6 experiment has eight test sections. The reduction in roughness resulting from different rehabilitation techniques for SPS-5 and SPS-6 experiments, as well as the development of roughness at the test sections, were studied.

6. Recommendations for Quality Assurance and Profiling Frequency.

On the basis of the analysis of the time-sequence IRI values at GPS sections, recommendations for quality assurance during profiling were developed. The trends in change in IRI observed at the test sections were used to develop guidelines for profiling frequency at the GPS sections.

1.3 ORGANIZATION OF THE REPORT

Chapter 2 describes the changes in IRI with time that were observed for the GPS sections. Chapter 3 presents a comparison between the IRI and RN. Chapter 4 describes the data elements that were selected for modeling the development of IRI and the data synthesis methods that were used with data obtained from NIMS. Chapter 5 analyzes the overall trends in IRI that were observed for each GPS experiment and presents the models that were developed to predict the development of IRI. Chapter 6 describes roughness characteristics at SPS-1 and SPS-2 projects, while chapter 7 describes roughness characteristics at SPS-5 and SPS-6 projects. Recommendations for quality assurance during profile data collection and recommendations for data collection frequency for GPS test sections are presented in chapter 8. Chapter 9 presents a summary of the key findings, while chapter 10 presents conclusions and recommendations for future research.

CHAPTER 2: ROUGHNESS DEVELOPMENT AT GPS SECTIONS

The development of roughness at GPS sections was studied using the IRI as the roughness index and the time-sequence IRI data that were available for each GPS section. The study of the development of roughness at GPS sections consisted of examining the time-sequence IRI data at each GPS section to study changes in IRI.

2.1 PROFILE DATA COLLECTION AT GPS SECTIONS

In the LTPP program, the United States and Canada are divided into four regions: North Atlantic, North Central, Southern, and Western. Figure 2.1.1 shows the area included in each region. A regional contractor in each of these regions performs data collection at all GPS sections located within the region. Each regional contractor uses a K.J. Law profiler that is equipped with optical sensors for profile data collection. These profilers collect elevation data at 25-mm (1-in) intervals, the collected data are averaged using a 305-mm (12-in) moving average, and the data are recorded at 152-mm (6-in) intervals.

All GPS sections are generally profiled annually, and the profile data along the left and the right wheel paths are collected. Although the time difference between two consequent dates when a section is profiled is generally close to a year, differences of several months can be present. This results in data being collected during different seasons at a section. For example, a given section may be profiled during fall in one year, and in the subsequent year, it may be profiled during winter. At each GPS section, the regional contractors collect data to obtain five profiler runs that satisfy the following criteria:

1. The both-wheel-path IRI (average IRI of left and right wheel path) of three profiler runs are within 1 percent of the mean both-wheel-path IRI computed from the five profiler runs.

2. The standard deviation of the both-wheel-path IRI for the five profiler runs is less than 2 percent of the mean both-wheel-path IRI computed from the five profiler runs.

If the profile data collected from the first five profiler runs do not satisfy the two criteria, additional profiler runs are performed at the section in order to obtain five profiler runs that satisfy the two criteria. However, the maximum number of profile runs performed at a section is limited to nine runs. The IRI computed from the profile data is stored in the RIMS maintained by the regional contractors. The IRI data are uploaded annually to the NIMS after they are

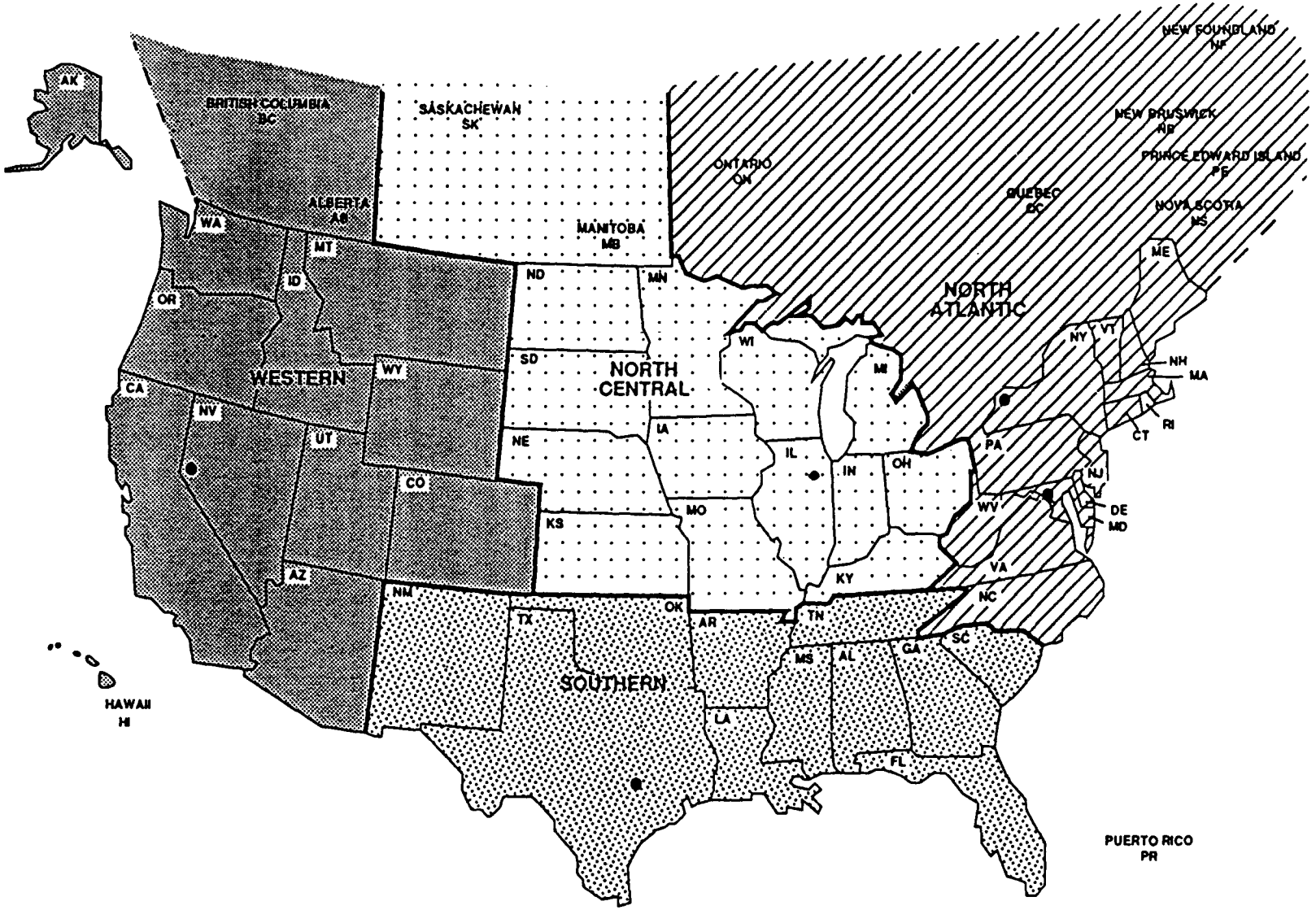

Figure 2.1.1. LTPP geographic regions.

subjected to quality-control checks. The profile elevation data collected by the profilers are also stored in the NIMS.

2.2 EXAMINATION OF CHANGES IN IRI AT GPS SECTIONS

2.2.1 Availability of Profile Data

Table 2.2.1 presents the number of GPS sections in the LTPP program categorized according to the GPS experiment and the LTPP region. In this table, GPS-6B and GPS-7B experiments are overlaid sections for which the condition of the pavement prior to the overlay is known. The time-sequence IRI data for the GPS sections were obtained from the NIMS. A review of the data indicated that recent IRI data were not available in the NIMS. As data that have not been uploaded to NIMS are available in RIMS, in order to use the latest available IRI data in the analysis, the IRI data of the GPS sections were obtained from RIMS. The percent distribution of test sections for each GPS experiment according to the number of times the sections have been profiled is presented in table 2.2.2. Generally, sections that have been profiled only once or twice for GPS experiments 1 through 5 have been dropped from the LTPP program or have been overlaid, and some of the overlaid sections are now either a GPS-6B or a GPS-7B section.

2.2.2 Analysis Procedure

The time-sequence IRI data at each GPS section were examined to study how the IRI changes over time. All GPS sections were included in this analysis. For each profile date at a GPS section, IRI for the five profiler runs performed on that day are available. The IRI of the five profiler runs for a given profile date were averaged to obtain the average IRI for each wheel path. For each GPS section, these data were used to prepare a plot showing the variations in IRI along the left and the right wheel path with pavement age. The pavement age corresponding to each profile date was computed by subtracting the construction date of the pavement from the profile date. For overlaid pavements (GPS-6, -7 and -9), the pavement age was computed with reference to the overlay date, which was treated as the construction date.

Figure 2.2.1 shows an example of a plot that was developed for each GPS section. The x-axis of the plot represents the pavement age, and the left- and right-wheel-path IRI corresponding to each profile date at that section are shown in the plot. The GPS section number; profile dates; age of the pavement; and the left-, right- and both-wheel-path IRI (average of left- and right-

Table 2.2.1. GPS sections in the LTPP program.

GPS Experiment	Number of Sections				
	LTPP Region				Total
	North Atlantic	North Central	Southern	Western	
GPS-1	46	34	78	65	223
GPS-2	28	6	67	35	136
GPS-3	15	50	28	36	129
GPS-4	13	37	16	0	66
GPS-5	15	25	35	9	84
GPS-6A	4	15	16	29	64
GPS-6B	7	9	11	11	38
GPS-7A	6	16	7	5	34
GPS-7B	4	17	0	0	21
GPS-9	3	11	9	5	28
TOTAL	141	220	267	195	823

Table 2.2.2. Percent distribution of test sections according to availability of time-sequence IRI data.

GPS Experiment	Number of Sections	Percent Distribution of Test Sections (%)							Total
		Number of Times Section Was Profiled							
		1	2	3	4	5	6	7	
GPS-1	223	5	9	19	19	16	18	14	100
GPS-2	136	4	2	38	21	10	16	9	100
GPS-3	129	2	5	18	27	27	15	6	100
GPS-4	66	3	13	13	34	18	12	7	100
GPS-5	84	5	7	21	36	12	13	6	100
GPS-6A	64	3	8	31	16	22	20	0	100
GPS-6B	38	18	11	18	13	24	16	0	100
GPS-7A	34	6	6	26	29	18	15	0	100
GPS-7B	21	10	14	27	29	10	10	0	100
GPS-9	28	4	11	32	18	25	11	0	100

wheel-path IRI) at each profile date are shown at the top of each plot. The both-wheel-path IRI represents the overall IRI for the section.

2.2.3 Examination of IRI Plots

The change in IRI over time at a GPS section is expected to fall into one of the following two categories:

1. Increase in IRI: The IRI along both the left and the right wheel paths will increase with time, as shown in figure 2.2.2. However, it is also possible for the IRI to increase in only one wheel path, while the IRI along the other wheel path remains stable, as shown in figure 2.2.3. For both cases, the both-wheel-path IRI increases with time.

GPS Section: 011019

Profile Date	Age of Pavement (yr)	IRI (in/mi)		
		Left Wheel Path	Right Wheel Path	Average
6/5/90	3.7	80	94	87
7/11/91	4.8	86	94	90
8/21/92	5.9	85	94	89
8/8/94	7.9	91	100	96

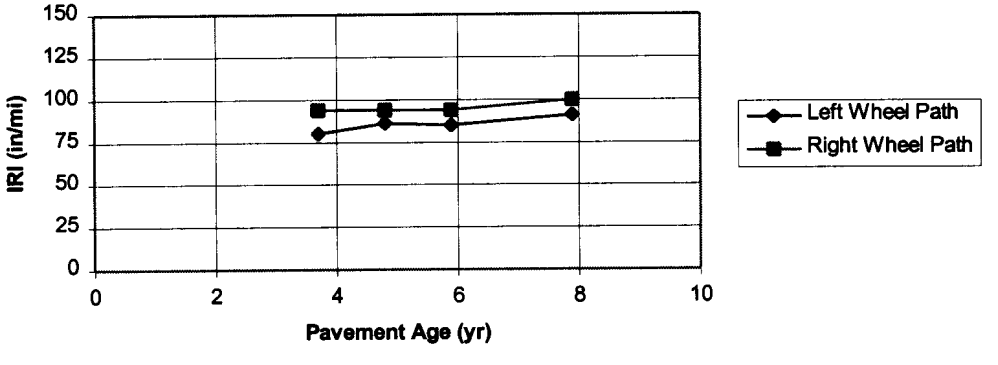

1 in/mi = 0.0158 m/km

Figure 2.2.1. Typical plot developed to examine changes in IRI with time.

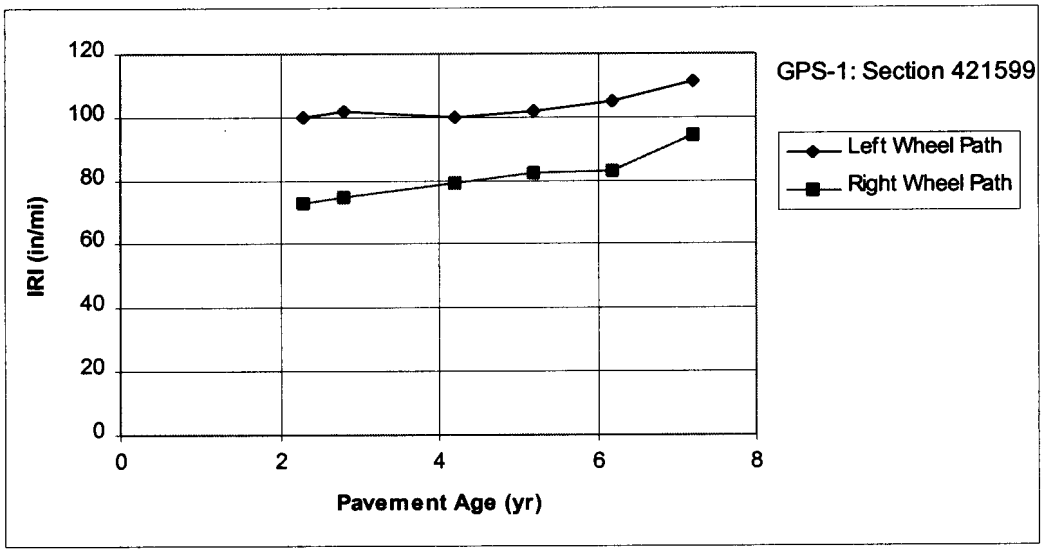

1 in/mi = 0.0158 m/km

Figure 2.2.2. Section showing an increase in IRI for both wheel paths.

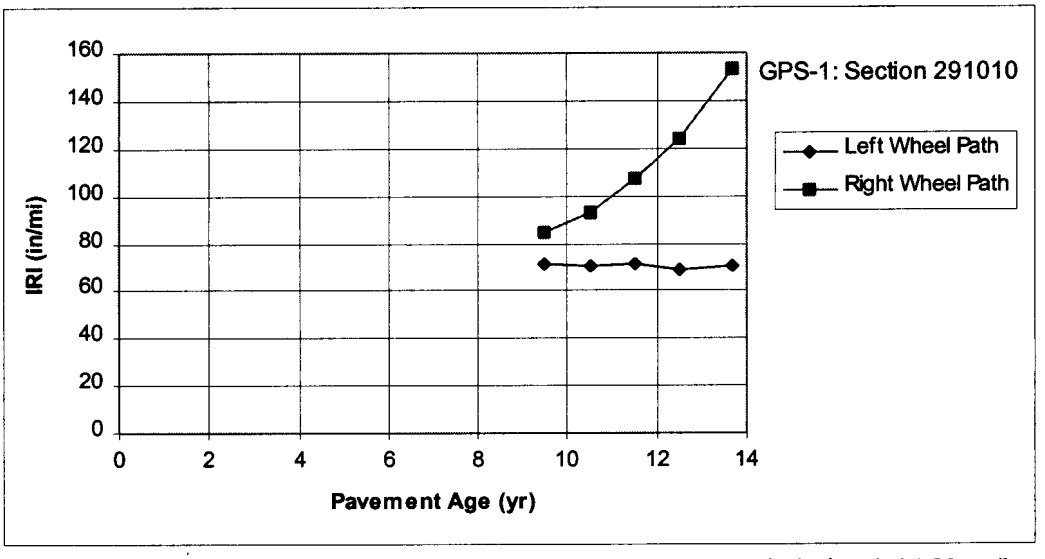

1 in/mi = 0.0158 m/km

Figure 2.2.3. Section showing an increase in IRI for one wheel path.

2. IRI Remains Stable: There may be minor variations in the IRI over the years, but overall, the IRI remains relatively stable. An example of such behavior is shown in figure 2.2.4, where the both-wheel-path IRI remains stable over the years, although there are minor variations in IRI along the left and the right wheel paths. The minor variations may be caused by differences in the profiled path or seasonal variations in the pavement profile.

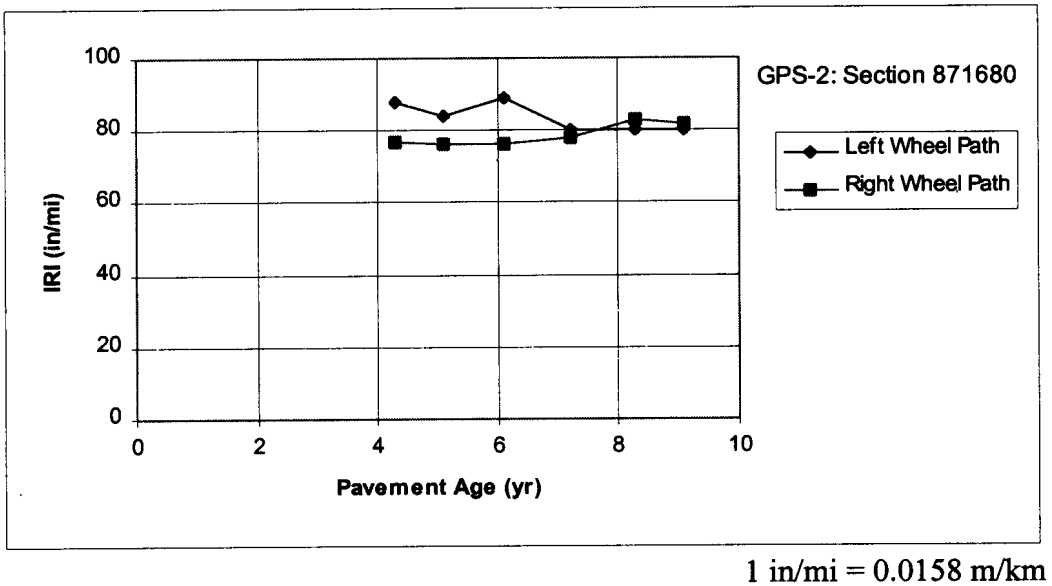

1 in/mi = 0.0158 m/km

Figure 2.2.4. Section with a relatively stable IRI over time.

An examination of the IRI versus age of pavement plots indicated that some GPS sections showed IRI trends that deviated from the two behavior patterns that were described. The GPS sections for which the IRI behavior deviated from these two patterns could be classified into one of the following four groups.

Group 1: The IRI of both the left and right wheel paths, or one of the wheel paths, for a given profiling date was considerably higher than the IRI obtained for the profiling dates before and after this date. An example of such behavior that occurs in both wheel-paths is shown in figure 2.2.5, while an example of such an occurrence in one wheel path is shown in figure 2.2.6.

Group 2: The IRI of both the left and the right wheel paths, or one of the wheel paths, for a specific profiling date was considerably lower than the IRI obtained for the profiling dates before and after this date. An example of such behavior that occurs in both wheel paths is shown in figure 2.2.7, while an example of such an occurrence in one wheel path is shown in figure 2.2.8.

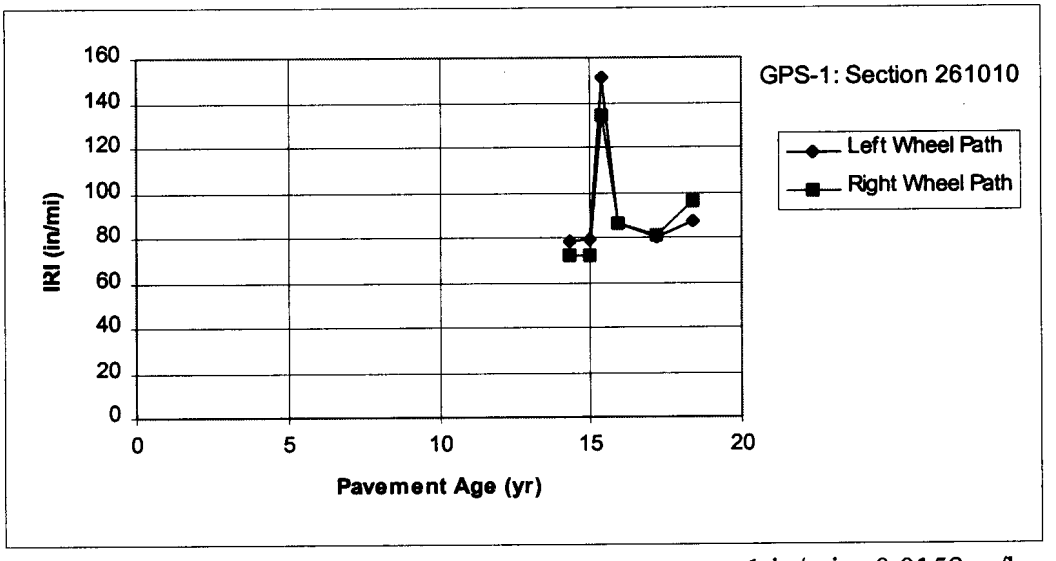

1 in/mi = 0.0158 m/km

Figure 2.2.5. Section showing Group1 behavior along both wheel paths.

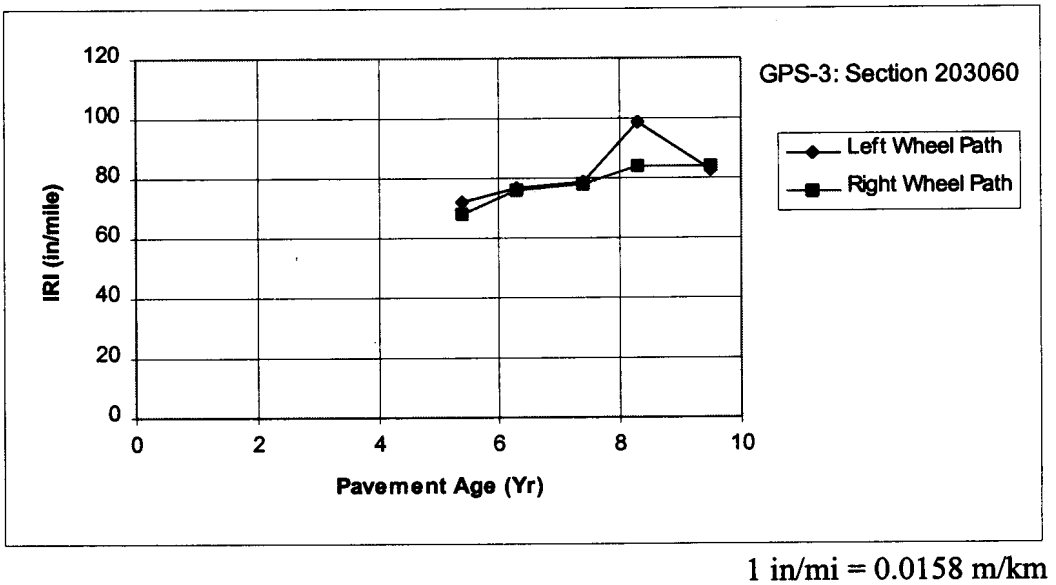

1 in/mi = 0.0158 m/km

Figure 2.2.6. Section showing Group 1 behavior along one wheel path.

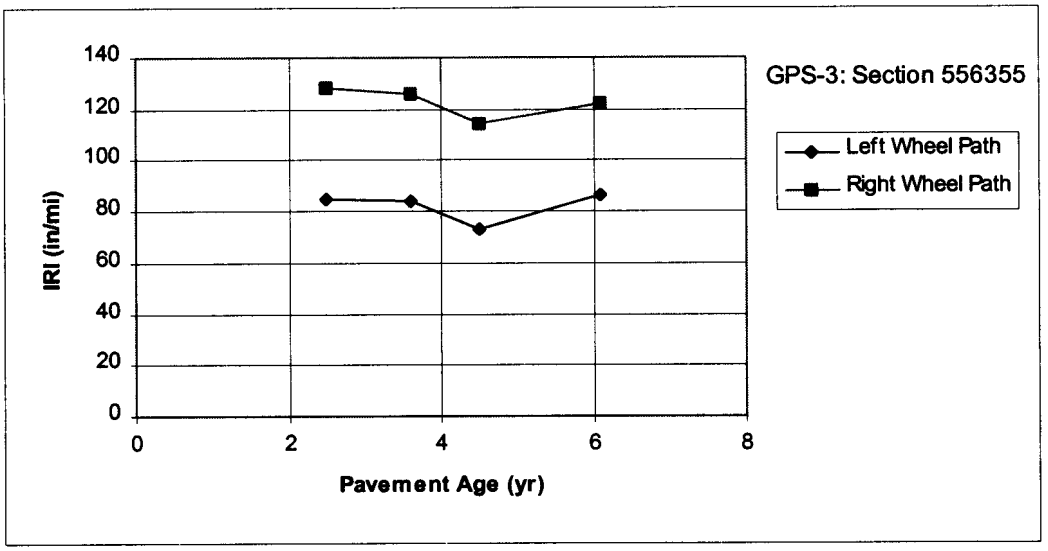

1 in/mi = 0.0158 m/km

Figure 2.2.7. Section showing Group 2 behavior along both wheel paths.

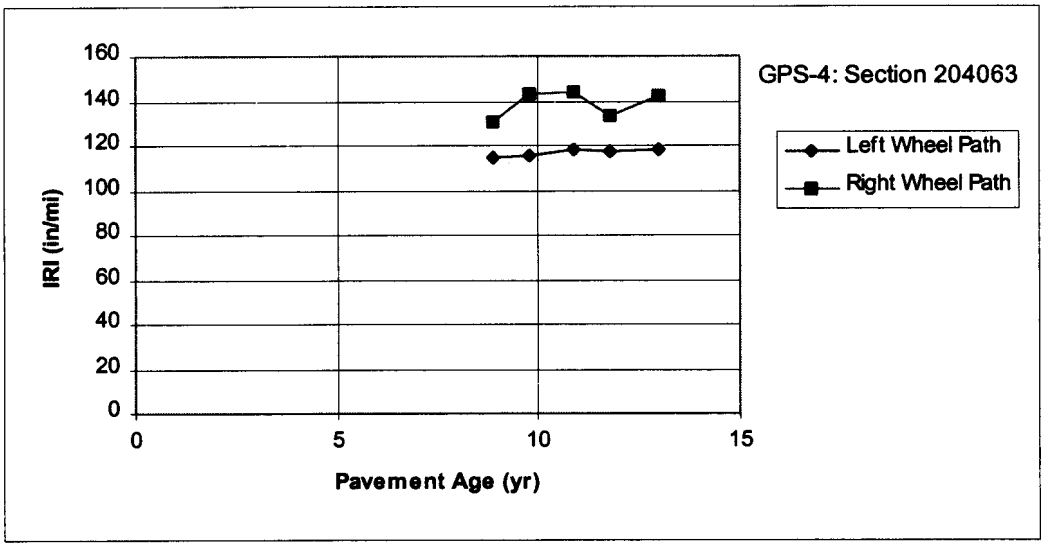

1 in/mi = 0.0158 m/km

Figure 2.2.8. Section showing Group 2 behavior along one wheel path.

Group 3: The IRI for both the left and the right wheel paths for different profiling dates were highly variable. An example of this behavior is shown in figure 2.2.9.

Group 4: An abrupt decrease in IRI was observed for both wheel paths, and the IRI at the subsequent profiling date remained close to this IRI. An example of this behavior is shown in figure 2.2.10.

The inconsistent IRI data that were observed at the sections may be caused by the following factors:

Variations in Profiled Path: A profile is a two-dimensional slice of road surface taken along a specific path. If a measurement is repeated, the same profile can only be expected if the same imaginary line is followed. Variations in the profiled wheel path for the different years can cause changes in the IRI. In some pavements, there is considerable transverse variability, which can cause considerable variations in the IRI, depending on the wheel path that is followed. If distresses are present in the vicinity of the wheel path, this can result in an IRI that is different between the years, and large variations in IRI can occur depending on whether the distress is included or omitted in the profile. For a given year, the profiler operator may follow a specific path and obtain five profiler runs that satisfy the data collection criteria. In the following year, at the same section, the operator may follow a different path and obtain five profiler runs that satisfy the data collection criteria, but whose IRI may be vastly different from the IRI of the previous year.

Temperature or Seasonal Effects: Changes in IRI can occur in pavements because of changes in profile caused by temperature or seasonal effects. In jointed PCC pavements, variations in the profile of the pavement can occur due to temperature effects. On days where the air temperature changes significantly over a 24-h cycle, the profile of a jointed PCC pavement can change during the day from curling actions caused by temperature variations. In the night and the early morning hours when the temperature at the pavement surface is lower than the temperature at the bottom of the pavement, the pavement surface contracts relative to the bottom, and the edges of the slab curl upward. In the afternoon hours, the slabs generally assume a flat shape. The magnitude of the slab curl depends on the slab length, slab thickness, support conditions below the slab, and the temperature gradient in the slab. Although the GPS sections are profiled annually, differences of several months can be present between subsequent profiling dates. This can result in the section being profiled during different seasons. The profile of a pavement can change because of moisture effects on the subgrade that cause the subgrade to swell or shrink, and during winter

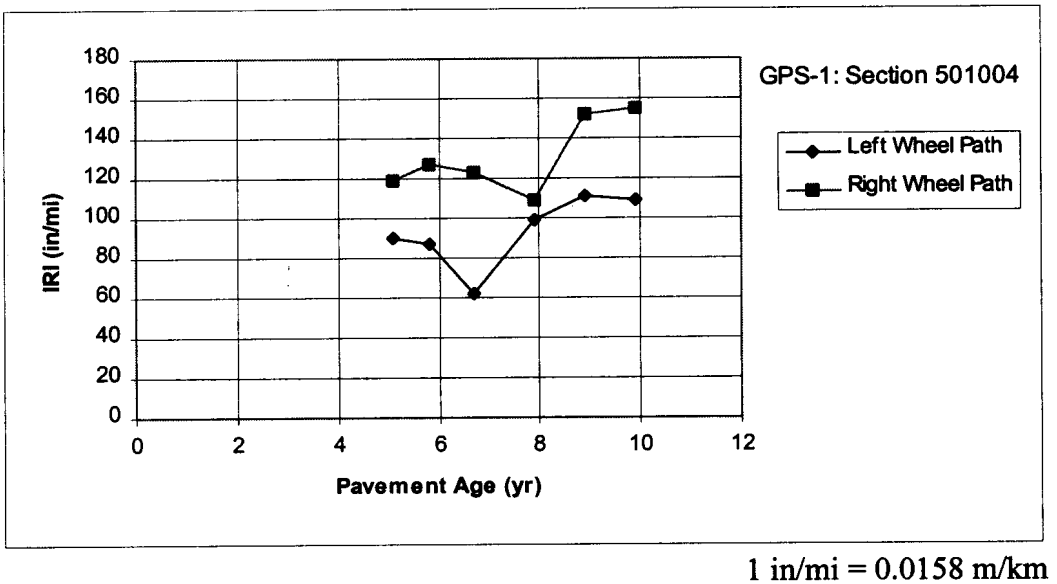

1 in/mi = 0.0158 m/km

Figure 2.2.9. Section showing Group 3 behavior.

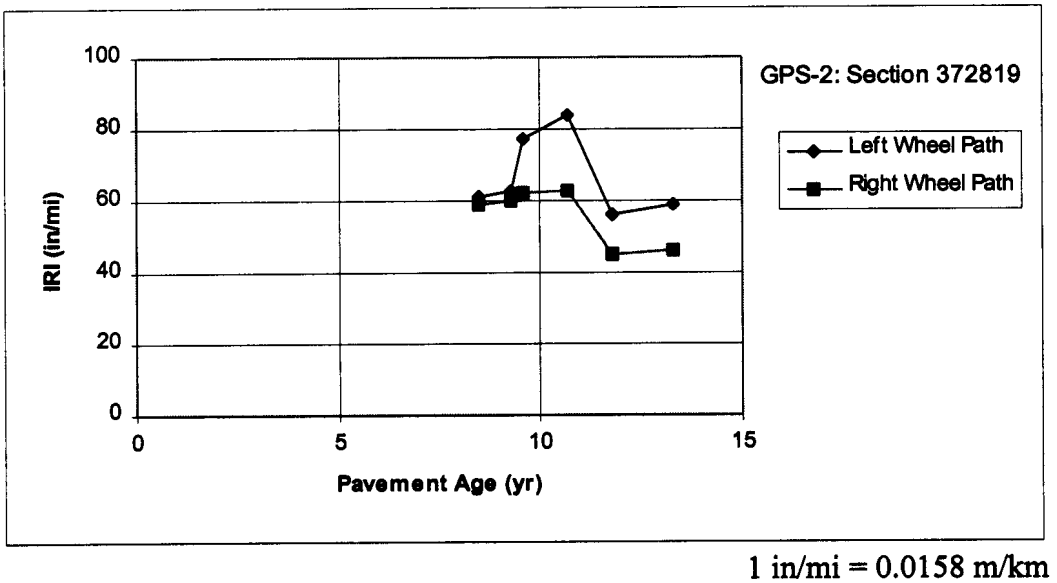

1 in/mi = 0.0158 m/km

Figure 2.2.10. Section showing Group 4 behavior.

months, frost heave of the subgrade and base layers can cause variations in the pavement profile. Both of these effects will contribute to variations in the IRI.

Maintenance Activities: Maintenance activities on a section can change the IRI of a section. Repair of distressed areas can lead to a reduction in IRI of the pavement. At a few sections, it was observed that the IRI showed an abrupt decrease in a particular year, and then remained generally close to this value in future profiling dates. This decrease in IRI may have been caused by maintenance activities on the section. Maintenance activities may also cause the IRI of the section to increase. When maintenance activities are carried out in the GPS sections, they are documented in the maintenance table in the NIMS. However, there were very few entries in these tables. The inconsistent IRI data that were observed could be attributed to maintenance activities for only three cases, on the basis of data available in the maintenance tables. There is a possibility that all the maintenance activities that have been performed on the sections have not been entered in these tables.

Data Collection Errors: Data collected by the K.J. Law optical profilers that are used in the LTPP program are affected by sunlight. The profilers have a shroud that prevents the sunlight from interfering with the optical sensors. Sunlight creeping under the shroud of the profiler can contaminate the collected data, which causes an increase in IRI. Malfunctions in the accelerometer, or incorrectly calibrated height sensors or accelerometers in the profiler may also cause invalid data to be collected. Equipment problems can also cause spikes to be introduced into the profile. All these conditions will cause erroneous profile data to be collected.

2.2.4 Investigation of Sections With Inconsistent IRI Data

GPS sections showing a behavior pattern similar to that described for Groups 1 through 4 were considered to have inconsistent IRI data. The profile elevation data of a selected group of GPS sections for GPS experiments 1 through 5 that had inconsistent IRI data were reviewed to determine if the cause of that behavior could be determined. The review of the data consisted of viewing the profile data for the year in which the IRI was questionable, as well as viewing the data for the previous and subsequent profile date. The profile elevation data were reviewed with the use of Profscan software.[2] This software is used in the LTPP program to review profile data and compute roughness indices.

The following are examples of test sections where the cause of the inconsistent IRI could be identified.

Case 1 - Spikes in Profile Data: Figure 2.2.11 shows a section where the left-wheel-path IRI for the fourth profile date was high when compared with the other years. A review of the profile elevation data indicated that there was a non-pavement-related spike in the data, which resulted in the high IRI. When the spike was removed, the left-wheel-path IRI decreased from 1.56 to 1.31 m/km (99 to 83 in/mi).

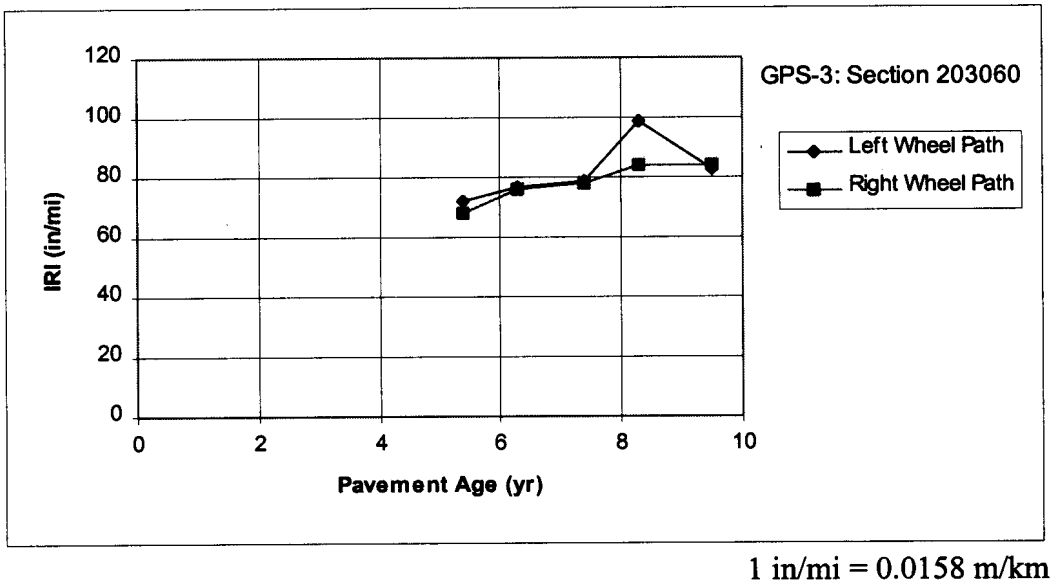

1 in/mi = 0.0158 m/km

Figure 2.2.11. Section with inconsistent IRI values caused by a spike in profile data.

Case 2 - Variations in the Wheel Path: For the section shown in figure 2.2.12, the right-wheel-path IRI for the second profile date was high when compared with the other dates. This section has transverse cracks. The driver appeared to have followed a wheel path closer to the shoulder during that year and picked up the wide cracks near the shoulder. This resulted in the increase in IRI observed for the section in that year.

Case 3 - Equipment Problems: In the third profile date for the section shown in figure 2.2.13, the IRI for both the left and right wheel paths were high when compared with the other years. A review of the data indicated that the accelerometer in the vehicle may not have been working properly for this profile date.

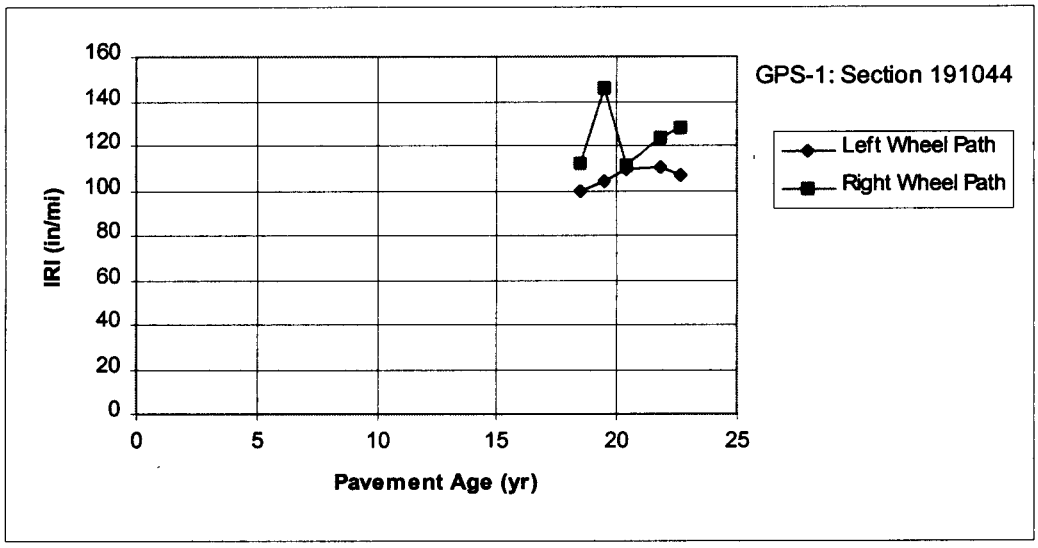

1 in/mi = 0.0158 m/km

Figure 2.2.12. Section with inconsistent IRI values caused by variations in the profiled path.

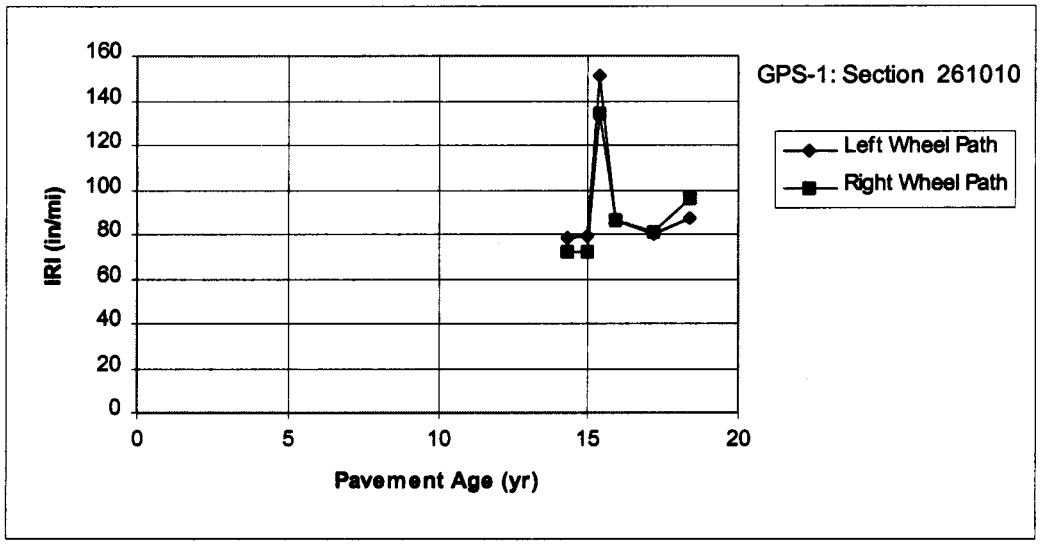

1 in/mi = 0.0158 m/km

Figure 2.2.13. Section with inconsistent IRI values caused by equipment problems.

Case 4 - Maintenance Activities on Section: Figure 2.2.14 shows a section whose IRI for both the left and the right wheel paths showed an abrupt reduction for the fifth profile date and, thereafter, remained close to this value at the sixth profile date. A review of the maintenance data files indicated that an aggregate seal coat had been placed on the section after the fourth profile date. The decrease in the IRI is attributed to the aggregate seal coat.

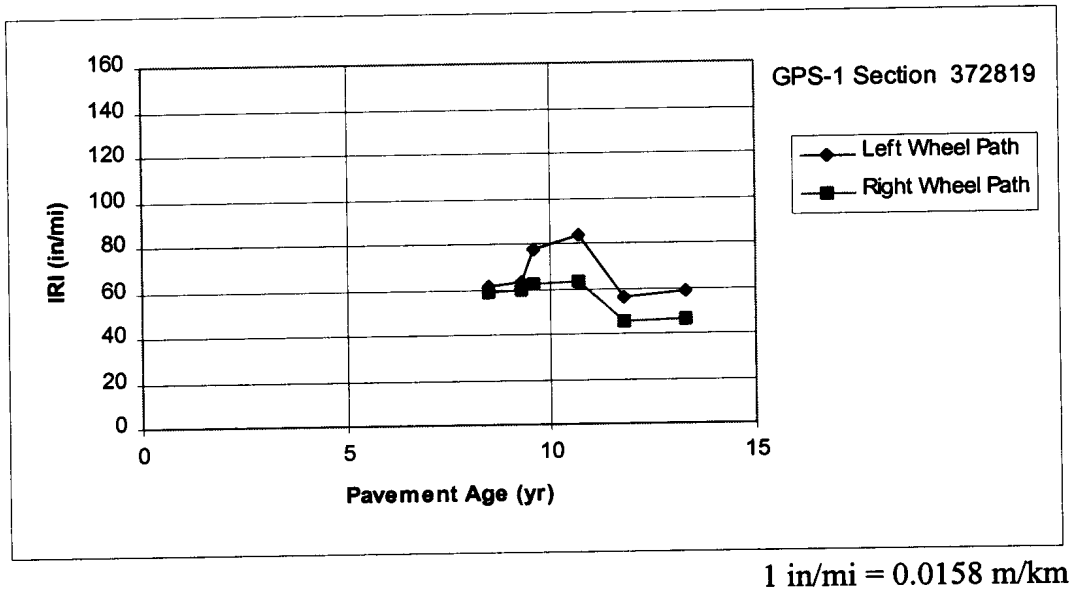

1 in/mi = 0.0158 m/km

Figure 2.2.14. Section with inconsistent IRI values caused by maintenance activities.

For the selected group of test sections reviewed, the cause of the inconsistent data could be identified for 53 percent of the cases. For 23 percent of the cases, the cause of the inconsistent data was attributed to variations in the profiled path. For most of the other 30 percent of the cases, the inconsistent IRI values were caused by spikes in the data. The review of the sections that had inconsistent IRI data was carried out by visually viewing the profile elevations using the Profscan program. A more detailed investigation of these sections could be carried out using filtering techniques. Such an analysis may explain the cause of the inconsistent IRI data for the sections for which a reason for the inconsistent IRI data could not be identified by reviewing the profile elevation data. However, this task was outside the scope of work for the contract. We recommend that an investigation of such behavior patterns be conducted with the use of filtering techniques, as such an investigation could yield valuable insight into variability of time-sequence IRI data.

In some sections, if only the both-wheel-path IRI is examined, a clear inconsistency in IRI is not seen. The averaging of the individual wheel-path data masks the performance. The IRI for two such sections are shown in table 2.2.3. At GPS section 421598, the left-wheel-path IRI for 12/17/92 is less than the IRI for the other dates. At GPS section 014929 for profile date 2/17/94, the left- as well as the right-wheel-path IRI are different from the values obtained for the previous years, with the left-wheel-path IRI being lower, and the right-wheel-path IRI being higher.

Table 2.2.3. IRI of two sections showing inconsistent IRI along one wheel path.

GPS Section Number	Profile Date	IRI (in/mi)		
		Left Wheel Path	Right Wheel Path	Both Wheel Path
421598	11/21/89	104	109	107
	5/17/90	108	105	107
	10/10/91	101	104	103
	12/17/92	91	108	100
	10/13/93	107	109	108
	9/15/94	108	109	109
014129	12/10/90	68	59	64
	4/6/92	67	61	64
	2/17/94	59	77	68

Note: 1 in/mile = 0.0158 m/km.

Table 2.2.4 presents the number of sections that had inconsistent IRI data for each GPS experiment, and also indicates whether the inconsistency is seen for the both-wheel-path IRI, or if individual wheel-path IRI has to be examined to see the inconsistency. Table 2.2.5 shows the number of sections in each region where inconsistent time-sequence IRI data were observed and categorized according to the GPS experiment. The percentage of sections that had inconsistent IRI data for the four LTPP regions were: North Atlantic - 38 percent, North Central - 30 percent, Southern - 15 percent, and Western - 28 percent. The lowest percentage was observed in the Southern region, where all sections are located in the no-freeze environmental zone. Appendix A includes a listing of all sections that show inconsistencies in IRI data.

Table 2.2.4. Sections with inconsistent IRI data summarized according to GPS experiment.

GPS Experiment	Number of Test Sections in GPS Experiment	Number of Sections			Percentage of Sites With Inconsistent IRI Data
		Inconsistent Both-Wheel-Path IRI (Note 1)	Inconsistent IRI in One Wheel Path (Note 2)	Total	
GPS1	223	46	12	58	26
GPS2	136	27	11	38	28
GPS3	129	30	10	40	31
GPS4	66	14	7	21	32
GPS5	84	9	4	13	15
GPS6	102	14	8	22	22
GPS7	55	10	8	18	33
GPS9	28	5	4	9	32
TOTAL	823	155	64	219	27

Note 1: Inconsistencies in IRI are noted when the both-wheel-path IRI is examined.

Note 2: The time-sequence data for the both-wheel-path IRI does not clearly indicate an inconsistency, but the IRI of a wheel path shows an inconsistency.

2.3 SUMMARY

The time-sequence IRI data at each GPS section were examined to study how the IRI changes over time. The IRI patterns observed for the sections were: (1) IRI along both the left and the right wheel path, or along one wheel path, increases with time; (2) IRI remains relatively stable over time, with minor variations between the profile dates; (3) IRI of both the left and the right wheel path or one of the wheel paths for a given profiling date is higher than the IRI obtained for the profiling dates before and after this date; (4) IRI of both the left and the right wheel paths or one of the wheel paths was lower than the IRI obtained for the profiling dates before and after this date, (5) IRI for both the left and the right wheel paths for different profiling dates were variable; and (6) An abrupt decrease in IRI was observed on both wheel paths, and the IRI at the subsequent dates remained close to this IRI. The sections that showed a IRI pattern similar to causes (3) through (6) were classified as sections that showed inconsistent IRI values, and 27 percent of GPS sections showed such a behavior.

The cause of this inconsistent IRI behavior can be attributed to one of the following causes: (1) variations in the profiled paths between the years; (2) temperature or seasonal effects; (3) maintenance activities at a section; or (4) data collection errors. A brief preliminary review

Table 2.2.5. Sections with inconsistent IRI data classified according to LTPP region.

Region	GPS Experiment	Total Test Sections in Experiment	Number of Sections			Percentage of Sections With Inconsistent IRI (%)
			Inconsistent Both-Wheel-Path IRI (Note 1)	Inconsistent IRI in One Wheel Path (Note 2)	Total	
North Atlantic	GPS1	46	15	3	18	39
	GPS2	28	9	1	10	36
	GPS3	15	5	1	6	40
	GPS4	13	5	0	5	38
	GPS5	15	2	2	4	27
	GPS6	11	3	1	4	36
	GPS7	10	3	2	5	50
	GPS9	3	2	0	2	67
North Central	GPS1	34	10	1	11	32
	GPS2	6	0	3	3	50
	GPS3	50	14	3	17	34
	GPS4	37	8	4	12	32
	GPS5	25	4	2	6	24
	GPS6	24	6	3	9	38
	GPS7	33	4	4	8	24
	GPS9	11	2	1	3	27
Southern	GPS1	78	8	5	13	17
	GPS2	67	8	5	13	19
	GPS3	28	1	3	4	14
	GPS4	16	1	3	4	25
	GPS5	35	2	0	2	6
	GPS6	27	0	2	2	7
	GPS7	7	0	1	1	14
	GPS9	9	0	2	2	22
Western	GPS1	65	13	3	16	25
	GPS2	35	10	2	12	34
	GPS3	36	10	3	13	36
	GPS4	0	0	0	0	0
	GPS5	9	1	0	1	11
	GPS6	40	5	2	7	18
	GPS7	5	3	1	4	80
	GPS9	5	1	1	2	40

Note 1: Inconsistencies in IRI are noted when the both-wheel-path IRI is examined.

Note 2: The time-sequence data for the both-wheel-path IRI does not clearly indicate an inconsistency, but the IRI of a wheel path shows an inconsistency.

was performed on a selected group of sections that showed inconsistent IRI to see if the cause of the behavior could be determined. For the selected group of test sections that were reviewed, the cause of the inconsistent data could be identified for 53 percent of the cases. For 23 percent of the cases, the cause of the inconsistent data was attributed to variations in the profiled path. For most of the other 30 percent of the cases, inconsistent IRI values were caused by spikes in the profile data.

CHAPTER 3: COMPARISON BETWEEN INTERNATIONAL ROUGHNESS INDEX AND RIDE NUMBER

Longitudinal profile data can be used to compute a variety of profile indices. Examples of such indices are International Roughness Index (IRI), Ride Number (RN), and Root Mean Square Vertical Acceleration (RMSVA). Profile indices are single numerical values used to quantify the ride quality of a pavement. For each profile index, a description of the ride quality is associated with a range of the ride index. Each ride index is sensitive to different components of road profile. Prior to developing predictive functions, a study of different indices was necessary. This chapter presents a comparison between IRI and RN, computed from the profile data measured at the GPS sections.

3.1 INTERNATIONAL ROUGHNESS INDEX (IRI)

The IRI is a widely accepted roughness index in the United States and elsewhere in the world. FHWA requires States to use the IRI as the standard roughness index for reporting the roughness at the Highway Performance Monitoring Sections. The IRI was developed from the data obtained from the International Road Roughness experiment, which was sponsored by the World Bank and conducted in 1982 in Brazil.[3] The research results from a NCHRP project that was performed in the late 1970's was utilized during the development of the IRI.[4] The computer programs required to compute the IRI are presented in the World Bank Technical Paper Number 46.[5] A primary requirement of the development of IRI was that it should correlate well with response-type roughness measuring equipment being used at the time. IRI has also been found to correlate well with subjective opinions of road users.

Technically, the IRI is a mathematical representation of the accumulated suspension stroke of a vehicle, divided by the distance traveled by the vehicle. The IRI is calculated mathematically from the measured longitudinal profile with use of a quarter car simulation along a single wheel path. The quarter car includes: one tire represented with a vertical spring, the mass of the axle supported by the tire, a suspension spring and a damper, and the mass of the body supported by the suspension for that tire. A simulation speed of 80 km/h (50 mi/h) is used for the quarter car, and the simulated suspension motion is linearly accumulated and divided by the length of the profile to yield the IRI. The coefficients used in the mathematical equations were those that provided the maximum correlation to the output of response-type roughness measuring systems. As inertial profilers typically measure longitudinal profiles along the two wheel paths, the average IRI for the section can be obtained by computing the IRI for each wheel path, and then averaging

the two values. The IRI is sensitive to wavelengths between 1 and 30 m (4 and 100 ft). The response of a sinusoidal input to the IRI quarter car filter is shown in figure 3.1.1.[6] The amplitude of the output sinusoid is the amplitude of the input multiplied by the gain shown in the figure. As seen in figure 3.1.1, the IRI filter has a maximum sensitivity at wavelengths of about 2.1 m (7 ft) and 15.2 m (50 ft).

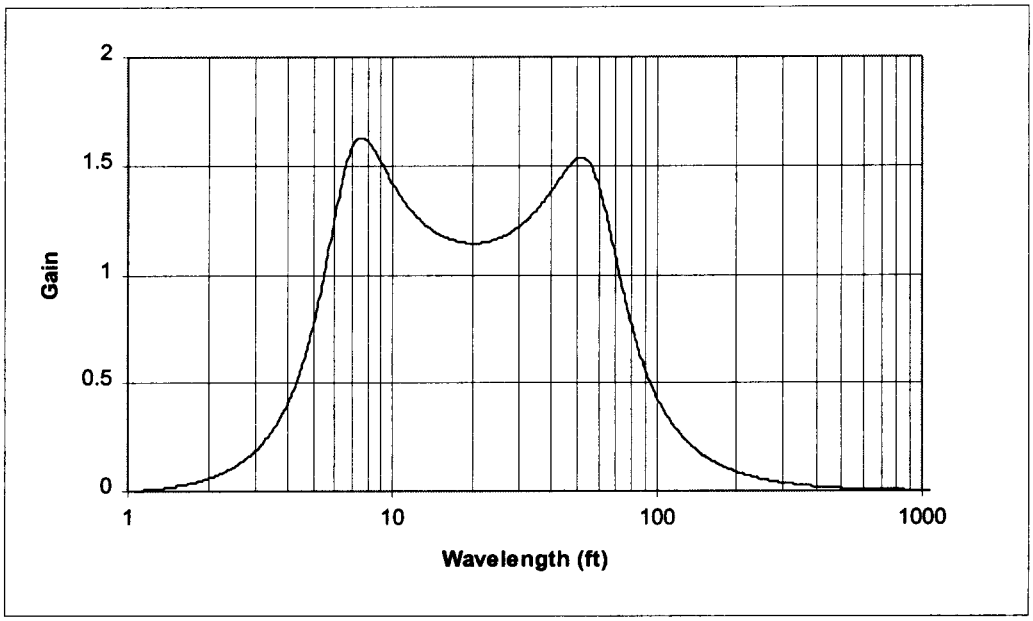

1 ft = 0.305 m

Figure 3.1.1. Response of IRI filter.

3.2 RIDE NUMBER (RN)

Long before the advent of high-speed profiling, highway engineers have been interested in estimating the opinion of the traveling public about the roughness of the roads. The Present Serviceability Index (PSI), which estimates the opinion of the road users of a pavement with the use of roughness and distress information, was developed during the AASHTO road test. The PSI has a scale from 0 to 5, with a score of 5 being assigned to a perfect pavement. Studies at the AASHTO road test have shown that about 95 percent of the information about the serviceability of the pavement is contributed by the roughness of its surface properties.

The RN assigns a score of between 0 and 5 for a pavement and is computed by an algorithm that provides a method to predict mean panel ratings from the measured profiles. The procedure for computing the RN was presented by Spangler and Kelly.[1] The research input for

the development of RN was provided through two research projects sponsored by the Ohio Department of Transportation[1,7] and two NCHRP projects.[8,9] In these experiments, panel ratings were obtained at test sections, and longitudinal profile data along the two wheel paths of the test sections were collected using a K.J. Law profiler. The data were used to develop a profile analysis algorithm to predict mean panel rating from measured profile. This was accomplished by using statistical techniques to find the spatial frequency bands of measured longitudinal profile roughness that correlate to subjective panel ratings of ride quality.

The RN ranges from 0 to 5, with 5 representing a perfect road, and 0 representing a road that is impassable. The RN computation method requires road profile data to be measured in two wheel paths at 25-mm (1-in) intervals, averaged over a 305-mm (12-in) distance, and stored at 152-mm (6-in) intervals. Profiles along both the left and the right wheel path are required for the computation of RN. Only wavelengths in the range of 0.48 to 2.4 m (1.6 to 8 ft) are considered in the computation of RN. The computation method computes a profile index for each wheel path. The profile index is the root mean square of the measured elevation profile after the amplitude of the long wave length content of elevation profiles has been attenuated by a second-order high-pass spatial filter having a natural frequency of 0.41 cycles/m (0.125 cycles/ft). A nonlinear transform is used to relate the profile index to the RN. The RN's computed for the left and the right wheel paths are then averaged to obtain the RN for the section. The RN computed by the algorithm had a coefficient of determination (R^2) of 0.84 with the actual measured subjective ride quality and a standard error of estimate of 0.29. The subjective ride quality estimates produced by this practice were found to be not significantly different in respect to pavement type, road class, and vehicle size.

3.3 COMPUTATION OF RN

The GPS sections are profiled annually, and the profile data along the left and the right wheel paths are collected. Multiple profiler runs are made over each section in order to obtain five profiler runs that satisfy the criteria described in section 2.1 of this report. The profile elevation data of the selected runs, as well as the IRI computed from the profile data, are stored in NIMS. However, the RN of these profiles is not computed.

All longitudinal profile elevation data for the GPS sections that are available in the NIMS were obtained to compute the RN. Examination of the profile elevation data revealed that data up to 1993 were available in the NIMS; for some sections, data were only available up to 1992. The computer program developed by Spangler and Kelly was used to compute the RN.[1] As

five profile runs are available in the NIMS for each profile date, the standard deviation and the coefficient of variation (COV) of the RN corresponding to each profile date were also computed.

3.4 COMPARISON BETWEEN COV OF IRI AND RN

For a given profile date, the COV of the RN for a specific GPS section was computed as described previously. For the same section, and the same profile date, the COV of the both-wheel-path IRI (average of left- and right-wheel-path IRI) was also computed. Thereafter, plots between the COV of RN and COV of IRI were prepared separately for GPS experiments 1 through 5. These plots are shown in figures 3.4.1 through 3.4.5. For each GPS experiment, all sections belonging to that experiment and all available profile dates were used in preparing these plots.

One profile data collection criterion at the GPS sections requires the standard deviation of the five selected profile runs to be less than 2 percent of the mean IRI (see section 2.1). This criterion is equivalent to specifying that the COV of the IRI computed from the five selected profile runs should be less than 2 percent. This value was 3 percent at the beginning of the LTPP program, and later it was reduced to 2 percent. Figures 3.4.1 through 3.4.5 indicate that, except

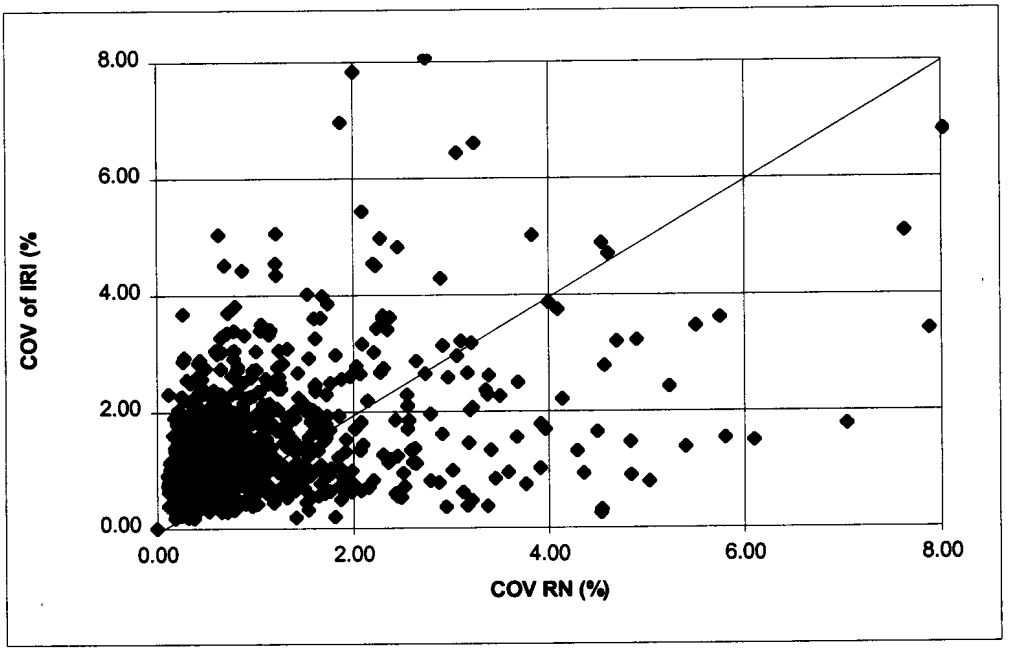

Figure 3.4.1. Relationship between COV of IRI and RN for GPS-1 sections.

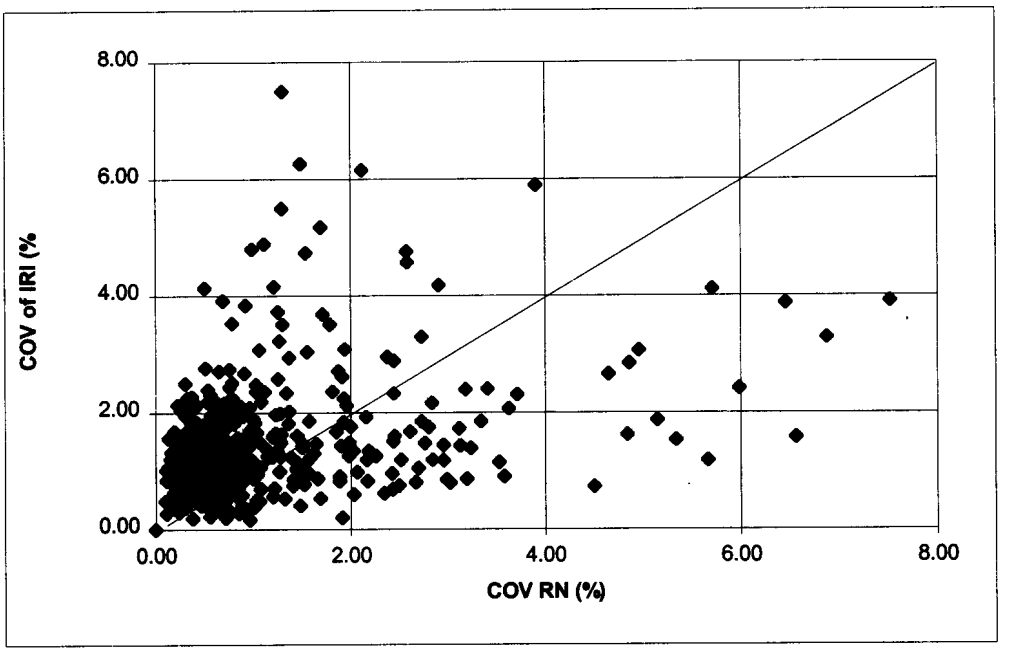

Figure 3.4.2. Relationship between COV of IRI and RN for GPS-2 sections.

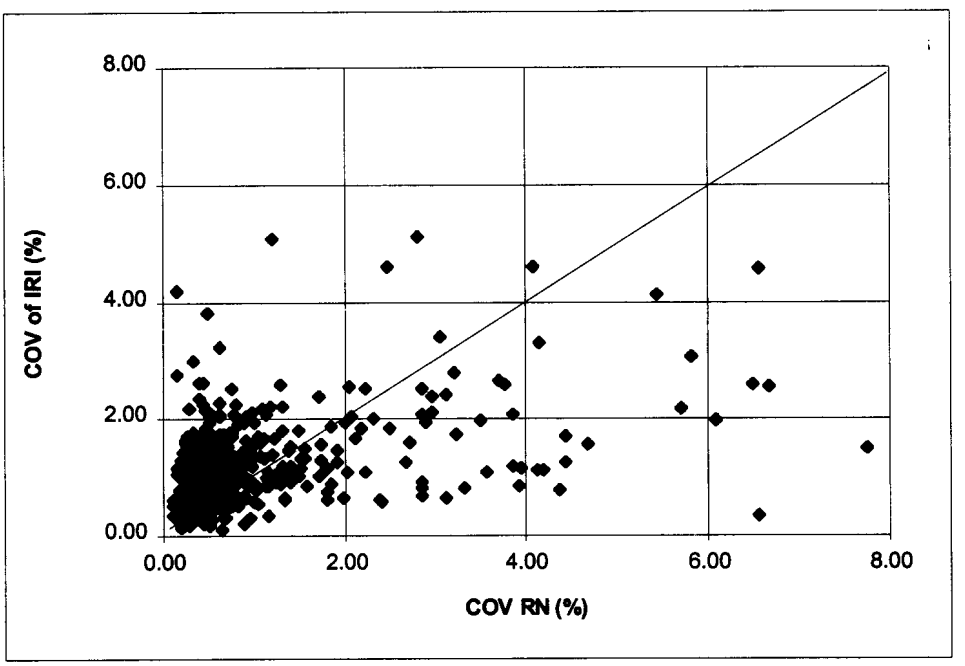

Figure 3.4.3. Relationship between COV of IRI and RN for GPS-3 sections.

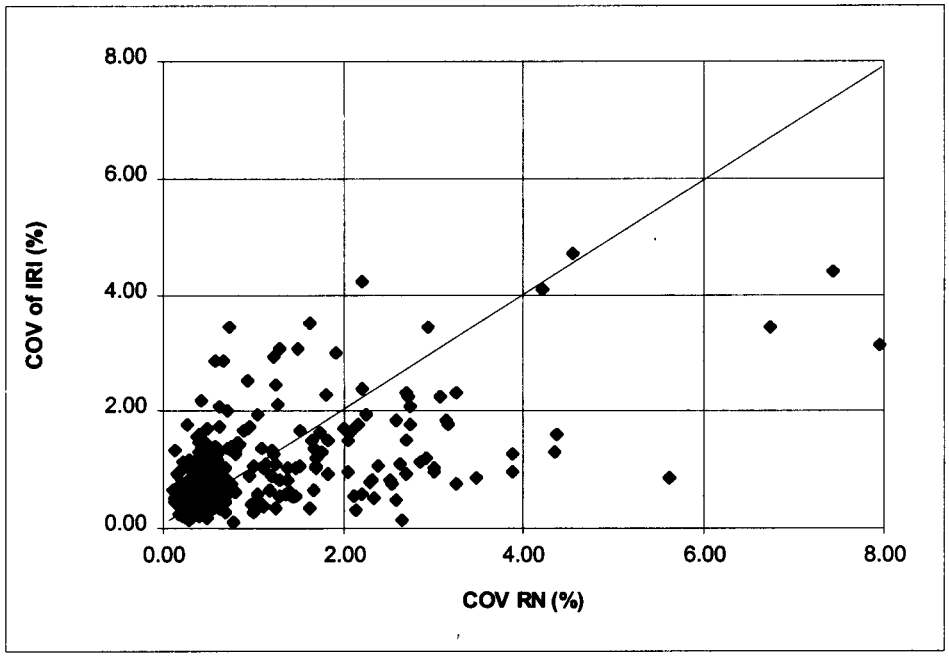

Figure 3.4.4. Relationship between COV of IRI and RN for GPS-4 sections.

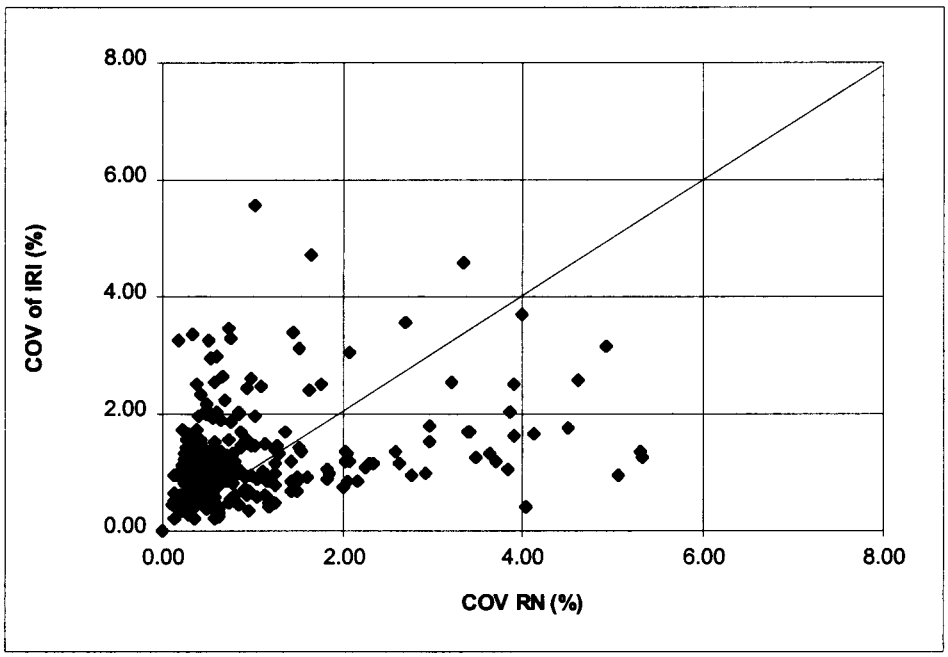

Figure 3.4.5. Relationship between COV of IRI and RN for GPS-5 sections.

for a few points, the majority of data points have a COV less than 3 percent. This indicates that the five profile runs for a specific test date that is available in NIMS have very repeatable IRI values.

Figures 3.4.1 through 3.4.5 show that the COV of IRI and RN can have different values at the same section. There are cases where low COV values of IRI have high COV values of RN, and vice versa. The range of wavelengths that contribute to the IRI, which is between 1.2 and 30 m (4 and 100 ft) is different than the range of wavelengths that contribute to RN, which is between 0.48 and 2.4 m (1.6 and 8 ft). Therefore, depending on the wavelength content of the multiple profiler runs, variability in the wheel paths can affect the two indices differently and cause differences in the COV between the two parameters.

3.5 COMPARISON BETWEEN INDICES

Figures 3.5.1 through 3.5.5 show the relationship between IRI and RN for GPS experiments 1 through 5. Each point in a plot represents the average IRI and the average RN computed from the five profiler runs available for a specific profiling date at a section. Each plot includes data for all sections and all profile dates that were considered in the analysis.

The plots for the AC-surfaced sections (GPS-1 and GPS-2) show a wider scatter in the relationship between IRI and RN at the higher IRI when compared with the PCC sections (GPS-3 through GPS-5). The GPS-3, -4 and -5 sections show a closer band than the AC sections. It appears that the roughness component wavelength of these sections is from the shorter wavelengths. These plots show that a unique relationship does not exist between IRI and RN. As these plots show, for a specific value of RN there is a wide range of IRI that would have the same RN. These variations are caused by differences in the wavelength content in the profiles.

For a simple illustration of this phenomenon, consider the two profiles shown in figure 3.5.6. Both profiles have IRI values that are close to each other, but the RN's are substantially different. The IRI is sensitive to wavelengths from 1.2 to 30 m (4 to 100 ft), while the RN is only sensitive to wavelengths from 0.48 to 2.4 m (1.6 to 8 ft). The short wavelength content in the first profile is larger than the second profile, and therefore it has a lower RN.

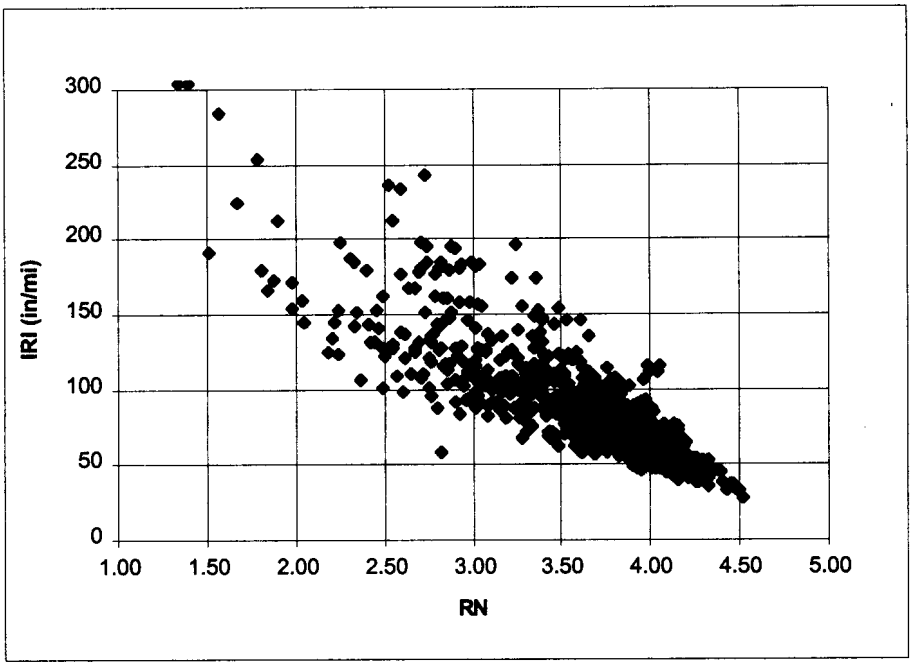

1 in/mile = 0.0158 m/km

Figure 3.5.1. Relationship between IRI and RN for GPS-1 sections.

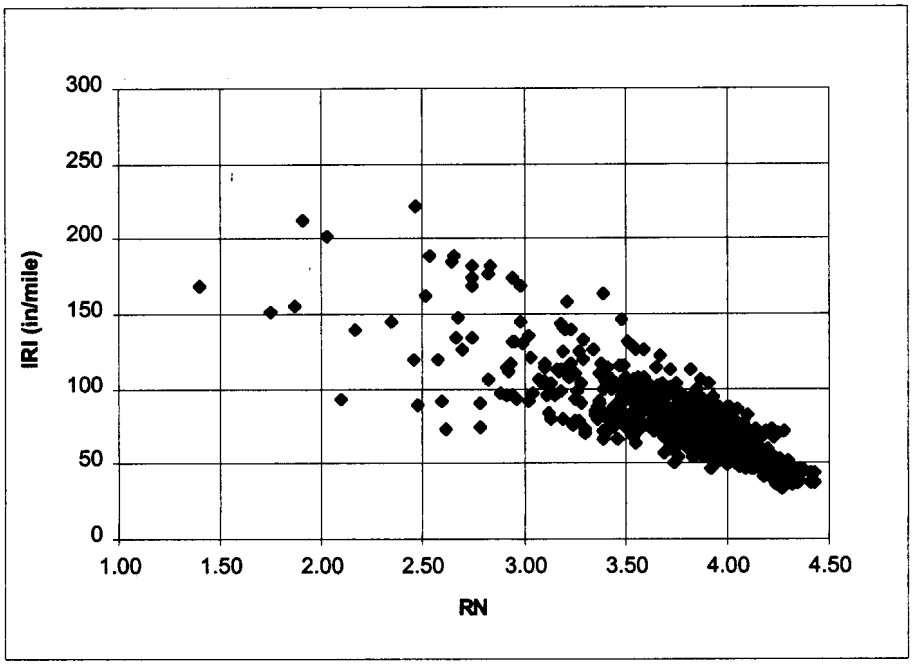

1 in/mile = 0.0158 m/km

Figure 3.5.2. Relationship between IRI and RN for GPS-2 sections.

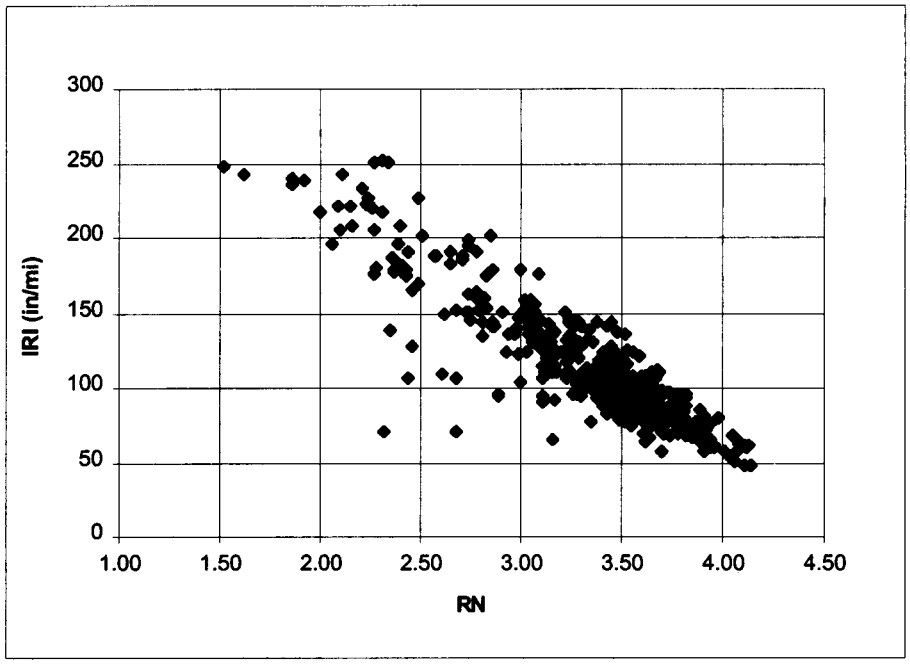

1 in/mile = 0.0158 m/km

Figure 3.5.3. Relationship between IRI and RN for GPS-3 sections.

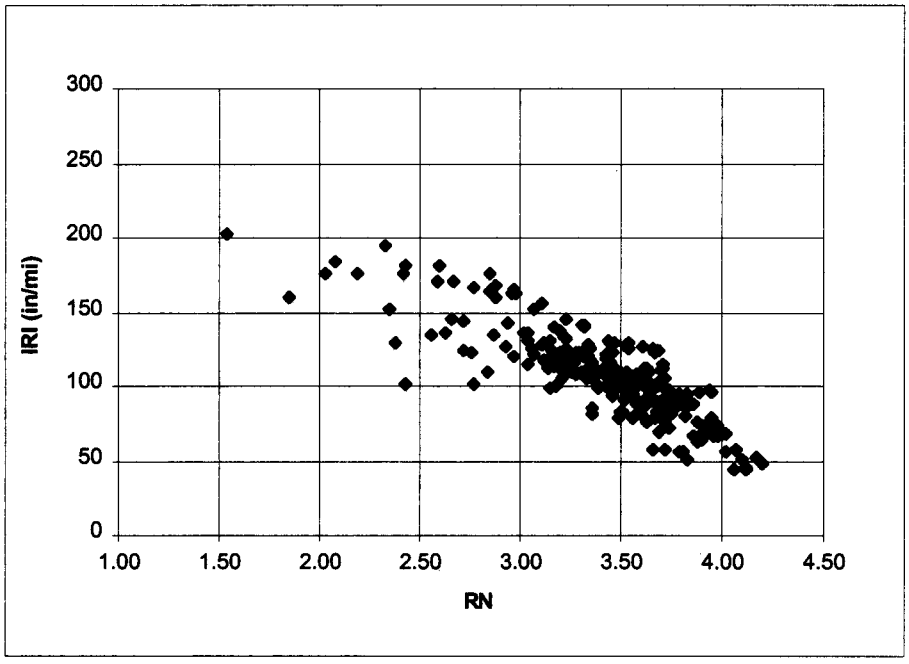

1 in/mile = 0.0158 m/km

Figure 3.5.4. Relationship between IRI and RN for GPS-4 sections.

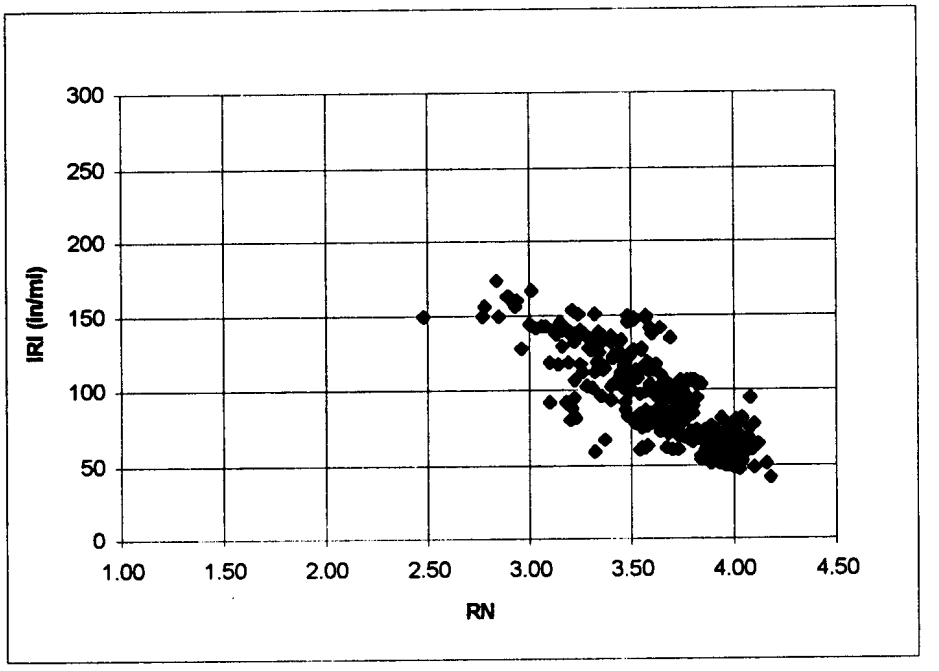

1 in/mile = 0.0158 m/km

Figure 3.5.5. Relationship between IRI and RN for GPS-5 sections.

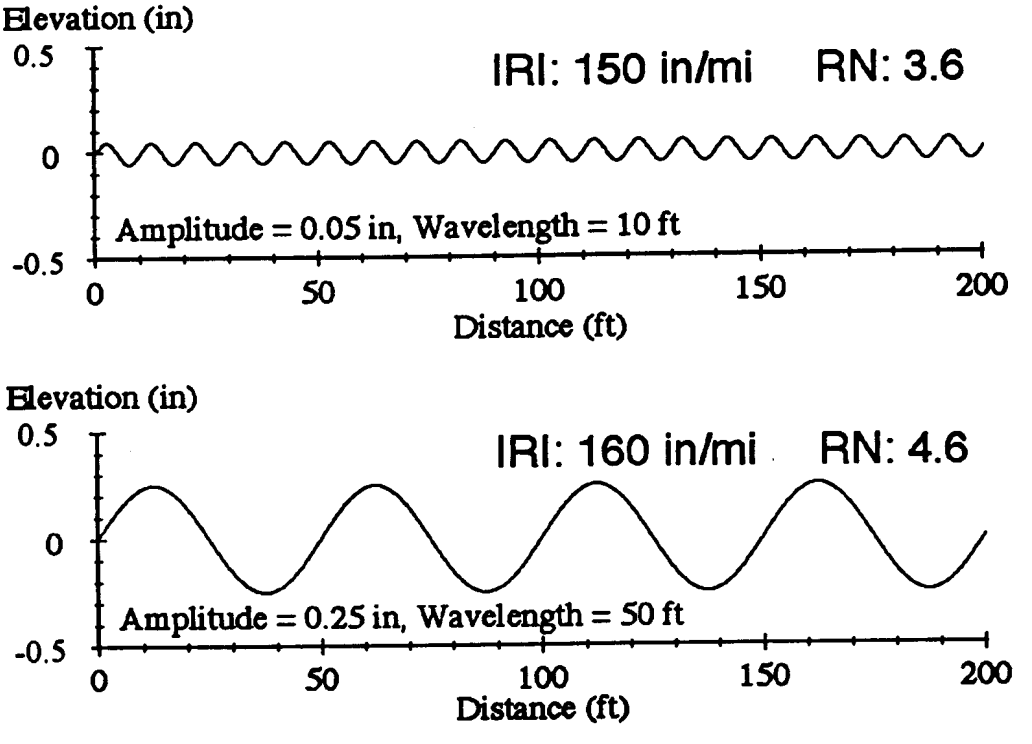

1 in = 25.4 mm, 1 ft = 0.305 m

Figure 3.5.6. Dependency of IRI and RN on wavelength content of profiles.

A specific IRI value does not indicate a unique profile associated with the IRI value. There could be numerous profiles, each having a different wavelength content, but the IRI of these profiles can be the same value. The RN of these profiles is only sensitive to wavelengths between 0.48 and 2.4 m (1.6 to 8 ft), and, depending on the wavelength content between these limits, the profiles that have the same IRI will have different values for RN. This is the cause of the nonuniqueness of the relationship between IRI and RN that is shown in figures 3.5.1 through 3.5.6.

3.6 COMPARISON OF TRENDS IN IRI AND RN AT SELECTED SECTIONS

A comparison between the variation of IRI and RN over time for a selected group of sections in GPS experiments 1 through 5 was performed. The IRI and RN that were computed from the time-sequence profile data at selected GPS sections were plotted against pavement age. Figures 3.6.1 through 3.6.5 present the comparison between these two parameters for four sections in GPS experiments 1 to 5, respectively. The selected sections presented for each GPS experiment include sections having low as well as high IRI values. These plots show that both the IRI and the RN follow the same trend.

3.7 NEW DEVELOPMENTS IN RIDEABILITY INDICES

The algorithm presented by Spangler and Kelly[1] for computing the RN is only valid for profiles obtained from profilers that obtain data at 25-mm (1-in) intervals, and then apply a 305-mm (12-in) moving average and record data at 152-mm (6-in) intervals. Currently only K.J. Law profilers satisfy these data collection criteria; this limitation prevents the RN from being computed for profiles collected by other profiling devices.

The University of Michigan Transportation Research Institute (UMTRI) developed a new ride index called the Rideability Number in a research project that was sponsored by the FHWA.[10] Data obtained from a panel rating study conducted in Minnesota, as well as the data collected for the NCHRP and Ohio Department of Transportation studies, were used in developing this parameter. The final report documenting this research was published in June 1996. This report was published after the analysis described previously in this chapter was performed. The Rideability Index developed by UMTRI is not restricted to a specific profiling sample interval, and can be computed for any data sampling interval. However, profiles obtained from ultrasonic devices do not have sufficient resolution to accurately measure short wavelengths,

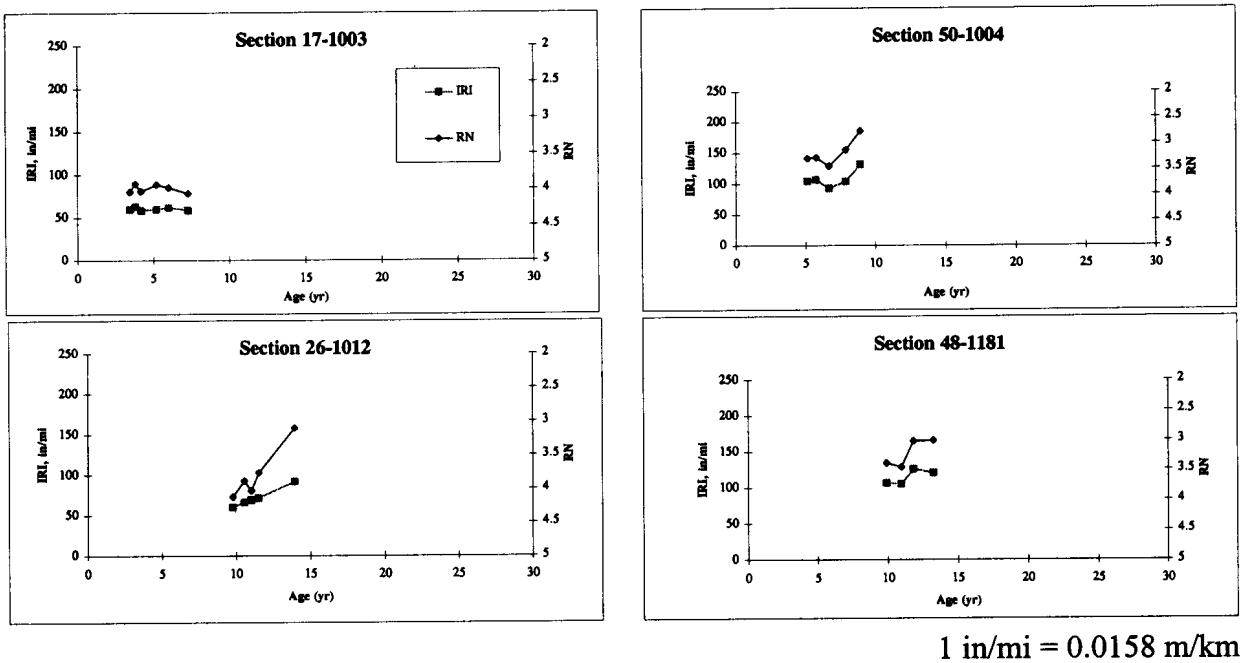

1 in/mi = 0.0158 m/km

Figure 3.6.1. Comparison of trends between RN and IRI for GPS-1 experiment.

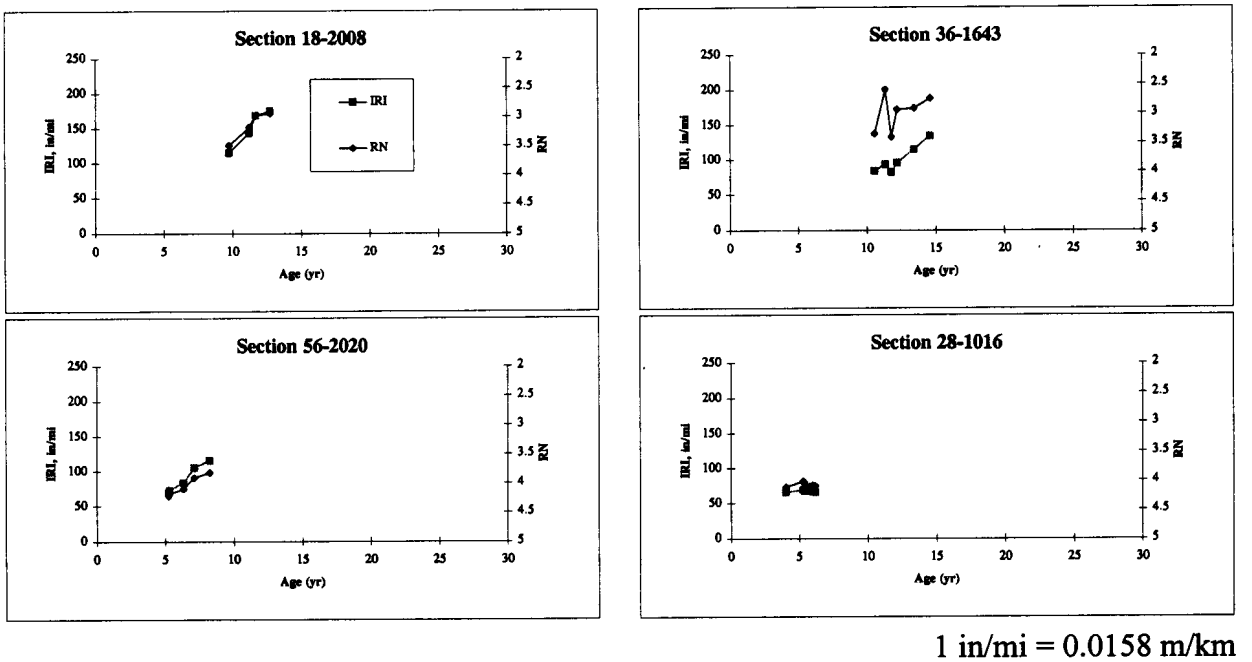

1 in/mi = 0.0158 m/km

Figure 3.6.2. Comparison of trends between RN and IRI for GPS-2 experiment.

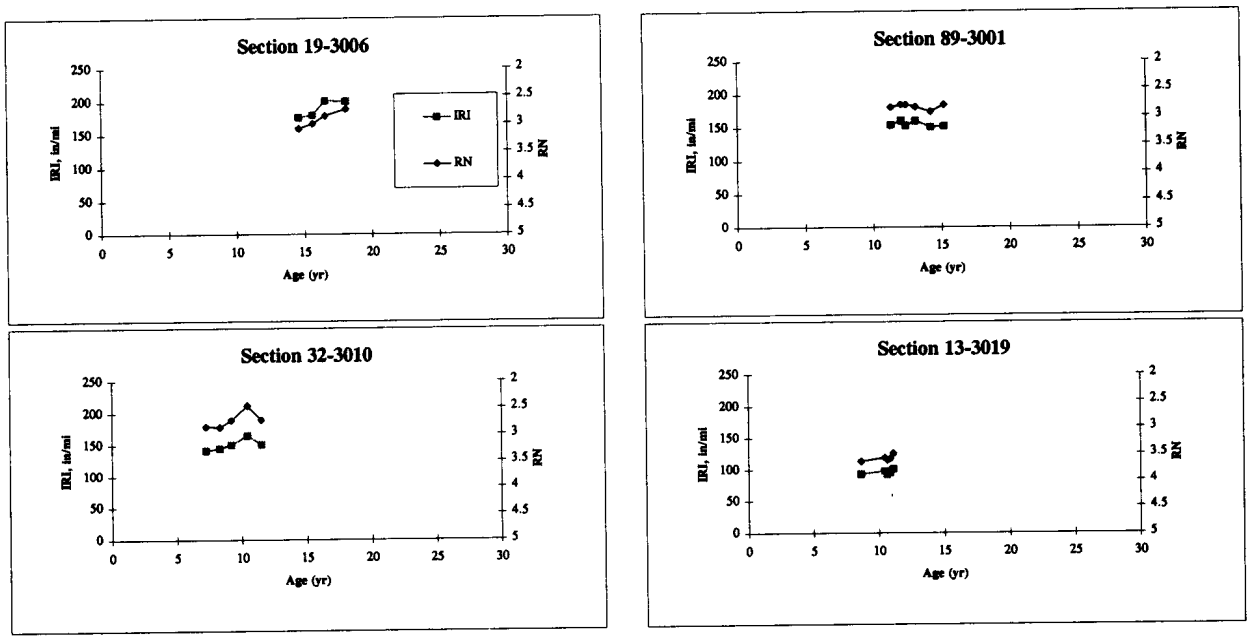

1 in/mi = 0.0158 m/km

Figure 3.6.3. Comparison of trends between RN and IRI for GPS-3 experiment.

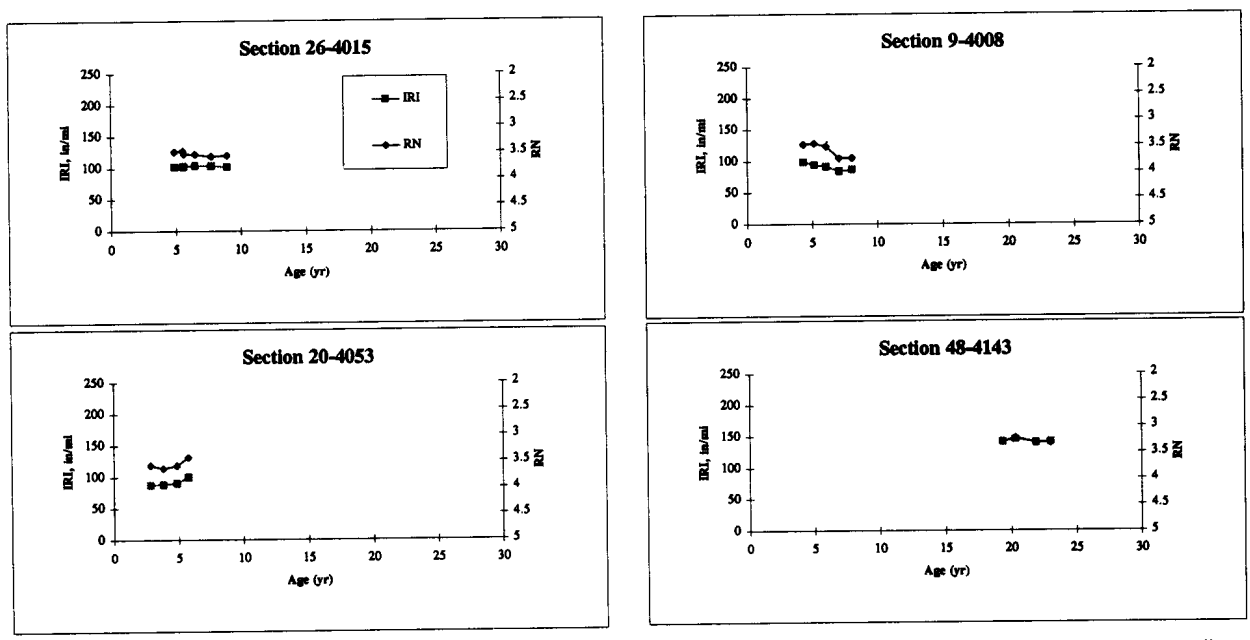

1 in/mi = 0.0158 m/km

Figure 3.6.4. Comparison of trends between RN and IRI for GPS-4 experiment.

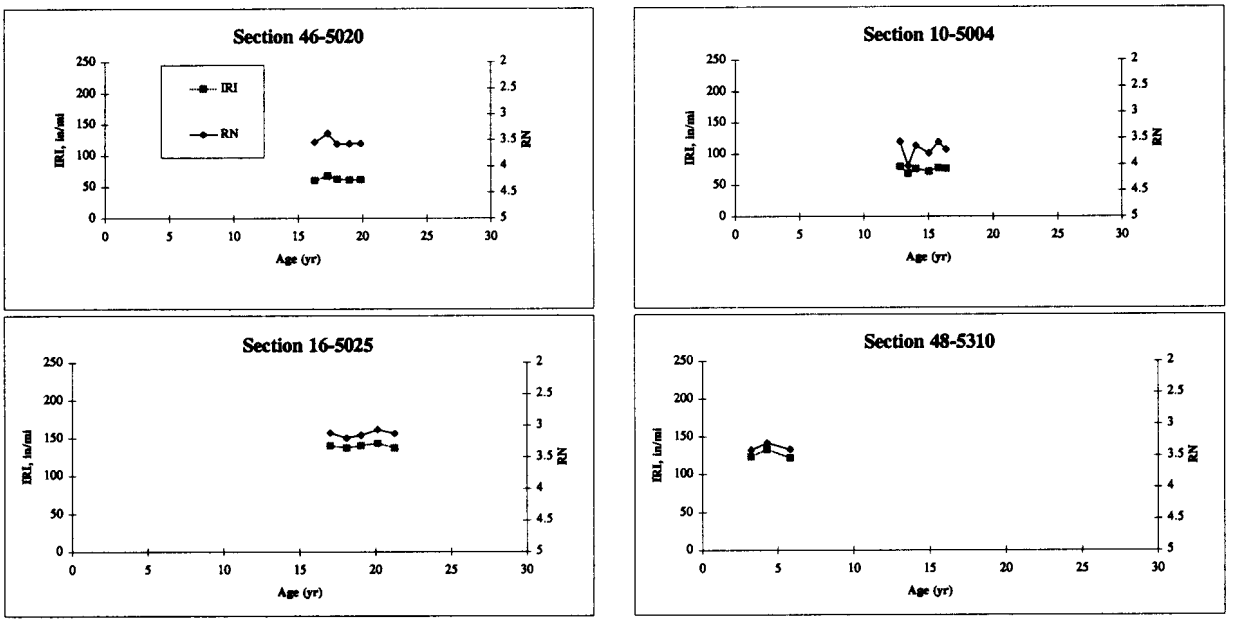

1 in/mi = 0.0158 m/km

Figure 3.6.5. Comparison of trends between RN and IRI for GPS-5 experiment

and the Rideability Index cannot be computed for profiles obtained from these devices. The Rideability Index is computed by: (1) first filtering the profile with a band-pass filter, (2) computing a Root Mean Square (RMS) value from the filtered profile called the profile index, and (3) transforming the profile index to the Rideability Index. The Rideability Index is influenced by wavelengths ranging from 0.6 to 9.1 m (2 to 30 ft). For a profile, the RN computed from the Spangler and Kelly algorithm is not equal to the Rideability Index developed by UMTRI. This is because the wavelengths and the gain factors that are used by the two indices are different. However, there is a very good correlation between these two indices. As there is a very good correlation between the RN and the Rideability Index, relationships between the Rideability Index and the IRI are expected to be similar to the relationships that were observed for the RN.

Currently, an American Society of Testing and Materials (ASTM) standard for computing the RN, which uses the algorithm for Rideability Index developed by UMTRI, has been proposed and is going through the balloting process of ASTM.

3.8 PROFILE STATISTIC TO BE USED IN ANALYSIS

An objective of the comparison between the IRI and the RN was to determine which of the two statistics would be used to develop models to predict roughness development. The IRI was selected as the parameter to be used in future analyses on the basis of the following factors:

1. A comparison of the trends in time-sequence IRI and RN that was performed at selected sections did not show a difference in the observed trends.

2. Profile elevation data are required for computing the RN, as this parameter is not a computed quantity that is stored in the NIMS. The latest profile elevation data that were available in the NIMS at the time the profile data were obtained for this study was 1993. For some sections, data were available only up to 1992. For most sections, this would provide profile data for less than 3 years. More recent IRI data for the GPS sections were available from the regional contractors in the RIMS. Therefore, at each test section, more time-sequence IRI data were available compared with time-sequence data for the RN. Because roughness trends can be better defined with more data points, using the IRI in the future analysis of this study presented a clear advantage.

3. The RN used in this analysis was based on the algorithm presented by Spangler and Kelly.[1] Efforts are currently under way by ASTM to introduce the Rideability Index (developed by UMTRI) as a standard method to compute a ride index. Basing our analysis on an index that is declining in relevance is not justifiable.

3.9 SUMMARY

A comparison between the IRI and the RN (computed from the algorithm developed by Spangler and Kelly) indicated that a unique relationship between the IRI and RN does not exist. The IRI is sensitive to wavelengths between 1.2 and 30 m (4 and 100 ft), while the RN is sensitive to wavelengths between 0.48 and 2.4 m (1.6 and 8 ft). For a specific value of RN, there could be a range of IRI values that correspond to that RN. For example, consider two profiles that have similar short wavelength contents, but different long wavelength contents. As the RN is sensitive to the short wavelength content, the two profiles can have the same RN, but as the long wavelength contents are different, they can have different IRI values. The study of trends in IRI and RN at selected sections indicated that these two parameters generally have similar trends. As the IRI has a maximum sensitivity at wavelengths of 2.1 m (7 ft) and 15.2 m (50 ft), short

wavelength content also has a significant contribution to the IRI. Therefore, short wavelength contents that are between 0.48 and 2.4 m (1.6 and 8 ft) that reduce the RN will cause an increase in the IRI. The RN computation method of Spangler and Kelly requires road profile data measured in two wheel paths at 25-mm (1-in) intervals, averaged over a 305-mm (12-in) distance, and stored at 152-mm (6-in) intervals. The UMTRI developed a new ride index called the Rideability Number in a research project that was sponsored by the FHWA. The Rideability Index can be computed from profiles obtained for any sampling interval. Efforts are currently under way by ASTM to introduce the Rideability Index (developed by UMTRI) as a standard method to compute a ride index.

CHAPTER 4: DATA SYNTHESIS

4.1 SELECTION OF DATA ELEMENTS

The data collected for the LTPP program are stored in the NIMS database. A description of the data that are available in the NIMS is presented in the *Long Term Pavement Performance Information Management System Data User's Guide.*[11] The data available in the NIMS can be divided into the following categories: inventory, maintenance, climatic, monitoring, traffic, materials testing, and rehabilitation. A brief description of the data elements contained in each category follows.

Inventory Data: Inventory tables contain information related to the location of the section and material characteristics of the pavement obtained from State transportation agency archives. Inventory data collection sheets were filled out by the State highway agencies for all GPS sections, and these data are included in the inventory tables in the database.

Maintenance Data: Data tables in this category record maintenance activities performed on the GPS test sections after the sections were included in the LTPP program.

Climatic Data: The climatic data available are derived from weather data originally collected by the National Oceanic and Atmospheric Administration and the Canadian Climatic Center (for Canadian test sections). Data collected from five weather stations that are close to each GPS section are available in these data tables.

Monitoring Data: Data tables in this category contain data recorded by monitoring equipment. These include profile data, deflection data, friction data, surface distress data, and transverse profile data.

Traffic Data: Traffic data tables contain historical traffic estimates provided by State highway agencies for each GPS section. Some limited section-specific monitored data collected by weigh in motion (WIM) equipment are also available.

Materials Testing: Extensive laboratory testing of materials performed on samples obtained just outside the 152-m- (500-ft-) long GPS section to characterize pavement layer and subgrade

properties. Laboratory test data for pavement and subgrade materials are contained in the tables that fall into this category.

Rehabilitation Data: Major improvements to a test section after it is included in the LTPP program are documented in the data tables that are in this category.

A goal in this study was to develop models to predict the development of roughness from the data available in the NIMS. The first step in the study was to identify variables that are available in the LTPP database that could be related to the development of roughness. A previous research effort to develop models to predict pavement roughness using LTPP data was performed by Simpson et al.[12] This report documents data elements that were identified by an expert panel as significant factors that affect the development of roughness. Models to predict roughness from data obtained from a study performed in Brazil is presented by Paterson.[13] These two reports were reviewed to identify data elements that have been related to roughness development in previous studies. The data elements that were available in the LTPP data tables were reviewed, and engineering judgment as well as information obtained from previous studies were used to identify data elements that may be relevant in this analysis. The tables containing the relevant data elements were obtained from the sixth informational release of NIMS, and are described later in this chapter. A review of the obtained data indicated that some of the desired information was not available. In these cases, the information was obtained from RIMS through the regional contractors.

4.2 DEVELOPMENT OF DATABASES FOR ANALYSIS

One of the most time-consuming portions of this study was the manipulation of the data files obtained from the NIMS and RIMS. Statistical analysis software requires databases that are row structured, where a dependent variable and the associated independent variables are contained in one row. The data files obtained from NIMS and RIMS were manipulated in order to develop such a structure for each GPS section.

Separate data tables were obtained for each GPS experiment from the NIMS. Each data table contains specific information by each GPS section, and the data element of interest for the analysis had to be extracted from the data file. Each data file obtained from NIMS was imported into a spreadsheet and the data elements that were to be used in the analysis were extracted. This resulted in separate spreadsheet files for each data element that contained the GPS identification number and the data element of interest in each row. Thereafter, an analysis

file was created for each GPS section. This file contained all data elements organized into a single row for each GPS section. This process was performed by importing the spreadsheets containing the data elements into a relational database, and then linking the tables to create a data table. All GPS sections, including the sections that had inconsistent IRI trends (see section 2.2.4) were included in the analysis. Prior to assembling the analysis database, certain manipulations had to be performed on several data elements, as described in section 4.3. A climatic database developed in a previous study was used to obtain the climatic data for this study.[12] Table 4.2.1 summarizes the information compiled for each GPS section and also presents the table name in the NIMS that contains this data element.

4.3 DATA MANIPULATIONS

The data files obtained from NIMS are structured in a row format, where the first column contains the GPS identification number, and the other columns contain the data associated with the section. However, there are typically many rows of data for the same GPS section within each data file. For example, where laboratory test results are available for multiple locations for a GPS section, each test result is contained in a separate row. The pavement layer thicknesses for GPS sections are contained in multiple rows, with each row containing data for one layer. The data file for historical traffic information can contain up to 25 rows of traffic information per GPS section, where each row contains the estimated traffic parameters for the GPS section for one year The data files must then be processed and arranged such that all the relevant information for each section is contained in one row before being imported to the relational database to create the analysis file. This process was generally performed in spreadsheets with the use of macros. The following sections describe examples of data manipulations that were performed on the data obtained from the NIMS.

4.3.1. Laboratory Test Data

For each GPS section, laboratory test data such as percentage passing the 75-μm (No. 200) sieve for subgrade, or PCC compressive strength, are available for multiple locations. These data elements were averaged to obtain a single representative value for each section.

4.3.2 Layer Thickness Data

The NIMS tables for layer thickness for a GPS section consist of a separate row for each layer. Even for AC, separate rows contain the layer thickness for the surface and leveling

Table 4.2.1. Data elements assembled into analysis database.

Data Element	Applicable Experiment	NIMS Table
Section Data		
Four-digit GPS section number	GPS 1 to 9	-
Two-digit State identification number	GPS 1 to 9	-
LTPP geographic region	GPS 1 to 9	-
LTPP GPS experiment number	GPS 1 to 9	EXPERIMENT_SECTION
Construction date	GPS 1 to 9	INV_AGE
Profile Data		
Age of pavement at time of profile measurement	GPS 1 to 9	Computed
IRI values	GPS 1 to 9	MON_PROFILE_MASTER
Pavement Layer Data		
AC Thickness from core data	GPS 1, 2, 6	TST_L05B
PCC thickness	GPS 3,4,5,7,9	TST_L05B
Overlay thickness	GPS 6, 7, 9	RHB_IMP, INV_MAJOR_IMP
Overlay date	GPS 6, 7, 9	RHB_IMP
Overlay code	GPS 6, 7, 9	RHB_IMP
Base thickness	GPS 1 to 9	TST_L05B
LTPP material code for the base	GPS 1 to 9	TST_L05B
Approximate structural number	GPS 1, 2, 6	Computed
Subgrade Data		
Subgrade liquid limit	GPS 1 to 9	TST_UG04_SS03
Subgrade plastic limit	GPS 1 to 9	TST_UG04_SS03
Subgrade plasticity index	GPS 1 to 9	TST_UG04_SS03
Subgrade percent passing No. 4 sieve	GPS 1 to 9	TST_SS01_UG01_UG02
Subgrade percent passing No. 200 sieve	GPS 1 to 9	TST_SS01_UG01_UG02
Subgrade moisture content	GPS 1 to 9	TST_SS01_UG01_UG02
Subgrade liquidity index	GPS 1 to 9	Computed
LTPP subgrade material code	GPS 1 to 9	TST_L05B
Overburden pressure on subgrade from pavement system	GPS 1 to 9	Computed
Climatic Data		
Annual precipitation	GPS 1 to 9	Previous study (reference 12)
Number of days below 32°F/yr	GPS 1 to 9	Previous study (reference 12)
Number of days above 90°F/yr	GPS 1 to 9	Previous study (reference 12)
Number of wet days/yr	GPS 1 to 9	Previous study (reference 12)
Number of days with >0.5 in. precipitation per/yr	GPS 1 to 9	Previous study (reference 12)
Number of freeze thaw cycles/yr	GPS 1 to 9	Previous study (reference 12)
Freeze index	GPS 1 to 9	Previous study (reference 12)

Table 4.2.1 (Continued). Data elements assembled into analysis database.

Traffic Data		
Historical Equivalent Single Axle Load (ESAL) data	GPS 1 to 9	TRF_EST_ANL_TOT_GPS_LN
Growth rate for KESAL (1000's of ESAL)	GPS 1 to 9	Computed
Average KESAL per year from historical data	GPS 1 to 9	Computed
Initial KESAL for section	GPS 1 to 9	Computed
Estimated truck factor	GPS 1 to 9	Computed
Estimated cumulative traffic	GPS 1 to 9	Computed
PCC Test Data		
PCC compressive strength	GPS 3, 4, 5, 7, 9	TST_PC01
PCC Poissons ratio	GPS 3, 4, 5, 7, 9	TST_PC04
PCC unit weight	GPS 3, 4, 5, 7, 9	TST_PC05
PCC elastic modulus	GPS 3, 4, 5, 7, 9	TST_PC04
PCC split tensile strength	GPS 3, 4, 5, 7, 9	TST_PC02
Shoulder Data		
Total width of outside shoulder	GPS 1 to 9	INV_SHOULDER
Paved width of outside shoulder	GPS 1 to 9	INV_SHOULDER
Thickness of outside shoulder	GPS 1 to 9	INV_SHOULDER
Thickness of shoulder base	GPS 1 to 9	INV_SHOULDER
Drainage		
Subdrainge information	GPS 1 to 9	INV_GENERAL
LTPP code for drain type	GPS 1 to 9	INV_GENERAL
LTPP code for drain location	GPS 1 to 9	INV_GENERAL
PCC Mix Data		
Water to cement ratio	GPS 3, 4, 5	INV_PCC_MIXTURE
Air content	GPS 3, 4, 5	INV_PCC_MIXTURE
Weight of coarse aggregate in mix	GPS 3, 4, 5	INV_PCC_MIXTURE
Weight of fine aggregate in mix	GPS 3, 4, 5	INV_PCC_MIXTURE
Weight of cement in mix	GPS 3, 4, 5	INV_PCC_MIXTURE
Weight of water in mix	GPS 3, 4, 5	INV_PCC_MIXTURE
PCC Steel Information		
Percent longitudinal steel by area	GPS 4, 5	INV_PCC_STEEL
PCC Joint Information		
Average contraction joint spacing, ft	GPS 3, 4	INV_PCC_JOINT
LTPP code for type of joint	GPS 3, 4	INV_PCC_JOINT

1 in = 25.4 mm, °C = (°F-32)/1.8

courses. The number of layers for the pavement structure for a GPS section can vary between two and six layers. For cases where the number of layers is six, the data are contained in six rows in the data file. Macro programs were used in the spreadsheet to reduce all these data to one row of information for each section. The structural number of AC-surfaced sections is not available in a data table in the NIMS, so the estimated structural number was computed from the layer thickness and by assigning structural coefficients to each layer on the basis of layer type. The overburden pressure on the top of subgrade was also computed on the basis of layer thickness and estimated density of the layers.

4.3.3 Traffic Data

WIM scales and Automatic Vehicle Classification systems have been installed at numerous GPS sections. At some GPS sections, portable equipment is used to collect data. The collected data are uploaded to the Central Traffic Database. The *Monitored Traffic Data Status Report,* published in October 20, 1995, provides a summary of monitored traffic data available at GPS sections.[14] A limited amount of annual Equivalent Single Axle Loads (ESALs) estimated from the monitored traffic data is available in the NIMS. This data table was reviewed to determine data availability. The number of days for which WIM data has been collected at a section ranged from 2 to 365, and the estimated annual ESALs by year have been computed from the available WIM data.

A review of the monitored traffic data indicated that at least 1 year of estimated ESALs was available at the following percentage of sections for GPS experiments 1 through 5: GPS-1, 43 percent; GPS-2, 37 percent; GPS-3, 43 percent; GPS-4, 76 percent; and GPS-5, 40 percent. A review of the data indicated that, for a specific section, the annual ESAL estimates vary significantly from 1 year to the next. For example, at GPS section 364018, the estimated annual Kilo Equivalent Axle Loads (KESALs) from WIM data was 249 in 1992, while the estimate for 1993 was 9. At GPS section 531006, the estimated KESALs from WIM data for 1992 was 34, while the estimate for 1993 was 72. The number of days of WIM data used to obtain the KESALs for the 2 years for both cases were different. One explanation for the variability seen in the ESAL data at a particular section is the varying number of days for which WIM data were collected from one year to the next. Because of the large variations in estimated ESALs that were noted at many sections, an accurate ESAL estimate could not be obtained for a GPS section from the WIM data. Therefore, it was decided to use historical traffic data that are available for the sections to estimate cumulative traffic loading applied at each section. The historical traffic data contain both truck counts and estimated ESAL counts for each year of

data. On the basis of these parameters, an estimate of truck factors (number of ESALs per truck) can also be computed from these data.

The cumulative traffic at any given profile date was desired for the analysis. The number of years for which historical traffic data exists is also variable. For some sections, historical traffic data began with the construction date, while for other sections, the historical traffic data were sporadic or did not begin at the date of construction. There were some sections for which traffic data were available for only 1 year. Figure 4.3.1 presents the traffic trends for several GPS-3 sections.

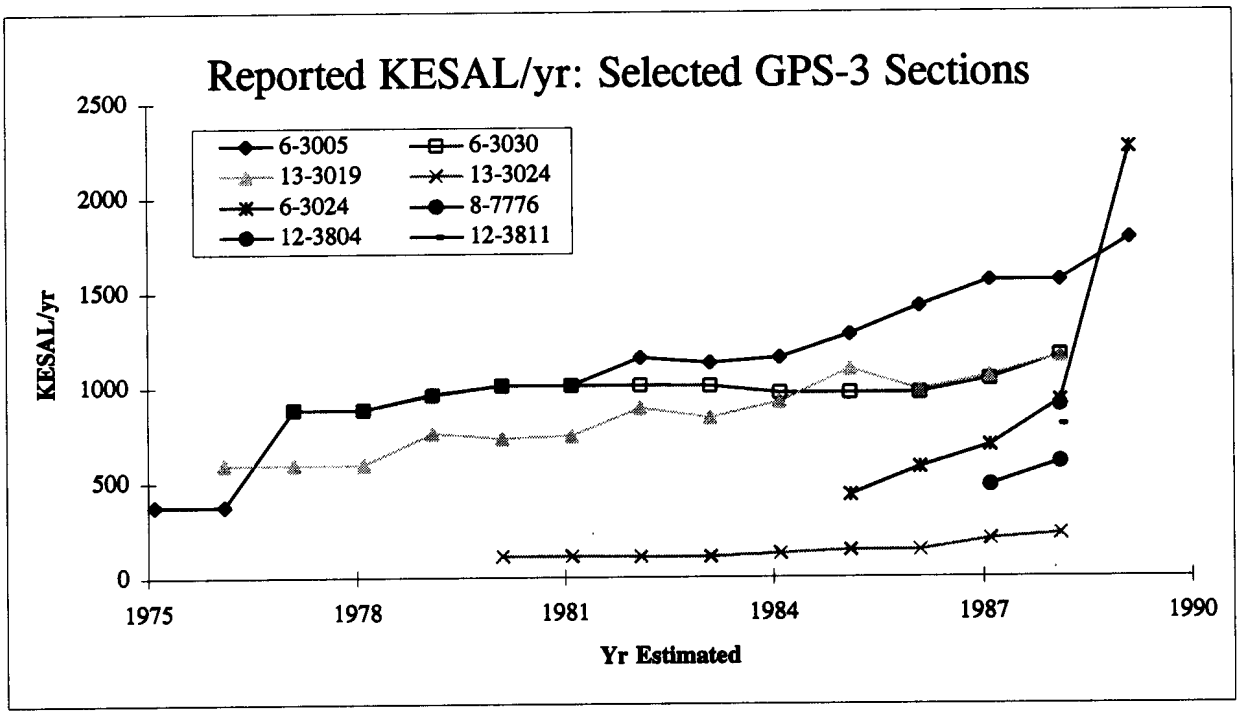

Figure 4.3.1. Plots of historical traffic data for selected GPS-3 sections.

Three approaches were used to compute cumulative traffic on the basis of the number of years of available traffic data. For sections that had 4 or more years of traffic data, cumulative traffic was computed based on an exponential growth type model, while for sections that had less than 4 years of traffic data, a linear projection that was based on a growth slope was used. For sections with only 1 year of traffic information, traffic was assumed to be constant at that rate over the life of the section. A brief description of the models that were used to compute cumulative traffic is presented next.

Exponential Growth: If the traffic growth rate is known along with the initial traffic rate, then the cumulative traffic at any point in time is defined by:

$$CumTraff = KESAL_0 \frac{(1+i)^n - 1}{\ln(1+i)}$$

where:

$CumTraff$ = the sum of the historical KESAL,
$KESAL_0$ = the first KESAL/yr noted in the historical data,
i = annual growth rate for KESAL/yr, and
n = number of years between first and last traffic date.

This equation can be manipulated into the form:

$$0 = -\frac{CumTraff}{KESAL_0}(\ln(1+i)) + ((1+i)^n - 1)$$

A macro was developed in a spreadsheet to iterate and obtain a solution for the growth rate for the above equation for each GPS section that had more than 4 years of traffic data. On the basis of the growth rate, the cumulative ESALs corresponding to each profile date were computed. Figure 4.3.2 graphically presents the approach used in this model.

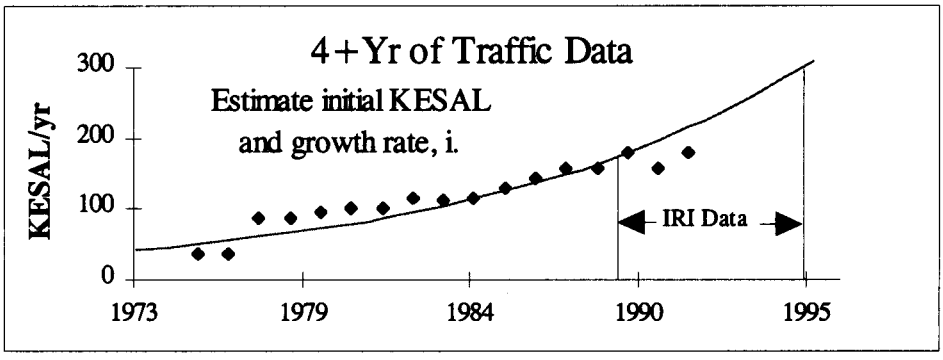

Figure 4.3.2. Graphical representation of traffic analysis scheme used for sections with more than 4 years of traffic data.

Linear Slope Type Growth: Traffic generally exhibits exponential growth over time. However, if the KESAL/yr were to increase linearly over time at a section, the cumulative traffic at any time can be defined by:

$$CumTraff = \int_0^t (KESAL_0 + bt)dt$$

where:

$CumTraff$ = cumulative traffic (KESAL),

$KESAL_0$ = the first KESAL/yr noted in the historical data,

b = linear traffic growth rate, and

t = time in yr between first and last traffic date.

Solving this equation, the slope can be expressed as:

$$b = \frac{2[CumTraff - KESAL_0 t]}{t^2}$$

An algorithm was developed to find the slope (b), which satisfies this relationship for each GPS section that had less than 4 years of traffic data. Figure 4.3.3 graphically presents the approach used in this model.

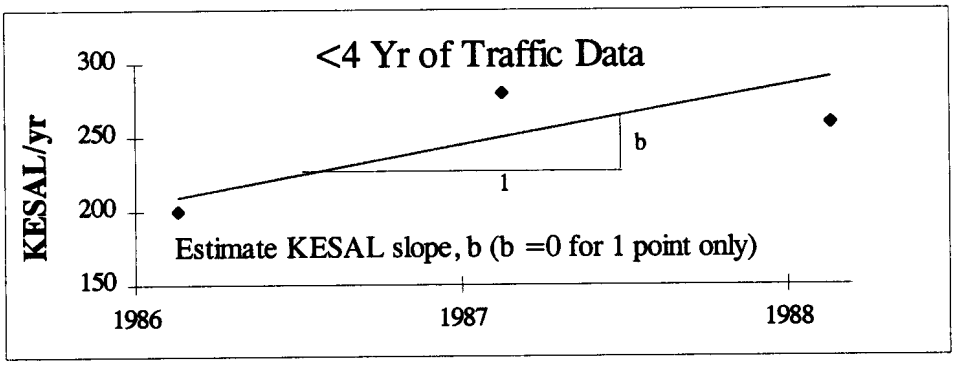

Figure 4.3.3. Graphical representation of traffic analysis scheme used for sections with less than 4 years of traffic data.

Most sections had data over only a portion of the pavement's life, and the traffic data for the initial years or the later years of the project were not available. In such cases, the above equations were used to estimate the traffic at the section immediately after construction by backcasting the growth rate. The cumulative traffic at each profile date was then computed on the basis of the initial traffic volume and the growth rate.

4.4 DATA AVAILABILITY

After the databases for each GPS experiment were assembled, the availability of each data element was evaluated. Generally, laboratory test data for GPS experiments 1 through 5 were available for the data elements that were considered in the analysis, except for resilient modulus test data, where data was limited. Some inventory data were missing for GPS experiments 1 through 5. An example is the load transfer type (doweled or aggregate) for the GPS-3 experiment, where the data were missing for 24 percent of the test sections. Laboratory test data for GPS experiments 6 through 9 were less complete compared with those of GPS experiments 1 through 5.

4.5 INITIAL PSI OF GPS SECTIONS

In the LTPP program, the GPS test sections were established on in-service pavements of varying ages. The initial IRI of these test sections were not available in the LTPP database. The researchers who performed an earlier analysis on roughness development[12] estimated the initial PSI of the test sections with the use of data from various sources. These initial PSI values were obtained and reviewed, and the review indicated that initial PSI estimates for 541 sections were available. The researchers[12] had used one of the following procedures to estimate the PSI of the sections: (1) estimate PSI on the basis of roughness measurement obtained at the test section soon after construction (148 sections); (2) extrapolate a roughness measurement made several years after construction to estimate the initial roughness and then estimate PSI (8 sections); (3) use multiple roughness measurements made over time and extrapolate back to estimate the initial roughness and estimate PSI from this value (122 sections); (4) tap the memory of an individual closely associated with the project during construction to get an estimate of PSI (18 sections); and (5) use general experience in initial PSI from research studies (248 sections). For cases where the PSI was estimated from roughness measurements, the data appeared to be from Mays meter measurements, and the roughness measurement was most likely to be for a segment length that included the 152-m- (500-ft-) long GPS section. Figure 4.5.1 presents the frequency distribution of the estimated PSI values. A review of the data indicated obvious biases. For example, Colorado had 16 GPS sections (comprising GPS-1, -2, -3, -6A, -7A, and -9 experiments) and all had an estimated PSI of 4.20. Arkansas had 14 GPS sections, where all the GPS-1, -2, and -7 experiments had an initial PSI of 4.20 while the 7 GPS-2 experiments had a PSI of 4.70. Because of these biases it was decided not to use these PSI data to estimate the initial IRI of the test sections.

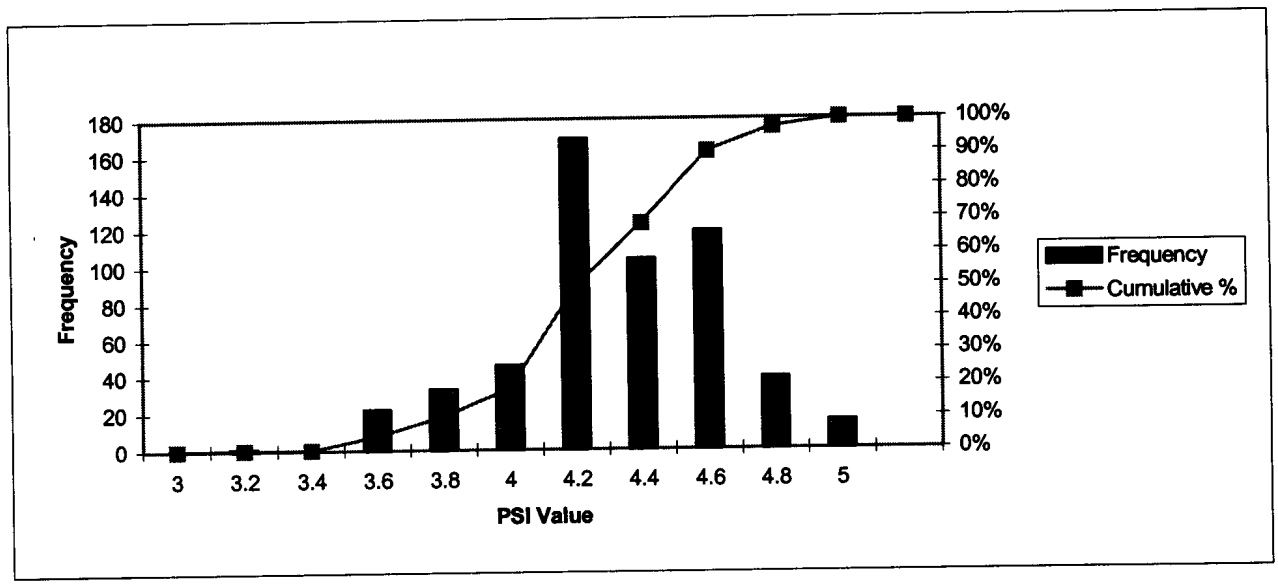

Figure 4.5.1. Frequency distribution of estimated initial PSI values for GPS sections.

4.6 DATA DISTRIBUTION AND CORRELATION ANALYSIS

Once the analysis databases containing the data elements that were to be analyzed were assembled, statistical procedures such as univariate analysis and bivarate analysis were performed on the data. The univariate analysis consisted of an investigation of the distribution of each data element that was selected for analysis, and was carried out separately for each GPS experiment. Histograms were developed to study the frequency distribution of the data elements. The histograms indicated that some biases existed for some of the data elements that were analyzed. For example, the study indicated that the distribution of the test sections for the GPS experiments have some bias related to the States. For example, 39 percent of the GPS-1 test sections are located in four states (Florida and North Carolina - 6 percent each, Arizona - 8 percent, and Texas - 19 percent). For the GPS-4 experiment, 37 percent of the test sections are located in three states (Missouri - 15 percent, Minnesota - 12 percent, and Arkansas - 10 percent).

Bivariate analysis consisted of computing the Pearson's correlation coefficient between the data elements selected for analysis and plotting two-way scatter plots. This correlation coefficient has a value between 1 and -1, with values approaching 1 indicating a strong positive correlation, values near zero indicating no correlation, and values approaching -1 indicating an inverse relation between parameters. As it is possible to have a strong correlation between two variables simply because of biases in the data distribution and influential observations, analyses of scatter plots were used to obtain insight into the relationship between two parameters to identify the true trends. For each GPS experiment, correlation coefficients were determined for

geographic regions, environmental regions, soil type, and many other parameters. The results of these analyses are described in chapter 5 of this report.

CHAPTER 5: MODELS TO PREDICT ROUGHNESS DEVELOPMENT AT GPS SECTIONS

The average IRI was used for all analyses described in this chapter. The average IRI is the mean of the IRI of the left and the right wheel paths. When the IRI of a section is referred to in this chapter, the average IRI is implied.

5.1 GENERAL TRENDS IN IRI DEVELOPMENT

5.1.1 IRI Trends for GPS Experiments

The first step in investigating general trends in IRI was to study plots of IRI versus pavement age for each GPS experiment. The general trends in IRI development that were noted for each GPS experiment are presented in this section.

Figure 5.1.1 shows the general trends for IRI development for the GPS-1 through GPS-5 pavement types. It can be seen that each pavement type has different roughness characteristics and rate of change. For example, the GPS-1 sections (flexible pavements on granular bases) generally show a higher rate of change of IRI than the GPS-5 sections, which consist of continuously reinforced concrete pavements (CRCP). Also, the GPS-3 sections, which are jointed plain concrete pavements (JPCP), exhibit only slight increases in IRI, but have much more variation in IRI over time. Figure 5.1.2 shows the general behavior of IRI for overlaid pavements (GPS-6, GPS-7, and GPS-9). The following four general behavioral patterns were observed in figures 5.1.1 and 5.1.2 for the GPS sections: (1) the IRI remained relatively stable over time, (2) IRI values were variable between the years with no clear overall trend for the section, (3) the IRI increased with time, and (4) pavements with an IRI in excess of 2.37 m/km (150 in/mi) exhibited larger increases in IRI over time.

A linear regression analysis was performed between the time sequence IRI values and the pavement age at each GPS section to identify the sections for which a linear relationship exists between these two parameters. All GPS sections that had 3 or more years of IRI data were subjected to the analysis. In the linear regression analysis, the IRI was the dependent variable, while the pavement age was the independent variable. The following statistical test was performed on the slope (ß1) obtained from the regression to see if a positive linear relationship exists between the IRI and the pavement age:

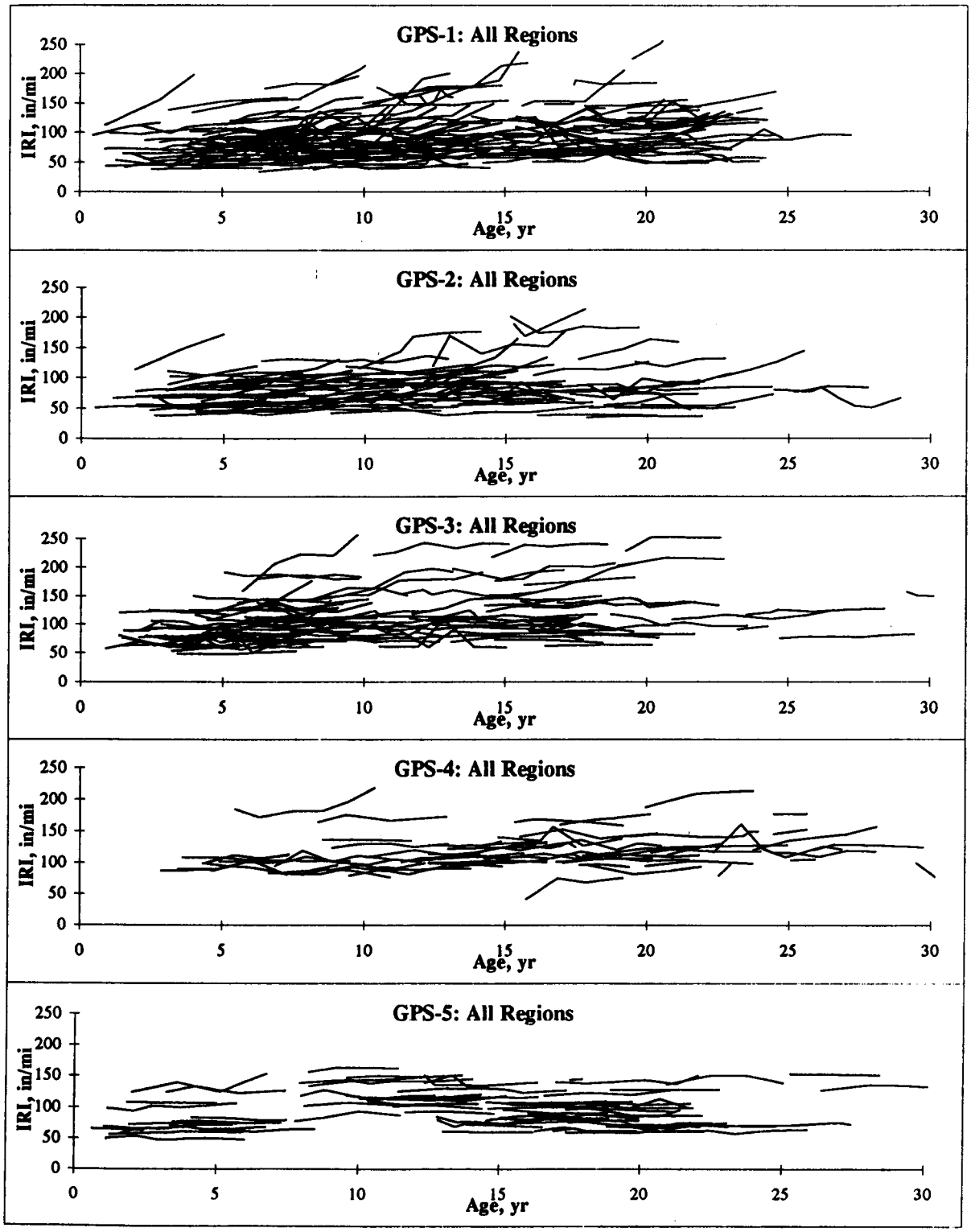

1 in/mi = 0.0158 m/km

Figure 5.1.1 Trends in IRI development for GPS-1 through GPS-5 sections (each line segment is one LTPP section)

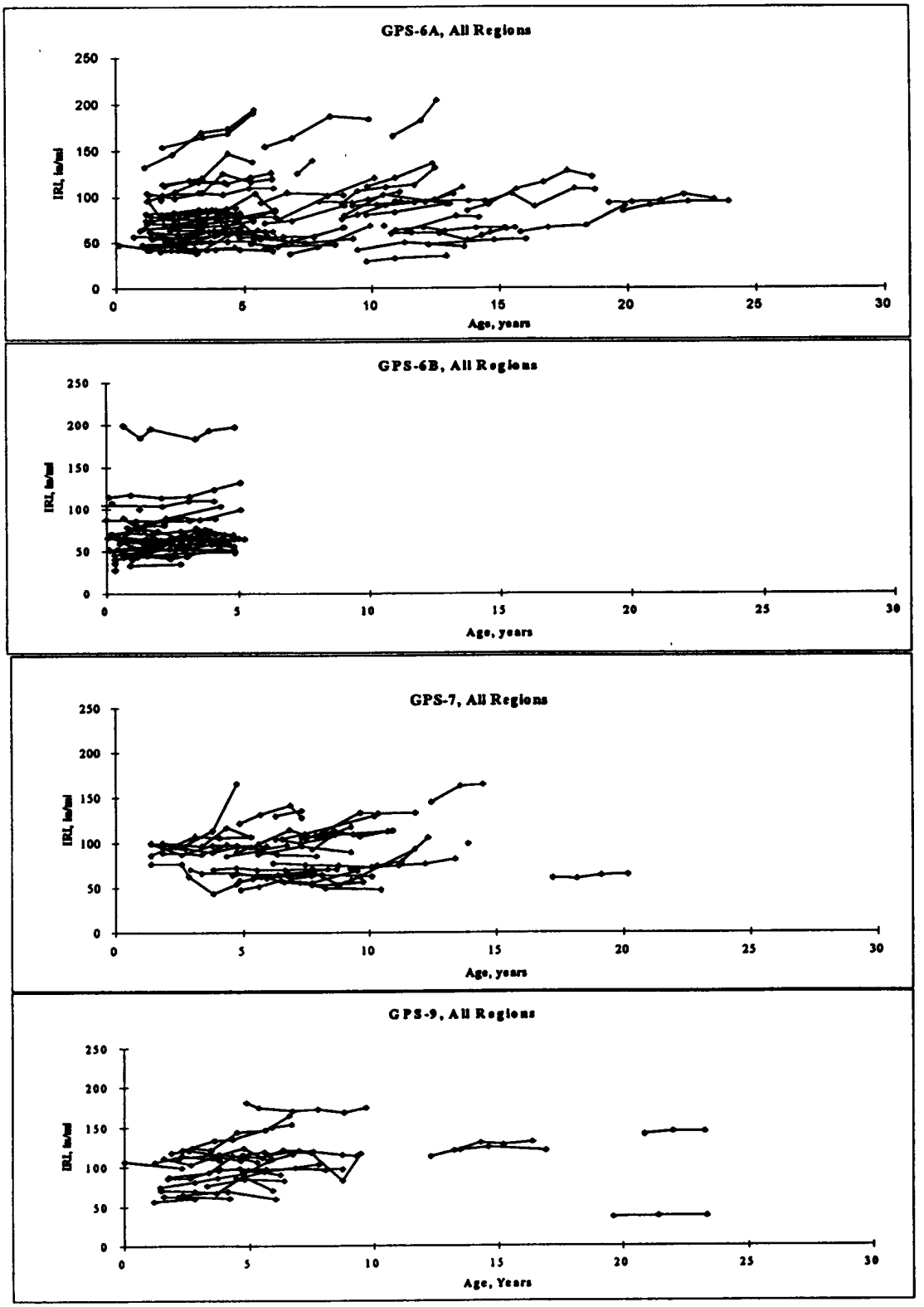

Figure 5.1.2. Trends in IRI development for overlaid pavements.

Ho: ß1 = 0

$H\alpha$: ß1> 0

Reject Ho if $t > t\alpha$ (where α was selected as 0.05).

It was noted that some sections exhibited a reduction in IRI with increase in pavement age. Another statistical test was performed at the GPS sections to determine if a negative linear relationship existed between the IRI and the pavement age. The following statistical test was performed on the slope (ß1) to examine if this condition existed:

Ho: ß1 = 0

$H\alpha$: ß1 < 0

Reject Ho if $t < -t\alpha$ (where α was selected as 0.05).

The percentage of sections for which a positive or negative linear relationship existed between the IRI and the pavement age classified according to the GPS experiment are presented in table 5.1.1. The following information obtained from the linear regression analysis is presented for each GPS section in appendix B: the intercept, the slope, the coefficient of determination (R^2), and if the t-test determined a linear relationship existed between IRI and pavement age. The time-sequence IRI data that are available at each site are also presented in appendix B. For nonoverlaid pavements, a higher percentage of AC pavements showed a statistically significant relationship between IRI and pavement age compared with the PCC pavements. A higher percentage of GPS-6 sections showed a statistically significant relationship between IRI and pavement age when compared with GPS-7 sections.

The frequency distribution of GPS sections according to the slope obtained from the linear regression analysis is presented in table 5.1.2. The slope from regression represents the rate of increase of IRI at the section. The percentage distribution of GPS sections according to the range of slopes is presented in table 5.1.3. It should be noted that the R^2 associated with these slopes ranged from zero to one. Therefore, the slopes that correspond to low R^2 values may not represent the actual rate of increase of IRI at the section. Table 5.1.4 presents the percentage distribution of GPS sections according to the range of R^2 values obtained from the linear regression. As seen from this table, for each GPS experiment a wide distribution of R^2 existed.

Table 5.1.1. Percentage of GPS sections showing statistically significant linear relationship between IRI and pavement age.

GPS Experiment	Number of Sites With 3 or More Yr of Profile Data	Percentage of Sections	
		Positive Linear Relationship	Negative Linear Relationship
GPS-1	188	38	3
GPS-2	124	30	0
GPS-3	120	18	2
GPS-4	56	17	0
GPS-5	73	4	4
GPS-6A	57	42	0
GPS-6B	27	22	0
GPS-7A	30	13	6
GPS-7B	16	18	12
GPS-9	24	16	4

Table 5.1.2. Distribution of sections according to rate of increase of IRI obtained from linear regression.

Rate of Change of IRI (in/mi/year)	Number of Sections									
	GPS Experiment									
	1	2	3	4	5	6A	6B	7A	7B	9
<0	32	24	50	17	34	7	11	7	8	7
0 - 2	58	43	36	24	32	19	8	11	5	9
2 - 4	40	23	18	8	5	12	4	3	1	1
4 - 6	14	15	6	3	1	5	2	4	1	2
6 - 8	23	6	3	3	0	5	2	2	1	3
8 - 10	8	4	2	1	0	5	0	1	0	1
>10	13	8	5	0	1	4	0	2	0	1
Total	188	123	120	56	73	57	27	30	16	24

Note: 1 in/mi = 0.0158 m/km.

Table 5.1.3. Percentage distribution of sections according to rate of change of IRI obtained from linear regression.

Rate of Change of IRI (in/mi/yr)	Percentage of Sections (%) GPS Experiment									
	1	2	3	4	5	6A	6B	7A	7B	9
<0	17	20	42	30	47	12	41	23	50	29
0 - 2	31	35	30	43	44	33	30	37	31	38
2 - 4	21	19	15	14	7	21	15	10	6	4
4 - 6	7	12	5	5	1	9	7	13	6	8
6 - 8	12	5	3	5	0	9	7	7	6	13
8 - 10	4	3	2	2	0	9	0	3	0	4
>10	7	7	4	0	1	7	0	7	0	4
Total	100	100	100	100	100	100	100	100	100	100

Note:1 in/mi = 0.0158 m/km.

Table 5.1.4. Percentage distribution of sections classified according to coefficient of determination (R^2) obtained from linear regression.

Range of Coefficient of Determination	Percentage of Sections (%) GPS Experiment									
	1	2	3	4	5	6A	6B	7A	7B	9
<0	3	2	8	7	5	2	4	3	0	4
0 - 0.25	20	20	32	39	36	18	26	27	25	33
0.25 - 0.50	16	16	26	16	30	18	26	13	13	21
0.50 - 0.75	20	19	19	14	19	14	11	30	19	17
0.75 - 1.00	41	44	16	23	10	49	33	27	44	25
TOTAL	100	100	100	100	100	100	100	100	100	100

Table 5.1.3 shows that, for each GPS experiment, a large number of sections had either a negative rate for the increase of IRI or a low rate that was between zero and 0.03 m/km/yr (2 in/mi/yr). The available IRI data indicated that the GPS sections have been profiled an average of four times. A rate of increase of IRI of 0.03 m/km/yr (2 in/mi/yr) corresponds to a change of 0.13 m/km (8 in/mi). This change represents a small value when considering the changes in IRI that can occur between the years due to environmental effects and variability in the profiled path. For nonoverlaid PCC pavements (GPS-3 to GPS-5), the percentage of sections that had a rate of increase of IRI less than 0.03 m/km/yr (2 in/mile/yr) or a negative rate were: GPS-3: 72 percent, GPS-4: 73 percent, and GPS-5: 91 percent. For nonoverlaid AC pavements (GPS-1 and GPS-2 sections), the percentage of sections exhibiting a similar behavior were 48 percent and 55 percent, respectively. GPS-6B and GPS-7B are overlaid pavements, and virtually all of these are less than

5 years old; 71 percent of GPS-6B and 81 percent of GPS-7B sections exhibited a growth rate that was negative or less than 0.03 m/km (2 in/mi/yr).

5.1.2 Methods Used For Modeling

In this study, for GPS experiments 1 through 4, considerable effort was placed on developing models that back predict the initial roughness on the basis of time-sequence IRI data and also predict the actual IRI value at any point in time. In the modeling effort, the sections that had relatively stable IRI values as well as sections that show an increase in IRI were considered. A growth rate parameter was also modeled such that the key parameters affecting both the initial IRI and growth of the IRI (including zero growth) could be determined. For the GPS-5 sections that showed virtually no increase in IRI, multiple linear regression was used to develop a model. For the overlaid sections, a rate of increase of IRI was determined by linear regression, and attempts were made to relate this parameter to factors that influence the increase in IRI. These concepts are discussed in greater detail in the following sections. All GPS sections that had a complete data set of the parameters that were evaluated for each model were included in the model development.

GPS-1 Through GPS-4 Experiments

The first step in model building consisted of observing the plots of IRI development over time. The observed shape of the development curves gives an indication of how the growth rate of the IRI changes over time. The IRI trends observed in the data were generally similar to exponential growth for GPS-1 and GPS-2 sections, while the GPS-3 and GPS-4 sections generally showed a logistic growth pattern.

Figure 5.1.3 shows examples of logistic and exponential growth rates and the resulting growth curves. In this figure, case 2 shows a constant growth rate while case 4 shows a growth rate that increases with time. For modeling of GPS-1, GPS-2, and GPS-4 sections, the growth rates that were used corresponded to case 4. The growth rate was characterized as follows:

$$r(t) = r_0(t^A/_B)$$

where:

$r(t)$ = growth rate value at any time t,

r_0 = growth rate constant,

A = constant between 0 and 2,

B = constant, and

t = time.

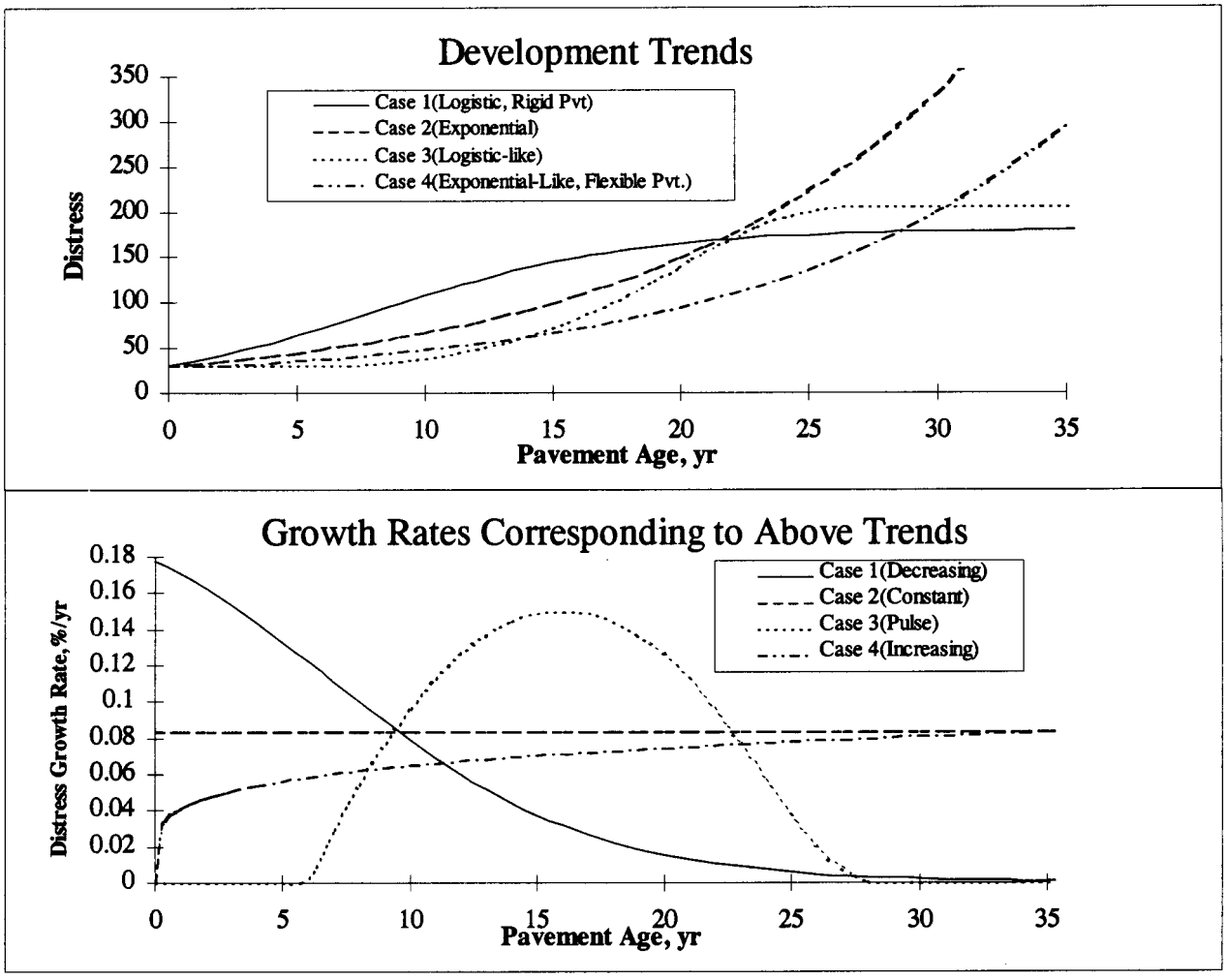

1 in/mi = 0.0158 m/km

Figure 5.1.3. Plots showing how different growth rate functions affect the development of an arbitrary distress type.

Logistic-like growth is characterized by a decreasing or single-pulse growth rate as a function of time that results in a somewhat stable value after some time period as the growth rate approaches zero. GPS-3 pavements were modeled using a logistic growth approach.

In reality, the growth rates in pavements are likely to oscillate seasonally, and are perhaps discontinuous in time, changing as the pavement condition changes and having a pulse-like increase during the passing of each load. A logistic trend appears similar to an exponential trend in early stages, but is characterized by a change in sign of the curvature in the resulting trend at later stages as the growth rate approaches zero. It is believed that all pavements would eventually exhibit logistic growth of IRI if measured for very long periods of time (i.e., IRI would not go to infinity but would eventually stabilize at some very high value) provided that the pavement system was not eroded away into an entirely impassable state.

One of the most challenging problems in modeling was the fact that the initial IRI values for the GPS sections were unknown. The modeling approach used in this study is shown graphically in figure 5.1.4. The initial IRI is typically back predicted as a nonlinear function of the structural properties of the pavement and subgrade properties. The growth rate is modeled as a nonlinear function of time, structural properties of the pavement, subgrade properties, climate parameters, and traffic loading. The results of the analyses indicate that initial IRI can generally be back predicted from the data within the LTPP IMS, yet most error in the models appear to be associated with back predicting initial IRI. This is likely associated with differences in construction practices, density specifications, and local subgrade variability and density.

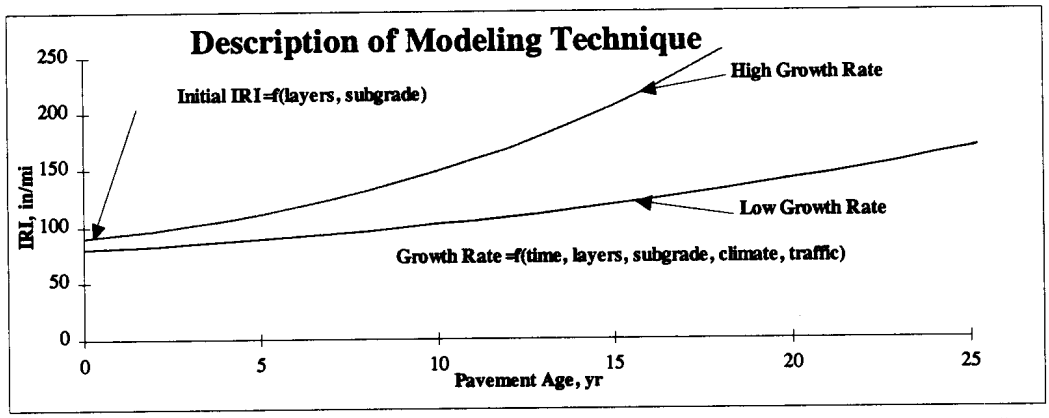

1 in/mi = 0.0158 m/km

Figure 5.1.4. General description of the modeling technique used for IRI prediction.

Correlations were determined for LTPP geographic regions, environmental regions, soil type, and many other parameters. The strongest correlations were typically observed when the data were sorted by environmental regions (figure 5.1.5) and subsorted by soil type for the wet regions. With the exception of the first model presented, only the 10 parameters that had the highest correlation to IRI for each data set are shown in this report. The first model presented

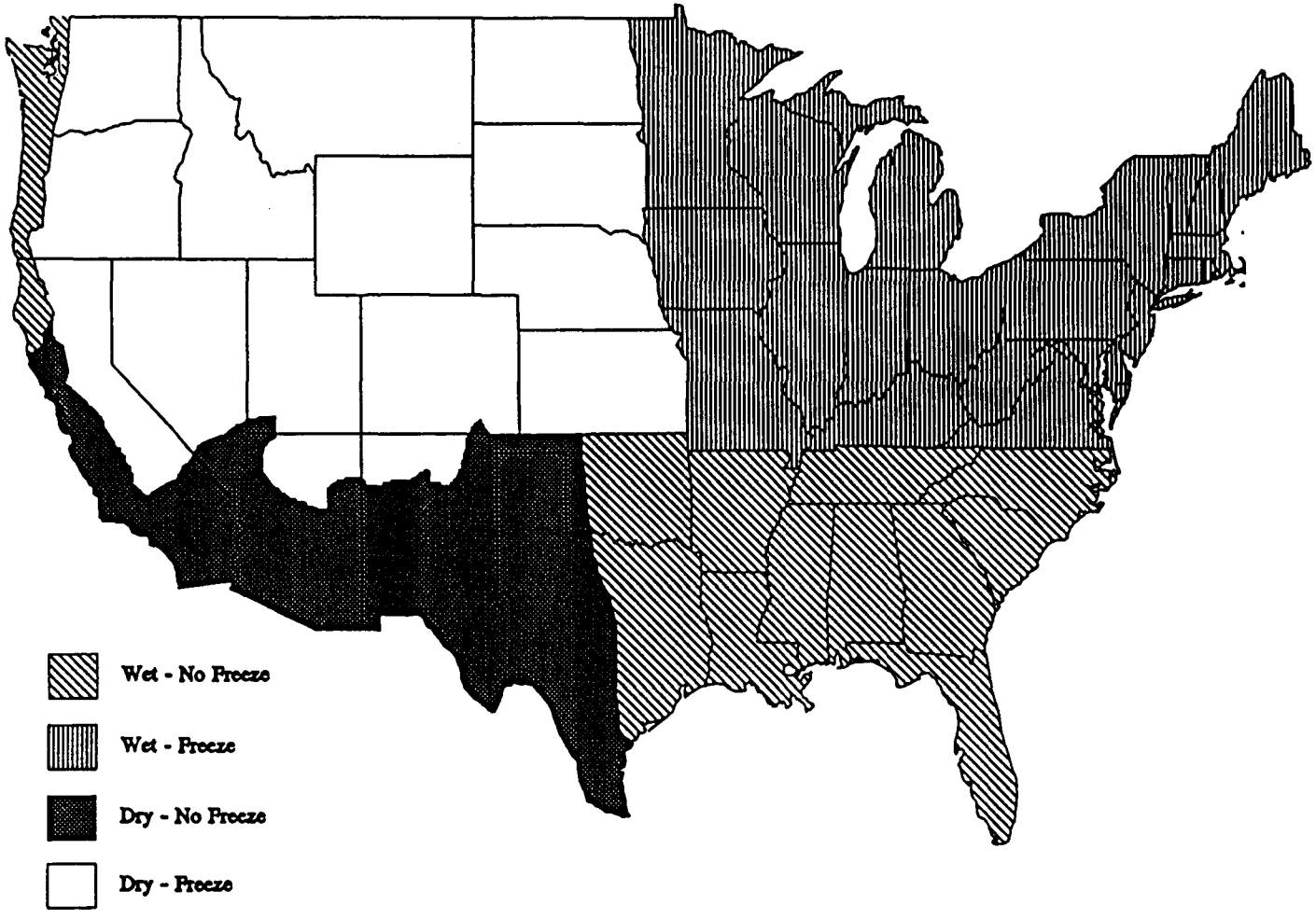

Figure 5.1.5. General distribution of the four climate classifications within the continental United States.

(GPS-1 dry freeze) shows an example of a correlation matrix and scatter plots of variables used in the modeling process.

After reviewing the correlations and scatter plots between the IRI and the parameters considered in the analysis, a model form for each data set was established using the parameters that showed the strongest correlation to IRI. For nonlinear modeling, a nonlinear optimization routine available in a commercial solver was used to vary the algebraic coefficients in the models for each data set to minimize the errors between measured and predicted IRI.

The modeling utilized a nonlinear optimization methodology developed by Leon Lasdon of the University of Texas at Austin, and Allen Waren of Cleveland State University.[15] This methodology is incorporated into what is referred to as the Generalized Reduced Gradient Algorithm (GRG2), which is used in the commercial solver. The solver varies the model coefficients slightly and monitors the partial derivatives of the dependent variables and the constraint variables with respect to the causative variables. The coefficients are varied until the partial derivatives are near zero, indicating a local minimum or optimal solution while maintaining constraint or boundary conditions.

During the modeling process the following constraints were used:

1. Range of Predicted Initial IRI = Estimated Range of Initial IRI: This constraint was used to hold the predicted initial IRI values within a reasonable range.
2. IRI Prediction Standard Deviation = IRI Measurement Standard Deviation: This constraint was used so that the standard deviation of the predicted IRI would fall within the standard deviation of IRI that was observed in the data set.
3. Range of Predicted IRI = Range of Estimated IRI: This constraint was used to so that the predicted IRI values would fall within a reasonable range of IRI values.
4. IRI Growth Rate ≥ 0: This constraint was used so that the IRI would not decrease over time.
5. Traffic Effects on IRI Growth Rate ≥ 0: Traffic had to be constrained as shown because of the tendency for thick, high traffic routes to have lower initial roughness and to develop roughness more slowly over time than thin, low traffic sections. In flexible pavement modeling, the ratio of traffic raised to some power divided by structural number to some power was used extensively in the growth rate constant estimate that generally produced good results and tended to result in positive trends for traffic effects.

The nonlinear modeling requires an initial estimate based on judgment for the coefficients. The optimization algorithm systematically varies the coefficients, minimizing the sum of errors between measured and predicted IRI. The results are sensitive to the initial estimate used for the coefficients.

In the optimization process, different strategies were used in the computation of errors that were used in the minimization process. The following methods were used to compute errors.

1. Sum of the absolute values of the average error per site: For each site, at each time-sequence IRI data point, the difference between the predicted and measured IRI values was computed. The absolute value of the differences were then averaged for each site. Then the average values at each site were summed.
2. Sum of the squared values of the average error per site: For each site, at each time-sequence IRI data point, the difference between the predicted and measured IRI values was computed. The squared values of the differences were summed and then averaged for each site. Then the average values at each site were summed.
3. Sum of the absolute values of errors: For each time-sequence IRI data point, the error was computed as the difference between the measured and the predicted IRI value. The absolute value of the error at each data point was then summed (for all time-sequence IRI data points for all sections).
4. Sum of squares of errors: For each time-sequence IRI value, the error was computed as the difference between the measured and the predicted IRI value. The errors were then squared and then summed (for all time-sequence IRI data points for all sections).

The initial iterations of the optimization were generally set up to minimize the sum of squares of errors. Some or all of the strategies that were described were then used in iterations until convergence. After a given solution converged, based on the initial estimate of the coefficients, it was reviewed to see if it gave realistic results and conformed with common sense. If not, the coefficients would be varied and the optimization run again. Using the average error per GPS site has the effect of weighting each site equally whether there was one IRI value or six IRI time-sequence values for the site. Using the error associated with each data point would weigh each measurement equally, weighting sites with more data more heavily in the resulting model.

When each model is described, the error for each model is defined as the average of the average errors per site for the sites used in the model. The average error for a site was computed as presented below:

$$\text{Average error per site} = E_j = \frac{1}{n}\sum_{i=1}^{n} \text{Abs (Predicted IRI}_i \text{ - Measured IRI}_i)$$

where: n = number of time-sequence IRI measurements at a site.

$$\text{Average error for model} = \frac{1}{m}\sum_{j=1}^{m} E_j$$

where: m = number of GPS sites used in model.

For each model developed for GPS-1 through GPS-4 experiments, the standard deviation of the errors are also presented. The standard deviation of the error for a model provides an indication on the dispersion of the errors.

It should be noted that the models are based on a data set that on average had four time-sequence IRI values that were obtained over a 4-year period. The models reflect the behavior pattern observed for the analyzed data set, and could reflect biases that were present in the data set. For the GPS sections used in the analysis, the applicability of these models can be evaluated as more time-sequence data become available. These models can be used to gain an insight into factors that affect the IRI development. The models are sensitive to input parameters, and care should be taken to use input parameters that are neither unrealistic nor beyond the range of data from which the model was developed.

GPS-5 Experiment

The modeling of IRI for the GPS-5 pavements was performed by using a step-wise multiple regression analysis that related the IRI of the pavement to a set of independent variables that could possibly affect the growth of IRI.

Overlaid Pavements (GPS-6,- 7,- 9)

For the overlaid pavements, a linear regression analysis was performed between the time-sequence IRI data and the pavement age to obtain the rate of increase of IRI, which is the slope of the regression equation. Correlation coefficients between the slope and parameters that could

affect the increase in IRI were computed to identify parameters that have strong correlations. Multiple regression analysis was then performed between the slope and these parameters to develop a relationship to predict the slope.

5.1.3 Definition of Variables Used in Modeling IRI

In sections 5.2 through 5.5, models for predicting IRI for GPS experiments 1 through 4 are presented. The resulting models are based on fitting exponential relations to parameters within the models. Some of the resulting exponents are large, and the models are sensitive to some parameters that are at extremes or are out of the range of data used to establish the models. For example, if the percentage passing the 75-μm (No. 200) sieve for subgrade (P200) value of 90 is placed into a model that was developed for subgrade having a P200 content less than 50, unrealistic predictions may result. Each of the models presented in sections 5.2 through 5.5 is followed by a figure showing the sensitivity of the model to various parameters. This figure can be used as a check when programming the model algorithm. These figures also show the range of each parameter encountered in the database. Table 5.1.5 provides the definitions of the parameters used in model building and used in the discussions presented in the following sections.

Climatic factors were found to have a strong influence on roughness development. Separate models were often developed for different climates for a given pavement type. Figure 5.1.5 shows the area included in each of the LTPP climatic zones. For the modeling conducted in this study, the boundary between wet and dry regions was taken as 508 mm (20 in) of annual precipitation, and the boundary between freezing and nonfreezing zones was taken as an annual freeze index of 89°C days (160°F days).

The following discussions present the terms used to describe PCC strength and elastic modulus. Concrete data were compiled for all GPS-3, GPS-4, and GPS-5 sections such that the average PCC properties could be determined. The average PCC properties for the entire GPS concrete pavement data (GPS-3 through GPS-5) are as follows:

1. Average split tensile strength = 4.44 MPa (643 psi)
2. Average elastic modulus = 31573 MPa (4570 ksi)
3. Average water to cement ratio = 0.48
4. Average compressive strength = 52.4 MPa (7584 psi)
5. Average unit weight = 87 kg/m^3 (147 pcf)

Table 5.1.5 Definition of Modeling Parameters

Parameter	Definition
%ACinSN	Percent of SN contributed by AC thickness
%Sand	P#4-P200, %
%Steel	Percent longitudinal steel by area, %
ACThick	AC thickness from core data, in
Age	Age of pavement, yr
air	PCC air content, %
AnnPrecip	Annual precipitation, in
BaseThick	Base thickness, in
c	Weight of coarse aggregate in PCC, lb/yd^3
c/f	Weight ratio of coarse to fine aggregate in PCC mix
cement	Weight of cement in mix, lb/yd3
Cum Traf	Estimated cumulative traffic, KESAL
Comp	PCC compressive strength, psi
Days32-	Number of days below 32°F per yr
Days90+	Number of days above 90°F per yr
Days.5"+	Number of days with >0.5" precipitation per yr
DaysWet/yr	Number of days with precipitation per yr
EMOD	PCC elastic modulus, psi
f	Weight of fine aggregate in PCC, lb/yd^3
FrzThwCyc	Number of freeze-thaw cycles per yr
FZI	Freeze Index, °F days per yr
Initial KESAL/yr	Estimated initial traffic level
JointSpace	Joint spacing, ft
KESAL/yr	Average KESAL per yr from historical data
LI	Subgrade liquidity index
LL	Subgrade liquid limit, %
P200	Subgrade percent passing No. 200 sieve
P#4	Subgrade percent passing No. 4 sieve
PCCth	PCC thickness, in
PI	Subgrade plasticity index, w%
PL	Subgrade plastic limit, w%
Po	Subgrade overburden pressure, psf
Poissons Ratio	PCC Poissons ratio
SN	Estimated Structural Number
SplitTensile	PCC split tensile strength, psi
t	Age of pavement at time of profile measurement
unitwt	PCC unit weight. lb/ft^3
w%	Subgrade moisture content, %
w/c	Water to cement ratio for PCC mix
water	Weight of water in PCC, lb/yd3

1 in = 25.4 mm, 1 psf = 0.048 kPa, 1 psi = 6.89 kPa, °C = (°F-32)/1.8

The split tensile strength and the elastic modulus of PCC can be related to the compressive strength (f_c') of PCC by the following American Concrete Institute (ACI) relations:

$$SplitTensile = 7.4\sqrt{f_c'}$$

$$ElasticModulus = 57000\sqrt{f_c'}$$

where:

SplitTensile	=	split tensile strength of PCC in psi,
ElasticModulus	=	elastic modulus of PCC in psi,
f_c'	=	compressive strength of PCC in psi.

The average values presented previously show good agreement with these two formulas. On the basis of the above two formulas, the ratio between the split tensile strength and the elastic modulus can be computed as shown below, where 10,000 is a scaling factor:

$$\frac{SplitTensile(10{,}000)}{ElasticModulus} = \frac{7.4(10{,}000)}{57{,}000} = 1.3$$

In the following discussions, a PCC that is referred to as higher strength-lower modulus is a PCC that has a ratio greater than 1.3 as computed from the above formula. For example, a PCC mixture that has higher split tensile strength with a low modulus is described qualitatively as a higher strength lower modulus mixture. The terms higher and lower are used in a relative sense. A mix with a low ratio is a stiff concrete that fails or cracks at low stress levels (more brittle behavior). A mix with a high ratio can experience more stress before failure or cracking (less brittle behavior). The above ratio at the various sites varies from 0.9 (E = 40590 MPa (5875 ksi), split tensile = 3.7 MPa (538 psi)) to 3.0 (E = 20900 MPa (3025 ksi), split tensile = 6.32 MPa (915 psi)), with an average of 1.43.

5.2 GPS-1: FLEXIBLE PAVEMENTS ON GRANULAR BASES

The time-sequence IRI values for each GPS-1 site were compiled and plotted against pavement age. Figure 5.2.1 shows the development of IRI for the GPS-1 sections classified according to LTPP regions. Trends in IRI observed in the different environmental regions and for

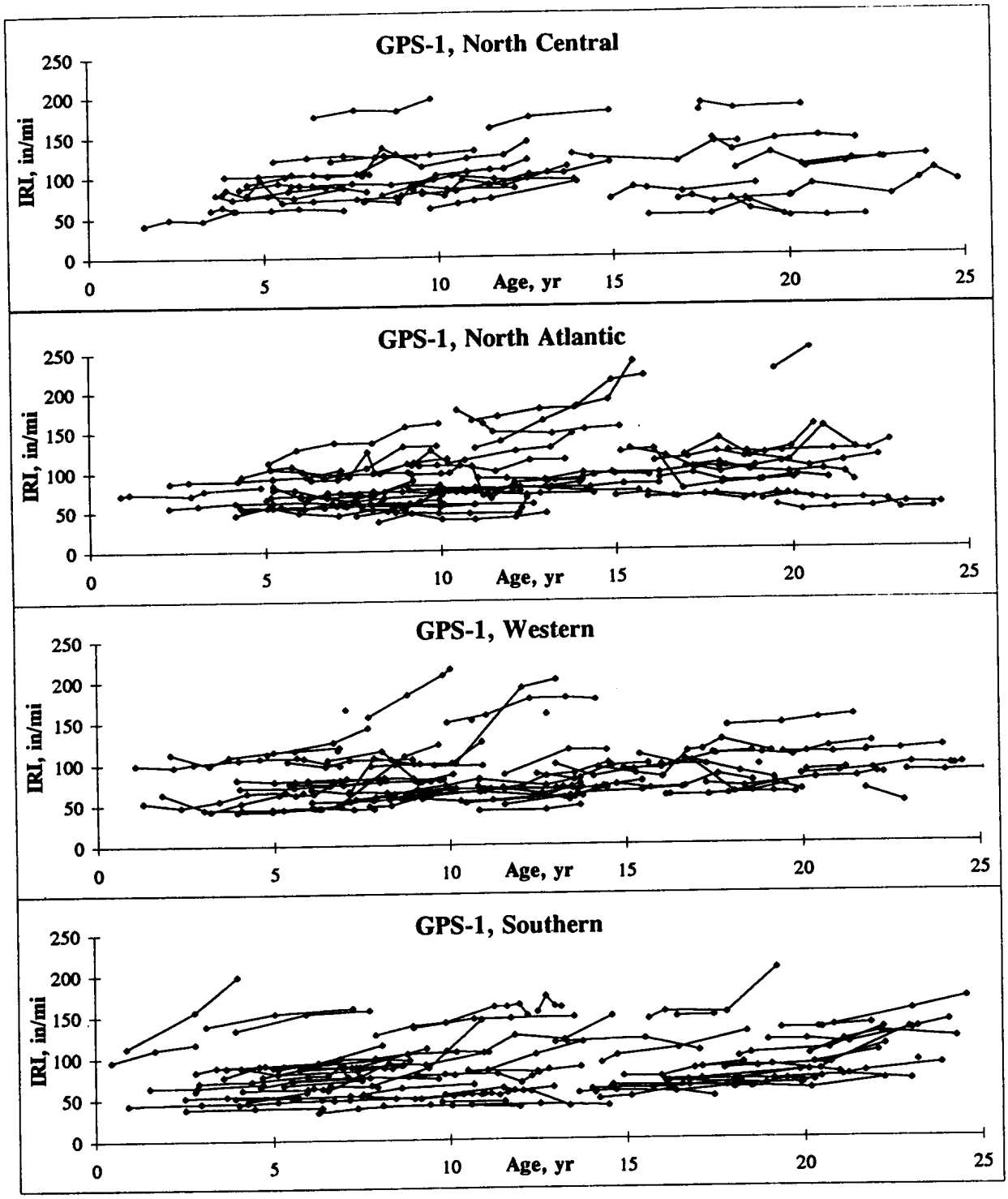

1 in/mi = 0.0158 m/km

Figure 5.2.1 IRI development over time for GPS-1 sections classified according to LTPP regions

different soil types are discussed later in the sections of the report that describe the models. Many of the GPS-1 sections show little change in IRI over time. The GPS-1 sections that do show an increase in IRI generally appear to have exponential growth of the IRI. A model based on exponential growth of the IRI can capture the general curve shapes observed. The model form that was used for flexible pavements is described below and shown graphically in figure 5.2.2:

$$IRI(t) = IRI_0 e^{r_0 t^A / B}$$

where:

IRI_0 = estimated initial IRI (after some initial traffic loading),
= f(the pavement structure and subgrade properties),
r_0 = growth rate constant,
= f(climate, traffic, subgrade, layer properties of the pavement),
t = time in years,
e = the exponential function, and
A and B = modeling constants.

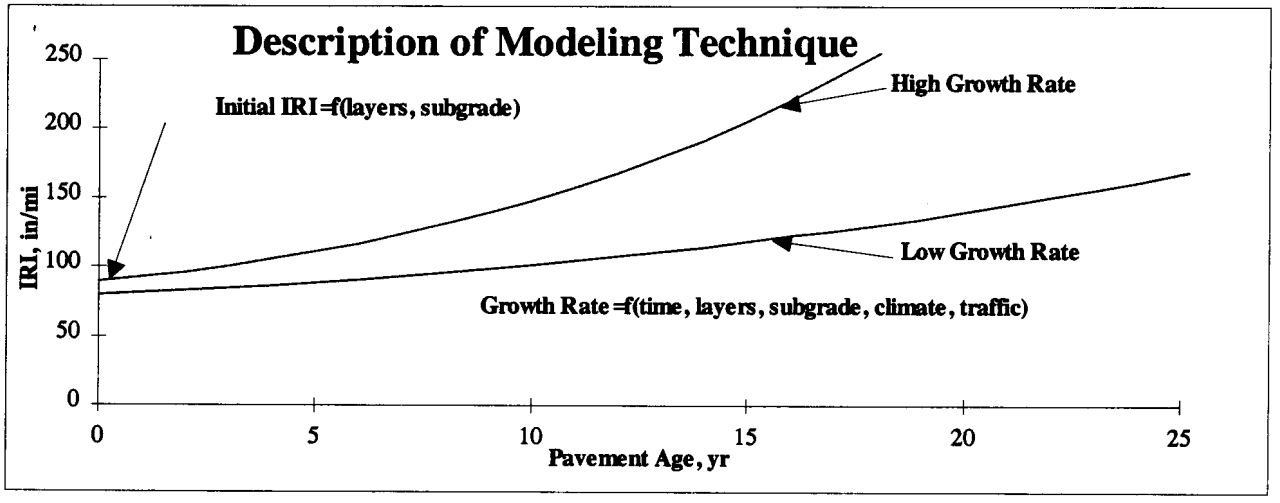

1 in/mi = 0.0158 m/km

Figure 5.2.2. Modeling technique used for GPS-1 sections.

In this model, IRI_0 represents the IRI value of the pavement after it has been opened to traffic and has been subjected to some initial traffic loading. In the initial phases of model building, the GPS-1 data were sorted in many ways, and correlation coefficients and scatter plots were generated and reviewed . The strongest correlations were observed when the data sets were divided into environmental regions and then again by the subgrade percent by weight passing the

75-μm (No. 200) sieve (P200) for the wet regions. The wet-freeze and wet-no freeze environments were split into three soil subgroups: (1) P200 > 50 percent, (2) P200 between 20 and 50 percent, and (3) P200 < 20 percent. These divisions appeared to divide the data on the basis of trends observed and resulted in relatively equal sizes of the data sets. Separate models were then developed for each data set. Scatter plots and statistical correlation matrices were used extensively during the model-building process. However, they are only presented for the first model discussed so that the methodology used during model building is understood. Table 5.2.1 shows the 10 parameters that had the highest Pearson correlation coefficients to IRI for the data sets used in GPS-1 model building.

In the following sections, each model is described along with a discussion on which types of pavements were showing high and low IRI values within each data set. The best and worst performers in each data set were roughly evaluated using the AASHTO pavement design equation (without considering serviceability loss due to climatic factors). This analysis provides an indication of what level of performance would be expected at the various sites that can be compared with the observed IRI values. By comparing the AASHTO-based anticipated life with the actual IRI behavior, sections that were performing well or sections that were failing prematurely could be better identified. In this evaluation, the cumulative traffic volume estimates at each section and an estimate of the subgrade modulus at each section (on the basis of laboratory test data for the subgrade) were used to obtain the structural number (SN) that is required for that section. This SN was then compared with the SN estimated for the test section from the pavement layer thickness. If any conclusions could be drawn from this analysis, they are indicated in the discussions.

5.2.1 Dry Freeze Environment

The dry freeze environment is defined for this study as a region that has less than 508 mm (20 in) of annual precipitation and a freezing index greater than 89 °C days (160 °F days). The pavements in this region are very sensitive to the amount of precipitation, freezing effects, and subgrade parameters. Higher fines content (P200) in the subgrade, coupled with higher precipitation and freezing, result in higher IRI. The effect of traffic could only be detected for very small SN values.

Figure 5.2.3 shows the model form developed for IRI prediction for the dry freeze region. This model was based on 124 IRI measurements from 26 sections and had an average

Table 5.2.1. Ten parameters that had highest correlation with IRI for GPS-1.

Wet-Freeze			Dry-Freeze	Dry-No Freeze
P200<20%	**20%<P200<50%**	**P200>50%**	**All Soils**	**All Soils**
P200(+.30)	%Sand(-.50)	PI(+.44)	AnnPrecip(+.48)	SN(-.31)
w%(+.28)	Po(-.45)	DaysWet/yr(-.42)	Age(+.47)	ACThick(-.27)
Age(+.24)	FrzThwCyc(+.42)	LL(+.38)	DaysWet/yr(+.44)	Age(+.19)
Days.5"+(+.21)	SN(-.39)	FZI(+.31)	Days.5"+(+.35)	Days90+(+.14)
FrzThwCyc(-.19)	AnnPrecip(-.35)	w%(+.29)	P200(+.33)	KESAL/yr(-.14)
Po(+.19)	P200(+.34)	ACThick(+.26)	Days32-(+.31)	Cum Traf(-.13)
DaysWet/yr(-.18)	Days.5"+(-.33)	Age(+.25)	FZI(+.28)	FZI(+.11)
FZI(+.16)	KESAL/yr(-.31)	PL(+.25)	w%(+.26)	Po(-.09)
AnnPrecip(+.14)	Truck Factor(-.23)	P200(+.23)	Cum Traf(+.24)	Days32-(+.08)
SN(+.11)	Age(+.23)	AnnPrecip(-.22)	%Sand(-.24)	P#4(+.08)

Wet-No Freeze		
P200<20%	**20%<P200<50%**	**P200>50%**
Days90+(+.59)	DaysWet/yr(-.40)	AnnPrecip(-.53)
ACThick(-.59)	KESAL/yr(-.30)	Days.5"+(-.52)
SN(-.34)	Po(-.27)	Days90+(+.37)
w%(-.51)	SN(-.25)	Age(+.35)
AnnPrecip(-.46)	w%(+.24)	Po(+.32)
Days32-(-.39)	Days90+(+.22)	PI(+.31)
%Sand(+.22)	FZI(-.21)	P200(+.31)
Age(+.21)	ACThick(-.16)	P#4(+.28)
P200(-.18)	P200(-.14)	LL(+.27)
KESAL/yr(+.15)	AnnPrecip(-.13)	FrzThwCyc(-.24)

error per section of 0.19 m/km (12.1 in/mi); the standard deviation of errors at the sections was 0.10 m/km (6.6 in/mi). Also included in the figure is a plot of measured versus predicted IRI and a plot of IRI versus pavement age for the measured and predicted IRI values from the data set. The measured and predicted values for a section can be identified by drawing a vertical line from the age axis through a white square, and then connecting it to a black triangle on the graph.

Figures 5.2.4 and 5.2.5 show the correlation matrices and scatter plots, respectively, for some of the key parameters related to GPS-1 dry freeze IRI development. There are no strong correlations with any of the variables, and several variables are correlated with each other. Many multi-variable clusters were calculated and reviewed in an attempt to find strong prediction variables to use in models. For example, one of the clusters used for freezing environments was:

P200*w%*FZI/ (10000*Po)

$$IRI(t) = IRI_0 e^{r_0 \frac{t^S}{T}}$$

$$IRI_0 = A(P200)^B + C(Po)^D + E(\%Sand)^F + G(\%ACinSN/100)^H$$

$$r_0 = \frac{I(KESAL/yr)^J}{K(SN)^L} + O(AnnPrecip)^P + Q(\frac{FZI * P200 * w\%}{Po})^R$$

A= 250.1471	F= 5.5503	K= 300	R= 1.5855
B= -0.0287	G= 203.8493	L= 4	S= 1.0952
C= -517.4179	H= 0.05983	O= 0.0006	T= 0.1879
D= -0.06407	I= 0.005	P= 0.6708	
E= -2.847E-10	J= 1.7	Q= 6.84E-09	

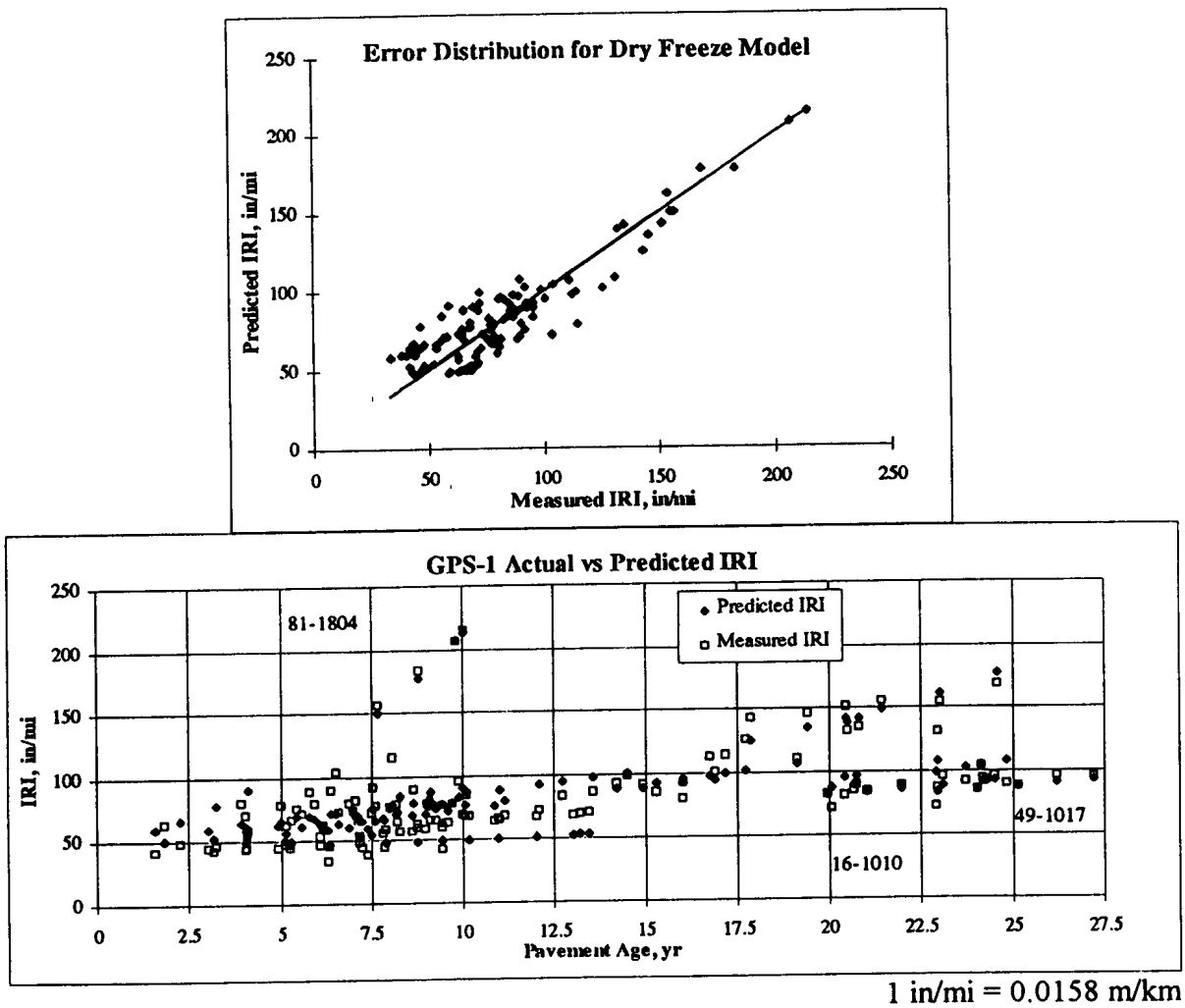

1 in/mi = 0.0158 m/km

Figure 5.2.3. GPS-1 dry freeze IRI model.

Dry-Freeze (FZI > 160, Ann Precip < 20)

	IRI	Age	P#4	P200	w%	SN	Po	ACThick	AnnPrecip	Days32-	Days90+	DaysWet/yr	Days.5"+	FrzThwCyc	FZI	KESAL/yr
IRI	1.000															
Age	0.474	1.000														
P#4	0.163	0.073	1.000													
P200	0.325	-0.098	0.497	1.000												
w%	0.261	-0.091	0.399	0.793	1.000											
SN	0.089	0.194	0.396	0.215	0.199	1.000										
Po	0.163	-0.234	0.315	0.608	0.596	0.368	1.000									
ACThick	-0.021	0.276	0.205	-0.120	-0.129	0.820	-0.155	1.000								
AnnPrecip	0.477	0.261	-0.052	0.124	0.250	-0.075	0.183	-0.286	1.000							
Days32-	0.308	0.130	0.126	-0.111	-0.052	0.075	0.048	0.010	0.058	1.000						
Days90+	-0.205	-0.060	0.140	0.263	0.139	-0.112	-0.110	-0.022	-0.275	-0.696	1.000					
DaysWet/yr	0.442	0.277	-0.121	-0.101	-0.078	0.188	0.245	-0.007	0.618	0.537	-0.776	1.000				
Days.5"+	0.355	0.161	0.119	0.230	0.359	-0.169	0.128	-0.354	0.901	-0.140	0.020	0.276	1.000			
FrzThwCyc	0.018	0.063	0.052	0.018	0.233	0.247	0.067	0.253	-0.380	0.372	-0.034	-0.183	-0.453	1.000		
FZI	0.283	0.077	0.163	-0.090	-0.152	-0.114	0.034	-0.209	0.299	0.785	-0.668	0.619	0.176	-0.266	1.000	
KESAL/yr	-0.088	-0.086	-0.222	-0.187	-0.210	0.105	-0.022	0.207	0.150	-0.104	-0.146	0.259	0.041	-0.119	-0.066	1

Dry-Freeze (FZI > 160, Ann Precip < 20)

	IRI	initKESAL	Truck F	Cum T	SN^3/(KESAL/yr	%ACinSN	Days90+*%ACinSN	FZI*p200*w%/Po	Annprecip*FrzThwCyc/Po	p200/Po	%sand	Days32-*FrzThwCyc	(KESAL/yr)^.1	(KESAL/yr)^.5
IRI	1.000													
initial KESAL/yr	-0.149	1.000												
Truck Factor	0.056	0.368	1.000											
Cum Traf	0.238	0.369	0.197	1.000										
SN^3/(KESAL/yr)	-0.161	-0.361	-0.442	-0.235	1.000									
%ACinSN	-0.145	0.128	0.085	0.440	0.117	1.000								
(Days90+)*%ACinSN	-0.184	-0.042	-0.146	0.054	0.060	0.461	1.000							
FZI*p200*w%/Po	0.364	-0.333	-0.171	-0.226	0.673	-0.239	-0.203	1.000						
Annprecip*FrzThwCyc/Po	0.271	0.185	0.209	0.167	0.053	0.205	-0.022	-0.042	1.000					
p200/Po	0.316	-0.164	-0.153	-0.018	0.342	-0.188	0.211	0.622	-0.004	1.000				
%sand	-0.242	-0.048	0.264	0.045	-0.109	0.390	0.039	-0.384	0.082	-0.624	1.000			
Days32-*FrzThwCyc	0.180	-0.100	0.265	-0.036	0.025	0.131	-0.356	0.173	0.200	-0.102	0.138	1.000		
(KESAL/yr)^.1	0.017	0.753	0.545	0.583	-0.749	0.167	-0.058	-0.548	-0.023	-0.295	0.096	-0.095	1.000	
(KESAL/yr)^.5	-0.045	0.852	0.511	0.621	-0.541	0.220	-0.063	-0.413	0.017	-0.238	0.068	-0.119	0.955	1.000

Figure 5.2.4. Correlation matrices used for review of GPS-1 dry-freeze data and model building.

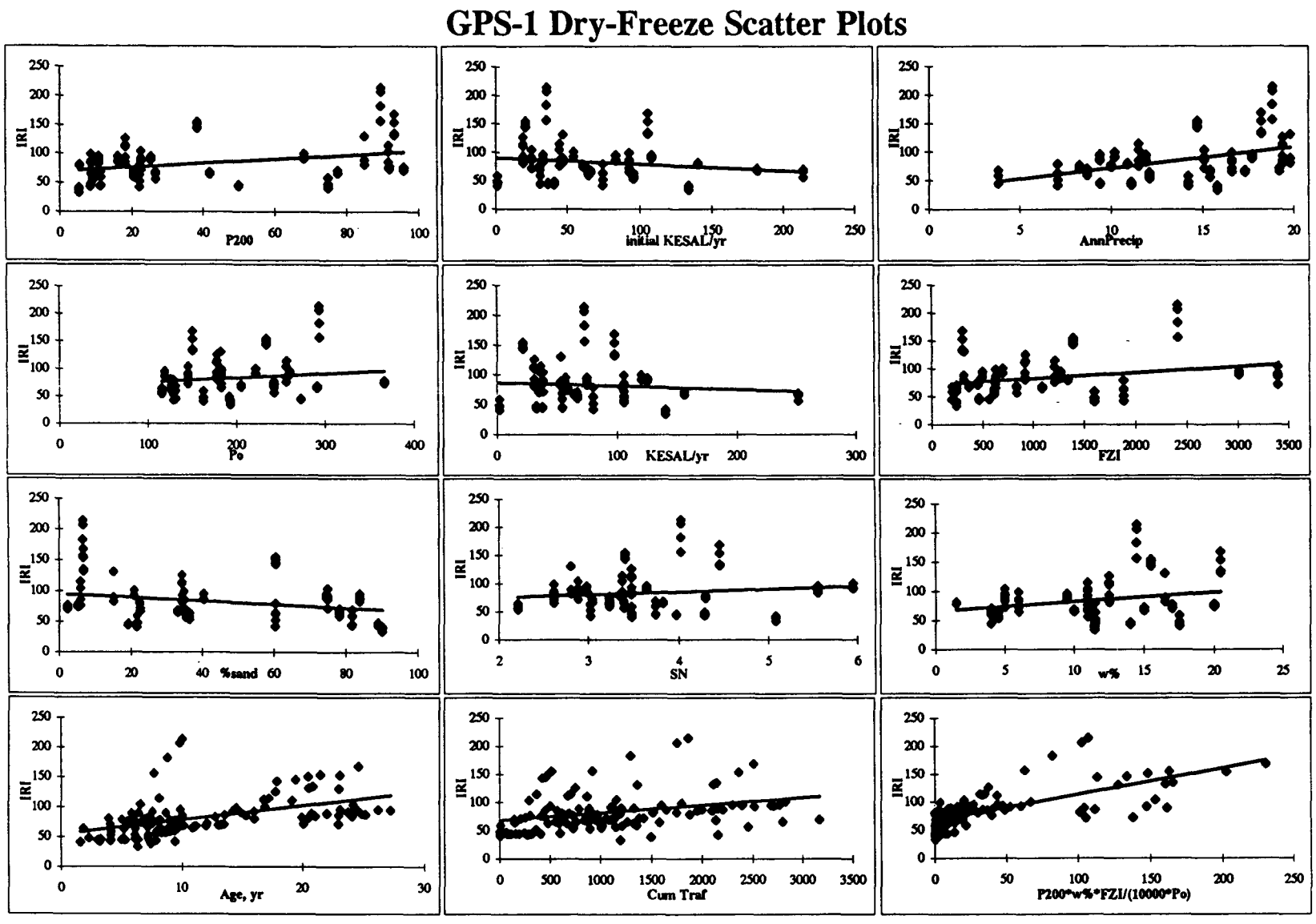

Figure 5.2.5. Scatter plots used for analysis of GPS-1 data and model building.

This parameter is thought to give an indication of the frost susceptibility of a given pavement system. This parameter shows strong correlation to the IRI values in freezing environments and is typically stronger than any of the individual parameters within the cluster.

Figure 5.2.6 shows the sensitivity of the dry freeze model when the subgrade conditions vary from a sandy gravel to soft clay. These models are very sensitive to the input parameters. Input parameters must be realistic and within typical ranges for dry freeze conditions, and within the range for parameters contained in the data set used for model building. Shown in parentheses next to the parameter name is the range of the parameter encountered in the LTPP data used to build the model.

Traffic rates for this data set varied from 2 to 250 KESAL/yr with an average of 74 KESAL/yr. The pavements in this subset that were poor performers generally existed on high-moisture-content clays, often with in-situ moisture contents that were higher than the plastic limit of the subgrade soil. The pavements in this subset that performed well generally rested on granular soils that contained 10 to 30 percent of P200 material and had relatively high AC layer thickness. Pavements with subgrades having P200 less than 10 percent appeared to have higher initial IRI values.

Sections 16-1010 and 49-1017, shown in figure 5.2.3, are considered to be the smoothest and oldest pavements in the data set. These sections had P200 values of 10 percent and 16 percent, respectively, subgrade moisture contents of 5 percent and 9 percent, respectively, traffic levels of 60 and 75 KESAL/yr, respectively, and annual precipitation values of 300 mm (12 in) and 225 mm (9 in), respectively. A preliminary evaluation of section 16-1010 based on the AASHTO equation indicates that the cumulative traffic volumes were below those expected to cause a terminal serviceability level. Section 49-1017 has a low estimated SN of 2.98; the subgrade is a clayey gravel with sand, with 56 percent passing the No. 4 sieve. This 28-year-old yet very smooth section is estimated to be near the end of its useful service life according to the AASHTO equation. Good subgrade conditions and low precipitation are factors that likely resulted in this section remaining smooth for over 25 years.

The poor performers generally existed on high-moisture-content clays, often with in-situ moisture contents that were higher than the plastic limit of the subgrade. Section 81-1804 (identified in figure 5.2.3) is less than 10 years old and has a rapidly increasing IRI. A preliminary analysis of this section with the AASHTO pavement design equation indicated that this section was at the end of its service life. This section has higher values for precipitation (475 mm (19

Parameter	(Data Range)	Case 1	Case 2	Case 3	Case 4	Case 5
%ACinSN	(25-85)	20	20	20	20	20
KESAL/yr	(2-250)	225	225	225	225	225
P200	(7-95)	10	25	45	65	95
w%	(2-20)	4	8	12	15	20
%Sand	(3-90)	60	65	60	33	4
Po, psf	(120-360)	200	200	200	200	200
SN	(2.2-5.9)	4	4	4	4	4
AnnPrecip, in	(3-20)	10	10	10	10	10
FZI, deg F*days	(160-3400)	1700	1700	1700	1700	1700
INITIAL IRI, in/mi =		49	41	39	38	36
Growth Rate Constant, r =		0.0035	0.0044	0.0078	0.0146	0.0356

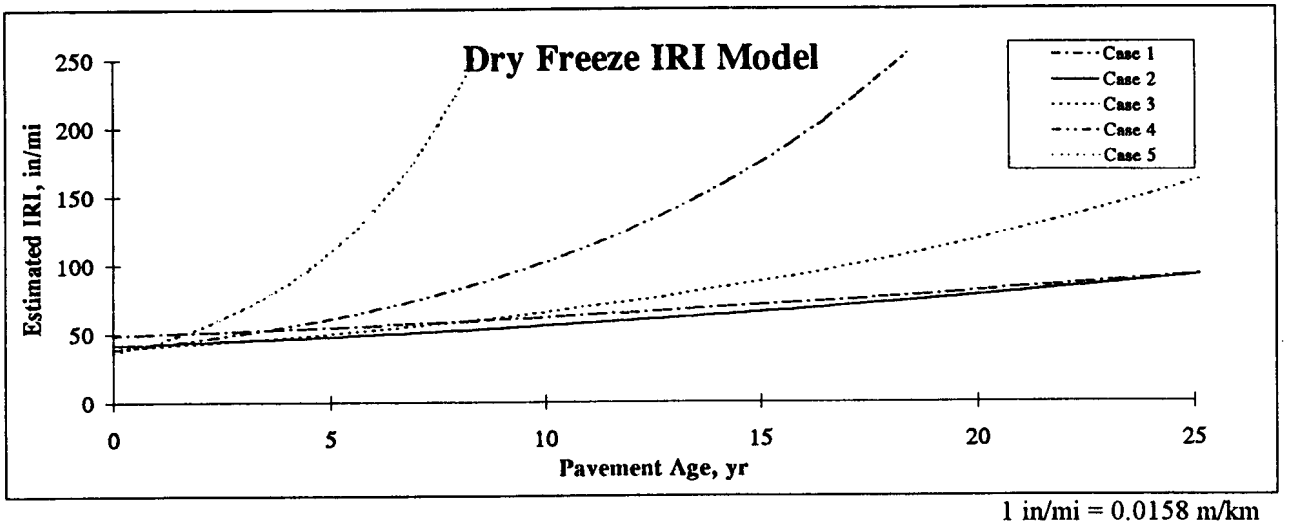

1 in/mi = 0.0158 m/km

Figure 5.2.6. Sensitivity of the dry freeze IRI prediction model to changes in subgrade conditions.

in)), freeze index (1339 °C days (2411 °F Days)), P200 (89 percent), and subgrade moisture content (14.5 percent), and has an estimated SN of 4 and is subjected to 74 KESAL/yr.

5.2.2 Dry-No Freeze Environment

The dry-no freeze environment is defined as a region that has less than 508 mm (20 in) of annual precipitation and a freezing index of less than 89 °C days (160 °F days). The roughness behavior of the pavements in this region appears to be controlled by the structural properties of the pavement, layer thickness, traffic, and subgrade parameters. Traffic rates for this data set varied from 30 KESAL/yr to 360 KESAL/yr, with an average of 110 KESAL/yr. Figure 5.2.7 shows the model developed to predict IRI for these pavements. This model was based on 79 IRI measurements from 22 sections and had an average error per section of 0.19 m/km (11.9 in/mi); the standard deviation of errors at the sections was 0.14 m/km (8.6 in/mi). Figure 5.2.8 shows the sensitivity of the resulting model to changes in traffic conditions. Shown in parentheses next to the parameter name is the range of the parameter encountered in the LTPP data used to build the model.

As shown in figure 5.2.7, the best long-term performers were sections 6-8535 (estimated SN = 5.5) and 6-8534 (estimated SN = 4.2). These sections are subject to very hot and dry conditions and high traffic (KESAL/yr = 360 and 240, days over 32°C (90°F) = 167). These sections are located on relatively high-P200-content but lower-moisture-content subgrades, but they utilize thick base and subbase layers such that the overburden pressures on the subgrade are greater than 14 kPa (300 lb/ft^2). Annual precipitation in the area where these sections are located is 75 mm (3 in) per year. The AASHTO equation predicts that 6-8535 is still within its anticipated service life. Section 6-8534, however, is estimated to be at the end of its service life according to the AASHTO equation, but has remained very smooth.

The section with the highest IRI in the data set was section 4-1002 (see figure 5.2.7). A preliminary evaluation of this section based on the AASHTO design equation indicated that this section was near the end of its estimated design life. This section has an AC thickness of 260 mm (10.4 in) and rests on a subgrade that is very dry and has a low percentage of P200 material. This site was the least predictable section in the data set. Another poorly performing section is section 4-1037 (see figure 5.2.7). A preliminary evaluation of this section based on the AASHTO equation indicated that it has exceeded its estimated design life. This site is located in a very hot region that has 180 days over 32°C (90°F); the pavement section has an estimated SN of 3.4.

$$IRI(t) = IRI_0 e^{r_0 \frac{t^S}{T}}$$

$$IRI_0 = A(P200/Po)^B + C(Po)^D + E(ACThick)^F + G(SN)^H$$

$$r_0 = \left[\frac{I(KESAL/yr)^J}{K(SN)^L} + M\left(\frac{AnnPrecip \times FzThwCyc}{Po}\right)^N + O(FZI)^P + Q(P200/Po)^R \right] \times \frac{1}{1000}$$

A= 70.163738	F= -1.0523933	K= 190	P= 3.6002489
B= 0.0719436	G= -309.87143	L= 3.5799804	Q= 2.7983612
C= -180.49308	H= -1.2513266	M= 8.032E-05	R= -0.9909045
D= -3.5455528	I= 130	N= 5.4828793	S= 1.0568
E= 370.09218	J= 1.65	O= 3.838E-06	T= 10

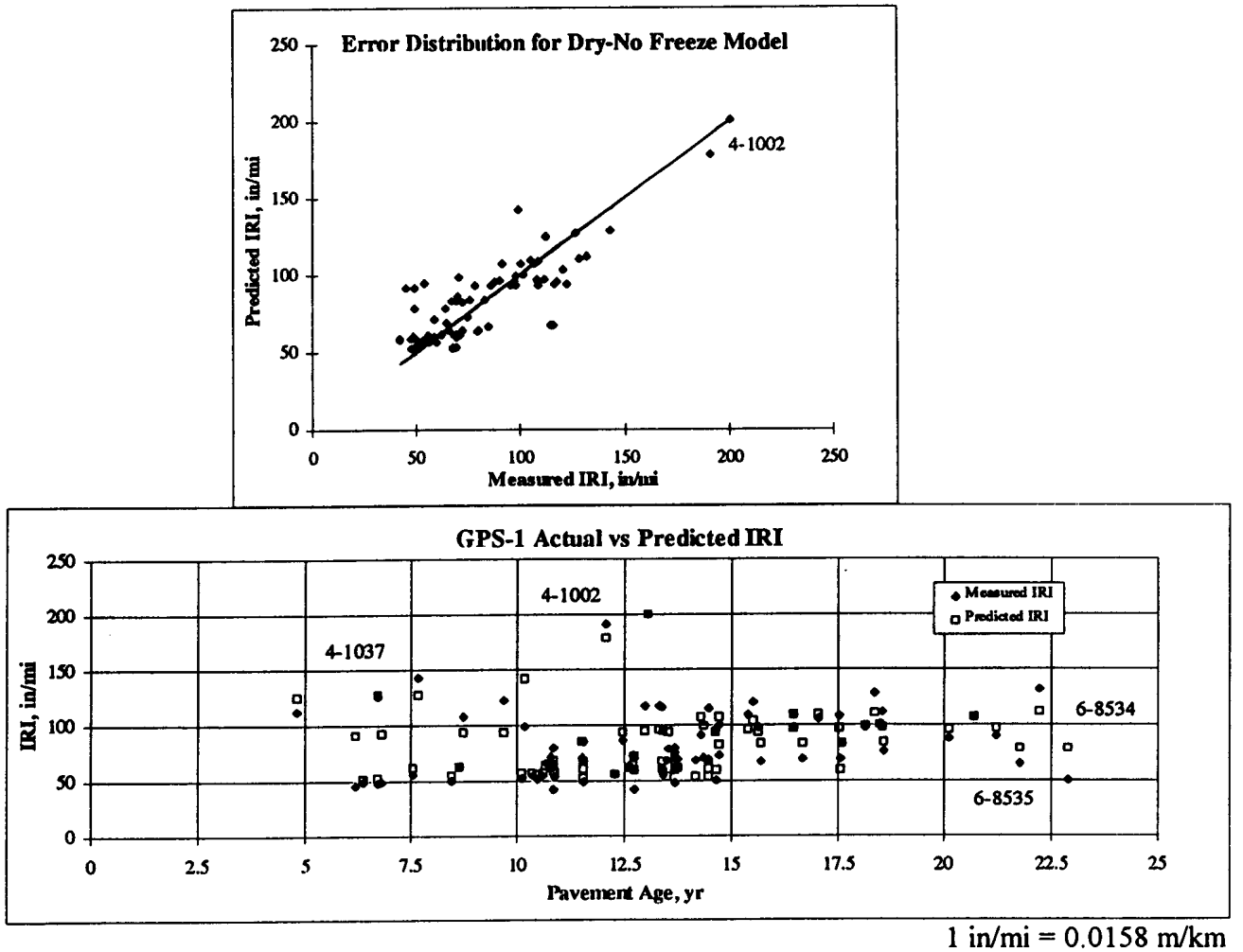

1 in/mi = 0.0158 m/km

Figure 5.2.7. GPS-1 dry-no freeze IRI model.

Parameter (Data Range)	Case 1	Case 2	Case 3	Case 4	Case 5
KESAL/yr (30-360)	30	100	170	265	360
SN (2.2-6.7)	2.70	2.70	2.70	2.70	2.70
ACThick, in (2.4-13)	5	5	5	5	5
P200 (4-70)	70	70	70	70	70
Po, psf (120-370)	140	140	140	140	140
FZI (0 to 145)	140	140	140	140	140
AnnPrecip, in (3-20)	20	20	20	20	20
FrzThwCyc (3-150)	110	110	110	110	110
INITIAL IRI, in/mi=	45	45	45	45	45
Growth Rate Constant, r=	0.506	0.540	0.595	0.697	0.826

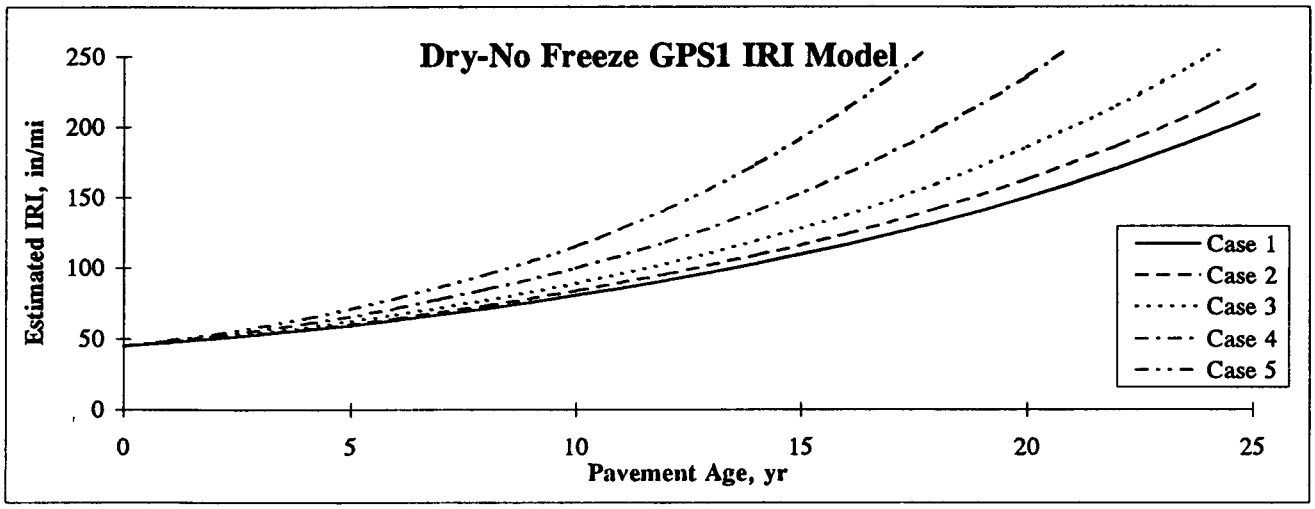

1 in/mi = 0.0158 m/km

Figure 5.2.8. Sensitivity of the dry-no freeze IRI prediction model to changes in traffic volume, holding all other parameters constant.

5.2.3 Wet Freeze Environment

The wet freeze environment is characterized by an annual precipitation greater than 508 mm (20 in) and a freezing index greater than 89 °C days (160 °F days). The data for this region were divided into three categories on the basis of the percent passing the 75-μm (No. 200) sieve (P200) for subgrade. The first model is for fine-grained soils (P200 > 50 percent), the second model is for coarse soils with P200 between 20 and 50 percent, and the third model is for coarse-grained soils with P200 less than 20 percent. The boundary of P200 equal to 50 percent is a standard boundary in the Unified Soil Classification System to differentiate between fine- and coarse- grained soil. The boundary of P200 equal to 20 percent was somewhat arbitrary, but coarse-grained soils with P200 greater than 20 percent often behave much differently than clean granular soils. This boundary also divided the data set somewhat equally.

The data appear to indicate that fine-grained soils are sensitive to the climate, subgrade conditions, and layer thickness. No strong correlation was noted with hot weather conditions for the wet freeze climate. Subgrade parameters and the severity of freezing are in general the controlling factors for roughness development in these conditions.

Wet Freeze GPS-1 (P200 > 50 percent) IRI Model

Figure 5.2.9 shows the model developed for the wet freeze climate for pavements with subgrade having a P200 greater than 50 percent. The least predictable sections with this model were thick AC sections that have very little base or subbase. This model was based on 96 IRI measurements from 19 sections and had an average error per section of 0.24 m/km (15.2 in/mi); the standard deviation of the errors at the sections was 0.19 m/km (11.9 in/mi). These pavements are sensitive to the Atterberg limits of the subgrade, moisture content of the subgrade, and the freezing index. Figure 5.2.10 shows the sensitivity of the resulting model to variations in the SN. Shown in parentheses next to the parameter name is the range of the parameter encountered in the LTPP data used to build the model. Traffic rates varied from 16 to 1600 KESAL/yr with an average of 160 KESAL/yr for this data set.

The best long-term IRI performer within this data set was section 21-1034 (see figure 5.2.9). A preliminary analysis of this section with the AASHTO equation indicated that this section is still within its service life. This section consists of a very thick AC surface and a low

$$IRI(t) = IRI_0 e^{r_0 \frac{t^S}{T}}$$

$$IRI_0 = A(P200)^B + C(1+PI)^D + E(ACThick)^F + G(Po)^H$$

$$r_0 = \left[\frac{I(KESAL/yr)^J}{K(SN)^L} + M(1+PI)^N + O\left(\frac{w\% \times P\#4 \times FZI}{Po}\right)^P + Q(P200)^R \right] \times \frac{1}{1000}$$

A=-9.014E-06	F=-0.1725499	K=180	P=2.3882482
B=3.4906533	G=8.361E+11	L=4	Q=2.062E-08
C=44.459606	H=-10.537378	M=0.0001832	R=5.9060862
D=0.142	I=3000	N=4.8077516	S=1.078564
E=56.917593	J=1.9	O=0.0465496	T=200

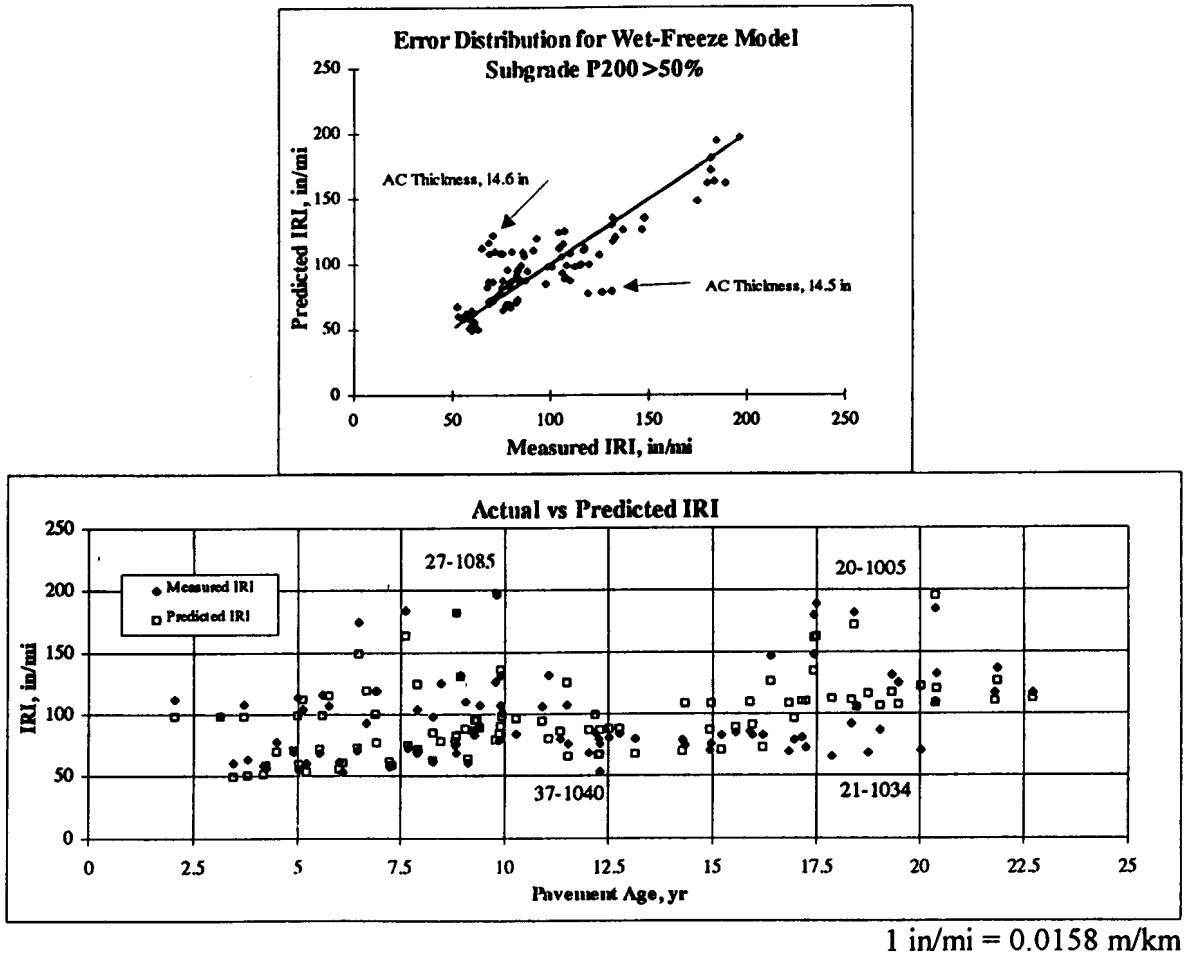

1 in/mi = 0.0158 m/km

Figure 5.2.9. GPS-1 wet-freeze (P200 > 50%) IRI model.

Parameter (Data Range)	Case 1	Case 2	Case 3	Case 4	Case 5
KESAL/yr (20-1600)	250	250	250	250	250
SN (2.8-10.3)	4.32	3.98	3.64	3.3	2.96
ACThick, in (2.2-16)	8	7	6	5	4
Po, psf (0-34)	180	180	180	180	180
PI (0-34)	15	15	15	15	15
P200 (50-100)	66	66	66	66	66
w% (7.5-27)	16	16	16	16	16
FZI (160-1730)	1400	1400	1400	1400	1400
INITIAL IRI, in/mi =	85	86	87	89	90
Growth Rate Constant, r =	7.67	8.34	9.37	11.01	13.77

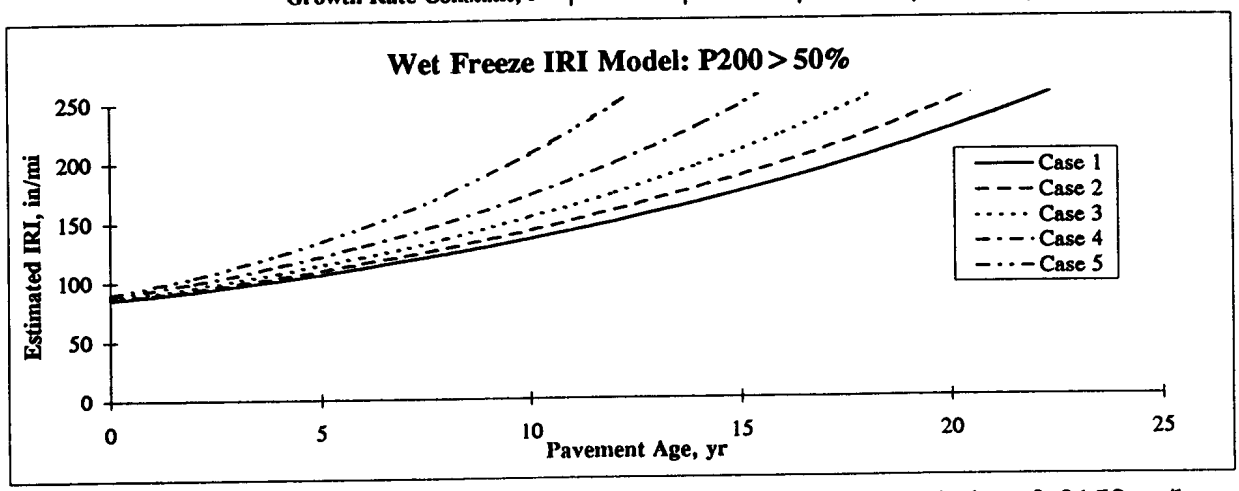

1 in/mi = 0.0158 m/km

Figure 5.2.10. Sensitivity of the wet-freeze IRI prediction model to changes in estimated SN, by varying AC thickness.

base thickness resting on a very high-water-content clay (P200 = 83 percent, w% = 27 percent). This section has low traffic (30 KESAL/yr), a low freeze index, and high precipitation.

The worst performers in this data set were sections 27-1085 and 20-1005 (see figure 5.2.9). These sections consist of thick AC layers with very little base or subbase. These sections are subjected to high freezing indices, and the frost-related effects appeared to be the cause of the high IRI values. Section 20-1005 is virtually identical in all respects to section 21-1034, which is identified as a good performer. The primary difference is that 20-1005 has a much higher freeze index. Section 27-1085 has even lower traffic but has a higher freeze index and has a higher IRI at an even earlier age.

Wet Freeze GPS-1 (20%<P200<50%) IRI Model

Soils of this type are frost susceptible. The correlation coefficients determined from these data fit the expected frost-related trends. The more sand present in the subgrade and the greater the overburden pressure on the subgrade, the lower IRI values tended to be. Surprisingly, a negative correlation to annual precipitation is noted. This may relate to the variation of precipitation over the year. Figure 5.2.11 shows the model developed for the wet freeze climate. This model was based on 88 IRI measurements from 15 sections and had an average error per section of 0.18 m/km (11.4 in/mi). The standard deviation of the errors at the sections was 0.10 m/km (6.9 in/mi). Traffic rates varied from 10 to 1030 KESAL/yr with an average of 230 KESAL/yr for this data set. Figure 5.2.12 shows the sensitivity of the resulting model to variations in the freeze-thaw cycles. Shown in parentheses next to the parameter name is the range of the parameter encountered in the LTPP data used to build the model.

The best long-term performer within this data set was section 37-1801 (see figure 5.2.11). This section is a fairly high-traffic (220 KESAL/yr) section with a low freeze index (91 °C days/yr (164 °F days/yr)) and a relatively thick AC surface (180 mm (7.2 in)) located on a relatively wet, higher P200 subgrade (w% = 19.5 percent, P200 = 43 percent). This section was at the margin between wet-no freeze and wet freeze conditions. It is believed that this section would not have done well in high freeze index conditions. According to the AASHTO equation, this very smooth section should be near the end of its service life.

One of the smoothest pavements in the data set is section 23-1012. This 8-year-old section experiences very high traffic (600 KESAL/yr) and has a high pavement thickness (SN = 7.3, Po = 22 kPa (460 lb/ft^2), AC thickness = 233 mm (9.3 in)) with a medium freeze index

$$IRI(t) = IRI_0 e^{r_0 \frac{t^S}{T}}$$

$$IRI_0 = A(P200/Po)^B + C(\%Sand)^D + E(SN)^F + G(\%ACinSN/100)^H$$

$$r_0 = \left[\frac{I(KESAL/yr)^J}{K(SN)^L} + M(FrzThwCyc)^N + O(\%Sand)^P + Q(Po)^R\right] \times \frac{1}{1000}$$

A= 61.978361	F= 1.08049	K= 70	P= 6.1837864
B= 0.321181	G= 0.0730219	L= 4.5	Q= 9.175E+12
C= 576.6484	H= -7.2190131	M= 2.576E-06	R= -4.9485028
D= -0.9128525	I= 240	N= 3.8083072	S= 1.1603307
E= 1.1868639	J= 1.352654	O= 5.238E-10	T= 10.265499

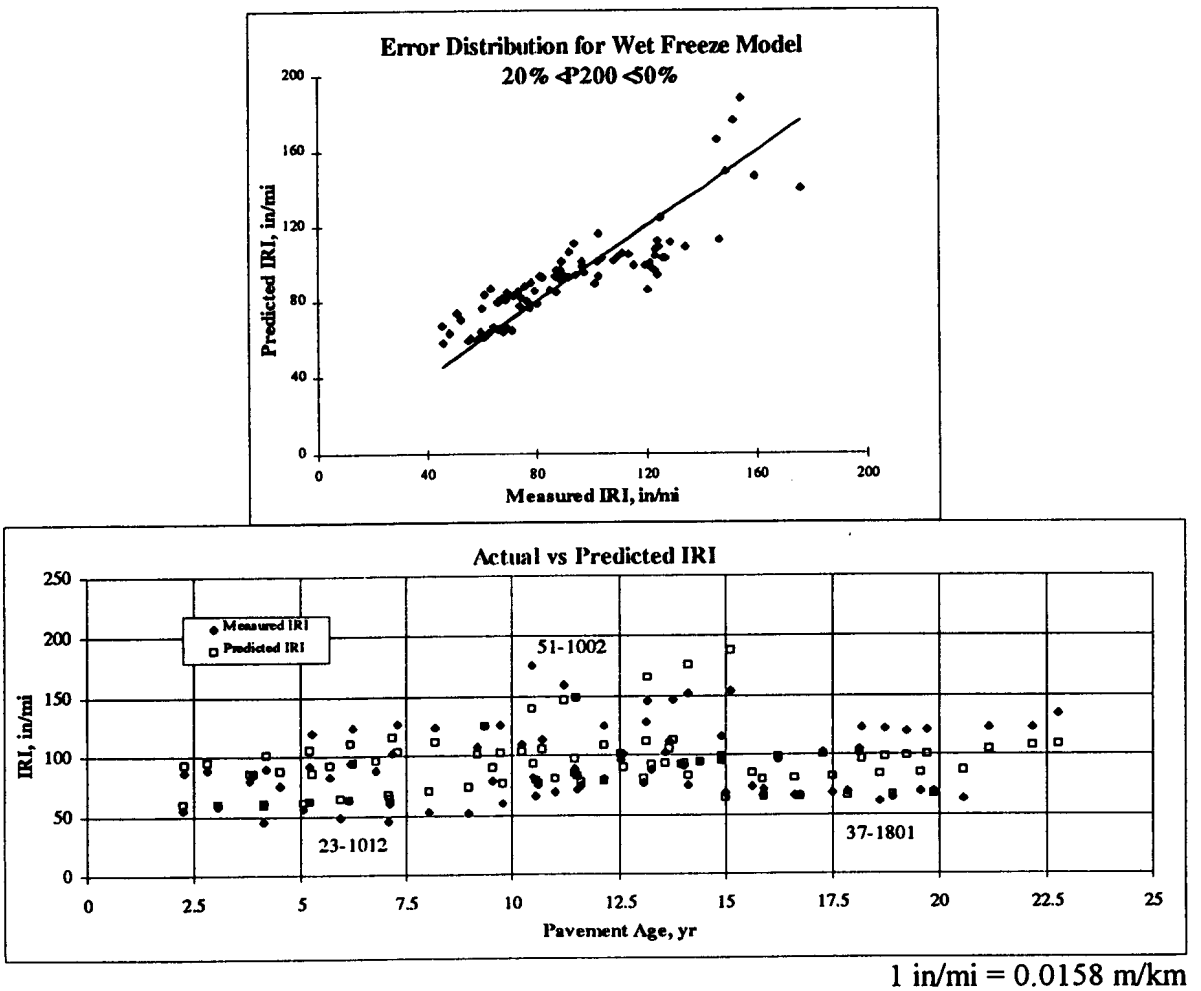

1 in/mi = 0.0158 m/km

Figure 5.2.11. GPS-1 wet-freeze (20% < P200 < 50%) IRI model.

Parameter (Data Range)	Case 1	Case 2	Case 3	Case 4	Case 5
KESAL/yr (10-1020)	350	350	350	350	350
SN (3.6-7.8)	5	5	5	5	5
%ACinSN (0.47-1.0)	0.66	0.66	0.66	0.66	0.66
Po, psf (125-460)	210	210	210	210	210
P200 (20-50)	20	20	20	20	20
%Sand (18-72)	70	70	70	70	70
FrzThwCyc (71-132)	70	85	100	115	130
INITIAL IRI, in/mi =	49	49	49	49	49
Growth Rate Constant, r =	0.198	0.228	0.277	0.352	0.460

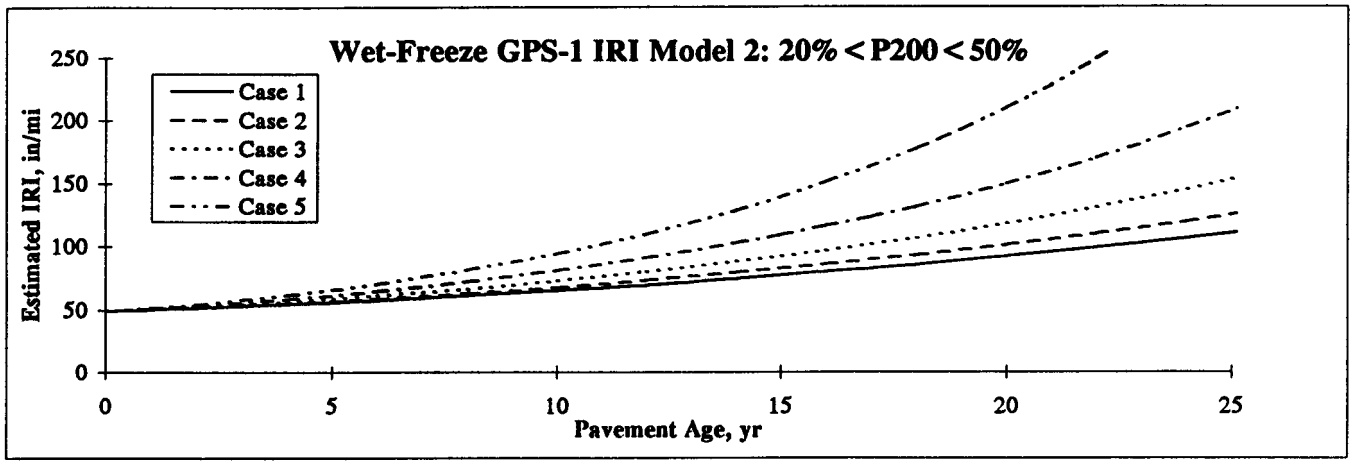

1 in/mi = 0.0158 m/km

Figure 5.2.12. Sensitivity of the wet-freeze model to changes in number of freeze-thaw cycles/yr.

(FZI=549 °C days/yr (988 °F days/yr)). The combination of good subgrade (P200 = 20%, w% = 12%) with high overburden pressures and thick AC layers likely resulted in this section having a very low initial IRI values.

The worst performer observed was section 51-1002. A preliminary analysis of this section with the AASHTO equation indicated that this section has exceeded its estimated design life.

Wet Freeze GPS-1 (P200 < 20 percent) IRI Model

Pavements existing within these conditions do not appear to be as susceptible to freezing effects compared with the higher P200 subgrades in the same climate. The number of days/yr with greater than 12 mm (0.5 in) of precipitation is the strongest climate factor that is correlated with IRI. Figure 5.2.13 shows the model developed for the wet freeze climate with a subgrade P200 less than 20 percent. This model was based on 157 IRI measurements from 32 sections and had an average error per section of 0.24 m/km (15.6 in/mi). The standard deviation of the errors at the sections was 0.19 m/km (11.9 in/mi). Pavement that had low SN values or pavements located in areas of high freeze indices had the highest errors for the developed model. For this data set, the traffic rates varied from 15 to 350 KESAL/yr with an average of 110 KESAL/yr. Figure 5.2.14 shows the sensitivity of the resulting model to changes in layer thickness for a constant SN. Shown in parentheses next to the parameter name is the range of the parameter encountered in the LTPP data used to build the model.

The best long-term performer in this data set was section 26-1001 (see figure 5.2.13). This is a very low-traffic (16 KESAL/yr) and low-SN (2.5) section resting on dry, clean sand (P200 = 4 percent, w% = 4.5 percent). The AC thickness was 55 mm (2.2 in) and the overburden pressure on the subgrade was 7.2 kPa (150 lb/ft^2). Another very smooth pavement is section 23-1009 (see figure 5.2.13). This 24-year-old section rests on similar subgrade conditions and utilizes thick base and subbase layers (Po = 19.2 kPa (400 lb/ft^2)). A preliminary evaluation of these two sections with the AASHTO equation indicated that the pavement sections are still within their estimated service life.

The worst long-term performers in the data set are sections 89-1127 and 89-1125 (see figure 5.2.13). Both of these are very thick sections (Po > 23 kPa (480 lb/ft^2)) located in a high freeze index environment (FI > 1167 °C days/yr (2100 °F days/yr)). Traffic levels are very different (25 and 350 KESAL/yr, respectively); however, their IRI behavior is similar. The only factor that explained the high IRI values for these sections was the high freezing indices,

$$IRI(t) = IRI_0 e^{r_0 \frac{t^U}{V}}$$

$$IRI_0 = A(P200 \times Po)^B + C(\%ACinSN/100)^D + E(ACThick)^F + G(w\%)^H$$

$$r_0 = \left[\frac{I(KESAL/yr)^J}{K(SN)^L} + M(FZI/100)^N + O(FZI/Po)^P + Q(Days.5"+))^R + S(ACThick)^T\right] \times \frac{1}{1000}$$

A=163.38286	F=-1.6724454	K=3.7680662	Q=3.004E-09
B=-0.0839446	G=-1922.9695	L=6.3120233	R=8.0280584
C=0.0130354	H=-5.7582451	M=0.0259789	S=-0.0008525
D=-8.4850338	I=31378.88	N=3.8343596	T=6.3945824
E=-329.31446	J=1.4836653	O=1559.7432	U=1.0489556
		P=-2.4342743	V=200

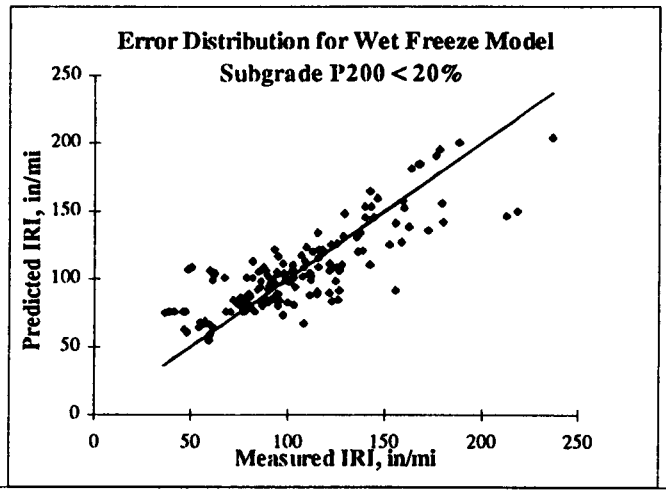

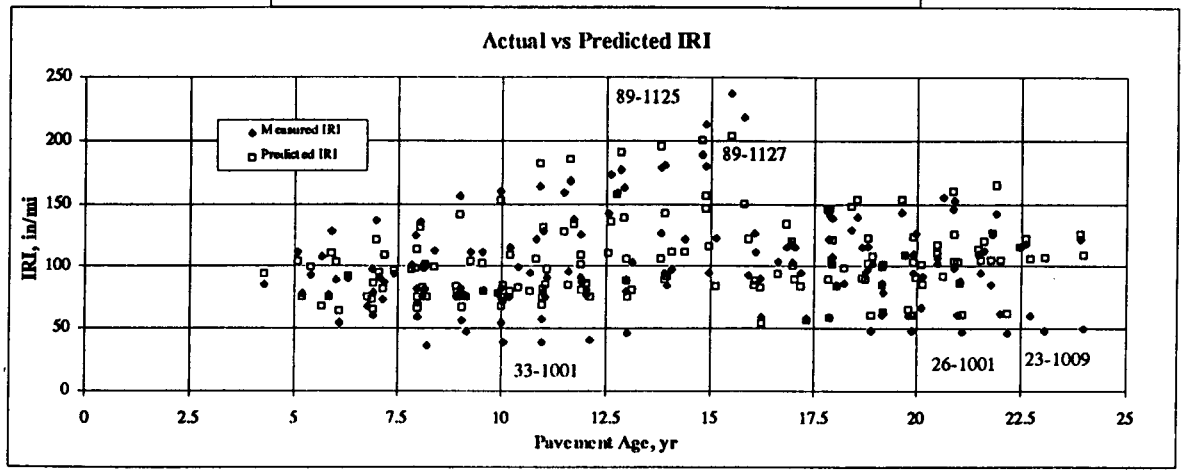

1 in/mi = 0.0158 m/km

Figure 5.2.13. GPS-1 wet-freeze (P200 < 20%) IRI model.

Parameter (Data Range)	Case 1	Case 2	Case 3	Case 4	Case 5
KESAL/yr (15-340)	120	120	120	120	120
SN (2.2-7.4)	3.0	3.0	3.0	3.0	3.0
ACThick (2.2-10.5)	5.6	4.8	4.1	3.3	2.5
%ACinSN (0.35-.95)	0.83	0.71	0.60	0.48	0.37
Po, psf (95-480)	120	150	180	210	240
P200 (1-15)	15	15	15	15	15
w% (2-11)	8	8	8	8	8
Days.5"+ (5-35)	25	25	25	25	25
FZI (160-2740)	1400	1400	1400	1400	1400
INITIAL IRI, in/mi=	69	62	53	44	73
Growth Rate Constant, r=	11.59	11.74	11.50	11.63	11.38

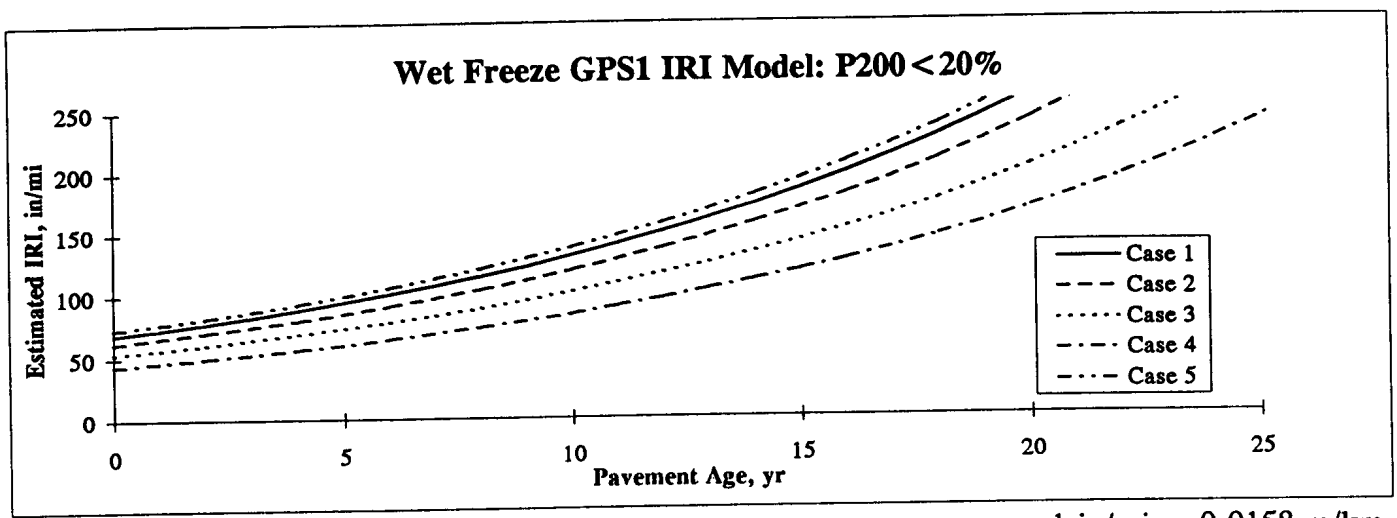

1 in/mi = 0.0158 m/km

Figure 5.2.14. Sensitivity of the wet-freeze model (P200<20%) to changes in layer properties at constant SN.

indicating that the environment is a controlling factor for these very thick sections in a severe climate. On the basis of AASHTO structural equation, these rough sections are estimated to be at the very beginning of their estimated service lives, indicating the strong effects of the severe climate on IRI and serviceability.

5.2.4 Wet-No Freeze Environment

The wet-no freeze environment is characterized by annual precipitation greater than 508 mm (20 in) and an annual freeze index of less than 89 °C days/yr (160 °F days/yr). The data for these sections were divided into three categories based on the percent passing the 75-μm (No. 200) sieve (P200) in the subgrade soils. The first model is for fine-grained soils (P200 > 50 percent), the second is for coarse-grained soils with P200 between 20 and 50 percent, and the third is for coarse-grained soils with P200 less than 20 percent. The boundary of P200 equal to 50 percent is a standard boundary in the Unified Soil Classification System to differentiate between fine-grained and coarse-grained soil. The boundary of P200 equal to 20 percent was somewhat arbitrary, but coarse soils with P200 greater than 20 percent often behave much differently than clean, granular soils. This boundary also divided the data set somewhat equally.

The pavements in this region are sensitive to the number of days above 32 °C (90 °F), which indicates that roughness is related to the softening of the asphalt concrete. Surprisingly, all subgroups show significant negative correlation to annual precipitation, which may indicate either a cooling effect from precipitation resulting in a higher AC stiffness over the year, or that areas with greater temperature and moisture variations over the year may have higher pavement roughness than more uniformly moist/uniform temperature climates.

Wet-No Freeze GPS-1 (P200>50 Percent)

Figure 5.2.15 shows the model developed for the wet-no freeze environment with fine-grained soils (P200 > 50 percent). This model was based on 97 IRI measurements from 24 sections and had an average error per section of 0.23 m/km (14.6 in/mi). The standard deviation of the errors at the sections was 0.17 m/km (10.5 in/mi). Traffic rates varied from 15 to 625 KESAL/yr with an average of 170 KESAL/yr for this data set. Traffic is not a strong factor in the IRI behavior of these pavements. Subgrade parameters such as plasticity index (PI), moisture content (w%), P200, and hot weather effects are the strongest factors that were correlated with IRI for these pavements. There is a strong negative correlation to precipitation, which is not

$$IRI(t) = IRI_0 e^{r_0 \frac{t^U}{V}}$$

$$IRI_0 = A(Po)^B + C(P200)^D + E(w\% \times \%sand \times Po)^F + G(ACThick/Po)^H$$

$$r_0 = \left[\frac{I(KESAL/yr)^J}{K(SN)^L} + M(0.5 + PI)^N + O(\frac{LI + .00001}{Po})^P + Q(FrzThwCyc \times Days90+)^R + S(DaysWet/yr)^T \right] \times \frac{1}{1000}$$

A=3069.239	F=0.0073774	K=1.8153442	Q=4.333E-07
B=-0.0076966	G=-443.09587	L=3.0510484	R=2.5926674
C=-5034.3994	H=0.0419734	M=-2384835.6	S=8.035E+17
D=-0.0292012	I=0.0029165	N=7.464E-05	T=-7.8133062
E=1794.5335	J=3	O=2388175.3	U=1.4938206
		P=7.636E-05	V=200

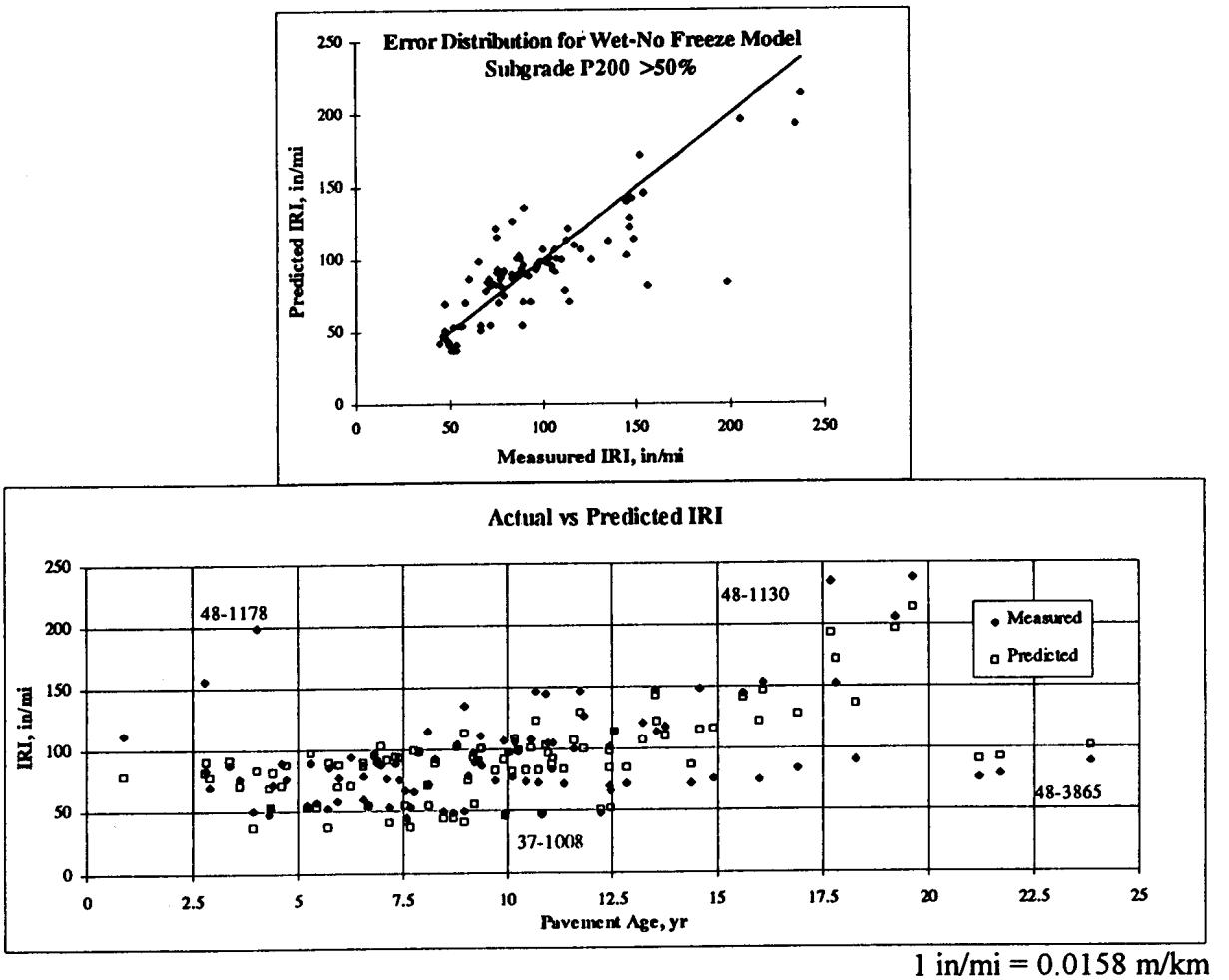

1 in/mi = 0.0158 m/km

Figure 5.2.15. GPS-1 wet-no freeze (P200 > 50%) IRI model.

clearly understood except from the perspective of reducing hot weather damage or reduced shrink-swell of soils from being wet more of the time. Figure 5.2.16 shows the sensitivity of the resulting model to varying SN. Shown in parentheses next to the parameter name is the range of the parameter encountered in the LTPP data used to build the model.

The best long-term performer in the data set was section 48-3865 (see figure 5.2.15). This section has a P200 of 57 percent, a moisture content of 11.5 percent, was at the lower end of precipitation (675 mm/yr (27 in/yr)), is subjected to low traffic (65 KESAL/yr), and has a thin AC layer (58 mm (2.3 in)) with overburden pressures on the subgrade of 10.5 kPa (220 lb/ft^2). This section has exceeded the AASHTO estimated traffic volumes that would cause terminal serviceability.

One of the smoothest pavements in the data set is section 37-1008 (see figure 5.2.15). This is a 12-year-old, high-traffic route (515 KESAL/yr), resting on a wet subgrade (P200 = 50 percent, w% = 31 percent), which experiences very little hot weather. The AC thickness is 233 mm (9.3 in) with a subgrade overburden pressure of 10 kPa (210 lb/ft^2). This section is estimated to be within its service life on the basis of the AASHTO equation.

The worst long-term performer in the data set was section 48-1130 (see figure 5.2.15), which was subjected to a low traffic level of 44 KESAL/yr. This section rests on a high-plasticity clay (LL = 53 percent, PI = 30 percent, P200 = 82 percent, w% = 26 percent) with the in-situ moisture content greater than the plastic limit of the soil (LI = 0.115). This section has an AC thickness of 68 mm (2.7 in), with the overburden pressure on the subgrade being approximately 15.3 kPa (320 lb/ft^2). The AASHTO equation indicated that this section is at the early stages of its service life.

Wet-No Freeze GPS-1 (20%<P200<50%)

Figure 5.2.17 shows the model developed for IRI prediction of pavements in wet-no freeze climates that have coarse soils with a lower P200 content (20 percent<P200<50 percent). This model was based on 96 IRI measurements from 21 sections and had an average error per section of 0.15 m/km (9.6 in/mi). The standard deviation of the errors at the sections was 0.17 m/km (10.6 in/mi). Traffic rates varied from 1 to 1180 KESAL/yr with an average of 180 KESAL/yr for this data set. These pavements are the best overall performers of all GPS-1 sections and are most sensitive to cross-section properties and warm weather effects. Figure 5.2.18 shows the sensitivity of the resulting model to variations in traffic volumes. Shown in

Parameter(Data Range)	Case 1	Case 2	Case 3	Case 4	Case 5
KESAL/yr (15-630)	300	300	300	300	300
SN (1.9-6.8)	2.5	3	3.5	4	4.5
ACThick, in (1.5-11)	3.5	3.5	3.5	3.5	3.5
Po, psf (120-330)	120	187	249	312	330
LI (0-0.3)	0.1	0.1	0.1	0.1	0.1
PI (0-30)	15	15	15	15	15
w% (11-31)	15	15	15	15	15
P200 (50-97)	66	66	66	66	66
%Sand (2.5-50)	27	27	27	27	27
DaysWet/yr (69-145)	85	85	85	85	85
Days90+ (1-130)	35	35	35	35	35
FrzThwCyc (4-86)	55	55	55	55	55
INITIAL IRI, in/mi=	65	68	70	72	72
Growth Rate Constant, r=	5.03	3.82	3.19	2.83	2.63

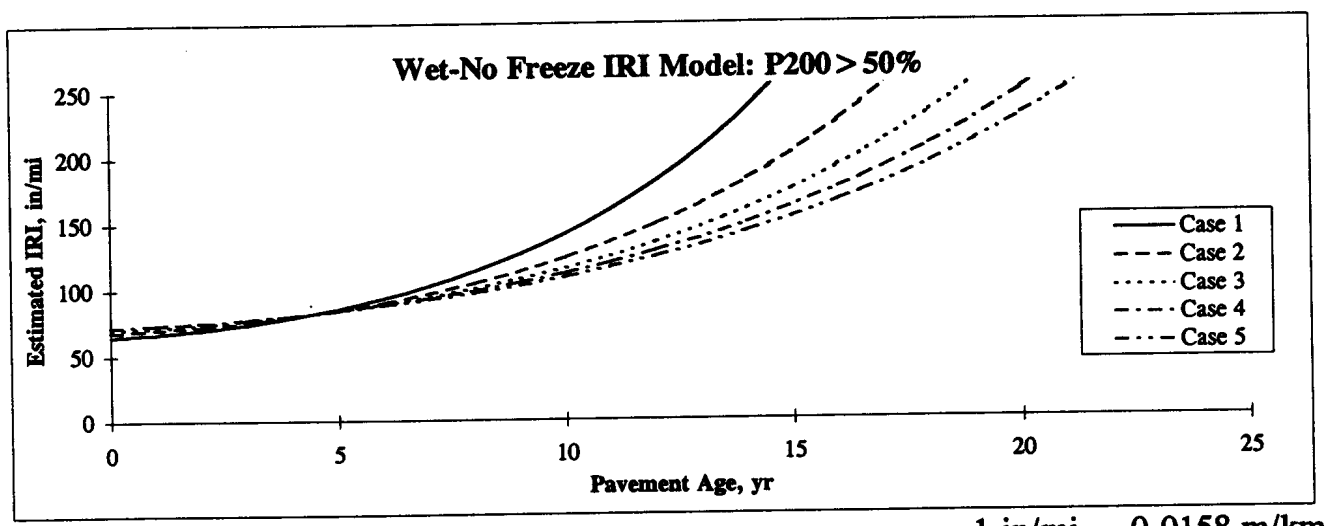

1 in/mi = 0.0158 m/km

Figure 5.2.16. Sensitivity of the wet-no freeze IRI prediction model (P200>50%) to changes in estimated SN, holding AC thickness constant.

$$IRI(t) = IRI_0 e^{r_0 \frac{t^S}{T}}$$

$$IRI_0 = A(w\%)^B + C(SN)^D + E(P200)^F + G(Po)^H$$

$$r_0 = \frac{I(KESAL/yr)^J}{K(SN)^L} + M(ACthick)^N + O(Days90+)^P + Q(DaysWet/yr)^R$$

A= 3.08E-01	F= -0.4208	K= 832.4608	P= 0.0414
B= 1.7353	G= -6.7049	L= 11.3978	Q= -0.00344
C= -0.3749	H= 0.29413	M= 0.0740552	R= 0.4553
D= -0.27133	I= 0.0573665	N= -6.6522	S= 1.7173
E= 312.61	J= 2.8032	O= 0.029425	T= 3.7776

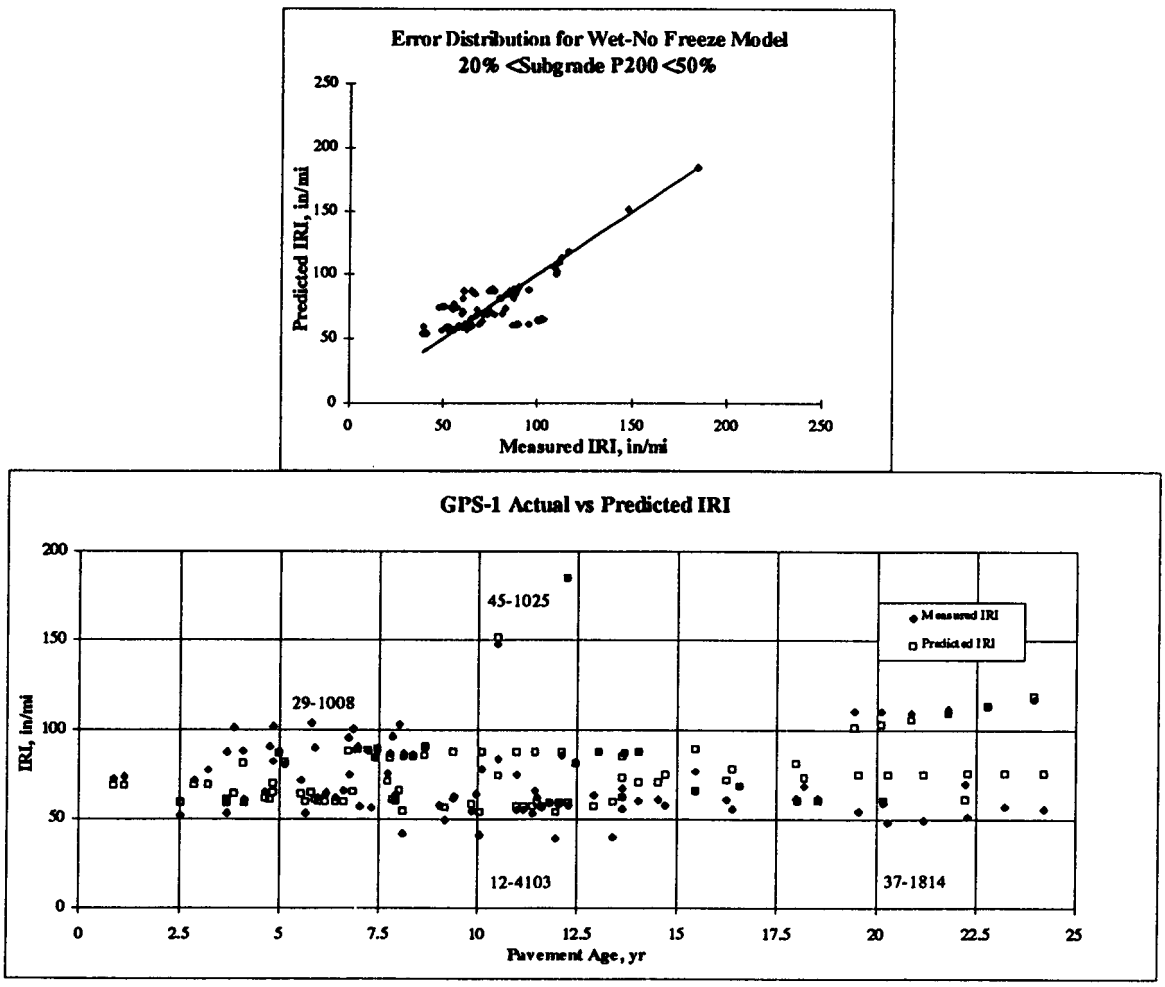

1 in/mi = 0.0158 m/km

Figure 5.2.17. GPS-1 wet-no freeze (20%<P200<50%) IRI model.

Parameter (Data Range)	Case 1	Case 2	Case 3	Case 4	Case 5
KESAL/yr (2-1100)	200	400	600	800	1000
SN (1.3-8.4)	3.2	3.2	3.2	3.2	3.2
Po, psf (75-430)	110	110	110	110	110
ACThick, in (1-13)	8	8	8	8	8
w% (1-18)	10	10	10	10	10
P200 (20-50)	30	30	30	30	30
Days90+ (8-103)	100	100	100	100	100
DaysWet/yr (80-165)	80	80	80	80	80
INITIAL IRI, in/mi =	64	64	64	64	64
Growth Rate Constant, r=	0.011	0.013	0.018	0.027	0.041

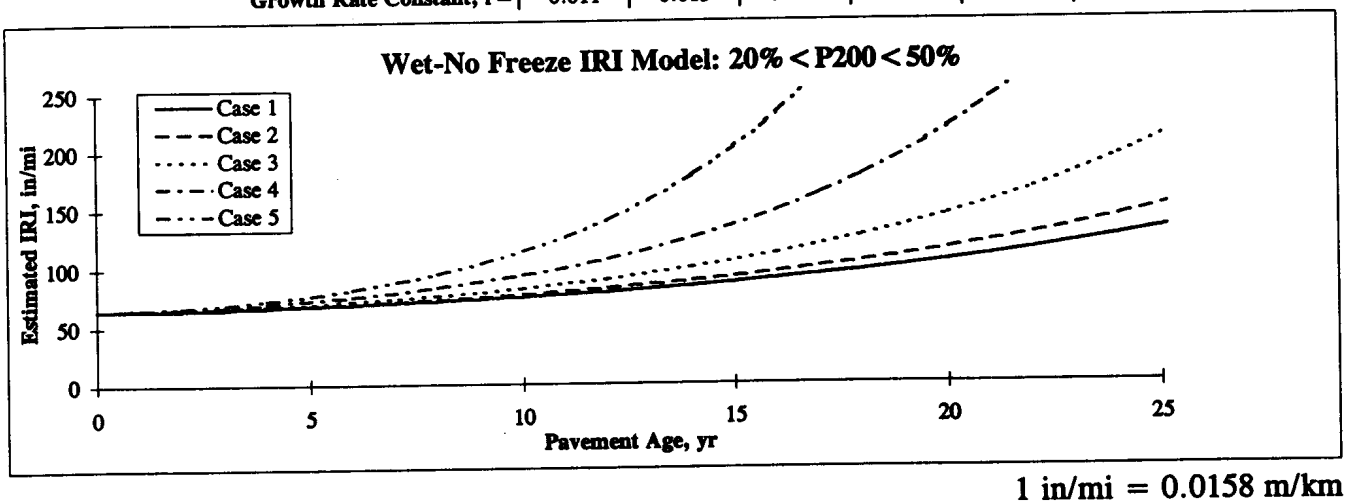

1 in/mi = 0.0158 m/km

Figure 5.2.18. Sensitivity of the wet-no freeze IRI prediction model (20% < P200 < 50%) to changes in traffic volume/yr, holding all other parameters constant.

parentheses next to the parameter name is the range of the parameter encountered in the LTPP data used to build the model.

The best long-term performer in this data set was section 37-1814 (see figure 5.2.17). This 24-year-old, 85 KESAL/yr section is characterized by high precipitation (1350 mm/yr (54 in/yr)) and very little hot weather (10 days over 32°C (90°F)). This smooth section is estimated to be approaching the end of its useful service life according to the AASHTO equation.

A very smooth pavement in this data set is section 12-4103 (see figure 5.2.17). This 12-year-old, very-high-traffic route (1126 KESAL/yr) has high precipitation (1425 mm/yr (57 in/yr)), moderate hot weather (55 days over 32°C (90°F)/yr), and has a high overburden pressure of 16.3 kPa (340 lb/ft^2) on a coarse-grained subgrade (P200 = 24 percent, w% = 7.5 percent). This section is estimated to be within its service life according to the AASHTO equation.

A poor performer in this data set was section 45-1025 (see figure 5.2.17). A preliminary analysis of this section with the AASHTO design equation indicated that this section should be approaching the end of its service life. This section has an estimated 5 KESAL/yr and has a SN of 1.65, and rests on a subgrade having a high moisture content and a high P200. Another rough pavement noted is section 29-1008 (see figure 5.2.17). This section utilizes a thick AC section of 285 mm (11.4 in) with low subgrade overburden pressure (Po = 5.6 kPa (178 lb/ft^2)). It is unclear why this section has such high IRI values early in life; perhaps construction related issues affected roughness.

Wet-No Freeze GPS-1 (P200<20 percent)

Figure 5.2.19 shows the model developed for the wet-no freeze environment with clean, coarse-grained soils (P200<20 percent). This model was based on 77 IRI measurements from 21 sections and had an average error per section of 0.19 m/km (12 in/mi). The standard deviation of the errors at the sections was 0.15 m/km (9.5 in/mi). Traffic rates varied from 36 to 660 KESAL/yr, with an average of 180 KESAL/yr for this data set. There are indications that for subgrades within this range, higher precipitation, higher P200, and higher moisture content reduce the IRI. Again, correlation of IRI to hot weather is very strong. Figure 5.2.20 shows the sensitivity of the resulting model to changes in traffic volume. Shown in parentheses next to the parameter name is the range of the parameter encountered in the LTPP data used to build the model.

$$IRI(t) = IRI_0 e^{r_0 \frac{t}{T} S}$$

$$IRI_0 = A(w\%)^B + C(SN)^D + E(P200)^F + G(ACThick)^H$$

$$r_0 = [\frac{I(KESAL/yr)^J}{K(SN)^L} + M(\frac{ACthick \times Po}{w\% \times KESAL/yr})^N + O(Days90+)^P + Q(DaysWet/yr)^R] \times 1/1000$$

A=31.966912	F=6.9990895	K=1	P=6.6583095
B=0.2839958	G=59.02204	L=77.998698	Q=2.471E+12
C=-9.857E-07	H=-1.6203565	M=33801.58	R=-4.6876717
D=9.3738374	I=2.5	N=-17.172621	S=1.0356619
E=-4.042E-08	J=1.2	O=1.595E-10	T=200

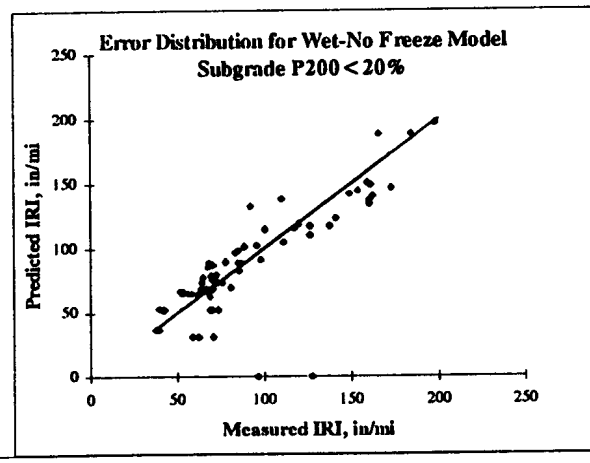

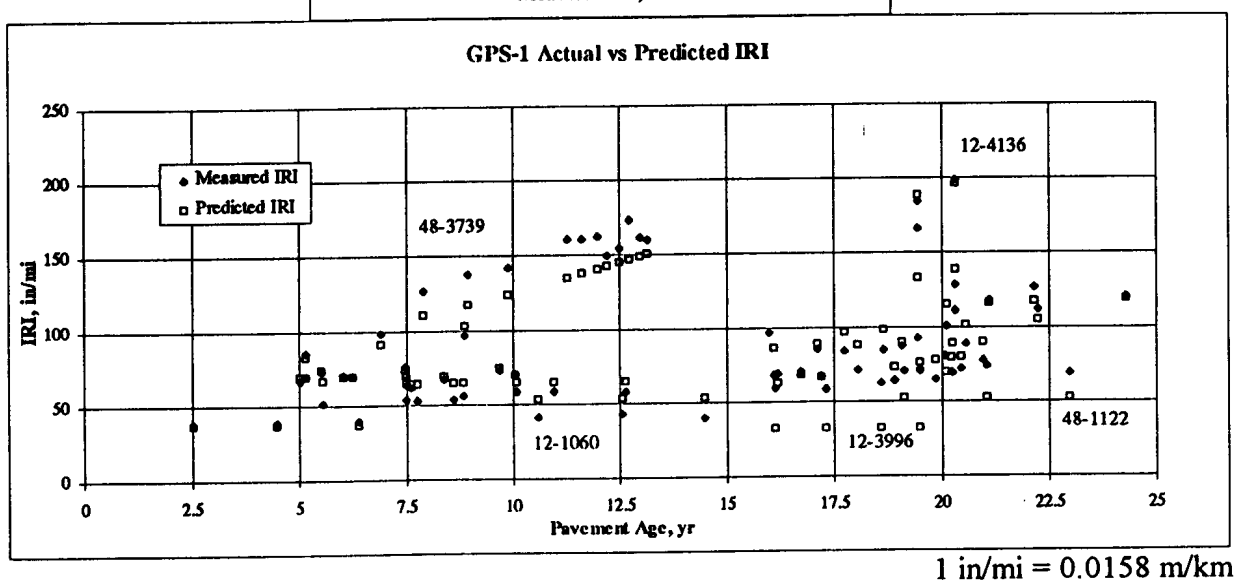

1 in/mi = 0.0158 m/km

Figure 5.2.19. GPS-1 wet-no freeze (P200<20%) IRI model.

Parameter (Data Range)	Case 1	Case 2	Case 3	Case 4	Case 5
KESAL/yr (36-660)	350	400	450	500	550
SN (1.8-6.0)	3.5	3.5	3.5	3.5	3.5
ACThick (1.3-9.4)	6	6	6	6	6
Po, psf (100-370)	120	120	120	120	120
w% (1-13)	13	13	13	13	13
P200 (0-20)	15	15	15	15	15
Days90+ (4-117)	90	90	90	90	90
DaysWet/yr (82-191)	85	85	85	85	85
INITIAL IRI, in/mi =	62	62	62	62	62
Growth Rate Constant, r=	3.88	4.00	4.83	9.71	33.86

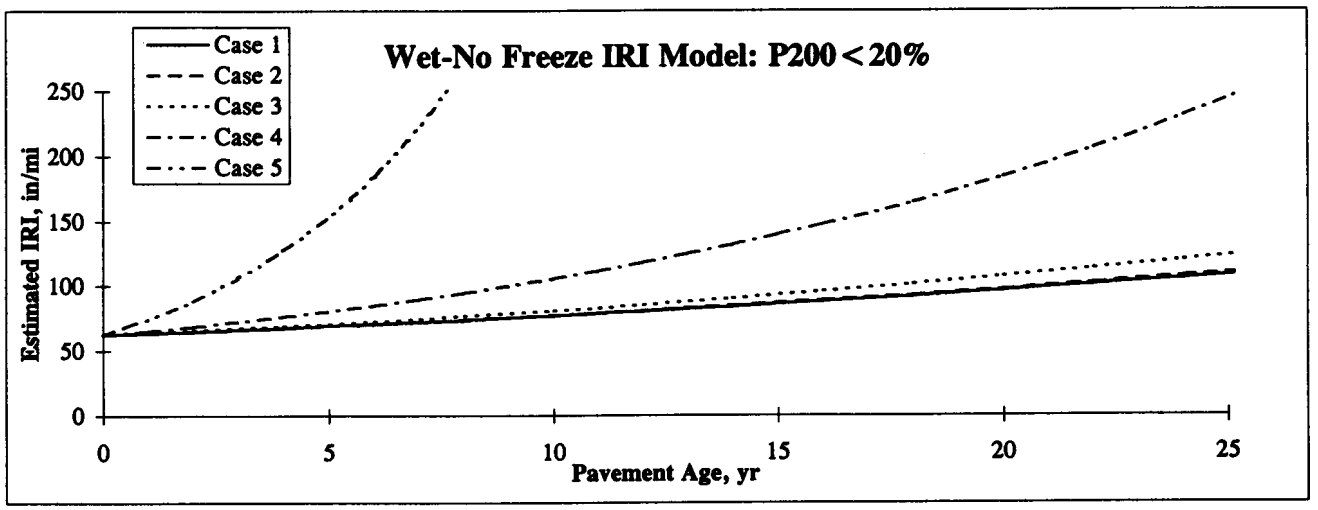

1 in/mi = 0.0158 m/km

Figure 5.2.20. Sensitivity of the wet-no freeze IRI prediction model (P200<20%) to changes in traffic volume/yr, holding all other parameters constant.

The best long-term performer in this data set was section 48-1122 (see figure 5.2.19). This 23-year-old pavement has an estimated SN of 4.3. A preliminary evaluation of this section with the AASHTO design equation indicated that the pavement section should still be within its service life. This section uses thick base and subbase layers, resulting in a subgrade overburden pressure of approximately 14.8 kPa (310 lb/ft^2). Subgrade conditions for this section are good, with a P200 content of 19.3 percent and a moisture content of 8.5 percent.

A poor performer noted in the data set is section 48-3739 (see figure 5.2.19). A preliminary evaluation of this section with the AASHTO design equation indicated that this section should still be within its service life. This section has an SN of 3.5, with a thin, 45-mm (1.8-in), AC surface, and is subjected to 155 KESAL/yr. The subgrade has a P200 of 5 percent and a moisture content of 4 percent. It is believed that the thin AC layer was the cause of the high IRI values at this section.

5.2.5 GPS-1 Summary

The models developed for the GPS-1 sections predict the development of IRI over time for flexible pavements according to the concept of exponential growth of IRI. The models predict two parameters: the initial IRI and the growth rate. The initial IRI is predicted on the basis of the structural properties of pavement layers and subgrade parameters. The growth rate is an exponentially increasing function of time and is a function of structural properties of pavement layers, subgrade and climate parameters, traffic loadings and time. The various models have average per site errors between 0.14 and 0.25 m/km (9 and 16 in/mi). Pavements in wet freeze environments resting on clean sands and gravel (P200 < 20 percent) were the least predictable type of GPS-1 pavement.

Structural factors such as SN and thickness of the AC layers have a larger role than climatic factors in roughness prediction for pavements in the no freeze environments. Performance of pavements over fine-grained soils is strongly related to the P200 and Atterberg limits of the subgrade soils. In hot climates, roughness is related to days above 32°C (90° F). In cold climates, roughness is related to freeze index and freeze-thaw cycles. In all data sets, the least predictable pavement types were pavements with thick AC layers and very thin base and/or subbase layers. These pavement types can perform either very well or very poorly but are obviously more sensitive to subgrade and climate conditions and construction procedures than pavements with thicker base and subbase layers. Higher overburden pressures on the subgrade, which reduce frost heave effects, appear to be critical for wet freeze environments and frost-

susceptible subgrades. In the wet regions, clean, coarse-grained soils with low P200, generally less than 5 percent by weight, had higher and more variable IRI than coarse-grained soils with P200 that was between 5 and 50 percent.

5.3 GPS-2: FLEXIBLE PAVEMENTS ON TREATED BASES

The time-sequence IRI values for each GPS-2 site were compiled and plotted against pavement age. Figure 5.3.1 shows the development of IRI for the GPS-2 sections classified according to LTPP regions. The general trend observed for roughness development for these sections was exponential growth. On the basis of observation of these plots, it was decided to pursue the development of prediction models based on exponential growth of IRI, as described in the previous section on GPS-1 pavements.

There are several base treatment types in the GPS-2 experiment. Table 5.3.1 shows the base types encountered in the GPS-2 database and the number of pavement sections for each base type. It was decided to build separate models for the different base types, except for the lean concrete base that did not have sufficient sections for model building. Table 5.3.2 indicates the 10 parameters that had the highest Pearson correlation coefficients to IRI, presented separately for the base types used in GPS-2 model building.

There are indications that, for the cement-treated aggregate bases, higher moisture in the subgrade and environment results in smoother conditions over time. Higher base thickness for the cement-treated aggregate bases indicate higher IRI values. The pavements with soil-cement bases showed a trend toward a lower IRI for increasing base thickness.

Traffic levels were not significant in the correlation analysis. The study of GPS-1 sections indicated that traffic effects on the IRI were generally detectable only for low SNs. Most of the GPS-2 sections have higher SN estimates, which may partially explain why traffic parameters did not correlate to IRI measurements for the GPS-2 sections.

Each model is described in the following sections along with a description of which pavement sections were showing good and poor performance within each data set. As described in section 5.2, the best and worst performers in each data set were evaluated with use of the AASHTO pavement design equation to determine if the best performers were within the service life and if the worst performers were at the end of their design life.

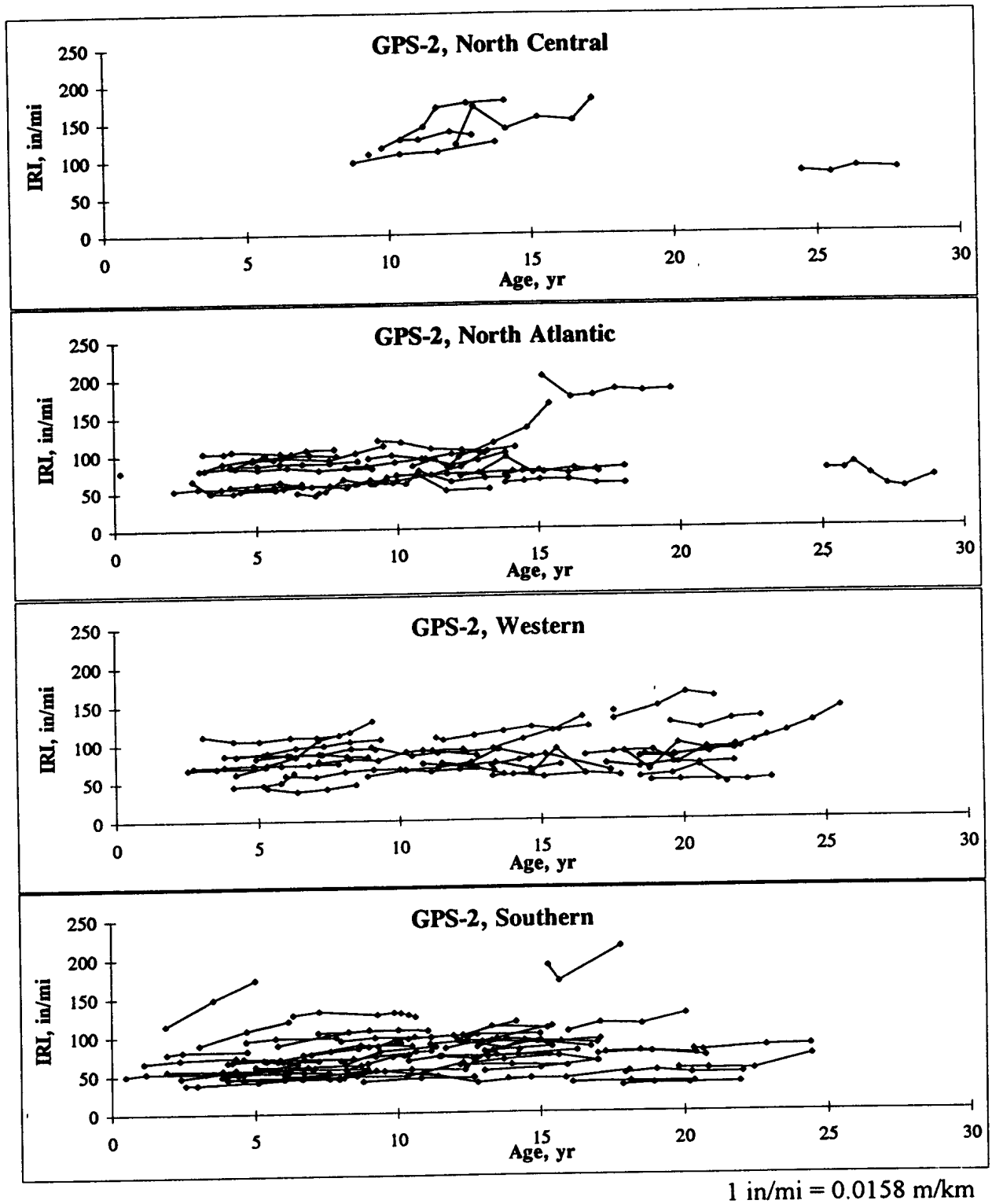

Figure 5.3.1. Plots showing the development of roughness for the GPS-2 sections within each LTPP geographical region.

Table 5.3.1. Base types included in the GPS-2 experiment.

Base Type	Number of Sections
Cement Aggregate Mixture	39
Hot Mix AC (HMAC)	27
Asphalt-Treated Mixture	18
Soil-Cement	14
Lean Concrete	6

Table 5.3.2. Parameters with highest correlation to IRI for the GPS-2 data sets (separated by base type).

AC Treated	HMAC
P200 (+.60)	SN (-.54)
P#4 (+.42)	P#4 (-.51)
PI (+.40)	Days32- (+.47)
Cum Traf (-.30)	AnnPrecip (-.46)
w% (+.22)	ACThick (-.46)
ACThick (+.17)	P200 (-.36)
SN (+.15)	BaseThick (+.24)
Days32- (+.14)	Po (-.21)
Po (-.08)	w% (+.15)
BaseThick (+.06)	LL (-.10)

Cement-Agg	Soil Cement
ACThick (-.30)	FZI (+.67)
ACThick/BaseThick (+.30)	Days32- (+.66)
%ACinSN (-.29)	BaseThick (-.56)
BaseThick (+.19)	AnnPrecip (+.39)
Days90+ (+.17)	Days90+ (-.39)
PL (-.16)	SN (-.36)
w% (-.10)	P#4 (-.32)
P200 (+.07)	Po (-.31)
-	P200 (+.29)
-	ACThick (-.23)

5.3.1 GPS-2 Asphalt-Treated Bases

Figure 5.3.2 shows the model form developed for this data set along with plots of measured versus predicted IRI shown as a line plot, and versus pavement age. This model was based on 59 IRI measurements from 15 sections and had an average error per section of 0.14 m/km (8.8 in/mi). The standard deviation of the errors at the sections was 0.11 m/km (6.7 in/mi). Traffic rates varied from 36 to 1010 KESAL/yr with an average of 230 KESAL/yr for this data

$$IRI(t) = IRI_0 e^{r_0 \frac{t^S}{T}}$$

$$IRI_0 = A(P200)^B + C(Po)^D + E(0.1 + PI)^F + G(SN)^H$$

$$r_0 = \left[\frac{I(KESAL/yr)^J}{K(SN)^L} + M(Days32-)^N + O(0.1 + PI)^P + Q(ACThick + BaseThick)^R \right] \times \frac{1}{1000}$$

A=5.375E+12	F=1.647102	K=2	P=5.973454
B=-16.515056	G=3.7768623	L=3	Q=35645608
C=1.405E+14	H=1.4903745	M=3.0725968	R=-5.2694928
D=-5.925719	I=800	N=1.4380862	S=1.01
E=-0.2137858	J=1.123564	O=3.333E-05	T=200

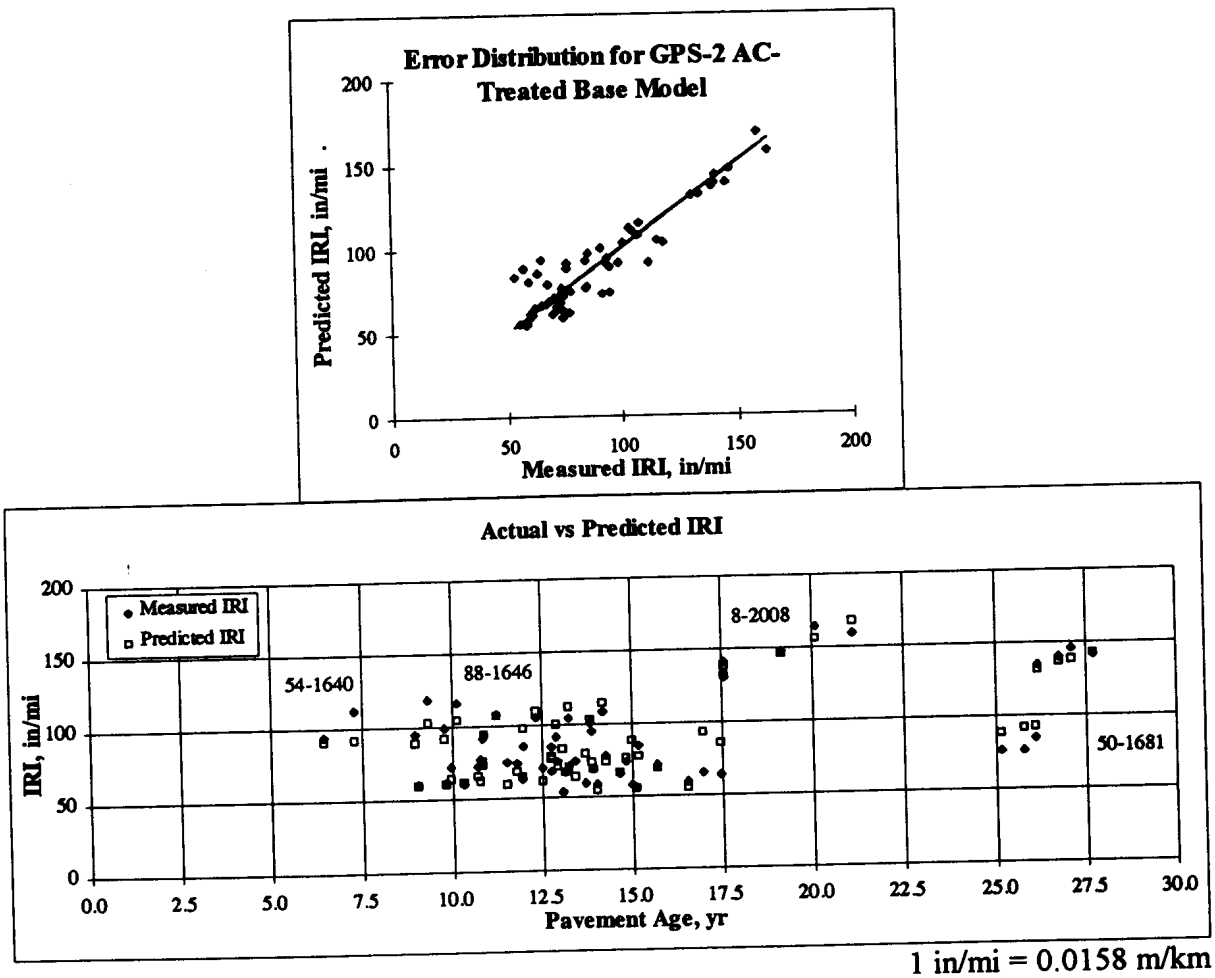

1 in/mi = 0.0158 m/km

Figure 5.3.2. GPS-2 AC-treated base IRI model.

set. Figure 5.3.3 shows the sensitivity of the resulting model to changes in subgrade conditions ranging from clean sand to fat clay. Shown in parentheses next to the parameter name is the range of the parameter encountered in the LTPP data used to build the model.

The best long-term performer is section 50-1681 (see figure 5.3.2). This 26-year-old, 70 KESAL/yr section is located in the wet freeze environment and has an estimated SN of 4.5. This section has a relatively thin AC surface layer of 58 mm (2.3 in), an asphalt-treated base layer of 85 mm (3.4 in), and a thick subbase. The subgrade is a clayey gravel with sand. A preliminary evaluation of this section with the AASHTO design equation indicated that the pavement section is still within its service life.

Section 8-2008 is a poor performer in this data set (see figure 5.3.2). A preliminary evaluation of this section with the AASHTO design equation indicated that this section is at the end of its design life. This section is located in the dry freeze region and has a AC surface of 93 mm (3.7 in) and an asphalt-treated base layer of 185 mm (7.4 in) thickness.

The other two rougher pavements noted in figure 5.3.2 are sections 88-1646 and 54-1640. Each section has approximately 500 mm (20 in) of asphalt-treated base plus AC thickness resting directly on the subgrade, and are located in the wet freeze environment. Both sections are subjected to low traffic, and a preliminary evaluation of these two sections did not indicate that they were underdesigned for the amount of traffic.

5.3.2 GPS-2 Hot Mix AC Bases

Figure 5.3.4 shows the model form developed for this data set along with plots of measured versus predicted IRI shown as a line plot, and versus pavement age. This model was based on 90 IRI measurements from 22 sections and had an average error per section of 0.22 m/km (11.8 in/mi). The standard deviation of the errors at the sections was 0.14 m/km (8.7 in/mi). Traffic rates varied from 40 to 1400 KESAL/yr with an average of 335 KESAL/yr for this data set. Figure 5.3.5 shows the sensitivity of the resulting model to changes in traffic rate for a pavement having a SN of 3, that is located in a wet environment. Shown in parentheses next to the parameter name is the range of the parameter encountered in the LTPP data used to build the model.

The best long-term performer in the data set is section 12-4100 (see figure 5.3.4), which is located in the wet-no freeze environment. This section is subjected to low traffic (46 KESAL/yr)

Parameter (Data Range)	Case 1	Case 2	Case 3	Case 4	Case 5
KESAL/yr (36-1010)	200	200	200	200	200
SN (3.8-8.4)	3.87	3.87	3.87	3.87	3.87
ACthick, in (2-15)	5.5	5.5	5.5	5.5	5.5
BaseThick, in (2-14)	5	5	5	5	5
Po, psf (118-508)	123	123	123	123	123
P200 (5-69)	5	20	33	55	69
PI (0-26)	0	3	12	22	26
Days32- (15-194)	180	180	180	180	180
INITIAL IRI, in/mi =	103	86	75	53	42
Growth Rate Constant, r=	8.19	8.19	8.29	11.77	17.86

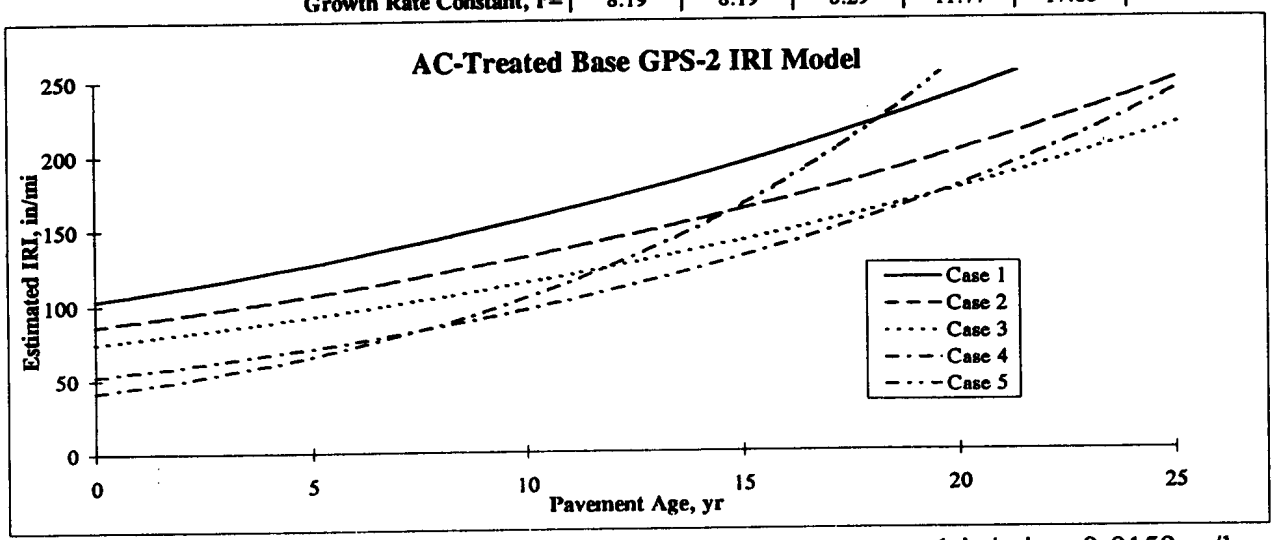

1 in/mi = 0.0158 m/km

Figure 5.3.3. Sensitivity of the AC-treated base GPS-2 model to changes in subgrade conditions.

$$IRI(t) = IRI_0 e^{r_0 \frac{t^S}{T}}$$

$$IRI_0 = A(ACThick)^B + C(BaseThick)^D + E(P\#4)^F + G(SN)^H$$

$$r_0 = \frac{I(KESAL/yr)^J}{K(SN)^L} + M(ACThick)^N + O(Days32-)^P + Q(AnnPrecip)^R$$

A= 40.8887	F= -0.8682	K= 20.7016	P= 2.3060
B= -0.5110	G= 40.0891	L= 12.00	Q= 9.70E-05
C= 1953.287	H= -0.75037	M= 2.00E-04	R= 0.1813
D= -2.95004	I= 101.57589	N= -0.2060	S= 1.2379
E= 349.64172	J= 0.6117952	O= 3.12E-09	T= 0.0226

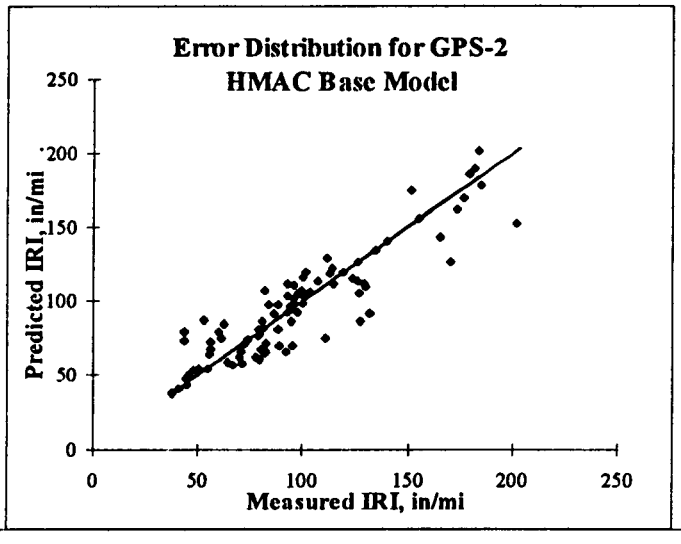

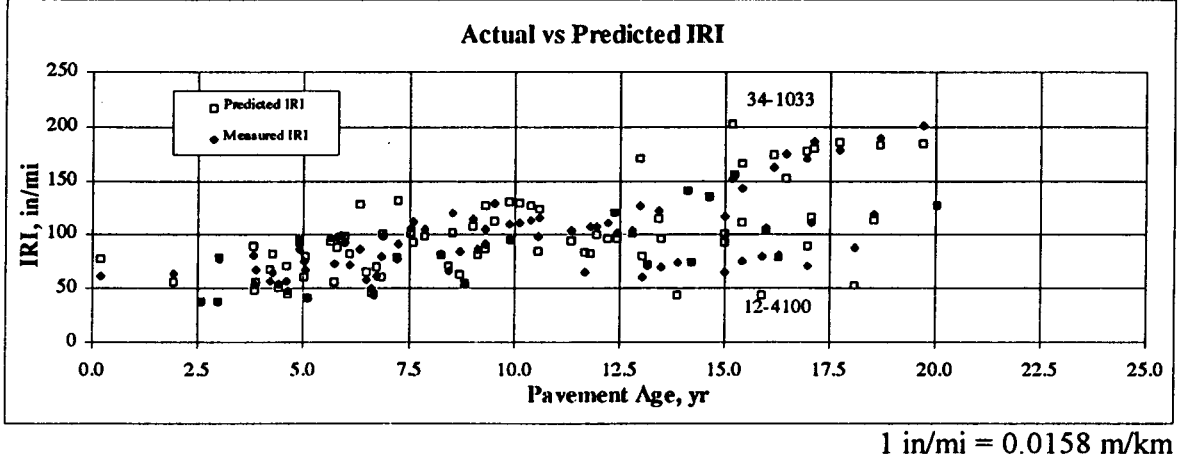

1 in/mi = 0.0158 m/km

Figure 5.3.4. GPS-2 HMAC base IRI model.

Parameter (Data Range)	Case 1	Case 2	Case 3	Case 4	Case 5
KESAL/yr (37-1400)	50	200	500	900	1400
SN (2.9-6.4)	3	3	3	3	3
ACthick, in (1-6)	4	4	4	4	4
BaseThick, in (4.5-12.7)	5	5	5	5	5
P#4 (50-100)	75	75	75	75	75
Days32- (16-190)	125	125	125	125	125
AnnPrecip, in (15-70)	24	24	24	24	24
INITIAL IRI, in/mi =	63	63	63	63	63
Growth Rate Constant, r =	0.0006	0.0008	0.0010	0.0011	0.0013

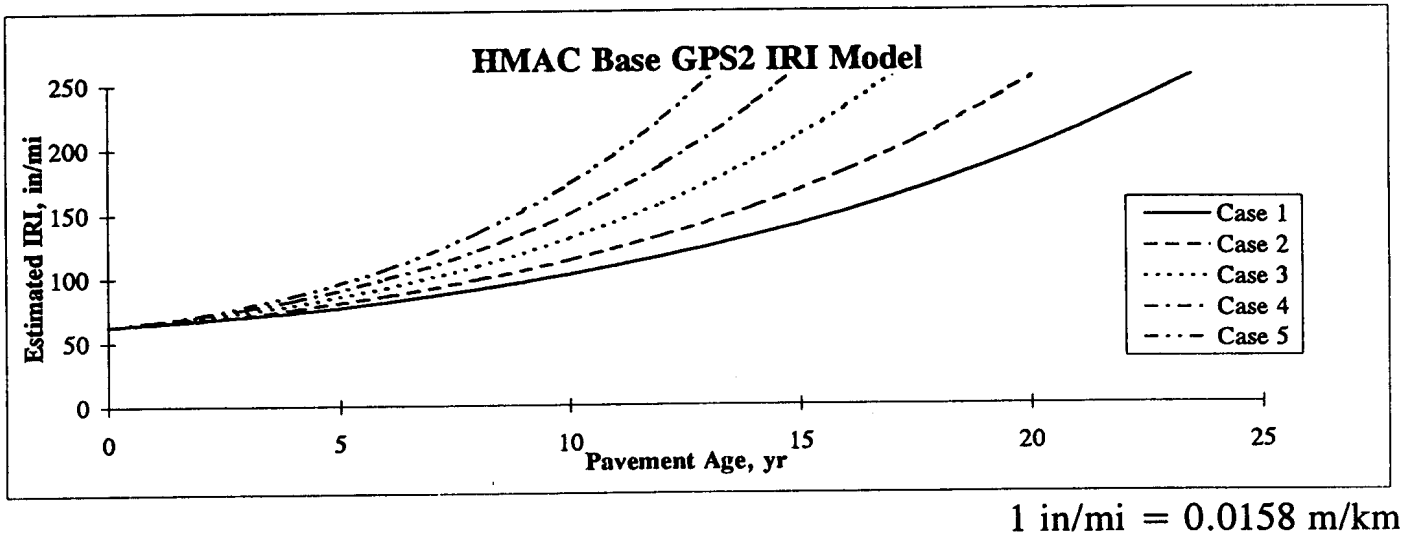

1 in/mi = 0.0158 m/km

Figure 5.3.5. Sensitivity of the HMAC base GPS-2 IRI model to changes in traffic volume, holding all other parameters constant.

and has a SN of approximately 4.7. The preliminary evaluation of this section with the AASHTO design equation indicated the pavement section is still within its service life. The annual precipitation at this location is very high with 1750 mm/yr (70 in/yr) but the section rests on a clean sand subgrade (P200 = 7 percent, w% = 3 percent). The section consists of 73 mm (2.9 in) of AC, 190 mm (7.6 in) of HMAC base, and approximately 300 mm (12 in) of subbase.

The section with the highest IRI is section 34-1033 (see figure 5.3.4), which is located in a wet freeze environment on a frost-susceptible subgrade (P200 = 23 percent, w% = 8 percent, FZI = 219 °C days/yr (395 °F days/yr) , precipitation = 1200 mm/yr (48 in/yr)). This section is subjected to a low traffic rate of 37 KESAL/yr, and the pavement section consists of 30 mm (1.2 in) of AC over 155 mm (6.2 in) of base.

5.3.3 GPS-2 Cement-Aggregate Mixture Bases

Figure 5.3.6 shows the model form developed for this data set along with plots of measured versus predicted IRI shown as a line plot, and versus pavement age. This model was based on 161 IRI measurements from 35 sections and had an average error per section of 0.21m/km (13 in/mi). The standard deviation of the errors at the sections was 0.17 m/km (13 in/mi). Traffic rates varied from 4 to 370 KESAL/yr with an average of 107 KESAL/yr for this data set. Figure 5.3.7 shows the sensitivity of the resulting model to changes in layer thickness, holding all other parameters constant for a dry environment. Shown in parentheses next to the parameter name is the range of the parameter encountered in the LTPP data used to build the model.

The best long-term performer in this data set is section 6-8149 (see figure 5.3.6). This 22- year-old section is located in a very hot and dry-no freeze environment, which has an annual precipitation of 175 mm (7 in) and 149 days above 32°C (90°F). This is a very-high-traffic (720 KESAL/yr) section with thin pavement layers (AC = 133 mm (5.3 in), Base = 125 mm (5 in)). The dry climate together with the good subgrade conditions (P200 = 20 percent, w% = 5 percent) may have been the primary factors that contributed to the excellent long-term performance.

The worst performer in the data set is section 5-2042 (see figure 5.3.6). A preliminary evaluation of this section with the AASHTO design equation indicated that it is approaching the end of its service life. This section is located in a wet no-freeze environment on a high P200 and high-water-content subgrade. Section 48-3679 (see figure 5.3.6) is showing a rapid increase in

$$IRI(t) = IRI_0 e^{r_0 \frac{t^U}{V}}$$

$$IRI_0 = A(ACThick)^B + C(w\%)^D + E(P200)^F + G(Po)^H$$

$$r_0 = \left[\frac{I(KESAL/yr)^J}{K(SN)^L} + M(AnnPrecip)^N + O\left(\frac{Days90}{ACThick}\right)^P + Q\left(\frac{P200 * w\% * FrzThwCyc}{ACThick * Po}\right)^R + S(ACThick)^T \right] \times \frac{1}{1000}$$

A=175.72255	F=-0.0412061	K=0.0885887	Q=0.2
B=-2.7528761	G=-829.64201	L=30.697898	R=1.3
C=-302.51141	H=-0.5603349	M=2.557E-08	S=4000
D=-1.9703234	I=20.989881	N=6.5330335	T=-0.15
E=123.57391	J=6.6289015	O=3.788E-08	U=1.01
		P=6.7857038	V=200

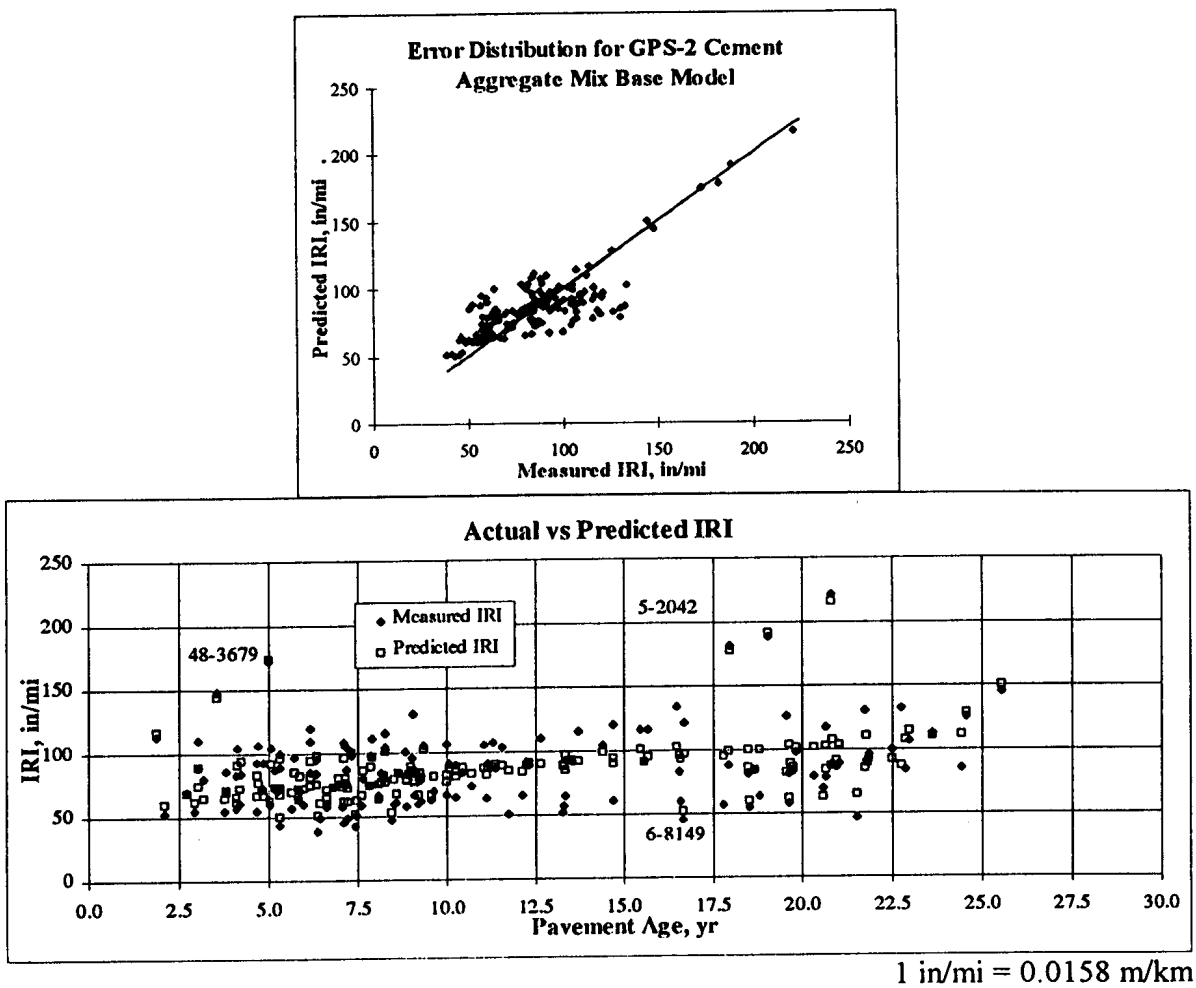

1 in/mi = 0.0158 m/km

Figure 5.3.6. GPS-2 cement-aggregate mixture base IRI model.

Parameter (Data Range)	Case 1	Case 2	Case 3	Case 4	Case 5
KESAL/yr (13-1057)	250	250	250	250	250
SN (3.5-7.5)	5.79	5.80	5.79	5.79	5.79
ACThick, in (1.6-9.9)	3	3.5	4	4.5	5
Po, psf (102-520)	220	217	213	210	206
w% (3-39)	9	9	9	9	9
P200 (9-94)	25	25	25	25	25
AnnPrecip, in (6-60)	10	10	10	10	10
FrzThwCyc (4-158)	12	12	12	12	12
Days90+ (0-159)	155	155	155	155	155
INITIAL IRI, in/mi =	72	69	67	66	64
Growth Rate Constant, r =	19.38	8.93	5.52	4.21	3.64

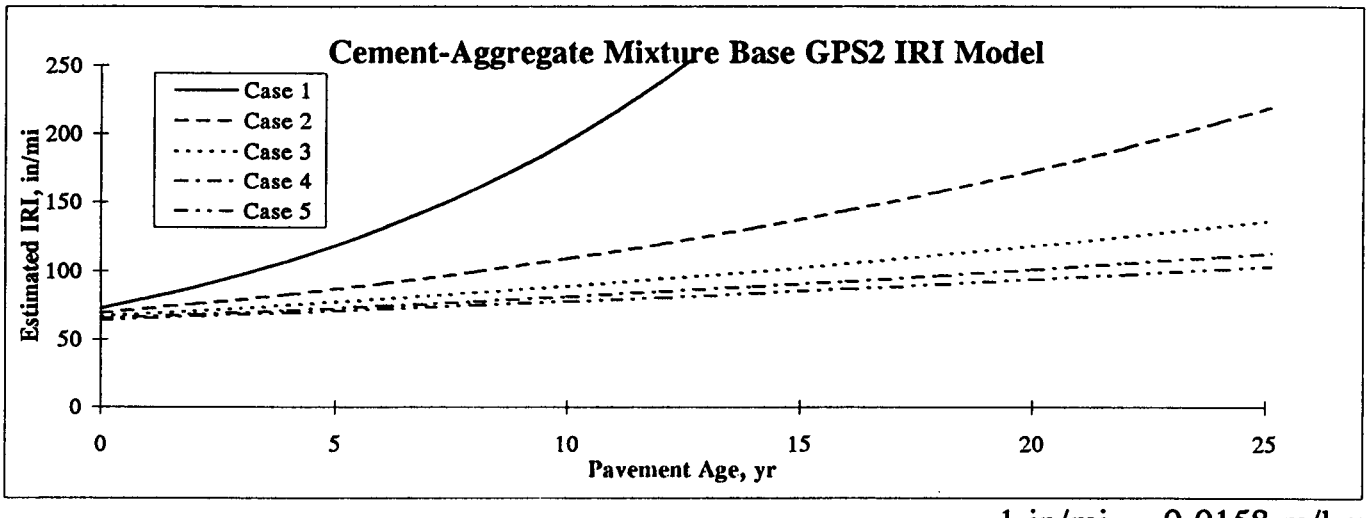

1 in/mi = 0.0158 m/km

Figure 5.3.7. Sensitivity of the cement-aggregate base model to changes in layer thickness, holding all other parameters constant.

IRI at a very early age. This section has a low AC thickness of 40 mm (1.6 in) over a thick base (210 mm (8.4 in)). The subgrade has a high P200 (66 percent) and a high plasticity index.

5.3.4 GPS-2 Soil-Cement Bases

Figure 5.3.8 shows the model form developed for this data set along with plots of measured versus predicted IRI shown as a line plot, and versus pavement age. This model was based on 47 IRI measurements from 14 sections and had an average error per section of 0.13 m/km (8 in/mi). The standard deviation of the errors at the sections was 0.10 m/km (6.6 in/mi). Figure 5.3.9 shows the sensitivity of the resulting model to changes in subgrade conditions, holding all other parameters constant, for a wet-no freeze environment. Shown in parentheses next to the parameter name is the range of the parameter encountered in the LTPP data used to build the model. There are very few sections in this data set, and little variation in behavior is seen between the pavements in this data set.

The best long-term performer in the data set is section 28-3090 (see figure 5.3.8). This section has extremely low traffic (5 KESAL/yr) with a fairly thick section (SN = 4.6, AC = 63 mm (2.5 in), base = 135 mm (5.4 in)). A preliminary evaluation of this section with the AASHTO design equation indicated that the pavement section is still within its service life.

5.3.5 GPS-2 Summary

The stabilized base types that are in the GPS-2 experiment are cement-aggregate mixtures, hot mix AC, asphalt-treated mixtures, soil-cement, and lean concrete. Models for predicting IRI were developed for all these base types except for lean concrete, which did not have sufficient sections for model building. The models that were developed predict the development of IRI over time according to the concept of exponential growth of IRI. The models predict two parameters: the initial IRI and the growth rate. The initial IRI is predicted on the basis of the structural properties of pavement layers and subgrade parameters. The growth rate is an exponentially increasing function of time and is a function of structural properties of pavement layers, subgrade and climate parameters, traffic loadings, and time.

The general trends for GPS-2 sections were similar to the trends observed for GPS-1 sections. Generally, poor performance was observed for GPS-2 sections that had a low total pavement thickness and were located in the freeze regions and also in cases where they were utilized over high-moisture-content subgrade. A reduction in the total pavement thickness can be

$$IRI(t) = IRI_0 e^{r_0 \frac{t^S}{T}}$$

$$IRI_0 = A(1+PI)^B + C(w\%)^D + E(Po)^F + G(P200/Po)^H$$

$$r_0 = \left[\frac{I(KESAL/yr)^J}{K(SN)^L} + M(w\% \times AnnPrecip \times FZI/10 \times Po)^N + O(AnnPrecip)^P + Q(\frac{100*P200*w\%}{Po})^R\right] \times \frac{1}{1000}$$

A=-38.971342	F=-0.0015447	K=2	P=-0.3137206
B=0.0927331	G=-14362.11	L=3.5	Q=0.1
C=6.135E-05	H=-0.0001067	M=77325.96	R=1
D=4.150747	I=2812.9537	N=0.0019983	S=1.01
E=14572.344	J=1.2901464	O=-257547.04	T=200

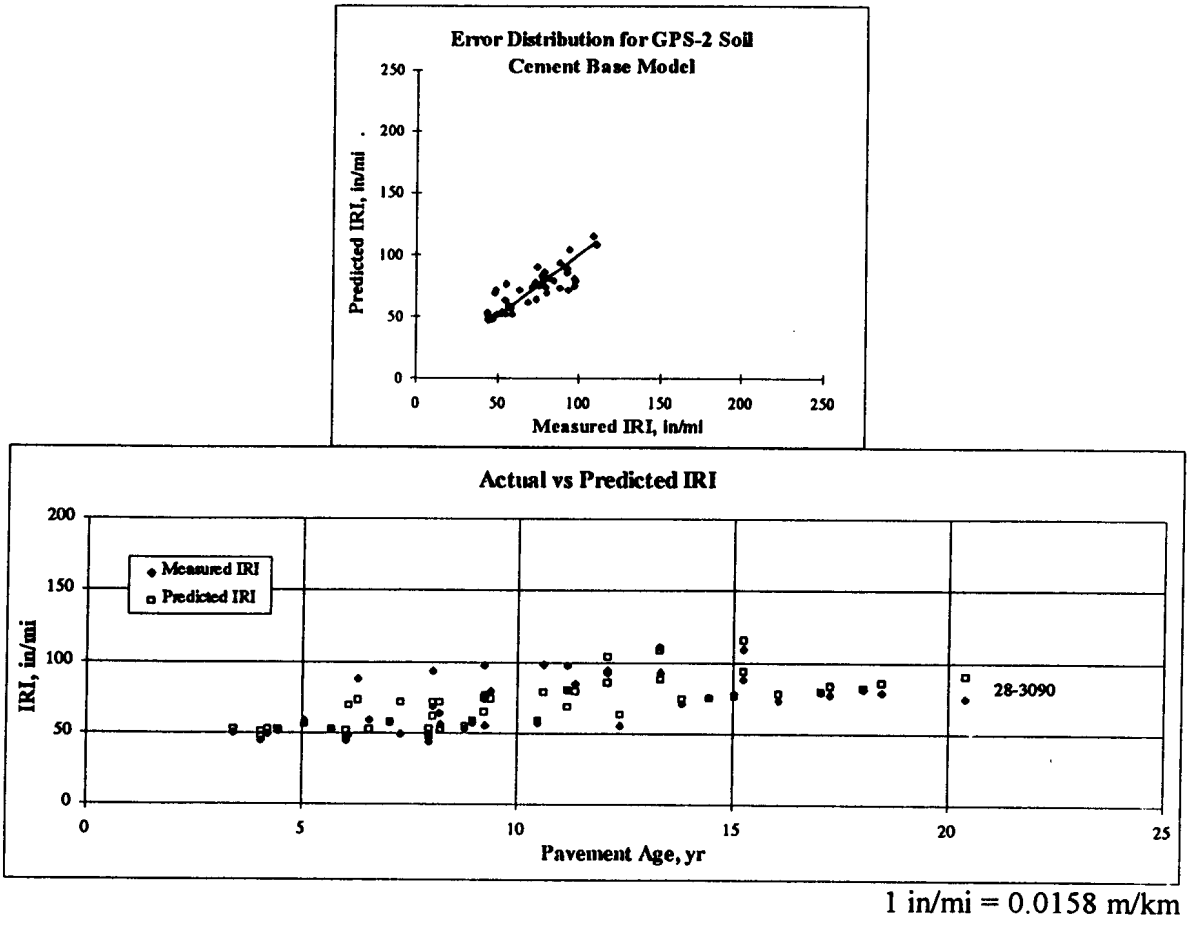

Figure 5.3.8. GPS-2 soil-cement base IRI model.

Parameter (Data Range)	Case 1	Case 2	Case 3	Case 4	Case 5
KESAL/yr (4-370)	120	120	120	120	120
SN (2.2-9)	3	3	3	3	3
Po, psf (70-300)	130	130	130	130	130
PI (0-11)	0	0	0	4	11
P200 (1.4-84)	1.4	20	50	70	84
w% (4-19)	4	8	12	16	19
AnnPrecip, in (44-63)	48	48	48	48	48
FZI (4-241)	150	150	150	150	150
INITIAL IRI, in/mi =	55	60	62	61	64
Growth Rate Constant, r =	15.83	15.95	16.04	16.13	16.19

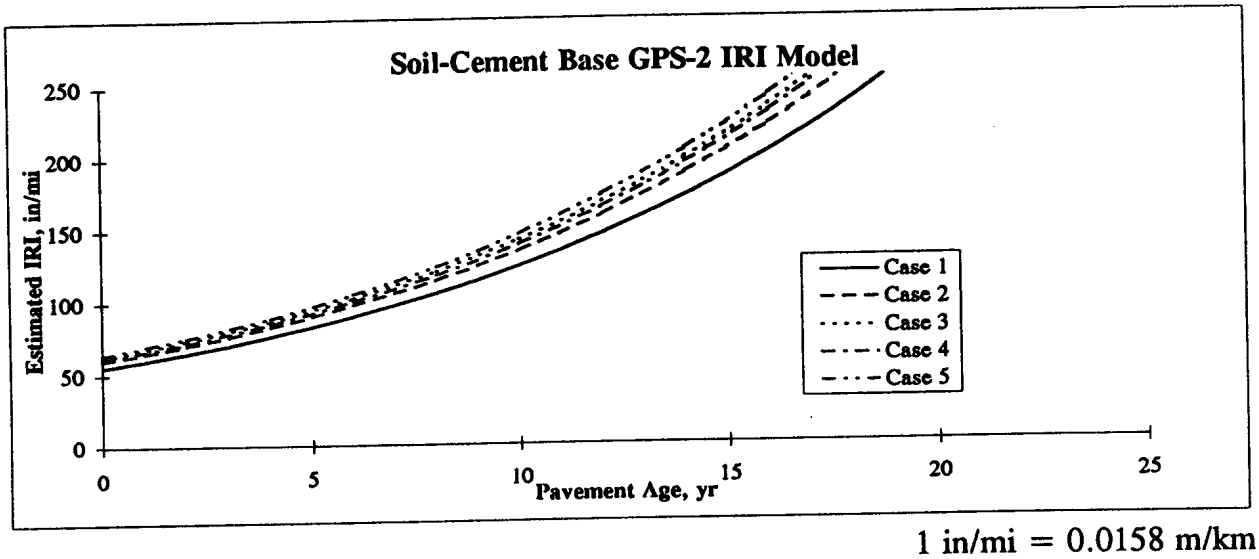

1 in/mi = 0.0158 m/km

Figure 5.3.9. Sensitivity of the GPS-2 soil cement base model to changes in subgrade conditions.

achieved by utilizing a stabilized base as opposed to a granular base or subbase layers. However, this results in a low overburden pressure on the subgrade, and was considered to be a primary cause for the poor performance that was described.

5.4 GPS-3: JOINTED PLAIN CONCRETE PAVEMENTS

The time-sequence IRI values for each GPS-3 site were compiled and plotted against pavement age. Figure 5.4.1 shows the development of IRI for the GPS-3 sections classified according to the LTPP regions. The general trend observed for roughness development over the typical range of IRI observed is either logistic or exponential growth. Logistic growth is characterized by a leveling off of the IRI development as the pavement ages. This is often referred to as S-curve type development. A logistic growth model appears similar to exponential growth in the early stages but then levels off over time. The general model form used for the GPS-3 pavements was:

$$IRI(t) = e^{r_0 t}\left[\frac{IRI_{\max} \times IRI_0}{IRI_0(e^{r_0 t} - 1) + IRI_{\max}}\right]$$

where:

IRI_0 = estimated initial IRI (after some initial traffic loading),
= f (design properties of pavement and subgrade properties),
IRI_{max} = estimated long-term IRI,
= f (design properties of pavement and subgrade properties),
r_0 = growth rate constant,
= f (climate, traffic, subgrade, and design properties of pavement),
t = time in years, and
e = the exponential function.

In this model, IRI_0 represents the IRI value of the pavement after it has been opened to traffic and has been subjected to some initial traffic loading. GPS-3 sections consist of sections that have doweled as well as undoweled joints. It is well known that doweled pavements behave differently than undoweled pavements. In wet regions (annual precipitation greater than 500 mm (20 in)), the data were divided according to the joint type. In dry regions (annual precipitation

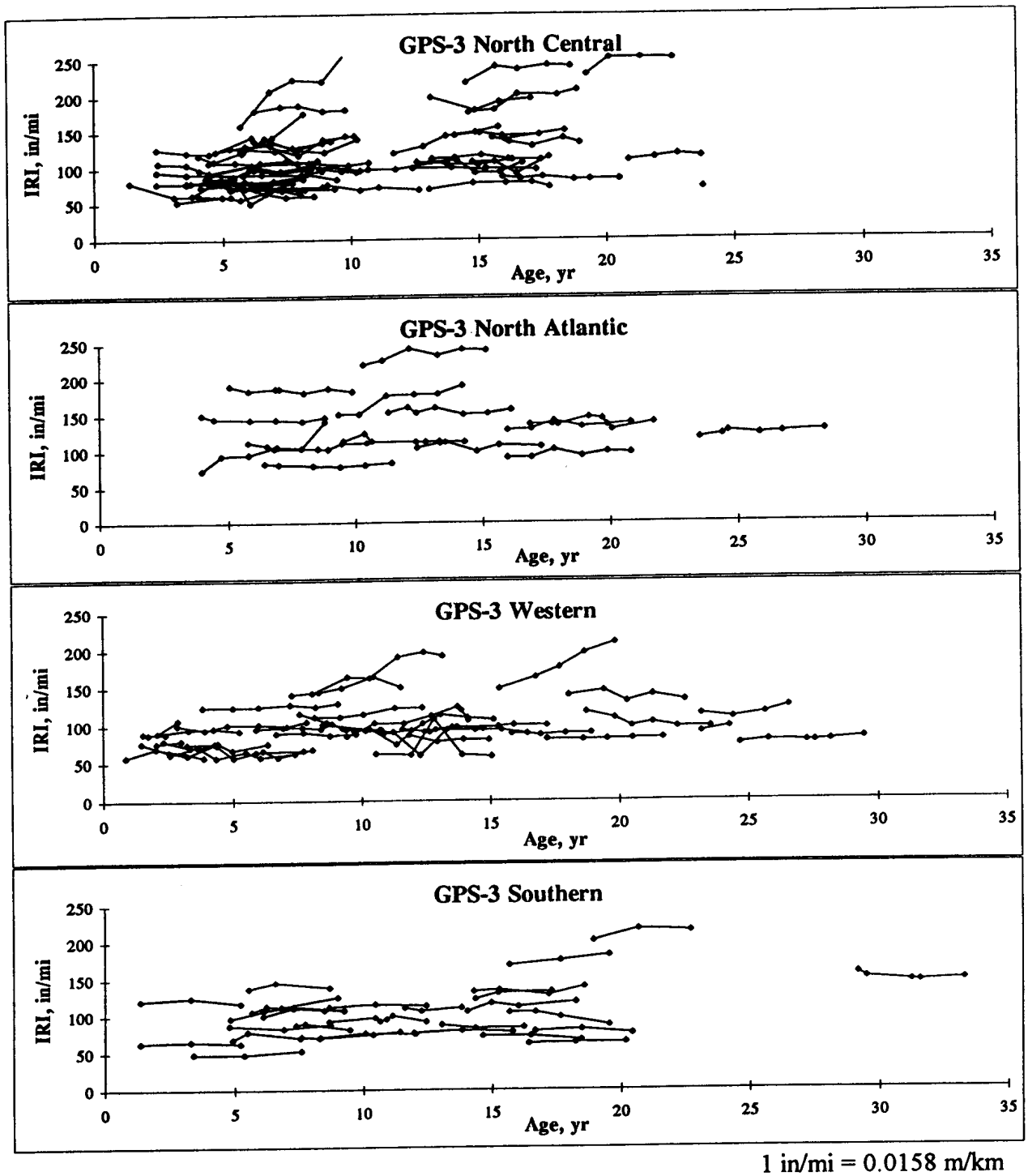

Figure 5.4.1. Trends in IRI development for GPS-3 sections according to LTPP regions.

less than 500 mm (20 in)), 69 percent of the pavements were undoweled, 13 percent were doweled, and the joint type was not known for 18 percent of the sections. Sufficient sections were not available in the dry regions to build a separate model for the doweled sections: therefore, it was decided to build one model for dry regions by considering all sections. Fairly good models were obtained for the undoweled pavements in the wet regions and for the pavements in the dry regions. Modeling attempts were not as successful for the doweled pavements in the wet regions. The correlations shown in table 5.4.1 reflect these trends.

Table 5.4.1. Ten parameters with highest correlations to IRI for GPS-3 sections.

Wet Regions Doweled GPS-3	Wet Regions Undoweled GPS-3	Dry Regions (All Joint Types)
Age (+.31)	EMOD (+.53)	Age(+.41)
Days90+ (-.21)	KESAL/yr (-.52)	PCCth (+.37)
FrzThwCyc (+.19)	Poissons Ratio (+.39)	JointSpace (+.31)
f, lb/cyd (+.18)	Comp (+.34)	Poissons Ratio (-.25)
cement (+.17)	Days90+ (-.34)	w% (+.23)
Days.5"+ (-.16)	P200 (+.33)	FrzThwCyc (+.22)
AnnPrecip (-.14)	c, lb/cyd (+.33)	Po (+.21)
air, % (-.13)	w/c (-.31)	f, lb/cyd (-.21)
SplitTensile (+.12)	DaysWet/yr (+.30)	BaseThick (+.15)
unitwt (-.12)	PCCth (+.27)	PL (-.13)

The correlations for the doweled sections located in wet regions, although rather insignificant, seem to indicate that pavements existing in cooler climates, with higher freezing, which utilize higher cement content and more fine aggregate will be rougher pavements. This can be explained in the context of brittleness and frost heave. Higher freezing, of course, means higher frost heave potential. Mixes with higher cement content and fine aggregate will generally have more brittle behavior and will suffer more shrinkage resulting in greater joint openings. This would result in higher dowel-bearing stresses. The joint spacings for the doweled GPS-3 pavements vary from 4.3 m (14 ft) to 9.1 m (30 ft), with an average of 5.8 m (19 ft). Most of these pavements are shorter than the critical slab length of $6\ell\sqrt{2}$, where ℓ is the radius of relative stiffness of the pavement system. For a 229-mm- (9-in-) thick slab on a typical granular subgrade, this critical slab length would be approximately 8 m (26 ft). As slab length approaches the critical slab length, bending stresses and deflections from combined curling, warping, and loads reach a maximum. There is a slight trend toward increasing IRI for increasing slab length (correlation coefficient of +.11) for the doweled GPS-3 sections.

The correlations for the undoweled sections show a strong negative correlation to traffic rates. This is due to the presence of several early-age sections that are very rough after very little cumulative traffic. These sections will be discussed in more detail later. In general, the trends show that higher precipitation, with more fines and water in the subgrade, tends to result in higher IRI values. This is intuitively correct as these trends in climate and subgrade conditions would tend to increase erosion/faulting potential. There is a slight trend for decreased IRI for increased joint spacing. The joint spacings for the GPS-3 pavements vary from 4.3 m (14 ft) to 9.1 m (30 ft), with an average of 5.8 m (19 ft). Most of these pavements are shorter than the critical slab length. Curling and warping effects should increase as slab length increases. However, it is believed that pavements with very short joint spacing would be more susceptible to slab rocking from settlement as the aggregate interlock diminishes over time at the joints. The PCC mix parameters are also strong factors relating to IRI. The trends seem to indicate that higher water to cement ratios with lower cement contents are resulting in smoother pavements. This can be explained in the context of workability and early-age curling and warping of the slabs. A very low water to cement ratio mix with very little cement and water would likely not be a workable mix. Low water to cement ratio mixes with high cement and water contents would likely generate more heat during hydration causing more extreme temperature gradients at set. This mix would also gain more strength at a faster rate, perhaps allowing more early-age curling effects because of less relaxation of stresses and strains during early temperature swings. However, this type of mix would be expected to be more durable over the long term.

The correlations for the dry regions seem to indicate that pavements that are thicker with longer joint spacing will have increased roughness. Dry environments would be more likely to develop significant moisture gradients through the thickness of the slab, perhaps developing more warping within the slabs. Higher subgrade moisture contents and higher freeze-thaw cycles per year indicate increased roughness.

5.4.1 Doweled GPS-3 in Wet Environment

IRI Prediction Model

Figure 5.4.2 shows the model that was developed for prediction of IRI for doweled GPS-3 sections in wet climates where annual precipitation is greater than 508 mm (20 in). This model was based on 136 IRI measurements from 30 sections and had an average error per section of 0.25 m/km (16.1 in/mi). The standard deviation of the errors at the sections was 0.21 m/km (13.6 in/mi). Traffic rates varied from 20 to 950 KESAL/yr with an average of 280 KESAL/yr for this

$$IRI(t) = e^{r_0 t}\left[\frac{IRI_{max} \times IRI_0}{IRI_0(e^{r_0 t} - 1) + IRI_{max}}\right]$$

$$IRI_0 = A(W/C \times 100)^B + C(\frac{P200}{Po})^D + E(JointSpace)^F + G(w\%)^H$$

$$IRI_{max} = W(PCCth)^X + Y(W/C \times 100)^Z + AA(P200 \times w\%)^{BB} + CC(JointSpace)^{DD}$$

$$r_0 = [I(PCCth)^J + K(SplitTensile/10)^L + M(EMOD/100000)^N + O(FrzThwCyc)^P + Q(cement)^R + S(DaysWet/yr)^T + U(KESAL/yr)^V] \times 1/10000$$

A= -6.554E+11	H= 0.08403437	O= 0.45640911	V= -1.9594221
B= -6.8246703	I= 126625.341	P= 1.26188093	W= 1512892.36
C= -8.470891	J= -3.7821891	Q= 0.1663822	X= -5.0282439
D= -0.0022624	K= -252.30118	R= 0.57651795	Y= -0.0001979
E= 0.01120562	L= 0.33965894	S= -4.8230202	Z= 3.21849506
F= 1.1341688	M= 223.618991	T= 0.96836712	AA= 0.00077479
G= 68.9381288	N= 0.53868136	U= -93734.541	BB= 1.74421201
			CC= 7.4137E-05
			DD= 5.4931273

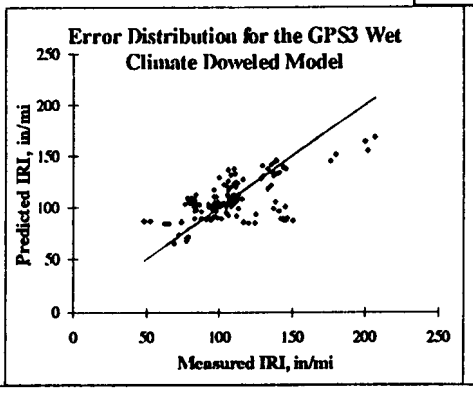

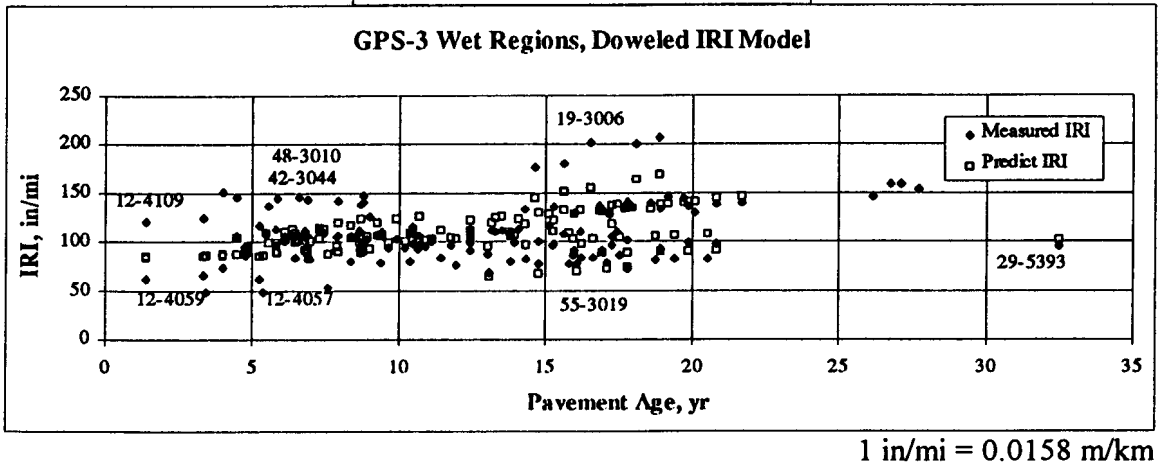

1 in/mi = 0.0158 m/km

Figure 5.4.2. GPS-3 wet regions, doweled joint IRI model.

data set. Most of the sections in this data set are less than 20 years old and have IRI values less than 2.37 m/km (150 in/mi). Figure 5.4.3 shows the sensitivity of the doweled GPS-3 model to changes in climate conditions. Shown in parentheses next to the parameter name is the range of the parameter encountered in the LTPP data used to build the model.

There was a very large variation in IRI values for sections less than 10 years old. For example, two sections in Florida, sections 12-4109 and 12-4059 (see figure 5.4.2), have virtually identical parameters but very different IRI. There are thick pavements at both extremes in IRI. There are pavements that are performing quite well as well as pavements that are performing poorly that are both located on poor subgrades. There are also sections of lower than average and higher than average split tensile strength on each extreme. All of these observations shed light on the reasons why correlations were small and modeling attempts were not as successful for these pavements as they were for the undoweled sections and the sections in the dry regions. The model is capturing the general trends but is not predicting the IRI values very accurately.

Performance of Specific Sections

The following discussion presents a qualitative analysis of the doweled GPS-3 pavement sections located in wet environments that exist at the extremes in performance. The analysis looks at high IRI pavements, low IRI pavements, and young pavements that had very different IRI values. The sections discussed are indicated in the bottom portion of figure 5.4.2.

The two smoothest pavements, which are more than 15 years old are sections 29-5393 and 55-3019. Section 29-5393 was approximately 33 years old at the time it was last profiled, and is subjected to a very low traffic level of 28 KESAL/yr. The section has 9-m (30-ft) joint spacing, 203-mm (8-in) slab thickness, and 32-mm (1.25-in) dowels resting on a thin granular base. The subgrade consisted of a wet clay (P200 = 70 percent, w% = 25 percent). The section is located in the wet freeze environment (precipitation = 950 mm/yr (38 in/yr), FZI=301 °C days/yr (542 °F days/yr)), with over 30 days above 32°C (90°F). Section 55-3019 is also a low traffic section (estimated 62 KESAL/yr), is 19 years old, and has an IRI of 1.1 m/km (72 in/mi). This section has a 4.6-m (15.1-ft) joint spacing, 224-mm (8.8-in) slab thickness, 25.4-mm (1-in) dowels, a granular base, and rests on a granular subgrade (P200 = 8.6 percent, w% = 5 percent). The section is located in the wet freeze environment (precipitation = 825 mm/yr (33 in/yr), FZI=1266 °C days/yr (2278 °F days/yr)). The low traffic volumes at these two sections may have been one reason for the low roughness.

Parameter (Data Range)	Case 1	Case 2	Case 3	Case 4	Case 5
PCCth, in (6 to 13)	9	9	9	9	9
SplitTensile, psi (486 to 738)	730	730	730	730	730
EMOD, psi (3,350,000 to 5,675,000)	5500000	5500000	5500000	5500000	5500000
w/c (0.31 to 0.7)	0.4	0.4	0.4	0.4	0.4
cement, lb (450 to 560)	550	550	550	550	550
Po, psf (100 to 440)	180	180	180	180	180
P200 (1 to 97)	95	95	95	95	95
w% (4 to 28)	25	25	25	25	25
DaysWet/yr (96 to 199)	96	110	130	150	170
FrzThwCyc (2 to 108) =	28	48	68	88	108
Kesal/yr (20 to 950)	650	650	650	650	650
JointSpace, ft (14.5 to 30)	20	20	20	20	20
IRI@25yr	244	230	208	189	172
INITIAL IRI, in/mi =	75	75	75	75	75
Growth Rate constant =	0.052	0.049	0.045	0.040	0.036
IRI(max) =	1634	1634	1634	1634	1634

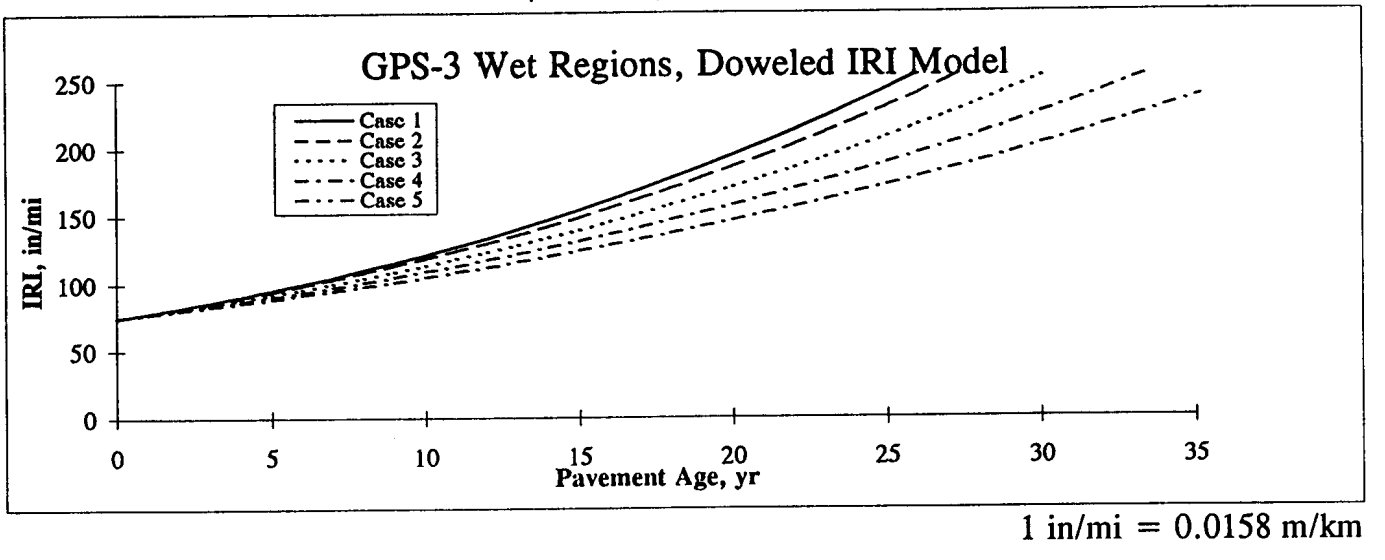

1 in/mi = 0.0158 m/km

Figure 5.4.3. Sensitivity of the GPS-3 (doweled) wet regions IRI model to changing climate conditions.

Sections 12-4109 and 12-4059 are both located in Florida and have similar parameters except for the IRI values and base type. These two sections had IRI measurements taken between the ages of 1 and 5 years. Both sections have low PCC thickness (180 mm (7.1 in) and 162 mm (6.4 in)), respectively, with medium traffic volume (169 KESAL/yr). The smoother section (12-4059) has a base that consists of a thin AC layer over a cement-aggregate mixture whereas the rougher section has only a cement-aggregate mixture. The PCC parameters reported indicate that the sections used a lower cement content of 301 kg/m^3 (508 lb/yd^3), but these values were higher than all of the other GPS-3 sections in Florida. With the exception of different base types, it is unclear as to why these similar sections have such different IRI at early ages.

The pavement that shows the highest IRI value in the data set is section 19-3006. This section consists of a 226-mm (8.9-in) thick slab with 6.1-m (20-ft) joint spacing resting on a 109-mm- (4.3-in-) thick cement-aggregate mixture base. Although this section has a low PCC split tensile strength 3403 kPa (494 psi), it has a relatively high elastic modulus and compressive strength.

5.4.2 Undoweled GPS-3 in Wet Environment

IRI Prediction Model

Figure 5.4.4 shows the IRI prediction model developed for undoweled pavements in the wet environment. This model was based on 104 IRI measurements from 24 sections and had an average error per section of 0.25 m/km (15.7 in/mi). The standard deviation of the errors at the sections was 0.18 m/km (11.7 in/mi). Traffic rates varied from 25 to 1490 KESAL/yr with an average of 410 KESAL/yr for this data set. The largest errors are associated with the two sections (55-3009 and 46-3012) that have very rapid IRI development. The model does predict these sections to have very high IRI growth rates but not quite as high as those observed from the IRI measurements. Figure 5.4.5 shows the sensitivity of the model to changes in traffic rates. Shown in parentheses next to the parameter name is the range of the parameter encountered in the LTPP data used to build the model.

Performance of Specific Sections

The following discussion presents a qualitative analysis of undoweled GPS-3 pavement sections located in wet environments that exist at the extremes in performance. The analysis looks at pavements that have remained very smooth over time, pavements that have become very

$$IRI(t) = e^{r_0 t}\left[\frac{IRI_{\max} \times IRI_0}{IRI_0(e^{r_0 t} - 1) + IRI_{\max}}\right]$$

$$IRI_0 = A(w/c \times 100)^B + C(\tfrac{P200}{Po})^D + E(JointSpace)^F + G(w\%)^H$$

$$IRI_{max} = W(PCCth)^X + Y(100 \times w/c)^Z + AA(P200 \times w\%)^{BB} + CC(JointSpace)^{DD}$$

$$r_0 = [I(PCCth)^J + K(SplitTensile/10)^L + M(EMOD/100000)^N + O(FZI)^P + Q(Days32-)^R + S(DaysWet/yr)^T + U(KESAL/yr)^V] \times 1/10000$$

A= -0.2480371	H= 0.0525586	O= -4.0215953	V= -0.3173752
B= 1.33362197	I= 4403.71574	P= 0.76147578	W= 7313.61265
C= -826.4683	J= -3.5134802	Q= 0.01759138	X= -2.476341
D= 0.01704857	K= -0.0132394	R= 2.33383558	Y= 0.00012248
E= 2.1071304	L= 2.38567734	S= 0.02570815	Z= 3.29949886
F= 0.00805606	M= 0.4798878	T= 1.95067852	AA= 2.8769925
G= 808.915445	N= 1.91694438	U= -3834.3217	BB= 0.52868067
			CC= 0.02633191
			DD= 3.01229593

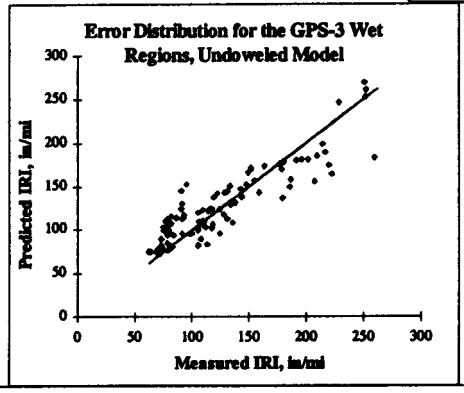

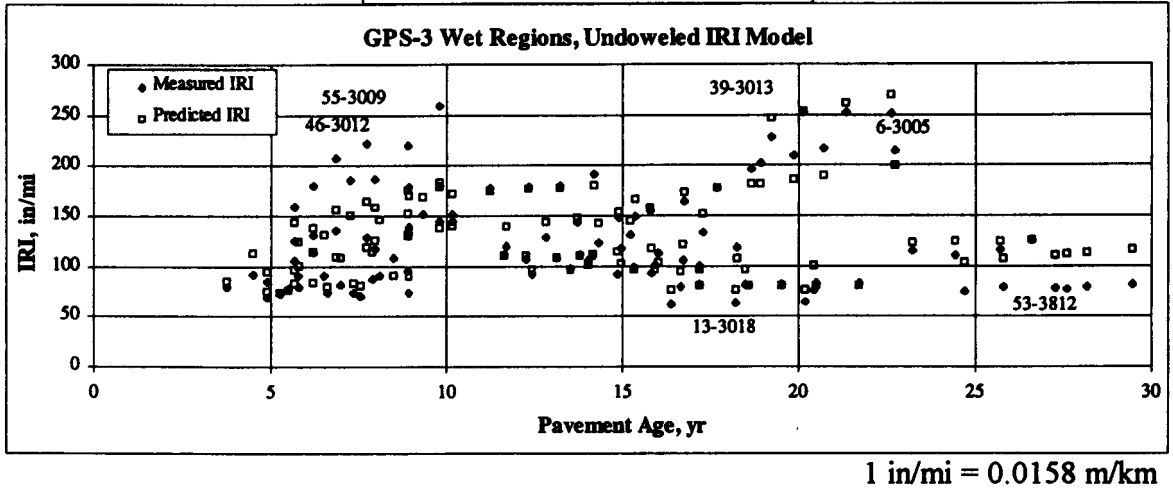

1 in/mi = 0.0158 m/km

Figure 5.4.4. GPS-3 wet regions, undoweled IRI model.

Parameter (Data Range)	Case 1	Case 2	Case 3	Case 4	Case 5
PCCth, in (8 to 14)	9	9	9	9	9
SplitTensile, psi (416 to 1014)	550	550	550	550	550
EMOD (2000000 to 6650000)	3500000	3500000	3500000	3500000	3500000
w/c (0.27 to 0.57)	0.51	0.51	0.51	0.51	0.51
Po, psf (120 to 680)	220	220	220	220	220
P200 (3 to 88)	88	88	88	88	88
w% (3 to 23)	12	12	12	12	12
DaysWet/yr (75 to 180)	80	80	80	80	80
FZI (1 to 1500)	1500	1500	1500	1500	1500
Days32- (8 to 160)	160	160	160	160	160
Kesal/yr (30 to 1400)	30	100	500	1000	1400
JointSpace, ft (11 to 20)	20	20	20	20	20
IRI@25yr	155	261	335	351	356
INITIAL IRI, in/mi =	63	63	63	63	63
Growth Rate constant, r =	0.048	0.089	0.125	0.135	0.140
IRI(max) =	417	417	417	417	417

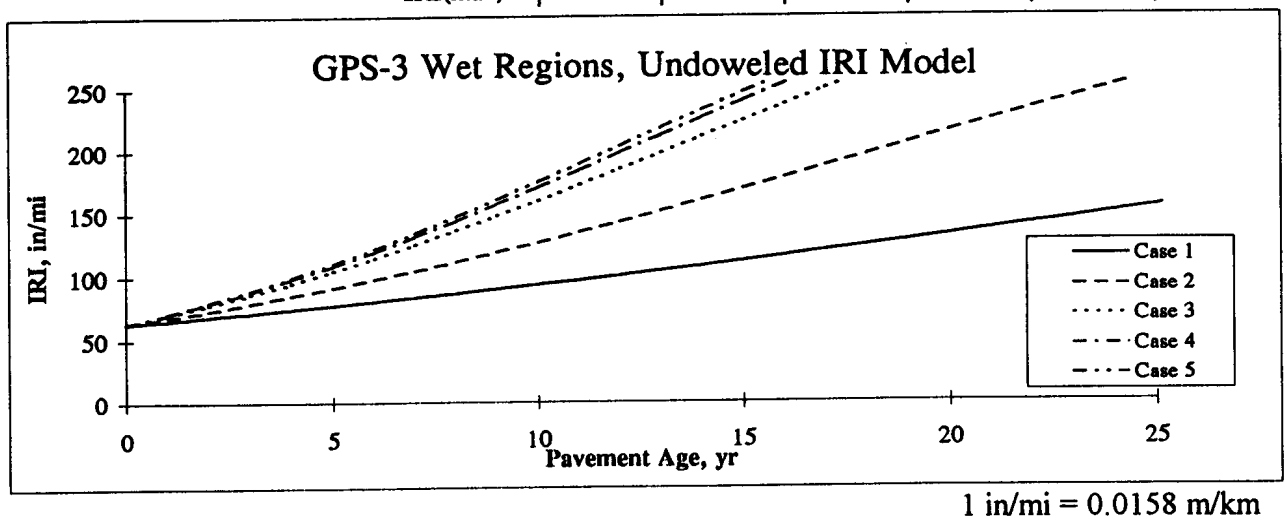

1 in/mi = 0.0158 m/km

Figure 5.4.5. Sensitivity of the GPS-3 (undoweled) wet regions IRI model to increasing traffic rates.

rough, and pavements that are developing roughness very quickly . The sections discussed are indicated in the bottom portion of figure 5.4.4.

Two pavements that are old but have low IRI values are sections 13-3018 and 53-3812. They have traffic levels of 280 and 710 KESAL/yr, respectively. Section 53-3812 has a split tensile strength that is near the upper limit of the split tensile strength data for the GPS-3 data set, whereas section 13-3018 has a split tensile strength that is near the lower limit of the split tensile strength data for the GPS-3 data set. Section 13-3018 used a low cement content of 307 kg/m^3 (517 lb/yd^3) with an estimated water to cement ratio of 0.51. Section 53-3812 used a low water to cement ratio (0.39) with typical cement content of 332 kg/m^3 (560 lb/yd^3), resulting in very high split tensile strength. The PCC mix for both sections used granite as a coarse aggregate with a low fine aggregate content.

Section 55-3009 shows rapid gain in IRI prior to reaching the age of 10 years. This section is located in the wet freeze environment on a high P200 subgrade that has a PI value just greater than 10. This section, which has a PCC thickness of 215 mm (8.6 in), is subjected to a traffic level of 312 KESAL/yr. The PCC for this section had a low split tensile strength and a high modulus, and the brittle nature of this mix may have contributed to pavement distress that resulted in a high IRI value.

There are two older pavements, sections 39-3013 and 6-3005, which were noted to have high IRI values. Section 6-3005 is a high traffic route (1101 KESAL/yr) located in a hot, wet-no freeze environment. This section has a 205-mm (8.2-in) slab, with 4.6-m (15-ft) joint spacing, and rests on a relatively high-moisture-content clay (P200 = 51 percent, w% = 17 percent, PI = 21 percent). A preliminary analysis of this section using the AASHTO equation indicated that it is likely to have reached the end of its design life. Section 39-3013 is a low traffic route (100 KESAL/yr) located in a mild wet freeze environment. This section has a 211-mm- (8.3-in-) thick slab, 5.2-m (17-ft) joint spacing, and a soil-cement type base. The subgrade is a high-moisture-content clay (P200 = 83 percent, w% = 21 percent). The PCC off this section had a low split tensile strength and a high modulus value. The brittle behavior of the PCC as well as the high moisture content of the subgrade may have been contributing factors to the high IRI of this section.

5.4.3 GPS-3 Sections in Dry Environment

IRI Prediction Model

Figure 5.4.6 shows the IRI prediction model developed for GPS-3 sections in the dry environments. This model was based on 135 IRI measurements from 26 sections and had an average error per section of 0.21 m/km (13.2 in/mi). The standard deviation of the errors at the sections was 0.11 m/km (7.1 in/mi). Traffic rates varied from 14 to 1610 KESAL/yr, with an average of 400 KESAL/yr for this data set. Figure 5.4.7 shows the sensitivity of the model to changes in climate conditions from very dry and hot to very cold and to the upper limit of the dry climatic range. Shown in parentheses next to the parameter name is the range of the parameter encountered in the LTPP data used to build the model.

Performance of Specific Sections

The following discussion presents a qualitative analysis of the GPS-3 pavement sections located in dry environments that exist at the extremes in performance. The analysis looks at pavements that have remained very smooth over time and pavements that are developing roughness very quickly. The sections discussed are indicated in the bottom portion of figure 5.4.6.

One notable good performer is section 6-3042. This section has carried an average of 1610 KESAL/yr is 15 years old, and still had an IRI value of 0.95 m/km (60 in/mi). The slab thickness is 224 mm (8.8 in) and rests on a subgrade with 64 percent P200 and 15 percent moisture content. The PCC used a cement content of 279 kg/m^3 (470 lb/yd^3) with a water to cement ratio of 0.61. These parameters combined with high coarse aggregate contents, resulted in a PCC mix that had a lower modulus (E = 24181 MPa (3500 ksi)) and a higher split tensile strength (split tensile strength = 5077 kPa (737 psi)).

Section 53-3013 has remained smooth over a long period. This section is located in the dry freeze environment, rests on a frost-susceptible subgrade (P200 = 37 percent, w% = 12 percent), and has a PCC thickness of 205 mm (8.2 in). This section is subjected to a low traffic level of 101 KESAL/yr. The PCC is a higher strength, lower modulus type concrete having a split tensile strength of 6079 kPa (894 psi). The low traffic levels, thick base and subbase layers that

$$IRI(t) = e^{r_0 t}\left[\frac{IRI_{max} \times IRI_0}{IRI_0(e^{r_0 t} - 1) + IRI_{max}}\right]$$

$$IRI_0 = A(JointSpace)^B + C(PCCth)^D + E(Po)^F + G(P200)^H$$

$$IRI_{max} = S(JointSpace)^T + U(P200)^V + W(PCCth)^X$$

$$r_0 = [I(Days32-)^J + K(AnnPrecip)^L + M(JointSpace)^N + O(c/f)^P + Q(KESAL/yr)^R] \times 1/10000$$

A= 1.57701354	G= 172.548119	M= 16.4129241	S= 9903.86557
B= 1.3932107	H= -0.7108349	N= 0.11943774	T= -1
C= 0.05750755	I= 1.3816E-05	O= -234.52103	U= 0.00713641
D= 2.96098324	J= 3.38379753	P= 0.11918564	V= 2.73962869
E= -76.984327	K= 218.96547	Q= -7986.4536	W= -124.32398
F= -0.0728376	L= 0.2534601	R= -1.002	X= 0.65113559

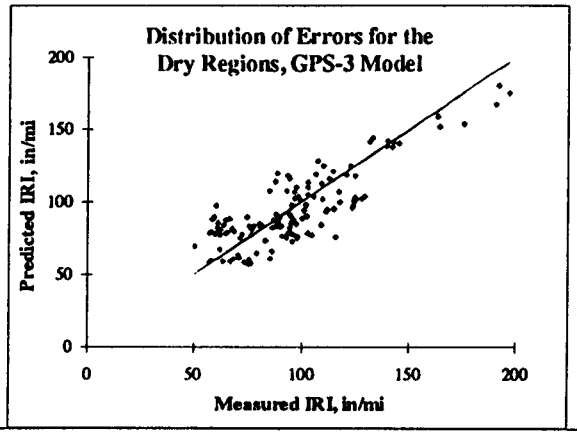

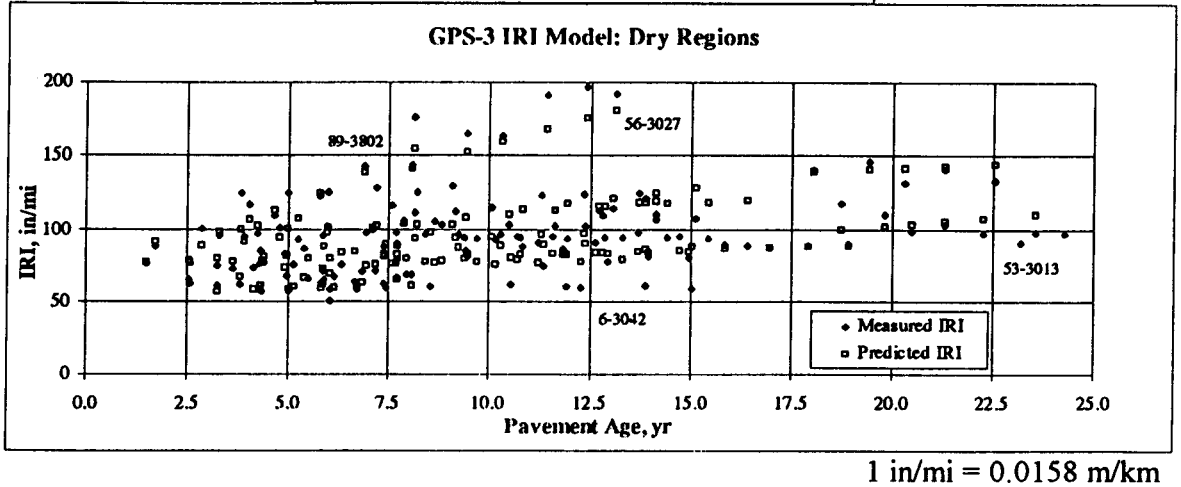

1 in/mi = 0.0158 m/km

Figure 5.4.6. GPS-3 dry regions IRI model.

Parameter (Data Range)	Case 1	Case 2	Case 3	Case 4	Case 5
PCCth, in (8 to 11.5)	9	9	9	9	9
c/f, lb/lb (1.13 to 2.17)	1.65	1.65	1.65	1.65	1.65
Po, psf (110 to 590)	150	150	150	150	150
P200 (6 to 93)	50	50	50	50	50
AnnPrecip, in (4 to 20)	4	8	12	16	20
Days32- (0 to 203)=	1	50	100	150	200
JointSpace, ft (11.5 to 15)	13.5	13.5	13.5	13.5	13.5
KESAL/yr (14 to 1600)	100	100	100	100	100
IRI@25yr	56	64	82	140	313
INITIAL IRI, in/mi =	55	55	55	55	55
Growth Rate constant, r = =	0.000	0.007	0.018	0.045	0.100
IRI(max) =	536	536	536	536	536

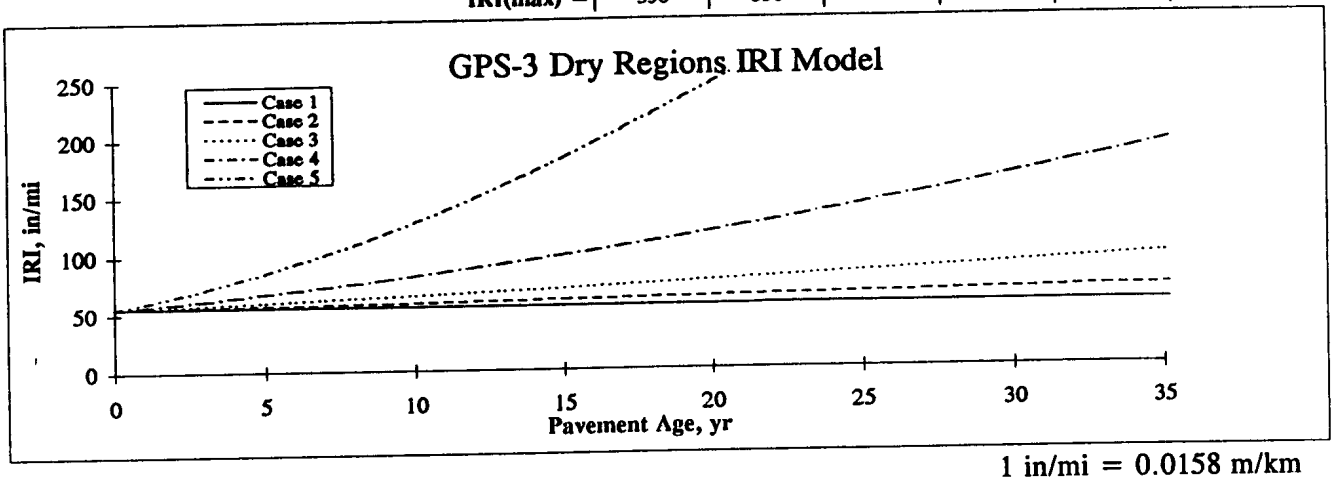

1 in/mi = 0.0158 m/km

Figure 5.4.7 . Sensitivity of the GPS-3 dry regions IRI model to changes in climate, holding all other parameters constant.

minimize frost heave effects, and the good PCC properties may have contributed to the excellent behavior of this section.

Section 56-3027 is shown to have rapidly developing IRI. This section has been subjected to 505 KESAL/yr, and the subgrade is very similar to that of a section discussed previously (53-3013). However, the freezing index at this location is much higher.

One pavement section that is apparently on a rapid course toward failure is section 89-3802. The IRI for this section has increased from 1.89 m/km (120 in/mi) at age 4 years to 2.84 m/km (180 in/mi) at age 8 years. This section is located in a severe dry freeze environment (precipitation = 463 mm/yr (18.5 in/yr), FZI=1887 °C days/yr (3396 °F days/yr), days wet=106)). This section is located on a very wet clay subgrade (P200 = 91 percent, w% = 34 percent, LL = 74 percent, PI = 41 percent). The section has a 249-mm (9.8-in) thick slab, 4.6-m (15-ft) joint spacing, and is subjected to 115 KESAL/yr. The PCC used limestone coarse aggregate with a relatively high fine aggregate content, and the cement content was 326 kg/m^3 (550 lb/yd^3) with a water to cement ratio of 0.4. The severe environment coupled with the subgrade type may be a cause of the high IRI at this section.

5.4.4 GPS-3 Summary

The models developed for the GPS-3 sections predict the development of IRI over time according to the concept of logistic growth of IRI. The models predict three parameters: the initial IRI as a function of design parameter of the pavement and subgrade parameters, a maximum long-term stable value of IRI as a function of design parameters of the pavement and subgrade parameters, and the growth rate constant that is a function of the design parameters of the pavement, subgrade, climate, and traffic parameters. The doweled and undoweled GPS-3 models for the wet region both have a mean error per GPS-3 section of 0.25 m/km (16 in/mi). The GPS-3 model for the dry regions has a mean error per GPS-3 section of 0.21 m/km (13 in/mi). Figure 5.4.8 shows the strong relation between IRI and the total amount of faulting observed at the undoweled GPS-3 sites. There are some indications that the relative values of the split tensile strength and elastic modulus in a PCC mix may have an effect on the IRI development of the pavement. However, this phenomenon needs further investigation.

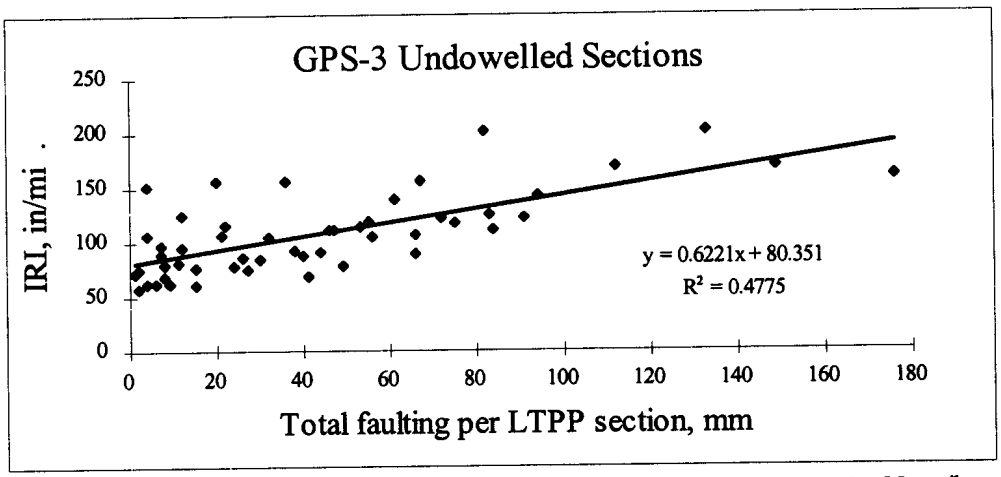

1 in/mi = 0.0158 m/km

Figure 5.4.8. Relationship between IRI and total faulting for undoweled GPS-3 sections.

5.5 GPS-4: JOINTED REINFORCED CONCRETE PAVEMENTS (JRCP)

The time-sequence IRI values for each GPS-4 site were compiled and plotted against pavement age. Figure 5.5.1 shows the development of IRI for the GPS-4 sections classified according to the LTPP regions. There are no GPS-4 sections in the western region. The general trend observed for roughness development for GPS-4 sections is exponential growth. The general model form used for the GPS-4 pavements is described below:

$$IRI(t) = IRI_0 e^{r_0 t^A / B}$$

where:

IRI_0 = estimated initial IRI (after some initial traffic loading),
= f(design parameters of pavement and subgrade properties),

r_0 = growth rate constant,
= f(climate, traffic, subgrade properties, design parameters of the pavement),

t = time in years,

e = the exponential function,

A and B = modeling constants.

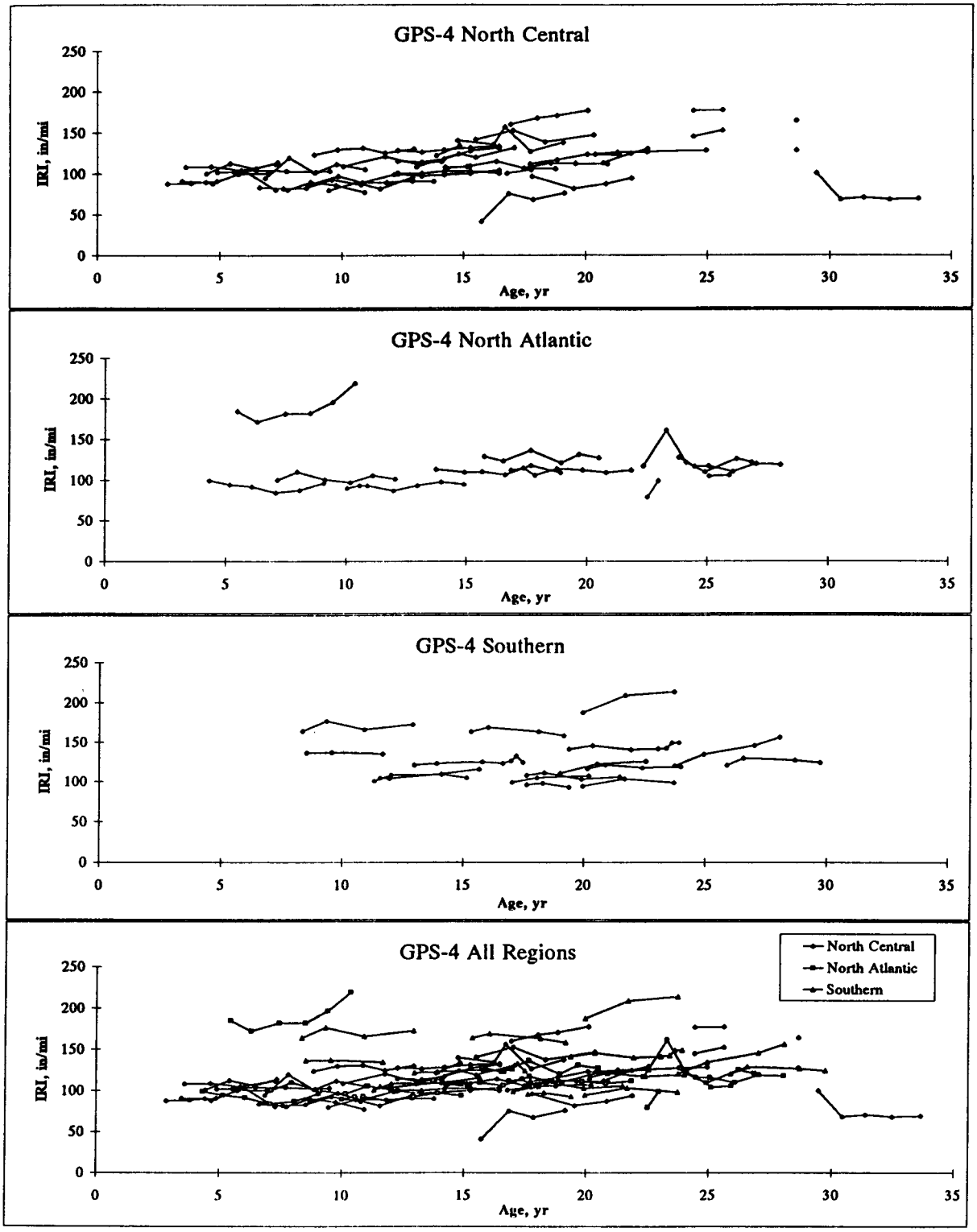

1 in/mi = 0.0158 m/km

Figure 5.5.1. Trends in IRI development for the GPS-4 sections according to LTPP regions.

In this model, IRI_0 represents the IRI value of the pavement after it has been opened to traffic and has been subjected to some initial traffic loading. Because of the relatively small number of GPS-4 sections, only one model was generated for the entire experiment. There were a total of 68 pavement sections with a total of 285 IRI values. Traffic rates at GPS-4 sections varied from 34 to 1610 KESAL/yr with an average of 350 KESAL/yr. Table 5.5.1 shows the ten parameters that had the highest correlation coefficients with IRI.

Table 5.5.1. Ten parameters with highest correlations to IRI for GPS-4 sections.

Parameter	Correlation Coefficient
water	-0.51
AnnPrecip	0.38
Days32-	-0.36
PCCth	0.34
cement	-0.33
FZI	-0.32
JointSpace	0.26
w/c	-0.24
w%	0.23
EMOD	-0.22

The correlations, although rather insignificant, seem to indicate that higher precipitation with more fines and water in the subgrade tend to result in higher IRI values. This is intuitively correct, as these trends in climate and subgrade conditions would tend to increase erosion/faulting potential. There is a slight trend for higher IRI for increased joint spacing. An increased joint spacing would likely result in a greater proportion of the transverse discontinuities (cracks and joints). This could increase the faulting potential over time.

The joint spacings for the GPS-4 pavements vary from 4.6 m (15 ft) to 30.5 m (100 ft), with an average of 15 m (49 ft). Most of these pavements are longer than the critical slab length of $6\ell\sqrt{2}$, where ℓ is the radius of relative stiffness of the pavement system. For a 229-mm- (9-in-) thick slab on a typical granular subgrade, this critical slab length would be approximately 9 m (30 ft). As slab length approaches the critical slab length, bending stresses and deflections due to combined curling, warping, and loads reach a maximum.

The PCC mix parameters are among the stronger factors relating to IRI. The trends seem to indicate that higher water to cement ratios with higher cement and water contents are resulting in smoother pavements. This can be explained in the context of workability and early- age curling and warping of the slabs. A concrete mix with a very low water to cement ratio and very little water would likely have workability problems. Low water to cement ratio mixes with high cement and water contents would likely generate more heat during hydration causing more extreme temperature gradients at set. This mix would also gain more strength at a faster rate, perhaps allowing more early-age curling effects because of less relaxation of stresses and strains during early temperature swings. However, this mix would be expected to be more durable over the long term.

5.5.1 GPS-4 IRI Prediction Model

Figure 5.5.2 shows the model developed for IRI prediction for the GPS-4 sections. The average error per section for the model was 0.16 m/km (10.3 in/mi). The standard deviation of the errors at the sections was 0.11 m/km (10.3 in/mi). Figure 5.5.3 shows the sensitivity of the resulting model to changes in slab thickness, holding all other input parameters constant. The sensitivity analysis indicates that, as slab thickness increases, the initial value of IRI increases but deterioration rates decrease. This indicates an optimum thickness in the 229 to 254 mm (9 to 10 in) range for the climate and traffic conditions shown. Shown in parentheses next to the parameter name is the range of the parameter encountered in the LTPP data used to build the model.

5.5.2 Performance of Specific GPS-4 Sections

The following discussion presents a qualitative analysis of the pavement sections that exist at the extremes in performance. The analysis looks at high IRI pavements, low IRI pavements, and old pavements that have carried very high traffic volumes and still have acceptable IRI values. The sections discussed are indicated in the bottom portion of figure 5.5.2.

Two sections, 54-4004 and 48-4152, are identified as having developed high IRI values at a relatively early age. Section 54-4004 is located in the wet freeze zone, and experiences 192 days with precipitation per year, which is the highest for the data set. The PCC slab thickness is 251 mm (9.9 in) and the slab rests on a granular base. This section has a high traffic volume (717 KESAL/yr); a preliminary analysis of this section with the AASHTO pavement design equation indicated that it is likely to have exceeded its design life. Section 48-4152 is located in the wet-no freeze zone, and is subjected to an annual precipitation of 1500 mm (60 in), with 34 days/yr

$$IRI(t) = IRI_0 e^{r_0 t^{AA}/BB}$$

$$IRI_0 = A(PCCth)^B + C(JointSpace)^D + E(1+PL)^F + G(Po)^H + I(w/c)^J + K(w\%)^L$$

$$r_0 = M(PCCth)^N + O(AnnPrecip)^P + Q(w/c)^R + S(\frac{P200 \times w\%}{100})^T + U(KESAL/yr/10)^V + W(\frac{EMOD}{100000})^X + Y(\frac{Comp}{1000})^Z$$

A= 1.056E-06	H= -1.68577	O= 6.32E-10	V= -0.8
B= 7.2505499	I= -997.43269	P= 7.638408	W= -2.309E-05
C= 1038.5954	J= 0.09401	Q= 118140340	X= 5.00354
D= -0.01149	K= 0.04133	R= 12.46117	Y= -1.91067
E= -0.00179	L= 1.99116	S= -19329.546	Z= 1.678449
F= 2.73034	M= 14669026	T= -0.0906444	AA= 0.51907
G= -52333.3	N= -2.49805	U= -50000	BB= 43.131

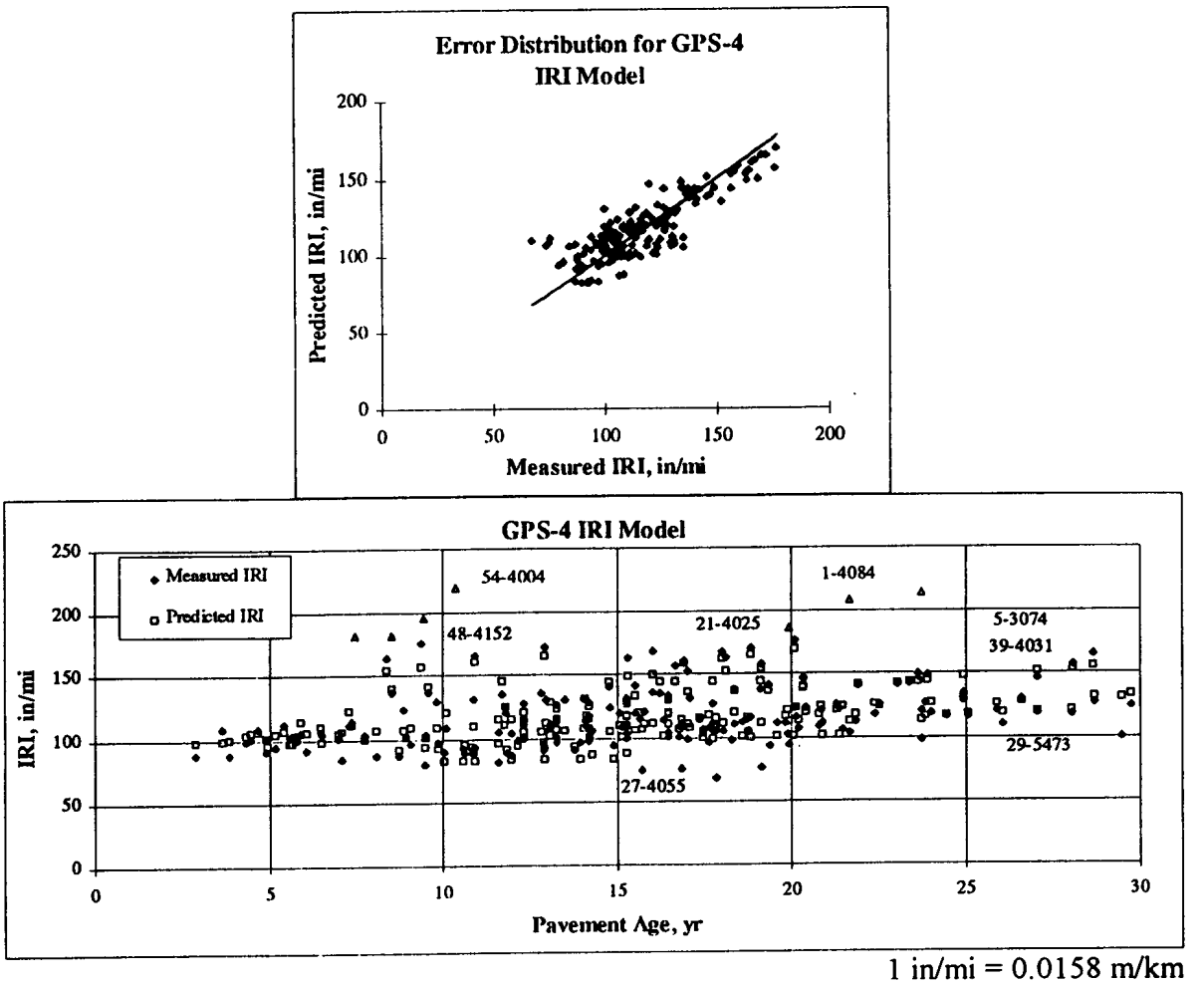

1 in/mi = 0.0158 m/km

Figure 5.5.2. GPS-4 IRI prediction model.

Parameter(Data Range)	Case 1	Case 2	Case 3	Case 4	Case 5
KESAL/yr (34 to 1600)	250	250	250	250	250
PL (0 to 24)	0	0	0	0	0
P200 (2 to 98)	3	3	3	3	3
w% (2 to 28)	3	3	3	3	3
Po, psf (135 to 335)	100	100	100	100	100
JointSpace, ft (15 to 61)	20	20	20	20	20
PCCth, in (7.9 to 11.4)	7	8	9	10	11
AnnPrecip (26 to 60)	50	50	50	50	50
w/c (.29 to .71)	0.55	0.55	0.55	0.55	0.55
EMOD, psi (3.5e+06 to 6.35e+06)	4500000	4500000	4500000	4500000	4500000
Compressive Strength, psi (4000 to 11000)	6000	6000	6000	6000	6000
INITIAL IRI, in/mi =	40	42	47	57	76
Growth Rate Constant, r =	15.43	12.21	10.13	8.73	7.74

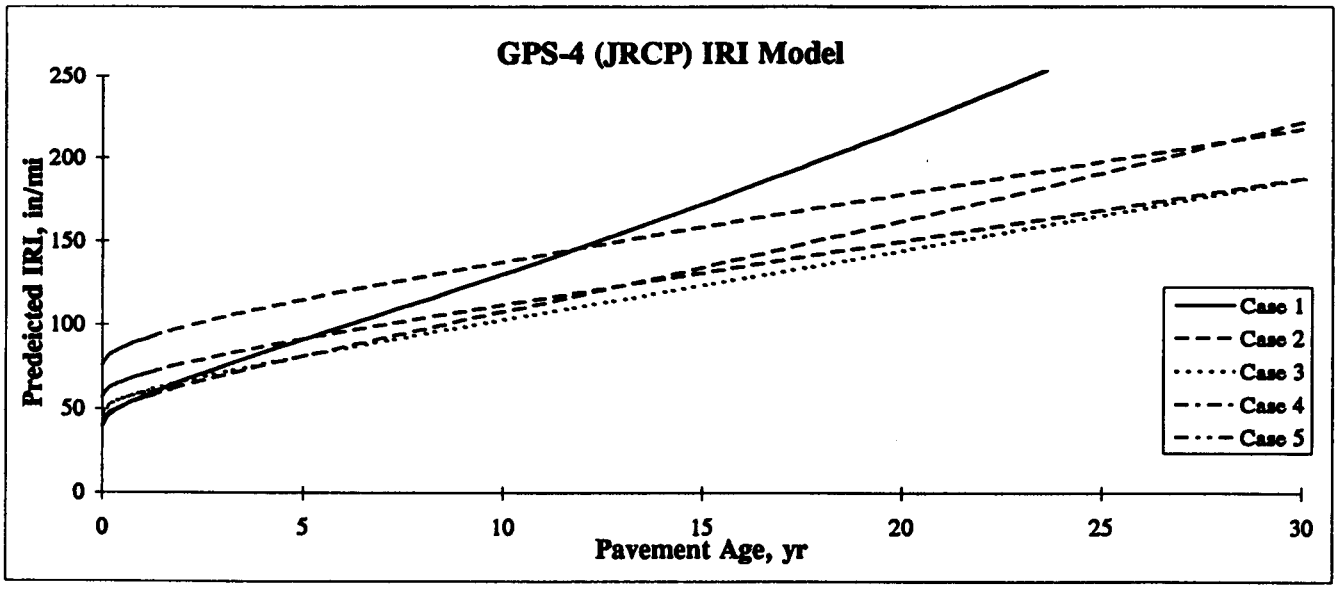

1 in/mi = 0.0158 m/km

Fig 5.5.3. Sensitivity of GPS-4 IRI model to changes in PCC thickness, holding all other parameters constant.

having a precipitation greater than 12.5 mm (0.5 in). This section has low traffic (79 KESAL/yr), a cement-aggregate mixture base, and a slab thickness of 290 mm (11.4 in).

The two smoothest sections noted in the GPS-4 data are sections 27-4055 and 29-5473. Section 27-4055 is a 226-mm- (8.9-in-) thick slab with a thin granular base resting on a coarse-grained subgrade (P200 = 10 percent, w% = 5.5 percent). The section experiences a medium traffic level (577 KESAL/yr) and has 8.2-m (27-ft) joint spacing. The annual precipitation is 737 mm (29 in), with a very high freeze index (1151 °C days/yr (2071 °F days/yr)). The PCC mix had a high coarse aggregate content and lower than average cement content which resulted in a relatively low modulus and high split tensile strength mix that was very dense. The combination of good subgrade and good PCC may have been one factor that resulted in exceptional performance of this section. Section 29-5473 is a 201-mm (7.9-in) thick slab with relatively high traffic (749 KESAL/yr). This section has a thin granular base and has a 18.7-m (61.5-ft) joint spacing. The subgrade has a P200 of 70 percent and a moisture content of 15 percent.

Sections 5-3074 and 39-4031 were identified as having supported heavy traffic volumes while maintaining low IRI values. Section 39-4031 is located in the wet freeze zone, and has carried an estimated 1600 KESAL/yr over its 30-year life. The section is a 234-mm- (9.2-in-) thick slab with 18.3-m (60-ft) joint spacing with a granular base and a subbase. The subgrade has a P200 of 64 percent and a moisture content of 12 percent. The PCC mix had a cement content of 362 kg/m^3 (611 lb/yd^3) and a water to cement ratio of 0.51. Laboratory test data for the PCC are not available at this section. Section 5-3074 is located in the wet-no freeze zone, and has carried an average of 1100 KESAL/yr over it's 25-year life. The section consists of a 259-mm-(10.2-in-) thick slab with 13.7-m (45-ft) joints and third point hinge joints at 4.5 m (15 ft). A 172-mm- (6.8-in-) thick cement-aggregate mixture base was used for this section. The subgrade consists of silt at 22 percent moisture content and 76 percent P200, which exists in a wet-no freeze environment. The PCC mix has a split tensile strength of 5385 kPa (805 psi), which is in the upper 5 percent of the GPS-4 data set, but had a relatively low elastic modulus.

5.5.3 GPS-4 Summary

The models developed for the GPS-4 sections predict the development of IRI over time for jointed reinforced concrete pavements according to the concept of exponential growth of IRI. The models predict two parameters: the initial IRI as a function of design parameters of the pavement and subgrade parameters, and the growth rate constant, which is a function of the

design parameters of the pavement, subgrade properties, climate parameters, and traffic loadings. The model has an average error per GPS-4 section of 0.16 m/km (10.3 in/mi). Generally, most of the sections that were performing well were resting on granular bases.

5.6 GPS-5: CONTINUOUSLY REINFORCED CONCRETE (CRC) PAVEMENTS

The IRI versus pavement age plots for continuously reinforced concrete pavements are shown in figure 5.6.1. These plots show that IRI remained relatively constant over time for most sections. Some sections showed some variability in IRI over the years, with the IRI for a specific year being either higher or lower than the previous and subsequent years. The pavements that were young (less than 5 years) as well as pavements that were old (over 20 years) showed the same IRI behavior pattern, which is a relatively constant IRI over time. This observation indicates that the CRC pavements appear to generally maintain their initial IRI over a long period of time.

To analyze the relationship between the current IRI and parameters that could affect roughness, the GPS-5 sections were divided into three data sets based on the environmental regions: dry (10 sections), wet-no freeze (36 sections), and wet freeze (39 sections). As only a few sections were in the dry freeze and dry-no freeze regions, they were combined into one category. Table 5.6.1 shows correlation coefficients between IRI and selected parameters for the different environmental regions. Consistent trends in correlations were observed for all three regions for percentage steel, elastic modulus of PCC and water to cement ratio. Low IRI values were associated with high percentages of steel and high water to cement ratios. Pavements with higher PCC elastic modulus had higher IRI values. The number of days above 32 °C (90 °F) was a strong climate factor for the wet-no freeze and dry regions that indicated higher IRI.

5.6.1 GPS-5 IRI Prediction Model

The analysis approach used in developing an IRI prediction model was multiple linear regression. The model to predict IRI for GPS-5 sections was developed by considering 70 sections for which data were available. The model developed for GPS-5 sections is:

$$IRI = 242.19 - 143.54 * PSTEEL - 127.12 * WCR + 2.55*10^{-4} * CUMT$$

Adjusted $R^2 = 0.14$, standard error = 27 and n = 70

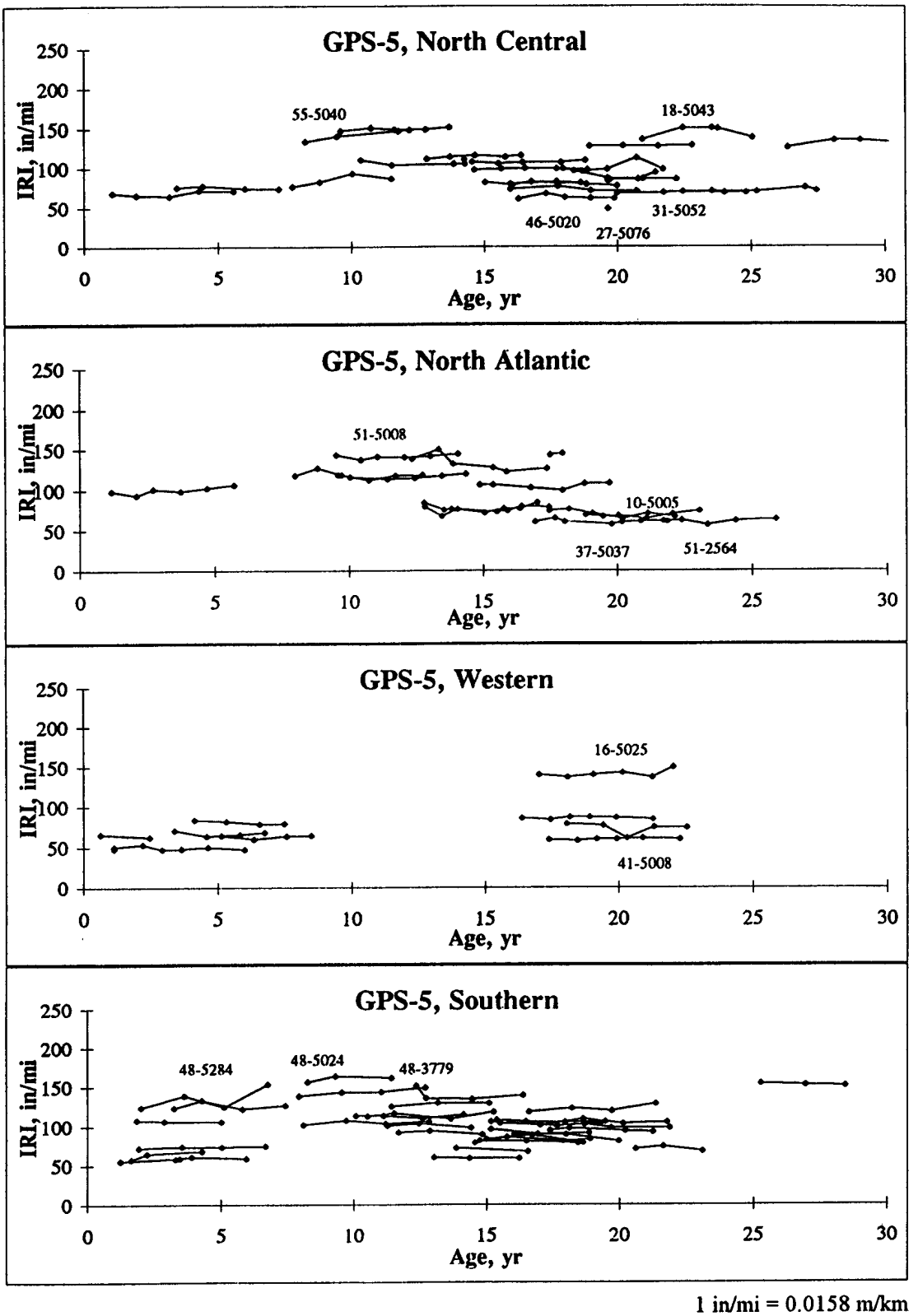

1 in/mi = 0.0158 m/km

Figure 5.6.1. IRI development for the GPS-5 sections classifed according to LTPP geographical regions.

Table 5.6.1. Ten parameters with highest correlation to IRI for the GPS-5 sections.

Dry Environments	Wet-No Freeze Environments	Wet Freeze Environments
water (-.80)	w/c (-.71)	EMOD (+.53)
w/c (-.65)	Days90+ (+.49)	Comp (+.45)
c/f (-.63)	DaysWet/yr (-.41)	w/c (-.41)
Cum traf (+.62)	FrzThwCyc (-.39)	BaseThick (+.38)
c (+.57)	water (-.36)	PL (+.36)
BaseThick (-.52)	BaseThick (-.33)	water (-.31)
Days90+ (+.43)	%Steel (-.33)	cement (+.28)
PCCth (-.41)	Poissons Ratio (+.27)	w% (+.28)
%Steel (-.23)	Comp (-.27)	DaysWet/yr (+.21)
EMOD(+.08)	EMOD (+.23)	%Steel (-.21)

where:

IRI = current IRI (in/mi),

WCR = water to cement ratio,

CUMT = cumulative KESAL (1000's of ESALs), and

PSTEEL = percent longitudinal steel (%).

Attempts were made to develop separate models for each environmental region. However, such attempts were not successful. The time versus IRI plots for the GPS-5 sections show a nearly constant IRI over time for virtually all the GPS-5 sections. This behavior is seen for pavements that are young (less than 5 years) as well as for sections that are old (over 20 years). These plots do not reveal any trends in IRI development for GPS-5 sections. It appears that the GPS-5 sections maintain a relatively constant IRI over their service life. The initial IRI of the pavement may be related to workability of the PCC, construction procedures, and the weather conditions at the time of placement of PCC. The cause of the low R^2 of the above relationship is most likely because these factors were not considered in the regression analysis.

5.6.2 Performance of Specific GPS-5 Sections

The characteristics of two pavements that have low IRI values and two pavements that have high IRI values are described in this section. These sections are indicated in figure 5.6.1. The average traffic rate for the GPS-5 data set was 456 KESAL/yr. There were several GPS-5 sections that were old (over 20 years) but still had low IRI values. Two such examples are section 41-5008, which is 22 years old and has an IRI of 0.95 m/km (60 in/mi) and section 46-5020, which is 20 years old and has an IRI of 0.98 m/km (62 in/mi). Section 41-5008 is located

in the dry freeze zone and is a high traffic route with an average of 566 KESAL/yr. The PCC slab is 205-mm (8.1-in) thick and the base is a cement-treated base, with the subgrade having a P200 of 11 percent and a moisture content of 10 percent. Section 46-5020 is also located in the dry freeze zone, and is a low traffic route with an average of 43 KESAL/yr. The PCC slab is 200-mm (7.9- in) thick and the base is a hot mix asphalt, with the subgrade having a P200 of 21 percent and a moisture content of 9 percent.

Two sections that have high IRI values and are less than 12 years old are sections 48-5284 and 48-5024. Both are located in Texas and are in the wet-no freeze zone. Both sections are located in areas that have a hot climate with days above 32°C (90°F) of 89 and 111 for sections 48-5284 and 48-5024, respectively. Section 48-5284 has an IRI of 2.4 m/km (153 in/mi) and is 7 years old, while section 48-5024 has an IRI of 2.55 m/km (162 in/mi) and is 11 years old. Section 48-5284 has a PCC slab thickness of 278 mm (11.1 in) resting on an asphalt-treated base, and is located over a subgrade that has a P200 of 41 percent and a moisture content of 16 percent. Section 48-5024 has a PCC slab that is 278-mm (11.1-in) thick that rests on an AC-treated base and is located on a subgrade that has a P200 of 24 percent and a moisture content of 12 percent. The traffic levels at sections 48-5284 and 48-5024 are 219 and 139 KESAL/yr, respectively.

5.6.3 GPS-5 Summary

A multiple regression analysis that was conducted on this data set developed a model for predicting the current IRI of the pavement, but the model has a very low R^2. Since all CRC pavements are maintaining a relatively constant IRI over the observed period, the roughness observed on these pavements is likely to be associated with the initial IRI of the pavement. The initial IRI of the pavement is probably related to factors that are associated with the conditions at the time of construction, such as workability of PCC, finishing procedures, and weather conditions during placement. These factors were not included in the regression analysis, and are likely to be the cause of the low R^2 value. The correlation analysis indicated that in all climatic regions, the percentage of longitudinal steel, water to cement ratio, and elastic modulus of PCC are related to the IRI of the pavement. Higher percentage of longitudinal steel and water to cement ratios generally result in a lower IRI, while higher PCC moduli result in a higher IRI.

5.7 ANALYSIS OF OVERLAID PAVEMENTS

5.7.1 Analysis Approach

Experiments GPS-6A and B, GPS-7A and B, and GPS-9 in the LTPP program involve the study of overlaid pavements. Experiment GPS-6A and B is the study of AC overlays of AC pavements, while GPS-7A and B is the study of AC overlays of PCC pavements, and GPS-9 is the study of unbonded PCC overlays of PCC pavements. Test sections for GPS experiments 6A, 7A, and 9, were established on in-service pavements, and the condition of the pavement prior to the overlay as well as the IRI of the pavement immediately after the overlay is not known for these sections. GPS-6B and GPS-7B experiments include sections that were overlaid after the beginning of the LTPP program, and the condition of the pavement prior to the overlay is known for these sections. Laboratory test data for overlaid sections in the NIMS and RIMS were less complete than the data that were available for GPS experiments 1 through 5. For the overlaid sections, various laboratory test data were missing for several sections.

The roughness development at the overlaid sections will be affected by applied traffic loading as well as climatic conditions. The condition of the pavement prior to the overlay as well as the amount of repairs performed on these sections prior to the overlay are expected to have a large influence on roughness development at these sections. However, the condition of the pavement prior to the overlay for these sections is not known except for the GPS-6B and GPS-7B sections. The increase in the IRI of a pavement after it is overlaid will be influenced by traffic, structural condition of the pavement, subgrade conditions, and climatic conditions. The current roughness of the pavement will depend on the initial roughness of the pavement and the increase in roughness caused by the described factors. Attempts to relate the current roughness of the pavement to the factors that would have an affect on the increase in roughness would not result in accurate models, as these factors are only related to the change in roughness. Predicting the initial IRI of overlaid pavements with use of an approach similar to that used for GPS-1 experiments will not provide realistic results for overlaid pavements. This is because the initial IRI of an overlaid pavement can vary depending on construction practices, such as milling prior to overlay, and the amount of repairs performed on the pavement prior to the overlay.

In the study of the overlaid pavements, the rate of increase of roughness at the sections was determined by using the time-sequence IRI data and performing a least square linear regression between IRI and time. The rate of increase of IRI obtained from the regression was then related to the possible factors that would cause an increase in IRI to see if significant factors

could be identified. The following sections describe the analysis that was carried out for GPS experiments 6, 7, and 9.

5.7.2 Roughness Development at GPS-6 Sections

Background

The GPS-6 experiment is the study of AC pavements that are overlaid with AC. The GPS-6 experiment is divided into two categories: GPS-6A and GPS-6B. The GPS-6A sections were established on existing overlaid pavements that were at different periods of their service life. The GPS-6B sections were overlaid after they were accepted to the LTPP program, and the IRI of these sections immediately after the overlay is known.

IRI before and After Overlay

There are 37 GPS-6B sections in the LTPP experiment for which profile data are available. Nineteen of these sections were profiled prior to being overlaid, and the IRI before the overlay are available for these sections. Figure 5.7.1 presents the IRI before the overlay, the IRI after the overlay, and the overlay thickness for these 19 sections. In this figure, the overlay thickness are arranged in ascending order. There are several cases, as shown in this figure, where the IRI before and after the overlay are very close to each other. The overlay date for the sections was determined by reviewing both the assign date (from data table experiment section in NIMS) and the overlay date indicated in the rehabilitation file. This overlay date was compared with the profile date for the section to determine if the profiling was performed before or after the overlay. For the sections where the IRI values before and after the overlay are approximately equal, there is a possibility that the overlay date in the database is incorrect and both these IRI values were values that were obtained after the section was overlaid. The data shown in figure 5.7.1 indicate that, in some cases, a substantial reduction in IRI can be obtained by a thin AC overlay.

As described before, there are 37 sections in the GPS-6B experiment, and the IRI before and after the overlay is known for 19 of these sections; for the other 18 sections only the IRI after the overlay is known. Therefore, there is a total of 37 sections for which the IRI after the overlay is known. The IRI after the overlay for these sections was analyzed to determine the distribution of the IRI values after overlay. The IRI of these sections ranged from 0.42 to 1.80 m/km (27 to 114 in/mi), with an average value of 0.95 m/km (60 in/mi). The frequency distribution of the IRI

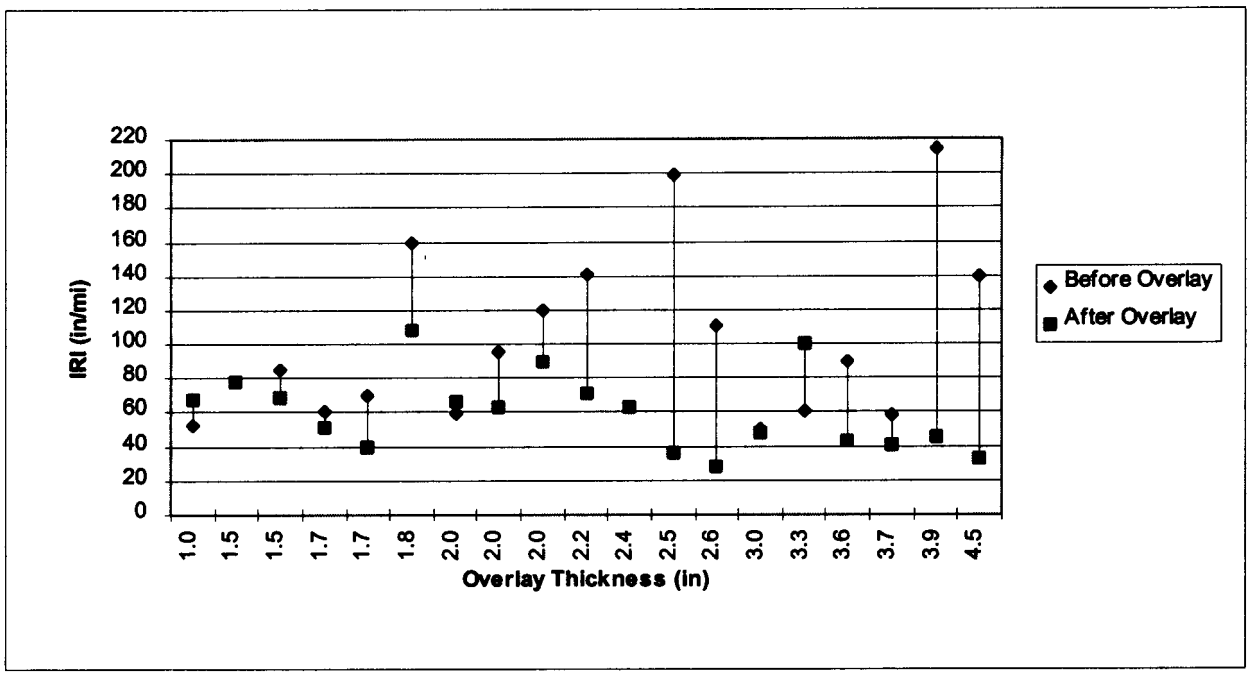

1 in/mi = 0.0158 m/km

Figure 5.7.1. IRI before and after overlay for GPS-6B sections.

of these sections after the overlay is shown in figure 5.7.2. As seen from this figure, the IRI of the overlay varied within a wide band; however, 73 percent of the IRI values were less than 1.10 m/km (70 in/mi). The factors that influence the IRI value of an overlaid pavement include: (1) the wavelength distribution in the pavement prior to the overlay, (2) the thickness of the overlay, (3) construction procedures, and (4) capability of the contractor.

Development of Roughness

Figure 5.7.3 presents the IRI versus age of pavement (after overlay) plots per region for the GPS-6B sections. This figure shows that virtually all sections maintain a relatively constant IRI over time. The age distribution of the sections shown in figure 5.7.3 indicate that 89 percent of the sections were less than 5 years old, with 45 percent of the pavement sections being less than 4 years old. Twenty-seven GPS-6B sections have been profiled three or more times. The statistical analysis described in section 5.1 of this report indicated that there was a statistically significant, positive linear relationship between IRI and age of overlay for only six sections. At 10 sections, the IRI at the last profile date was less than the IRI at the first profile date. Because only a small number of sections showed an increase in IRI, a meaningful analysis to statistically quantify the change in IRI cannot be carried out yet for the GPS-6B sections.

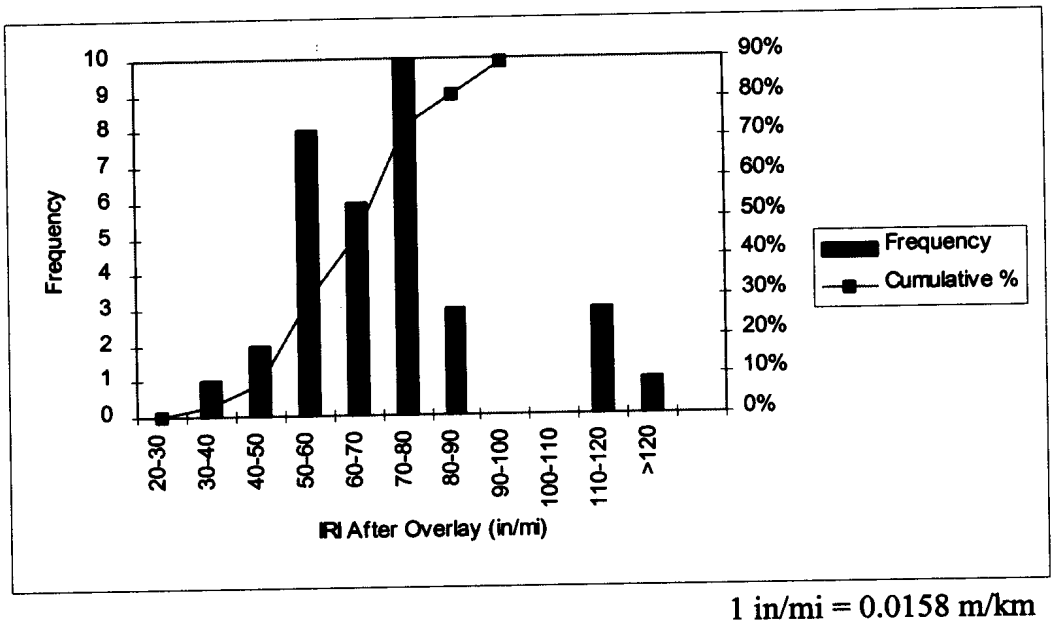

1 in/mi = 0.0158 m/km

Figure 5.7.2. Frequency distribution of IRI after overlay for GPS-6B sections.

In the LTPP program, GPS-6A sections were established on in-service pavements, and the IRI of the pavement immediately after the overlay is not known for these sections. The overlay thickness for these sections are recorded in an inventory file in the NIMS database, but were not available for many of the sections. Figure 5.7.4 presents the IRI versus pavement age (after overlay) relationship for the GPS-6A sections. The date when a section was overlaid is indicated by the assign date in the database file called experiment section. In the Western region it was noted that all GPS-6A sections had a similar assign date. As the age of the pavement after overlay was computed on the basis of this date, the pavement age shown in figure 5.7.4 for the sections in the Western region may be incorrect.

As seen in figure 5.7.4, some sections showed a relatively constant IRI with time, but some sections were exhibiting an increase in IRI with time. Fifty-seven GPS-6A sections had been profiled three or more times, and the statistical analysis described in section 5.1 of this report indicated that 24 sections showed a statistically significant linear increase in IRI with time. The slope from the least square regression indicates the rate of increase of IRI for each section, and the frequency distribution of the slopes for all GPS-6A sections are presented in table 5.7.1.

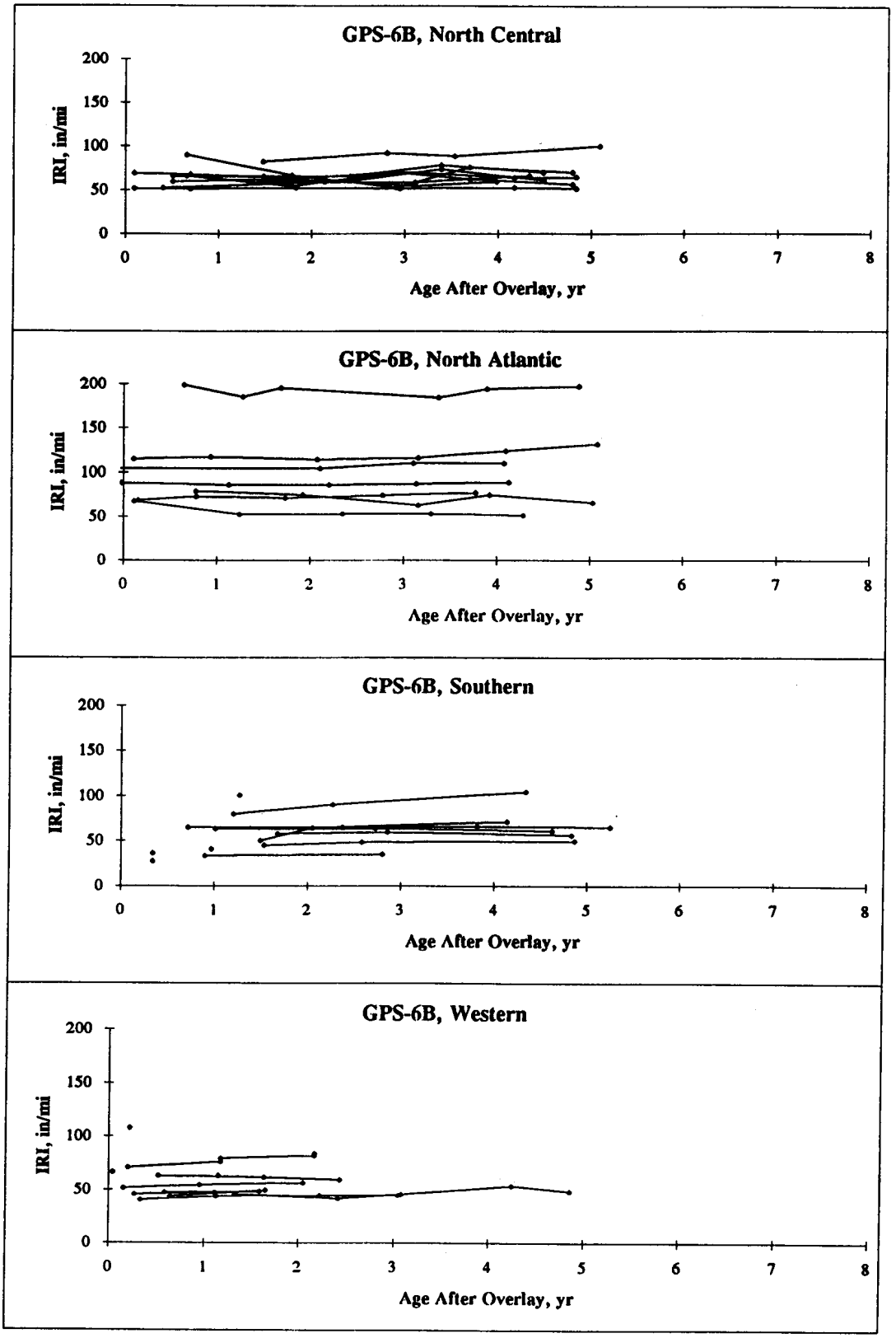

Figure 5.7.3. Trends in IRI development for the GPS-6B sections.

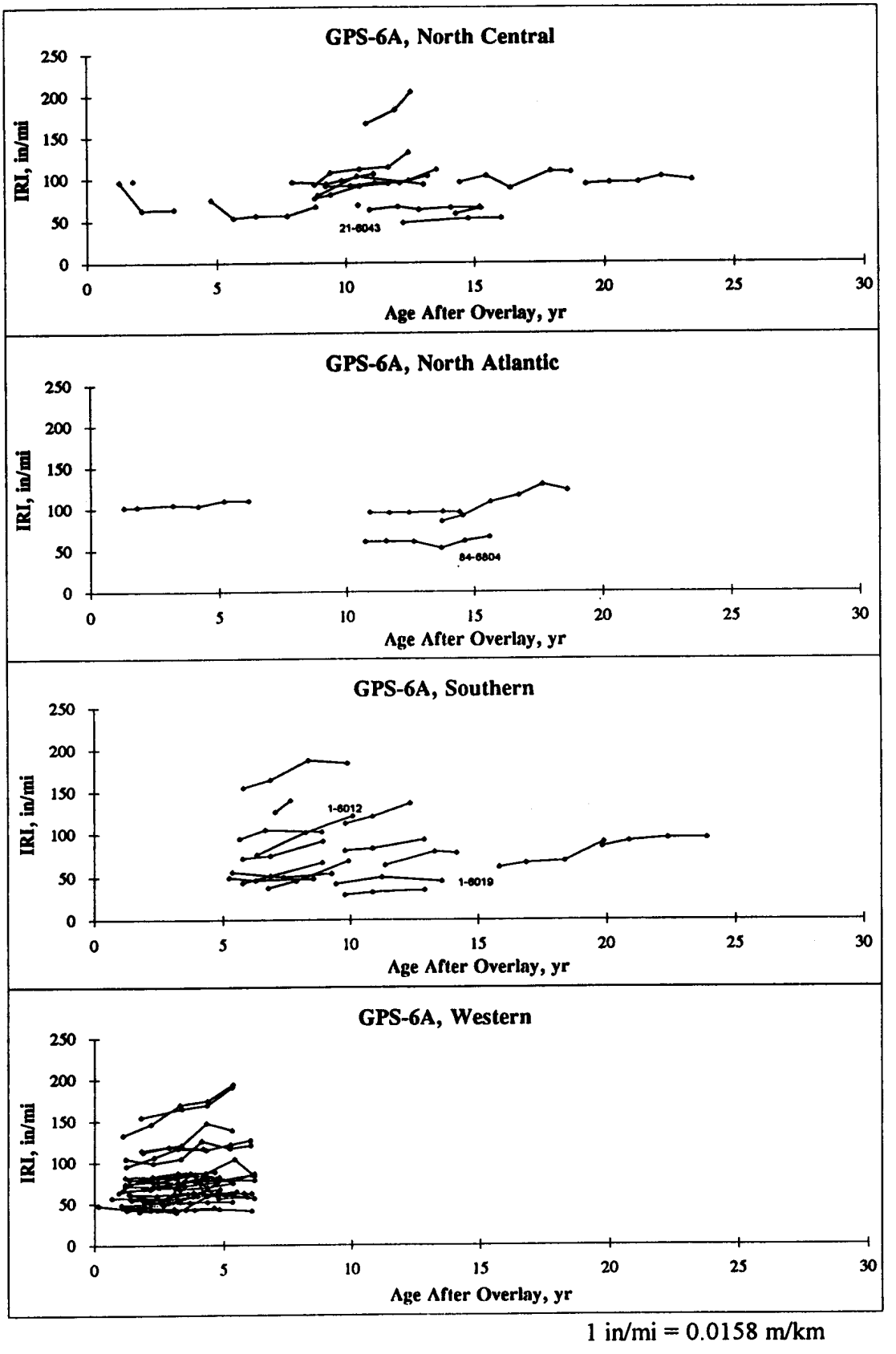

1 in/mi = 0.0158 m/km

Figure 5.7.4. Trends in IRI development for the GPS-6A sections.

Table 5.7.1. Frequency distribution of slope for GPS-6A sections.

Range of Slope (in/mi/yr)	Number of Sections	Percentage of Sections (%)
0	7	12
0 - 2	19	33
2 - 4	12	21
4 - 6	5	9
6 - 8	5	9
>8	9	16

Note: 1 in/mi = 0.0158 m/km.

The correlation coefficients between the slope and a selected group of parameters that could affect the rate of development of IRI are presented in table 5.7.2. Correlations considering all GPS-6A sections as well as considering those that have a slope greater than 2 in/mi/yr (0.03 m/km/yr) are shown in this table. When performing the correlation analysis for all sections, the slope of the sections that had a negative slope was set to zero. Correlation coefficients are affected by data distribution, and the cause of some illogical correlations in table 5.7.2 were caused by such occurrences.

When all sections were considered, the highest correlation of the slope occurred for minimum surface modulus (-0.32), which was obtained from deflection data. When the sections that showed a slope greater than 0.03 m/km/yr (2 in/mi/yr) were considered, the highest correlation coefficient (-0.49) was with the SN estimated from thickness of the pavement layers. Multiple regression analysis was performed for these two cases separately by considering the slope as the dependent variable. When all sections were considered in the analysis, the following equation was obtained:

$$\text{Slope} = 5.26 + 0.03 * \text{Frzthaw} - 1.566 * 10^{-4} * \text{Minsur} \quad \text{..... (5.7.1)}$$

$R^2 = 0.30$, Standard Error = 3.26, n = 44

where:

Slope = rate of increase of IRI (in/mi/yr),
Frzthaw = number of freeze-thaw cycles/yr, and
Minsur = minimum surface modulus (psi).

Table 5.7.2. Correlation coefficients of slopes for GPS-6A sections

Parameter	All Sections	Sections With Slope > 2 in/mi/yr
Annual Precipitation	-0.29	-0.23
Average Annual Days Below 32 °F	0.27	0.07
Average Annual Days Above 90 °F	0.07	0.07
Average Annual Wet Days	-0.24	-0.20
Average Annual Freeze-Thaw Cycles	0.30	0.13
Average Annual Freeze Index	0.14	-0.02
Percent Passing No. 200 Sieve for Subgrade	-0.14	-0.32
Subgrade Moisture Content	-0.25	-0.39
Liquid Limit of Subgrade	-0.19	-0.47
Plastic Limit of Subgrade	-0.28	-0.48
Plasticity Index of Subgrade	-0.09	-0.37
Annual KESALs	-0.04	-0.26
Base Thickness	-0.09	-0.10
Structural Number	-0.17	-0.49
AC Thickness	-0.13	-0.44
Minimum Surface Modulus	-0.32	-0.30
Dynamic Stiffness Modulus	-0.38	-0.28

Note: 1 in/mi = 0.0158 m/km.

When only the sections that showed a slope greater than 0.03 m/km/yr (2 in/mi/yr) were considered in the analysis, the following equation was obtained:

Slope = 11.15 - 0.96*SN

R^2 = 0.19, standard error = 3.09, and n = 31

where:

SN = structural number.

Performance of Specific GPS-6A Sections

Characteristics of two sections that have similar traffic levels but different behavior, as well as two sections that have low IRI values are described in this section. These sections are noted in figure 5.7.4.

There were two GPS-6A sections 1-6012 and 1-6019 that were noted to have carried an estimated 1050 KESAL/yr over their 10 to 13 years of service after overlay but had different IRI behavior (see figure 5.7.4). Both these sections are located in high precipitation environments with very minimal freeze-thaw cycles, and have similar SN. The subgrade properties at the two locations are likely to have been a major factor in the difference in their performance. The better performer (1-6109) has approximately 305 mm (12 in) of AC, which is located on a well-draining sand subgrade with no drains. This section has an IRI of 0.71 m/km (45 in/mi) 14 years after the overlay. The pavement section for the poorer performer (1-6012) consisted of 127-mm (5-in) AC thickness on 127-mm (5-in) of AC-treated base that is located on a silty sand subgrade (P200 = 21 percent , w% = 11 percent) with continuous well-type drains. This section had an IRI value of 1.91 m/km (121 in/mi) 10 years after the overlay.

Section 84-6804 was noted to be performing well under high traffic (730 KESAL/yr), high precipitation, and high freeze index conditions (see figure 5.7.4) . This is a very thick section (SN = 6.3) consisting of 152-mm (6-in) AC, over 76 mm (3 in) of AC-treated base, and a thick subbase providing high overburden on the subgrade. The subgrade has a P200 content of 22 percent and a moisture content of 5 percent. The IRI value for this section was 0.84 m/km (53 in/mi) 16 years after the overlay. Another good performer in wet freeze conditions was section 21-6043 (see figure 5.7.4). This is a high traffic route (970 KESAL/yr) located on a subgrade that is similar to that discussed in the previous section. This section had an estimated SN of 5.1 with a thick subbase, but the freezing index at this site was less than for section 84-6804. This section had a IRI of 1.04 m/km (66 in/mi) 15 years after overlay.

5.7.3 Roughness Development at GPS-7 Sections

Background

The GPS-7 experiment is the study of PCC pavements that are overlaid with AC. The PCC pavements include jointed plain concrete pavements (JPCP), jointed reinforced concrete pavements (JRCP), and continuously reinforced concrete pavements (CRCP). The GPS-7 experiment is divided into two categories: GPS-7A and GPS-7B. The GPS-7A sections were existing overlaid pavements that were at different periods of their service life when they were accepted into the LTPP program. The GPS-7B sections were overlaid after they were accepted to the LTPP program, and the IRI of these sections immediately after the overlay is known.

IRI Before and After Overlay

There are 21 GPS-7B sections in the LTPP experiment for which profile data are available; 15 of these sections had been profiled prior to being overlaid, and therefore the IRI of these sections before the overlay is known. Figure 5.7.5 presents the IRI before the overlay, the IRI after the overlay, and the overlay thickness for the 15 sections for which the IRI before and after the overlay is known. In this figure, the overlay thickness are arranged in ascending order. The IRI after the overlay of 12 of the sections shown in figure 5.7.5 ranged from 0.73 to 1.06 m/km (46 to 67 in/mi), with three sections having an IRI between 1.32 and 1.51 m/km (84 and 96 in/mi). The data shown in figure 5.7.5 indicate that even a relatively thin overlay that is less than 88 mm (3.5 in) can substantially reduce the IRI of a pavement. For three cases shown in figure 5.7.5, the IRI of the pavement after the AC overlay was more than 1.26 m/km (80 in/mi). For these three cases, the AC overlay reduced the IRI of the pavement by a very small amount.

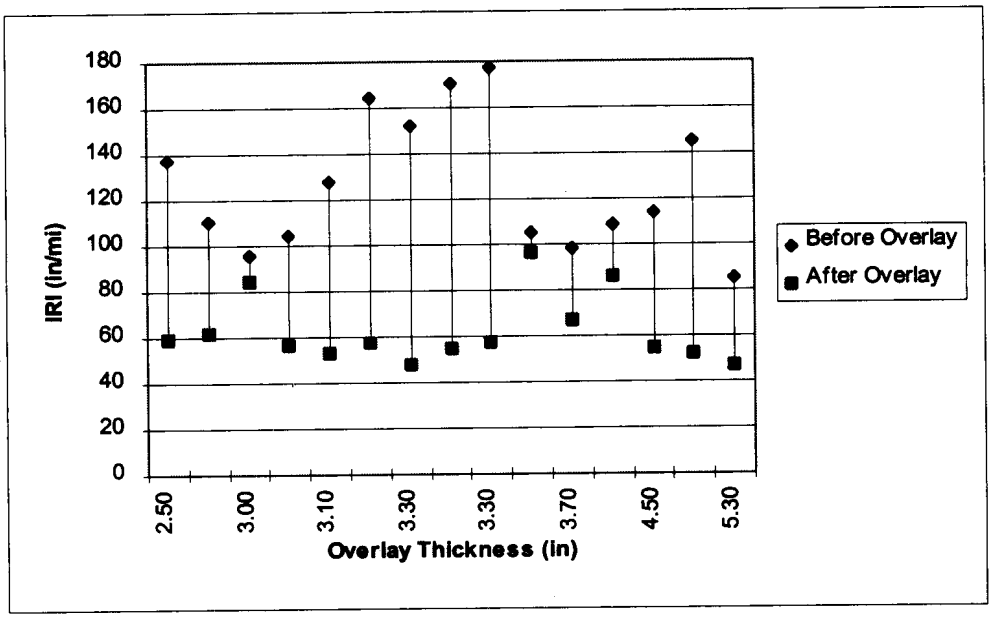

1 in/mi = 0.0158 m/km

Figure 5.7.5. IRI before and after overlay for GPS-7B sections.

As described previously, there are 21 sections in the GPS-7B experiment, and the IRI before and after the overlay is known for 15 of these sections; for the other six sections only the IRI after the overlay is known. Therefore, the IRI after overlay is known for 21 sections. The

frequency distribution of the IRI after overlay of all 21 GPS-6B sections is shown in figure 5.7.6. As shown in this figure, the IRI after overlay ranged from 0.6 to 1.58 m/km (40 to 100 in/mi), with 76 percent of the IRI values after the overlay being less than 1.10 m/km (70 in/mi). The factors that influence the IRI value of an overlaid pavement include: (1) the wavelength distribution in the pavement prior to the overlay, (2) the thickness of the overlay, (3) construction procedures, and (4) capability of the contractor.

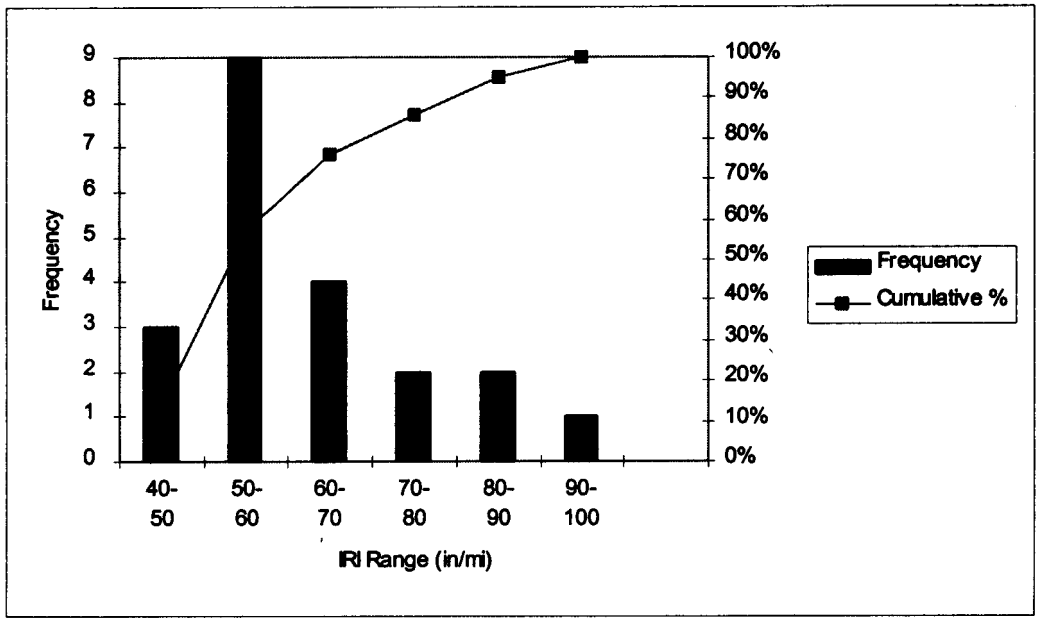

1 in/mi = 0.0158 m/km

Figure 5.7.6. Frequency distribution of IRI after overlay for GPS-7B sections.

Development of Roughness

GPS-7B sections are located only in the North Atlantic and North Central regions, and the IRI versus pavement age (after overlay) plots for the GPS-7B sections in these two regions are presented in figure 5.7.7. The age of all the GPS-7B sections at the last profile date was less than 6 years, with 72 percent of the sections being less than 4 years old. As shown in figure 5.7.7, virtually all sections are showing a flat response of IRI over time. Of the GPS-7B sections, 16 sections had been profiled three or more times. The linear regression analysis described in section 5.1 of this report computed a slope for each section that is the rate of increase of IRI for the section. The analysis indicated that the slope for eight of the sections to be negative, and a statistically significant linear relationship between IRI and pavement age existed only for three

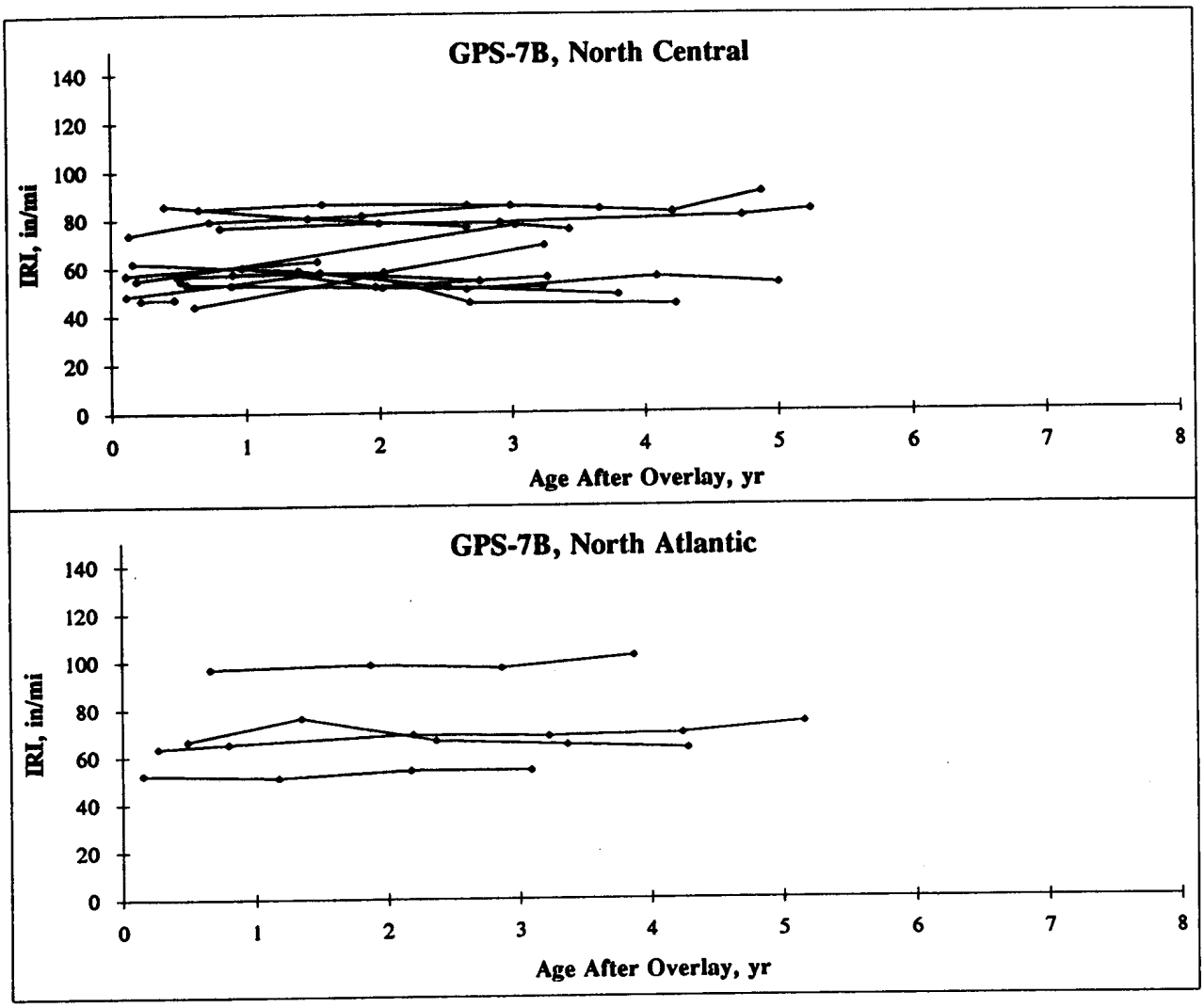

1 in/mi = 0.0158 m/km

Figure 5.7.7. Trends in IRI development for the GPS-7B sections.

sections. Therefore, a statistical analysis to quantify the change in IRI for GPS-7B sections cannot be carried out yet.

In the LTPP program, GPS-7A sections were established on in-service pavements, and the IRI of the pavement immediately after the overlay is not known for these sections. The IRI versus pavement age (after overlay) plots for the GPS-7A sections are presented in figure 5.7.8. The age of the GPS-7A sections in the Western region at last profile date are all less than 5 years. As seen in figure 5.7.8, most GPS-7A sections show a flat response of IRI over time, with a few sections showing an increase of IRI with time. Thirty GPS-7A sections had been profiled three or more times, and the linear regression analysis described in section 5.1 of this report computed a slope (rate of increase of IRI) for each section. These values are presented in appendix B. The frequency distribution of the slopes is presented in table 5.7.3. Twenty-three percent of sections had negative values for the rate of change of IRI, with 37 percent of sections having a rate of increase of IRI of between zero and 0.03 m/km (2 in/mi).

Table 5.7.3. Frequency distribution of slope for GPS-7A sections.

Range of Slope (in/mi/yr)	Number of Sections	Percentage of Sections (%)
<0	7	23
0 - 1	6	20
1 - 2	5	17
2 - 3	1	3
3 - 4	2	7
> 4	9	30

Note: 1 in/mi = 0.0158 m/km.

A correlation analysis was performed between the slope and possible factors that could cause an increase in roughness. The analysis was carried out separately for all GPS-7A sections and for sections that showed a slope greater than 0.03 m/km (2 in/mi/yr). When the analysis was carried out for all GPS-7A sections, the slope of sections that had a negative value was set to zero. The results of this correlation analysis are presented in table 5.7.4. PCC properties such as compressive strength, elastic modulus, and split tensile strength were not available for many GPS sections and were not used in the analysis. Correlation coefficients are affected by the biases in the distribution of the data, and some of the illogical correlations are attributed to these biases. None of the factors that were explored had a high and logical correlation with the slope.

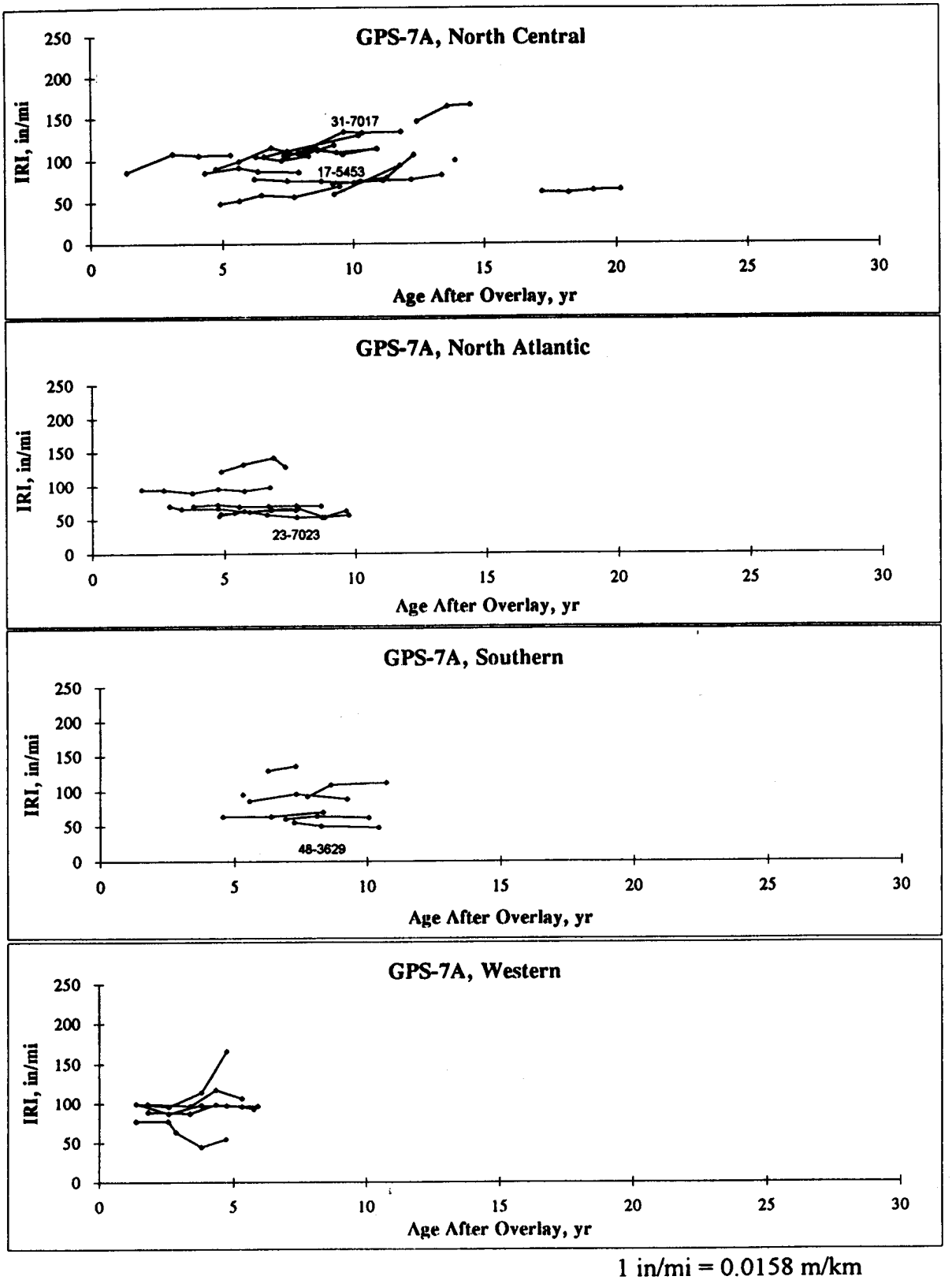

Figure 5.7.8. Trends in IRI development for the GPS-7A sections.

Table 5.7.4. Correlation coefficients of slope for GPS-7A sections.

Variable	All Sections	Sections With Slope > 2 in/mi/yr
Annual Precipitation	-0.11	0.38
Average Annual Days Below 32°F	-0.10	-0.68
Average Annual Days Above 90°F	-0.02	0.20
Average Annual Wet Days	-0.08	0.09
Average Annual Freeze-Thaw Cycles	-0.15	-0.62
Average Annual Freeze Index	0.01	-0.48
Percent Passing No. 200 Sieve for Subgrade	-0.12	-0.63
Subgrade Moisture Content	-0.09	-0.44
Liquid Limit of Subgrade	-0.20	-0.81
Plastic Limit of Subgrade	-0.20	-0.84
Plasticity Index of Subgrade	-0.16	-0.64
Annual KESALs	-0.11	-0.07
Overlay Thickness	0.01	0.55
PCC Thickness	-0.02	0.27
Base Thickness	-0.12	-0.40

Note: 1 in/mi = 0.0158 m/km.

Therefore, models for predicting the IRI development for GPS-7A experiment could not be developed. Distresses in AC overlays of PCC pavements primarily occur at joints and working cracks, and generally begin with reflection cracks that deteriorate and spall with time. The IRI will therefore be affected by the joint spacing of the PCC pavement. The development of roughness will also be affected by the type of joint repairs that are carried out prior to the overlay. The joint repairs can consist of full-depth PCC or AC patches, partial-depth PCC or AC patches, and load transfer restoration. Strategies such as placing a paving fabric at joints prior to overlay to retard reflection cracking, or sawing and sealing of joints in the AC overlay will also influence the development of roughness. The factors that were described previously, as well as the properties of PCC that control temperature-related movement of the PCC slab, are expected to be the primary factors that relate to roughness development in AC overlays of PCC pavements.

Performance of Specific GPS-7A Sections

Characteristics of three sections that have low IRI values and a section that has a high IRI value are described in this section. The described sections are indicated in figure 5.7.8.

A section that is performing well is section 23-7023, which is located in the wet freeze zone. The IRI value of this section is 1.0 m/km (63 in/mi) 10 years after the overlay. This is a 196-mm-(7.7-in-) thick JRCP that was 27 years old when overlaid with 157 mm (6.2 in) of AC. The section experiences approximately 1100 KESAL/yr. The combination of thicker overlay and subgrade conditions (P200 = 23 percent, w% = 6 percent) can be attributed to the good performance of this section.

A poor performer that is noted is section 31-7017, which is located in the wet freeze zone. The IRI of the pavement 11 years after the overlay is 2.1 m/km (133 in/mi). This is a section that is subjected to a low traffic rate of 50 KESAL/yr, and the pavement section is a 201-mm (7.9-in) thick JRCP slab that was 30 years old when overlaid with 81 mm (3.2 in) of AC. This section rests on subgrade with a P200 of 91 percent and a moisture content of 28 percent.

There are two sections that are AC overlays of CRCP sections that have performed well (48-3629 and 17-5453). The IRI of section 48-3629 is 0.76 m/km (48 in/mi) 10 years after the overlay, while the IRI of section 17-5453 is 1.15 m/km (73 in/mi) 10 years after the overlay. The pavement section for both of these sections is approximately 66-mm (2.6- in) AC overlay of 203-mm (8-in) CRCP slab. Both sections rest on subgrades with relatively high P200 and high moisture contents and are subjected to high traffic volumes.

5.7.4 Roughness Development at GPS-9 Sections

Background

The GPS-9 experiment is the study of unbonded PCC overlays of PCC pavements. The PCC pavement types can include jointed plain concrete pavement (JPCP), jointed reinforced concrete pavement (JRCP) and continuously reinforced concrete pavement (CRCP). There were 28 GPS-9 test sections for which profile data were available. There were six combinations of pavement types included in this experiment, as shown in table 5.7.5.

Roughness Development

The IRI versus age of pavement (after overlay) plots for GPS-9 sections are shown in figure 5.7.9. At the latest profile date for these sections, 60 percent of the sections were less than 5 years old after the overlay. As seen in figure 5.7.9, some sections showed a relatively flat

Table 5.7.5. Pavement types in the GPS-9 experiment.

Original Pavement	Type of PCC Overlay	Number of Sections
CRCP	JRCP	4
JPCP	CRCP	7
JPCP	JPCP	6
JPCP	JRCP	4
JRCP	CRCP	2
JRCP	JRCP	2

response of IRI over age, with some sections showing a variable IRI pattern over the years, and some sections showing an increase in IRI with age.

Twenty-four GPS-9 sections had been profiled three or more times, and the linear regression analysis described in section 5.1 of this report computed a slope (rate of increase of IRI) for each section. These values are presented in appendix B. The frequency distribution of the slopes are presented in table 5.7.6. A statistically significant linear relationship between IRI and pavement age existed for only four sections. Twenty-nine percent of sections had negative values for the rate of change of IRI, with 38 percent of sections having a rate of increase of IRI between zero and 0.03 m/km (2 in/mi). Concrete strength data from laboratory tests (such as compressive strength) are not available for the majority of the sections.

Table 5.7.6. Frequency distribution of slope for GPS-9 sections.

Range of Slope (in/mi/yr)	Number of Sections	Percentage of Sections (%)
<0	7	29
0 - 2	9	38
2 - 4	1	4
4 - 6	2	8
6 - 8	3	13
>8	2	8

Note: 1 in/mi = 0.0158 m/km.

A correlation analysis was performed between the slope and the parameters presented in table 5.7.4 to see if the slope could be related to these parameters. The analysis was carried out separately for all sections and then for the sections that showed a slope greater than 0.03 m/km (2

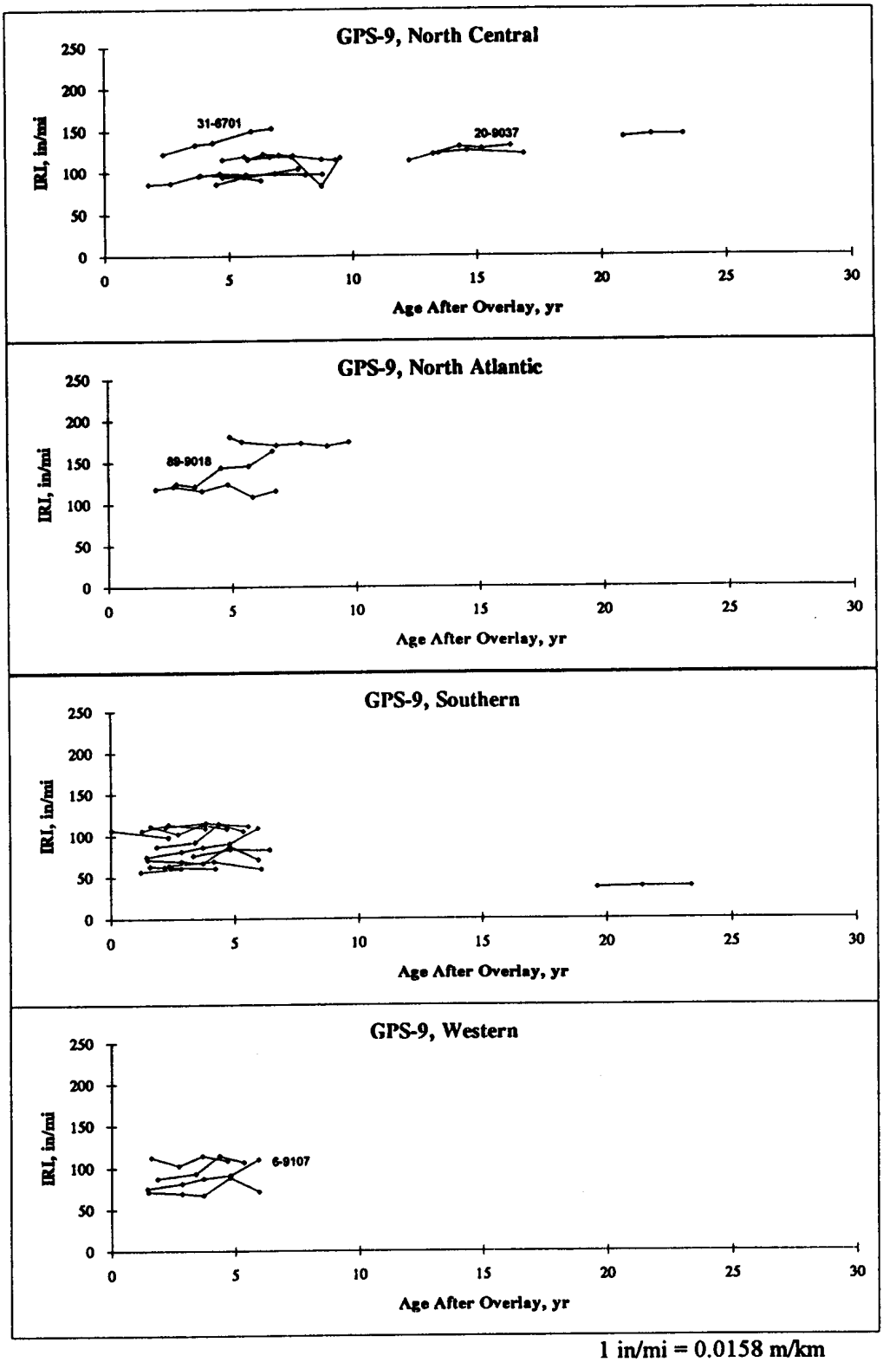

Figure 5.7.9. Trends in IRI development for the GPS-9 sections.

in/mi/yr). However, no strong logical correlations could be obtained. Therefore, a model to predict the development of IRI for GPS-9 sections could not be developed. The roughness development characteristics that are associated with the six combinations of pavement types included in this experiment (see table 5.7.5) are expected to be different. The low number of test sections for each pavement type prevents a detailed analysis from being performed on each pavement type.

Performance of Specific Sections

Characteristics of four GPS-9 sections that have a high rate of increase of IRI are described in this section. Only four GPS-9 sections had a statistically significant relationship between IRI and pavement age, and all these sections had a high rate of increase of IRI. These sections are shown in figure 5.7.9. The rate of increase of IRI for these sections are: (1) section 06-9107: 0.11 m/km/yr (7.2 in/mi/yr), (2) section 20-9037: 0.07 m/km/yr (4.2 in/mi/yr), (3) section 31-6701: 0.11 m/km/yr (7.2 in/mi/yr), and (4) section 89-9018: 0.16 m/km/yr (10.4 in/mi/yr).

For these four sections, test data for concrete were available only for section 06-9107, which was a 220-mm (8.8-in) thick JPCP overlay of a JPC pavement. The average compression strength and the split tensile strength of concrete for this site were 29.7 MPa (4315 psi) and 3.1 MPa (447 psi), respectively. These were the lowest values in the entire GPS-9 data set. The original PCC was much stronger than the overlay. It is believed that this low overlay strength combined with high traffic volume (800 KESAL/yr) led to the high rate of IRI development at this site. The average thickness of the unbonded PCC overlay determined from cores at test sections 89-9018 (JPC overlay of a JPC pavement) and test section 20-9037 (JPC overlay of a JRC pavement) were 160 mm (6.4 in) and 145 mm (5.8 in), respectively, which are relatively low overlay thicknesses. Both sections had low traffic volumes (<180 KESAL/yr).

5.7.5 Summary for Overlaid Pavements

The IRI values before and after the overlay were available for 19 GPS-6B and 15 GPS-7B sections. A review of the IRI data at these sites indicated there is little effect of the roughness prior to overlay on the roughness immediately after the overlay. The IRI after overlay of the GPS-6B sections ranged from 0.42 to 1.80 m/km (27 to 114 in/mi), with 73 percent of the sections having an IRI less than 1.10 m/km (70 in/mi). For GPS-7B sections, the IRI after the overlay ranged from 0.73 to 1.58 m/km (46 to 100 in/mi), with 76 percent of the IRI values being

less than 1.10 m/km (70 in/mi). The trend in the data of the GPS-6A versus GPS-6B experiments indicates on a qualitative basis that roughness starts to develop after about 10 years of service. The continued monitoring of these sections is considered important. It could be seen that the trend in increase in IRI after 10 years is a larger rate of increase than that for the GPS-1 or GPS-2 pavements.

GPS-6B and GPS-7B sections are generally less than 5 years old. Very little change in IRI has occurred at most of these sections after the overlay. Therefore, a statistical analysis on the data cannot be performed yet. For GPS-6A, -7A and -9 sections, a linear regression analysis was performed on the time-sequence IRI data to determine the rate of increase of IRI. Correlation analyses were performed separately for each experiment to relate the rate of increase of IRI with parameters that could affect the increase of IRI. For GPS-7A and GPS-9 experiments, strong and logical correlations were not observed, and models to predict IRI development could not be developed. For GPS-6A sections, a relationship between the rate of increase of IRI and the minimum surface modulus was developed by considering all sections, while a relationship between the rate of increase of IRI and SN was developed for the sections that had a rate of increase of IRI that was greater than 0.03 m/km/yr (2 in/mi/yr). However, both these relationships had low R^2 values and high standard errors of estimates.

5.8 IRI PREDICTION USING LINEAR MODELS

The increase in IRI of a pavement after construction will depend on factors such as pavement layer thickness, subgrade properties, climatic factors, and applied traffic. If the initial IRI of the pavement is known, the current IRI of the pavement can be used to find the change in IRI. The change in IRI can then be related to the variables that affect the development of IRI to develop models. An approach that has been used in some research efforts to develop roughness models is to treat the current IRI as the dependent variable and relate it to a set of independent variables that are associated with the development of roughness. However, these independent variables are related to the change in roughness, which is the difference between the current roughness and the initial roughness, and not simply to the current roughness. Therefore, simply developing models by relating the current IRI with parameters that may cause the IRI to increase, without considering the initial IRI of the pavement, will not result in accurate models.

Initially, in this research effort models were developed by relating the current IRI of the pavement to factors that may cause an increase in IRI. Multiple regression analysis was performed using computerized stepwise regression procedures to develop these models. The

following is an example of a model that was developed for the GPS-3 sections by considering all GPS-3 sections.

IRI = 0.73 + 2.09* TIME + 3.14 * PCCTH + 0.18 * AVG32 + 0.52 * PI + 0.29 * AVGWET

Adjusted R^2 = 0.23 and standard error = 36
where:

IRI = current IRI (in/mi),
TIME = age of pavement (yr),
PCCTH = PCC thickness (in),
AVG32 = average days below 32°F,
PI = plasticity index, and
AVGWET = average wet days/yr

A residual analysis of this model performed by plotting the residuals with the predicted IRI indicated a pattern in the residuals. The pattern showed that this model overpredicts the IRI of pavements that have low IRI values and underpredicts the IRI of pavements that have high IRI values. Therefore, such models are not considered to be accurate in correctly predicting the IRI of the pavement.

A model developed for the GPS-9 sections using a similar approach yielded the following model:
IRI = -45.4 + 4.08 * TIME + 0.43 * AVG32 + 5.34 * PCCOL + 0.72 * ANNP
R^2 = 0.45 and standard error = 21

where:

IRI = current IRI (in/mi),
TIME = age of pavement after overlay (yr),
AVG32 = average days below °F.
PCCOL = PCC overlay thickness (in), and
ANNP = annual precipitation (in).

The R^2 of this model may suggest that an approximate IRI of the pavement can be obtained by this model. However, a residual analysis of this model performed by plotting the residuals versus the predicted IRI indicated a pattern in the residuals. The residuals showed that

this model overpredicts the IRI of pavements that have low IRI values and underpredicts the IRI of pavements that have high IRI values.

CHAPTER 6: ROUGHNESS CHARACTERISTICS OF SPS-1 AND SPS-2 PROJECTS

6.1 ROUGHNESS CHARACTERISTICS OF SPS-1 PROJECTS

6.1.1 Description of SPS-1 Experiment

The Specific Pavement Studies SPS-1 experiment is titled the Strategic Study of Structural Factors for Flexible Pavements. The SPS-1 experiment was developed to investigate the effect of selected structural factors on the long-term performance of flexible pavements constructed on different subgrade types in different environmental regions. The subgrade types considered in this experiment are classified as fine grained and coarse grained, while the environmental regions considered are the four LTPP environmental regions: wet freeze, wet-no freeze, dry freeze and dry-no freeze.

Table 6.1.1 presents the structural properties of the test sections in the SPS-1 experiment. These 24 sections are to be constructed for each combination of subgrade type and environmental region, with test sections 1 through 12 being constructed at one site, and test sections 13 through 24 being constructed at a different site. In a SPS-1 project, the layout of the test sections can be in any sequence; however, it is recommended that the expected life of the test section and base type be considered when deciding on the layout. The structural factors considered in this experiment are: surface layer thickness, base type, base course thickness, and drainability. Two different surface course thicknesses of AC, 100 mm (4 in) and 175 mm (7 in), and five different base types are used in the experiment. The base types are: dense-graded aggregate base, asphalt-treated base, asphalt-treated base over dense-graded aggregate base, permeable asphalt-treated base over dense-graded aggregate base, and asphalt-treated base over permeable asphalt-treated base. The total base thickness at the test sections ranges from 200 mm (8 in) to 400 mm (16 in), with underdrains being provided at all sections that have a permeable asphalt-treated base. The estimated SN for each test section is also presented in table 6.1.1. The layer coefficients that were used to compute the SNs are: AC - 0.40, asphalt-treated base - 0.32, permeable asphalt-treated base - 0.22, and dense-graded aggregate base - 0.12. Each test section is constructed over a minimum length of 182 m (600 ft), and 152 m (500 ft) of the section is used for monitoring.

Table 6.1.1. Structural properties of SPS-1 sections.

Test Section Number	Asphalt Concrete Thickness (in)	Layer 2		Layer 3		Estimated Structural Number
		Material	Thickness (in)	Material	Thickness (in)	
1	7	DGAB	8	-	-	3.76
2	4	DGAB	12	-	-	3.04
3	4	ATB	8	-	-	4.16
4	7	ATB	12	-	-	6.64
5	4	ATB	4	DGAB	4	3.36
6	7	ATB	8	DGAB	4	5.84
7	4	PATB	4	DGAB	4	2.96
8	7	PATB	4	DGAB	8	4.64
9	7	PATB	4	DGAB	12	5.12
10	7	ATB	4	PATB	4	4.96
11	4	ATB	8	PATB	4	5.04
12	4	ATB	12	PATB	4	6.32
13	4	DGAB	8	-	-	2.50
14	7	DGAB	12	-	-	4.24
15	7	ATB	8	-	-	5.36
16	4	ATB	12	-	-	5.44
17	7	ATB	4	DGAB	4	4.56
18	4	ATB	8	DGAB	4	4.64
19	7	PATB	4	DGAB	4	4.16
20	4	PATB	4	DGAB	8	3.44
21	4	PATB	4	DGAB	12	3.92
22	4	ATB	4	PATB	4	3.70
23	7	ATB	8	PATB	4	6.24
24	7	ATB	12	PATB	4	7.52

Note 1: DGAB - dense-graded aggregate base, ATB - asphalt-treated base, PATB - permeable asphalt-treated base.

Note 2: 1 in = 25.4 mm.

6.1.2 Data Availability for SPS-1 Projects

The IRI values of the SPS-1 test sections were obtained from the RIMS, through the regional contractors. Table 6.1.2 presents the SPS-1 projects for which IRI data were available. This table also presents the test section numbers constructed at each site, the number of times the project has been profiled, the subgrade type, the LTPP environmental region, and the estimated annual ESALs applied to the test section. As shown in table 6.1.2, profile data are available for six SPS-1 projects. One project has been profiled three times, while three projects have been

profiled twice, and the other two projects have been profiled only once. The SPS-1 projects are generally first profiled within a month after they are opened to traffic; thereafter, they are profiled annually.

Table 6.1.2. SPS-1 projects for which IRI data were available.

Project Location	State Code	Test Section Numbers	Number of Times Profiled	Subgrade Type	Environmental Region	Annual ESALs
Alabama	AL	1 - 12	1	Fine Grained	Wet-No Freeze	237,000
Arizona	AZ	13 - 24	2	Coarse Grained	Dry-No Freeze	200,000
Iowa	IA	1 - 12	3	Fine Grained	Wet Freeze	130,000
Kansas	KS	1 - 12	2	Fine Grained	Dry Freeze	469,000
Nebraska	NE	13 - 24	2	Fine Grained	Dry Freeze	119,000
Virginia	VA	13 - 24	1	Fine Grained	Wet Freeze	N/A

Extensive sampling is performed at the SPS-1 projects to obtain samples from the subgrade, base, and surface layers. Laboratory tests are performed on the samples to characterize material properties. Data files containing laboratory test data were obtained from the RIMS, through the regional contractors. A review of these data files indicated that very few data were available in these files. Therefore, it was not possible to conduct an analysis to relate material properties to the roughness at the test sites.

6.1.3 IRI After Construction for SPS-1 Sections

The IRI referred to in this section is the average IRI of the left and right wheel paths, unless specifically mentioned otherwise. The IRI values at the test sections immediately after construction were examined to study the IRI characteristics of new pavements. The average IRI of all test sections at a SPS-1 project was computed by averaging the individual IRI of the test sections. Figure 6.1.1 presents the average IRI for each SPS-1 project. The SPS-1 project in Arizona was constructed on a coarse-grained subgrade, while all other SPS-1 projects were constructed on a fine-grained subgrade. The average IRI for the SPS-1 projects in Alabama, Arizona, Iowa, and Kansas ranged between 0.74 and 0.88 m/km (47 and 55 in/mi), with the project in Nebraska having the highest average IRI of 1.13 m/km (72 in/mi). The COV of the IRI between the test sections in each project is shown in figure 6.1.2. The COV of IRI indicates the variability of IRI between the test sections. The SPS-1 projects in Virginia and Alabama had the lowest variability in IRI between the test sections, with the COV for these two projects being 6 and 8 percent, respectively.

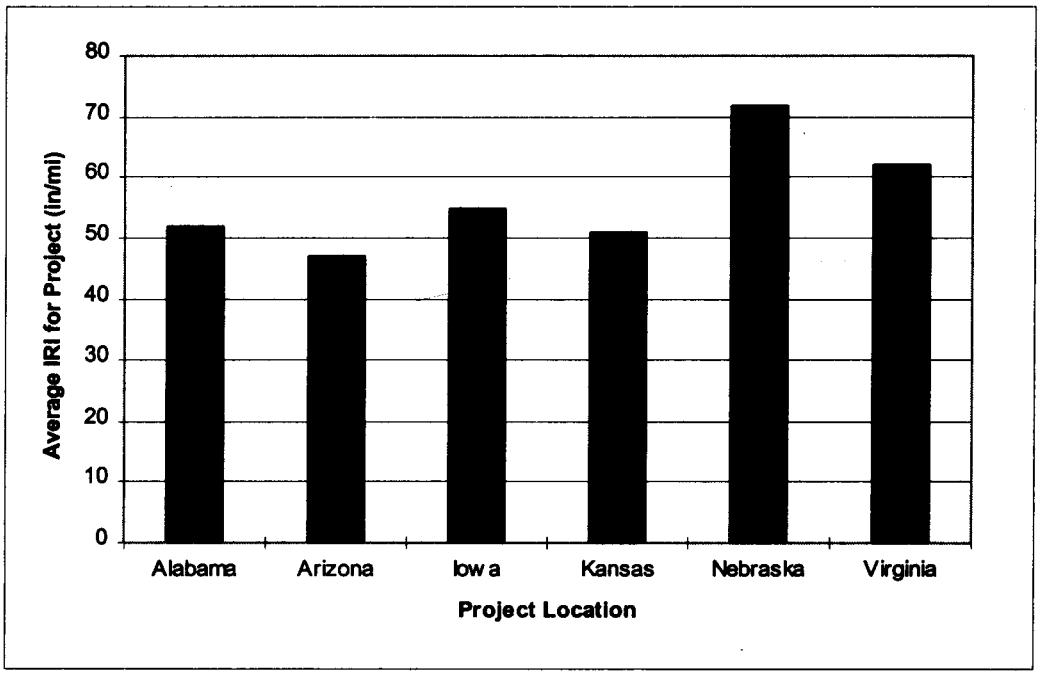

1 in/mi = 0.0158 m/km

Figure 6.1.1. Average IRI for SPS-1 projects.

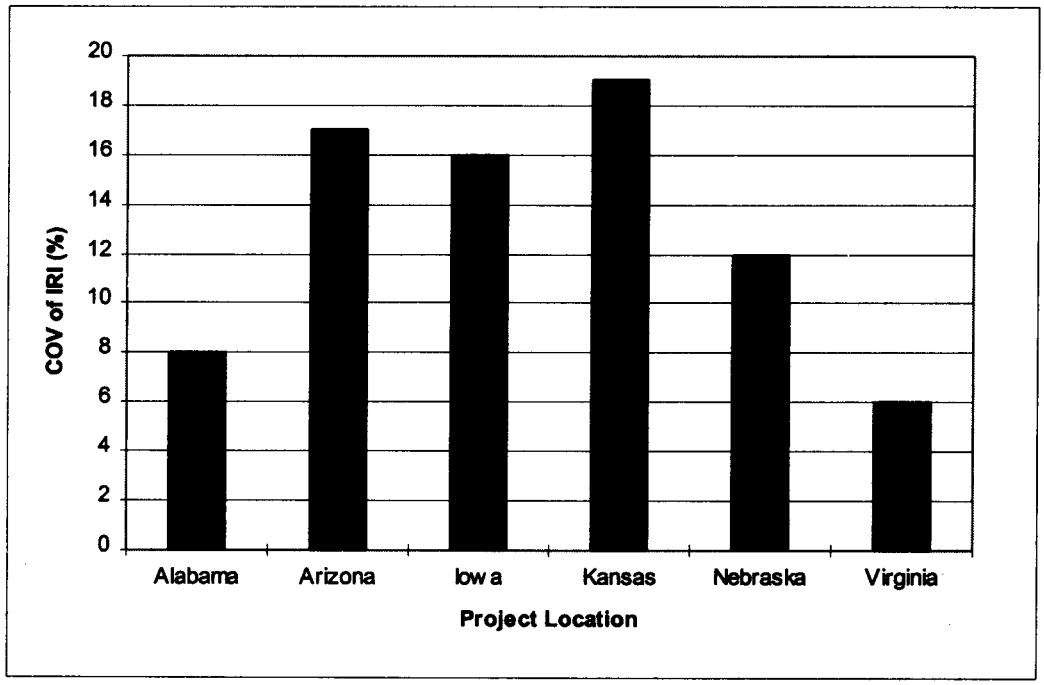

1 in/mi = 0.0158 m/km

Figure 6.1.2. COV of IRI of test sections in SPS-1 projects.

The IRI values after construction of the test sections in the SPS-1 projects in Alabama, Iowa, and Kansas which consist of test sections 1 through 12 (see table 6.1.1), are shown in figure 6.1.3. The IRI values after construction for the test sections in the SPS-1 projects in Arizona, Nebraska, and Virginia which contain test sections 13 through 24, are shown in figure 6.1.4 The subgrade at all projects was fine-grained, except for the project in Arizona, which had a coarse-grained subgrade. These figures show that varying IRI values were obtained for the same pavement section in projects constructed at different locations.

Large differences in IRI between the right and the left wheel paths were observed for the SPS-1 projects in Alabama and Arizona, with the right-wheel-path IRI being higher than the left-wheel-path IRI. The average difference in IRI between the right and left wheel paths of the test sites for the projects in Alabama and Arizona was 0.32 and 0.30 m/km (20 and 19 in/mi), respectively. Figure 6.1.5 shows the difference in IRI between the right and the left wheel paths for the test sections in the SPS-1 project in Alabama. The largest difference in IRI between the wheel paths occurred at sections 1 and 4 in Alabama, and was 0.44 m/km (28 in/mi). In the Arizona SPS-1 project, the largest difference between right- and left-wheel-path IRI at a test section was 0.55 m/km (35 in/mi). At the other four SPS-1 projects, the average difference in IRI between the right and the left wheel paths ranged from 0.02 to 0.08 m/km (1 to 5 in/mi). Figure 6.1.6 shows the relationship between the left- and the right-wheel-path IRI for the individual test sites for the SPS-1 projects shown in table 6.1.2. Each point in the plot represents an SPS test section. The set of data that show high right-wheel-path IRI compared with the left-wheel-path IRI occurred in the test sections from the Alabama and Arizona SPS-1 projects.

6.1.4 Roughness Development at SPS-1 Sections

The IRI referred to in this section is the average IRI of the left and the right wheel paths. The SPS-1 projects in Arizona, Kansas, and Nebraska have been profiled twice, while the SPS-1 project in Iowa has been profiled three times. The SPS-1 projects in Arizona and Nebraska consist of test sections 13 through 24, while the test sections in Iowa and Kansas correspond to test sections 1 through 12. The IRI of all test sections in these four projects for all profile dates is shown in figures 6.1.7 through 6.1.10. The first profile date corresponds to the profile run immediately after construction.

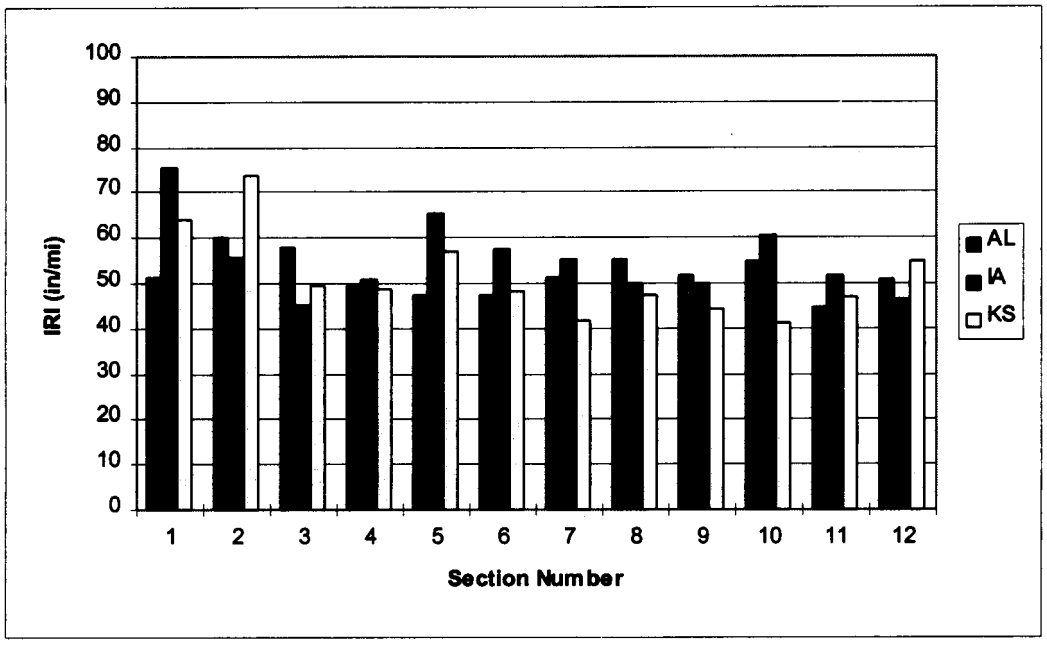

1 in/mi = 0.0158 m/km

Figure 6.1.3. IRI after construction for test sections 1-12 in SPS-1 projects.

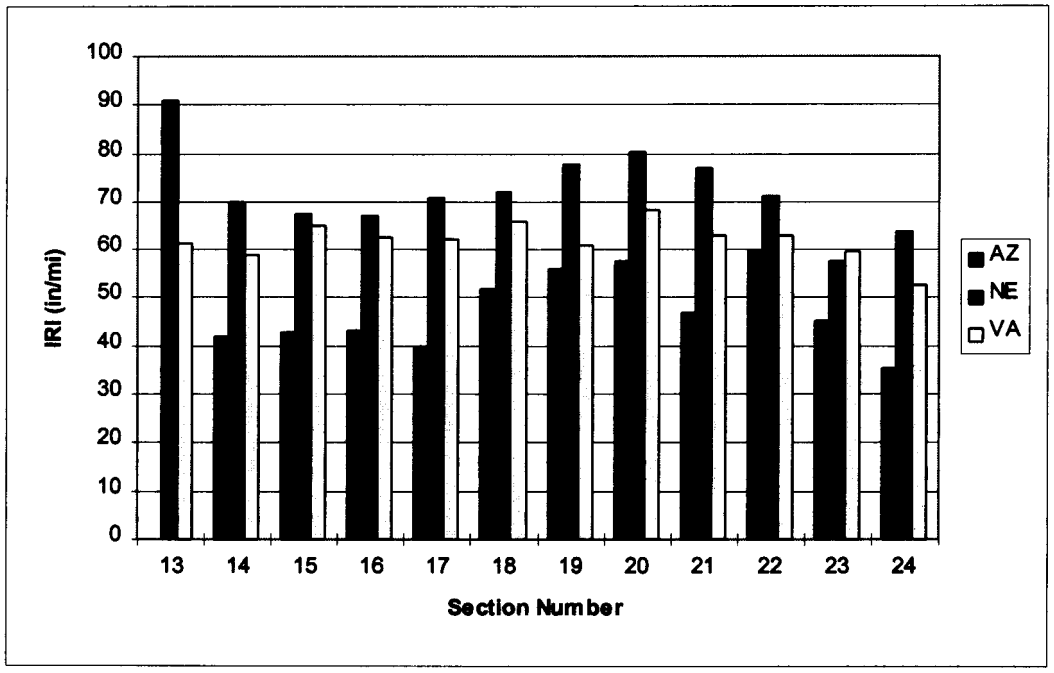

1 in/mi = 0.0158 m/km

Figure 6.1.4. IRI after construction for test sections 13-24 in SPS-1 projects.

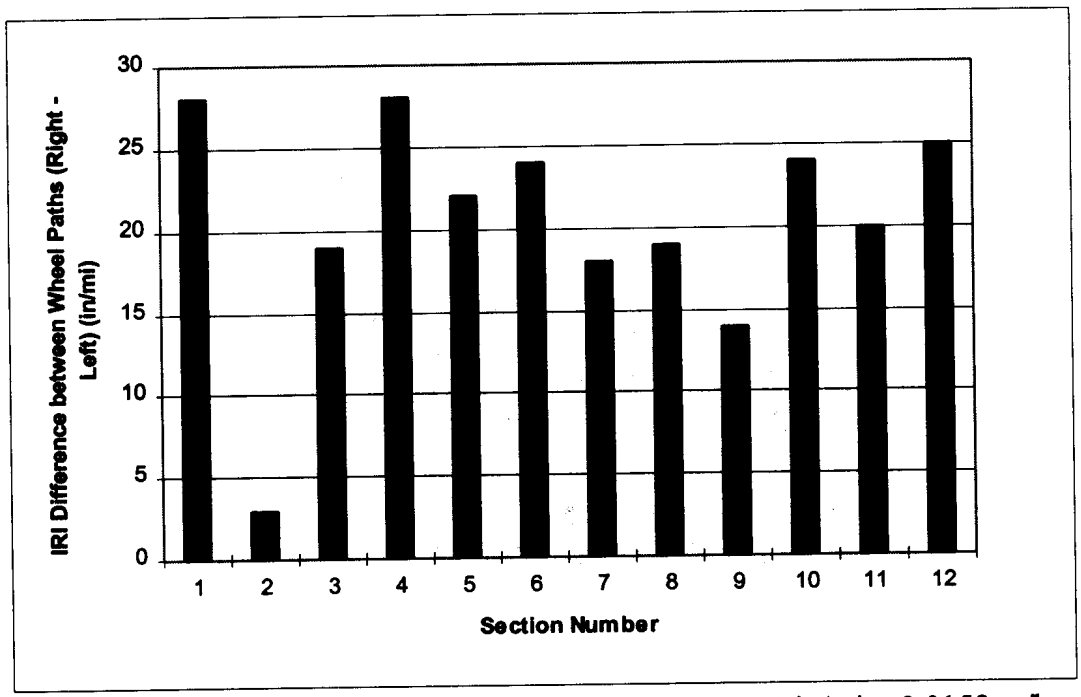

1 in/mi = 0.0158 m/km

Figure 6.1.5. Difference in IRI between right and left wheel path for test sections in the SPS-1 project in Alabama.

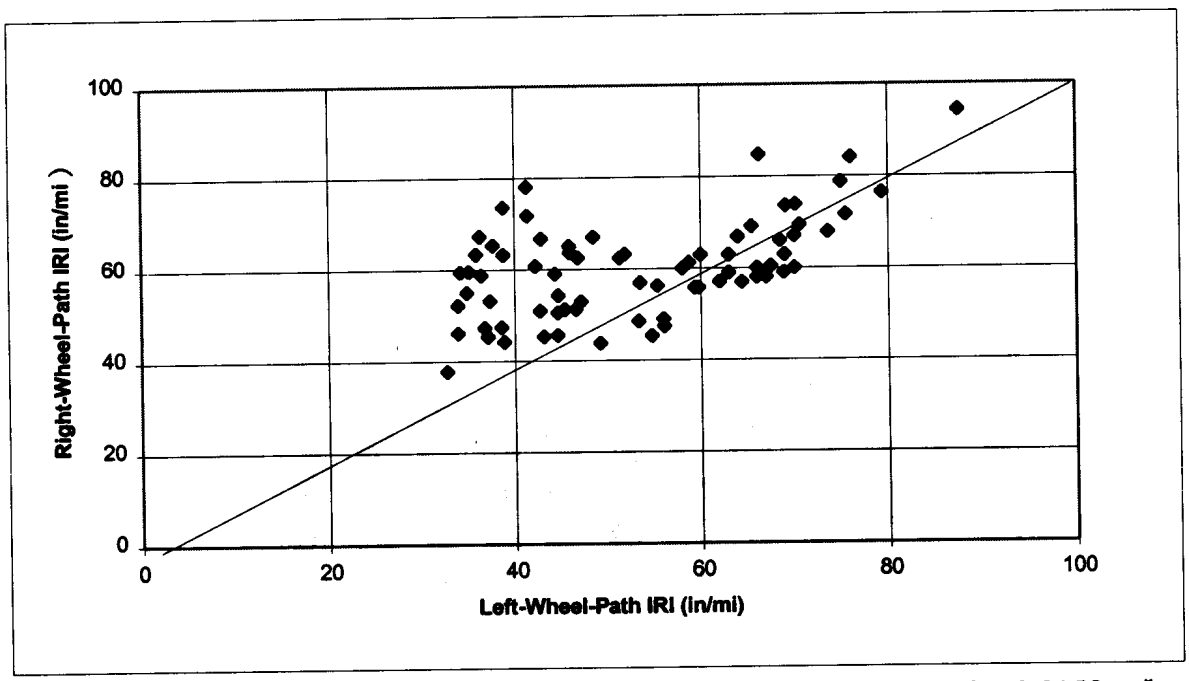

1 in/mi = 0.0158 m/km

Figure 6.1.6. Comparison between left- and right-wheel-path IRI for SPS-1 test sections.

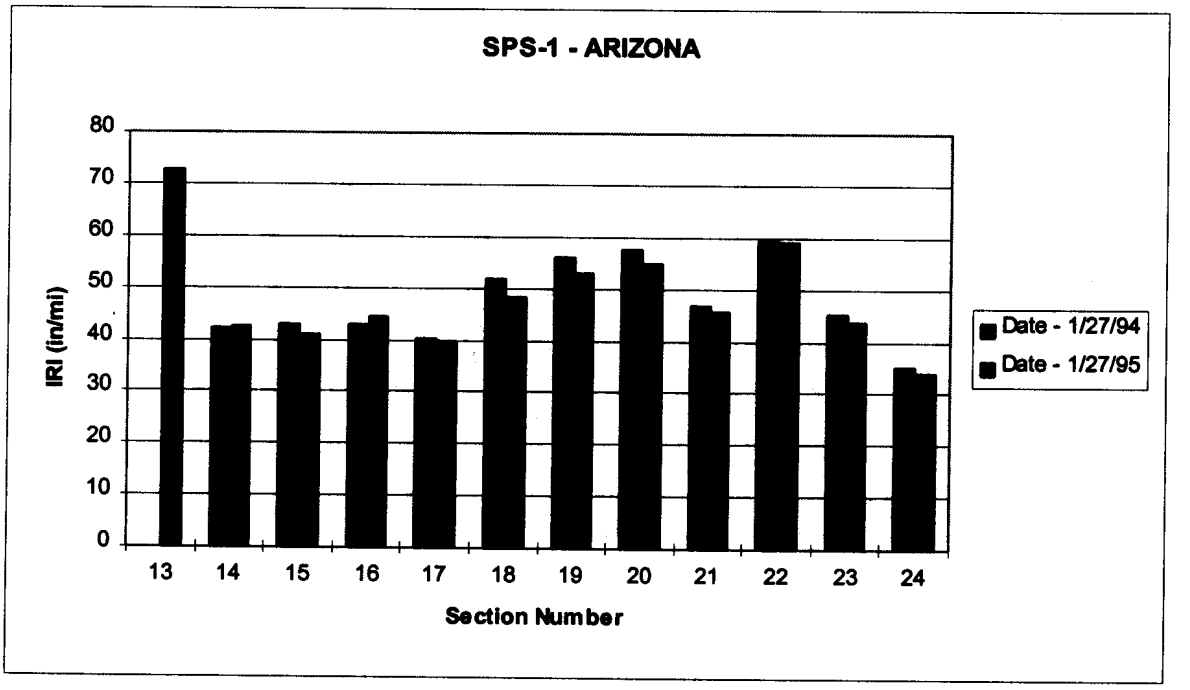

1 in/mi = 0.0158 m/km

Figure 6.1.7. IRI for SPS-1 project in Arizona.

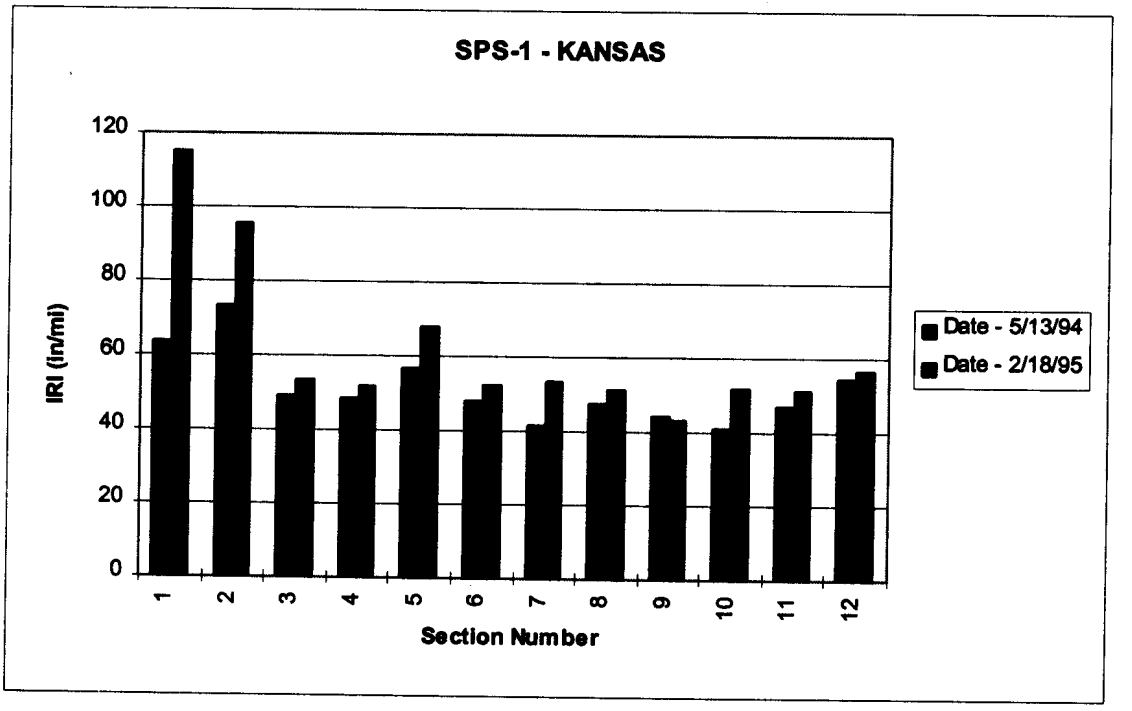

1 in/mi = 0.0158 m/km

Figure 6.1.8. IRI for SPS-1 project in Kansas.

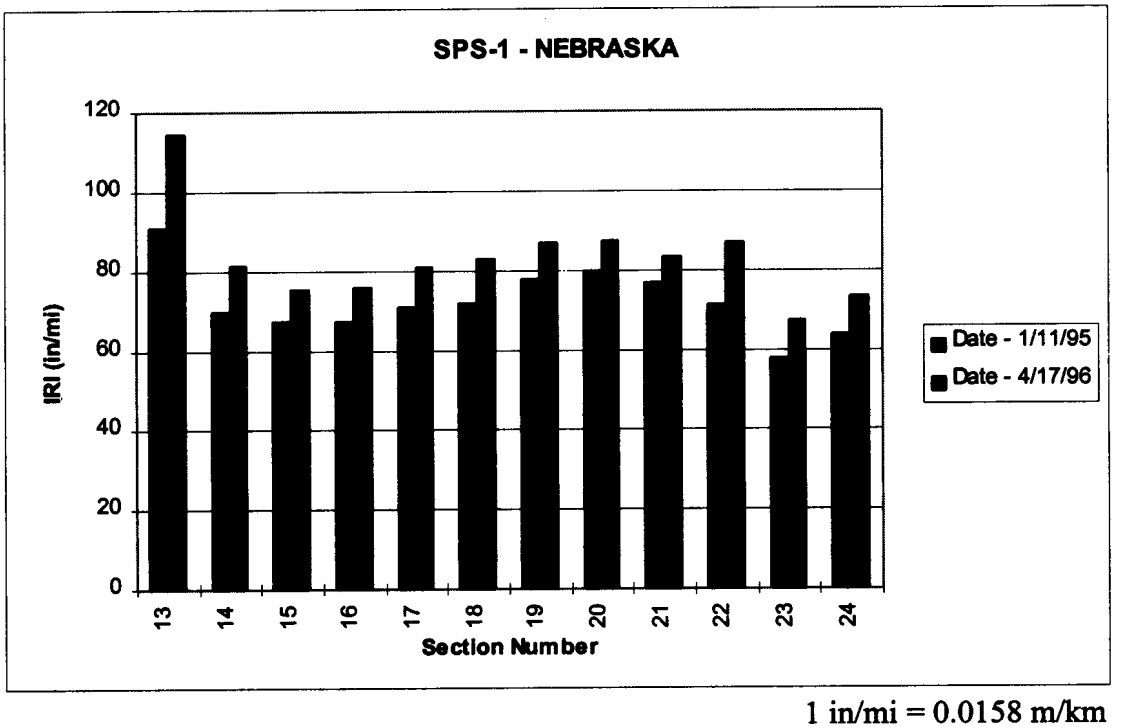

1 in/mi = 0.0158 m/km

Figure 6.1.9. IRI for SPS-1 project in Nebraska.

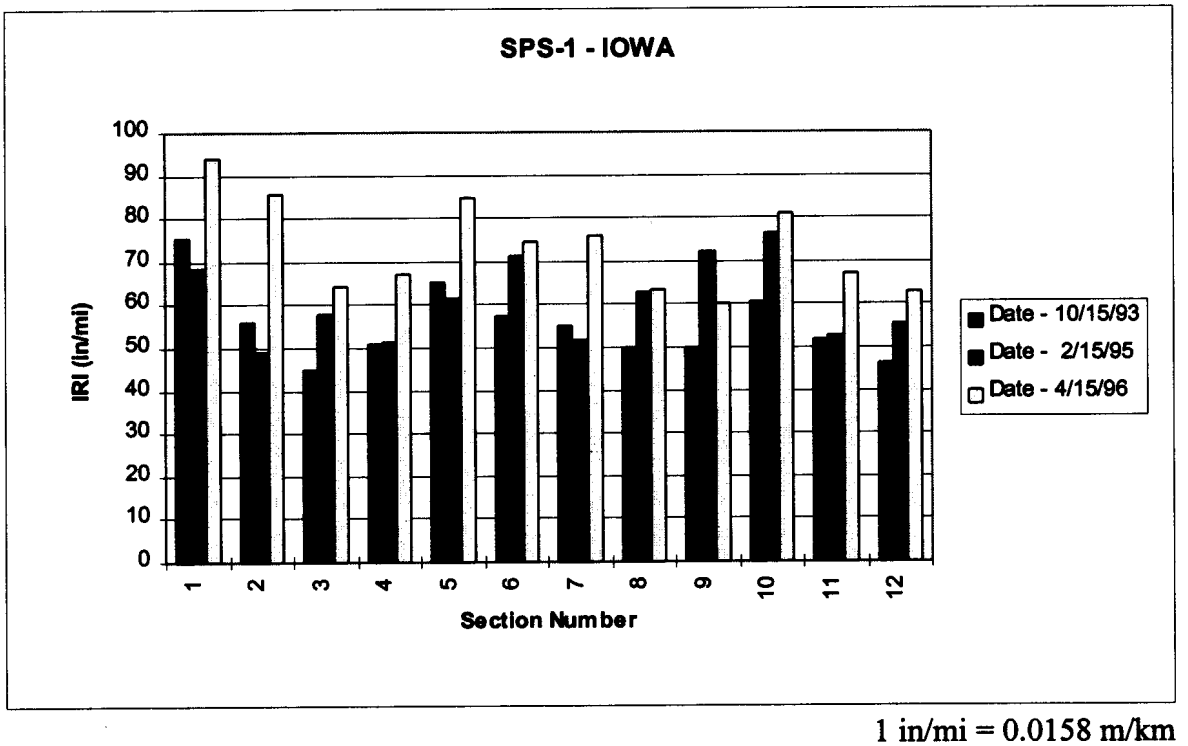

1 in/mi = 0.0158 m/km

Figure 6.1.10. IRI for SPS-1 project in Iowa.

The rates of increase of IRI at each test section in these SPS-1 projects were computed relative to the IRI after construction, using the following formula:

$$\text{Rate of increase of IRI} = \frac{\text{IRI (t) - IRI (0)}}{\text{Time}} \quad \ldots\ldots\ldots\ldots (6.1)$$

where:

IRI (t) = IRI at latest profile date,
IRI (0) = IRI after construction, and
Time = time in years between the profile dates.

The rate of increase in IRI for the SPS-1 test sections computed from the above formula is presented in figure 6.1.11 as a function of the estimated SN of the section. In this figure, the rate of increase in IRI for the projects in Arizona, Kansas, and Nebraska represents the rate of increase of IRI at approximately 1 year after being subjected to traffic; for the project in Iowa it reflects the rate of increase in IRI that occurred over a 2-year period. Section 1 in Kansas, which had an estimated SN of 3.76, had a rate of increase of IRI of 1.04 m/km/yr (66 in/mi/yr), which is not shown in the plot because of scaling effects.

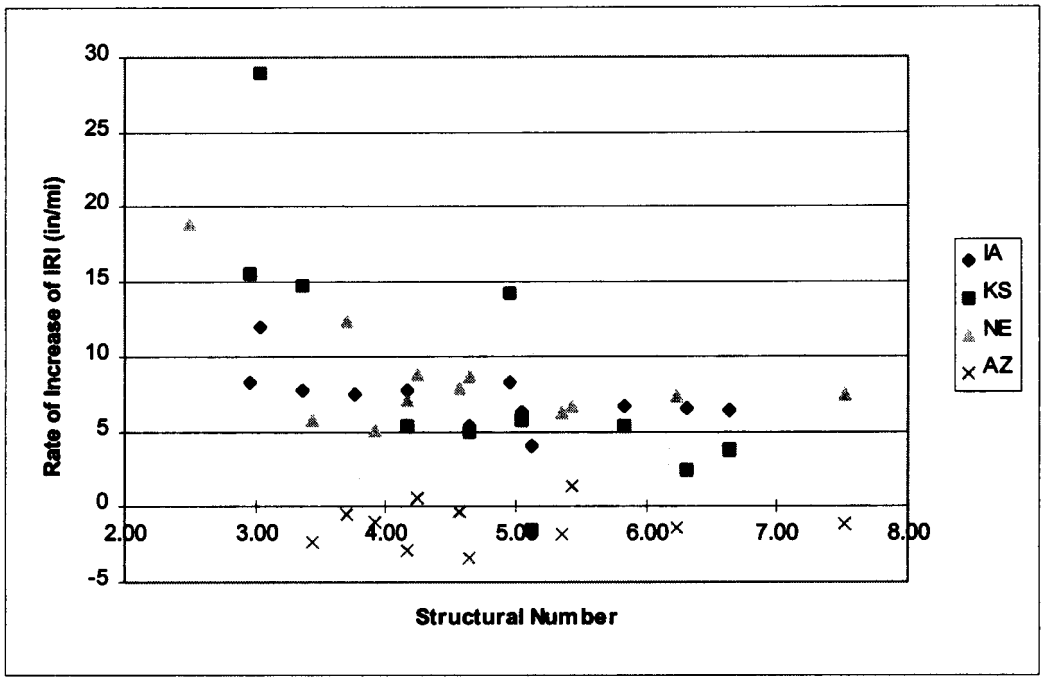

1 in/mi = 0.0158 m/km

Figure 6.1.11. Rate of increase of IRI for SPS-1 sections as a function of SN.

Approximately 1 year after construction, the majority of sections in Arizona had an IRI that was less than that after construction. However, the IRI value after construction for test section 13 in Arizona (which had an estimated SN of 2.50) was not available; therefore, the rate of development of IRI for that section could not be computed. Apart from the project in Arizona, all other projects showed a high rate of increase of IRI for the sections that had a low SN..

Figure 6.1.10 shows the IRI at the test sections in the SPS-1 project in Iowa, which reflect variable IRI trends. The IRI at the second profile date was higher than the IRI at the first profile date at all sections except for test sections 1, 2, 5, and 7. However, at the third profile date, all sections had IRI values that were higher than the IRI at the first profile date. These variations may have been caused by environmental factors, as the second profile date at this project was in winter, and the third profile date was in early spring.

In the Kansas SPS-1 project, test sections 1, 2, 5, and 7 had estimated SNs that were less than 4, and all these sections showed high rates of increase of IRI. The rate of increase of IRI at test section 1 was 1.05 m/km/yr (66.3 in/mi/yr), while at sections 2, 5, and 7 the rate ranged from 0.23 to 0.46 m/km/yr (14.8 to 28.8 in/mi/yr). The Kansas and Iowa SPS-1 projects have the same series of test sections (see table 6.1.1). The high rate of increase of IRI that was observed at some test sections in the Kansas project was not seen at the corresponding test sections in the Iowa project, where all sections had a rate of increase of IRI that was between 0.06 and 0.19 m/km/yr (4 to 12 in/mi/yr). The SPS-1 project in Iowa and Kansas are both located on fine-grade subgrade; the Iowa project is in the wet-no freeze zone and the Kansas project is in the dry freeze zone. However, the Kansas project is subjected to over three times the ESAL rate as the Iowa project. The high traffic rate as well as different subgrade conditions may have caused the higher rates of increase in IRI for these sections in Kansas.

The effects of seasonal variability in IRI of AC pavements is not known at this time. Subgrade movements in fine-grained soils can occur due to variations in moisture and freezing effects. Although the SPS-1 projects are to be profiled annually, changes of several months can occur between profile dates. For example, the profile dates for the Iowa SPS-1 project were: (1) October 15, 1993, (2) February 15, 1995, and (3) April 15, 1996. The first profiling date was in the fall, the second profiling date was in the winter, and the third profiling date was in the spring. The variability in subgrade conditions caused by seasonal effects may influence the profile of the pavement, resulting in differences in IRI. The rates of increase of IRI that were discussed will be affected if such conditions occur.

6.1.5 SUMMARY FOR SPS-1 PROJECTS

Profile data were available for six SPS-1 projects. Of these, one project has been profiled three times, three projects had been profiled twice, and two projects had been profiled only once. Therefore, only a limited amount of profile data were available for analysis. The average IRI of the SPS-1 projects, which is the average of the 12 test sections in the project, ranged from 0.74 m/km (47 in/mi) for the SPS-1 project in Arizona to 1.13 m/km (72 in/mi) to the SPS-1 project in Nebraska. The COV of the IRI of the test sections within a project ranged from 8 percent for the project in Alabama to 19 percent for the project in Kansas. There were large differences between the right- and the left-wheel-path IRI for the SPS-1 projects in Alabama and Arizona, where the right-wheel-path IRI was higher than the left-wheel-path IRI. The average difference between the IRI of the wheel paths for the SPS-1 projects in Alabama and Arizona was 0.32 and 0.30 m/km (20 and 19 in/mi), respectively. This average difference for the other four projects ranged from 0.02 to 0.08 m/km (1 to 5 in/mi). The test sections in the SPS-1 project in Arizona, which is located on a coarse-grained subgrade in a dry-no freeze environment, showed little change in IRI when it was profiled approximately 1 year after construction. The test sections in the Kansas project that have estimated SNs less than 4 showed a large increase in IRI when they were profiled approximately 1 year after construction. The test sections in Kansas are located on a fine-grained subgrade and are subjected to an estimated 469 KESAL/yr. Apart from the SPS-1 project in Arizona, all other SPS-1 projects generally indicated that the sections that had low SNs had a higher rate of increase of IRI when compared with the sections that had high SNs.

6.2 ROUGHNESS CHARACTERISTICS OF SPS-2 PROJECTS

6.2.1 Description of SPS-2 Experiment

The Specific Pavement Studies SPS-2 experiment is titled the Strategic Study of Structural Factors for Rigid Pavements. The SPS-2 experiment was developed to investigate the effect of selected structural factors on the long-term performance of rigid pavements constructed on different subgrade types in different environmental regions. All rigid pavement test sections are doweled, jointed PCC with a joint spacing of 4.6 m (15 ft). The subgrade types considered in this experiment are classified as fine-grained and coarse-grained. The environmental regions considered in this experiment correspond to the four LTPP environmental regions: wet freeze, wet-no freeze, dry freeze and dry-no freeze.

Table 6.2.1 presents the structural properties of the test sections in the SPS-2 experiment. These 24 sections are to be constructed for each combination of subgrade type and environmental region, with half of the test sections (sections 1 through 12) being constructed at one site, and the other half (sections 13 through 24) being constructed at a different site. The structural factors considered in this experiment are: thickness of PCC layer, flexural strength of the PCC, base type, drainability, and lane width. The two PCC slab thickness considered in this experiment are 200 mm (8 in) and 275 mm (11 in), while the two PCC flexural strengths that are used are 3.8 MPa (550 psi) and 6.2 MPa (900 psi). The three base types used are: lean concrete base of 150 mm (6 in) thickness, dense-graded aggregate base of 150-mm (6-in) thickness, and a 100-mm (4-in) thick permeable asphalt-treated base over a 100-mm (4-in) thick dense-graded aggregate base. Underdrains are provided in the test sections that have a permeable asphalt treated base. The lane widths considered in this experiment are 3.66 m (12 ft) and 4.27 m (14 ft). Each test section is constructed over a minimum length of 183 m (600 ft), and 152 m (500 ft) of the section is used for monitoring.

6.2.2 Data Availability for SPS-2 Projects

The IRI values of the SPS-2 test sections were obtained from the RIMS through the regional contractors. Table 6.2.2 presents the SPS-2 projects for which IRI data were available. This table also presents the test section numbers constructed at each site, the number of times the project had been profiled, the subgrade type, environmental region, and the estimated ESALs in the study lane. As shown in table 6.2.2, profile data are available for seven SPS-2 projects. Two projects have been profiled four times, one project has been profiled three times, two projects have been profiled twice and two projects have been profiled once. The SPS-2 projects are generally first profiled within a month after they are opened to traffic; thereafter, they are profiled annually.

Extensive sampling is performed at the SPS-2 projects to obtain samples from subgrade, base, and surface layers. Laboratory tests are performed on the samples to characterize material properties. Data files containing laboratory test data were obtained from the RIMS, through the regional contractors. A review of these data files indicated that very few data were available in these files. Therefore, it was not possible to conduct an analysis to relate material properties to the roughness at the test sites.

Table 6.2.1. Structural properties of SPS-2 sections.

Section Number	PCC Thickness (in)	Flexural Strength (psi)	Lane Width (ft)	Layer 2		Layer 3	
				Material	Thickness (in)	Material	Thickness (in)
1	8	550	12	DGAB	6	-	-
2	8	900	14	DGAB	6	-	-
3	11	550	14	DGAB	6	-	-
4	11	900	12	DGAB	6	-	-
5	8	550	12	LCB	6	-	-
6	8	900	14	LCB	6	-	-
7	11	550	14	LCB	6	-	-
8	11	900	12	LCB	6	-	-
9	8	550	12	PATB	4	DGAB	4
10	8	900	14	PATB	4	DGAB	4
11	11	550	14	PATB	4	DGAB	4
12	11	900	12	PATB	4	DGAB	4
13	8	550	14	DGAB	6	-	-
14	8	900	12	DGAB	6	-	-
15	11	550	12	DGAB	6	-	-
16	11	900	14	DGAB	6	-	-
17	8	550	14	LCB	6	-	-
18	8	900	12	LCB	6	-	-
19	11	550	12	LCB	6	-	-
20	11	900	14	LCB	6	-	-
21	8	550	14	PATB	4	DGAB	4
22	8	900	12	PATB	4	DGAB	4
23	11	550	12	PATB	4	DGAB	4
24	11	900	14	PATB	4	DGAB	4

Note 1: DGAB - dense-graded aggregate base, LCB - lean concrete base, PATB - permeable asphalt-treated base.
Note 2: 1 in. = 25.4 mm, 1 ft = 0.3 m, 1 psi = 6.89 kPa.

Table 6.2.2. SPS-2 projects for which profile data are available.

Project Location	State Code	Test Section Numbers	Number of Times Profiled	Subgrade Type	Environmental Region	Annual ESALs
Arizona	AZ	13 - 24	2	Coarse Grained	Dry-No Freeze	1,320,000
Colorado	CO	13 - 24	1	Coarse Grained	Dry Freeze	480,000
Iowa	IA	1 - 12	2	Fine Grained	Wet Freeze	329,000
Kansas	KA	1 - 12	4	Fine Grained	Dry Freeze	1,300,000
Michigan	MI	13 - 24	4	Fine Grained	Wet Freeze	890,000
North Carolina	NC	1 - 12	3	Fine Grained	Wet-No Freeze	539,000
Washington	WA	1 - 12	1	Fine Grained	Dry Freeze	N/A

6.2.3 IRI After Construction for SPS-2 Sections

The IRI values at the test sites immediately after construction were examined to study the IRI characteristics. The average IRI for each SPS-2 project was computed by averaging the IRI values of the test sections in the project. The average IRI for each SPS-2 project, computed by averaging the IRI of each test section, is presented in figure 6.2.1. The average IRI for the SPS-2 projects ranged from 1.12 to 1.47 m/km (71 to 93 in/mi). The COV of IRI between the test sections in each project is shown in figure 6.2.2. The COV presents the variability in IRI between the test sections. The COV for the projects ranged from 11 to 24 percent.

The IRI values after construction of the test sections in the SPS-2 projects in Iowa, Kansas, North Carolina, and Washington that contain test sections 1 through 12 (see table 6.2.1) are shown in figure 6.2.3. The IRI after construction for the test sections in the SPS-1 projects in Arizona, Colorado, and Michigan that contain test sections 13 through 24 are shown in figure 6.2.4 The subgrade at the projects in Arizona and Colorado was coarse grained, while the subgrade at the other projects was fine grained. These figures show that varying IRI values were obtained for the same pavement section in the projects constructed at different locations.

The average left- and right-wheel-path IRI values for the different SPS-2 projects were close to each other for all projects, with the average difference between the right- and left-wheel-path IRI (right IRI - left IRI) ranging from -0.09 to 0.14 m/km (-6 to 9 in/mi). Figure 6.2.5 presents the relationship between the left- and the right-wheel-path IRI for the individual test sites for the SPS-2 projects shown in table 6.2.1. Each point in the plot represents an SPS test section. For most of the test sites, the difference in IRI between the wheel paths at a test section was less than 0.16 m/km (10 in/mi).

The average IRI values of the test sections that have similar base types in each SPS project were computed to examine if trends could be identified. The three base types present in an SPS-2 project are: (1) dense-graded aggregate base, (2) lean concrete base, and (3) permeable asphalt-treated base over dense-graded aggregate base. Each SPS-2 project has four sections that have each of these base types. The average IRI for each base type for all SPS-2 projects is presented in table 6.2.3 and shown in figure 6.2.6. The test sections that are included in each base type have different slab thickness, flexural strengths, and lane widths. Although some SPS projects showed clear differences in the IRI values for a specific base type, an overall trend was not evident when all projects were considered. For example, in the SPS-2 project in Colorado (see figure 6.2.7) test sections 13 through 16, which are on a dense-graded aggregate base have a

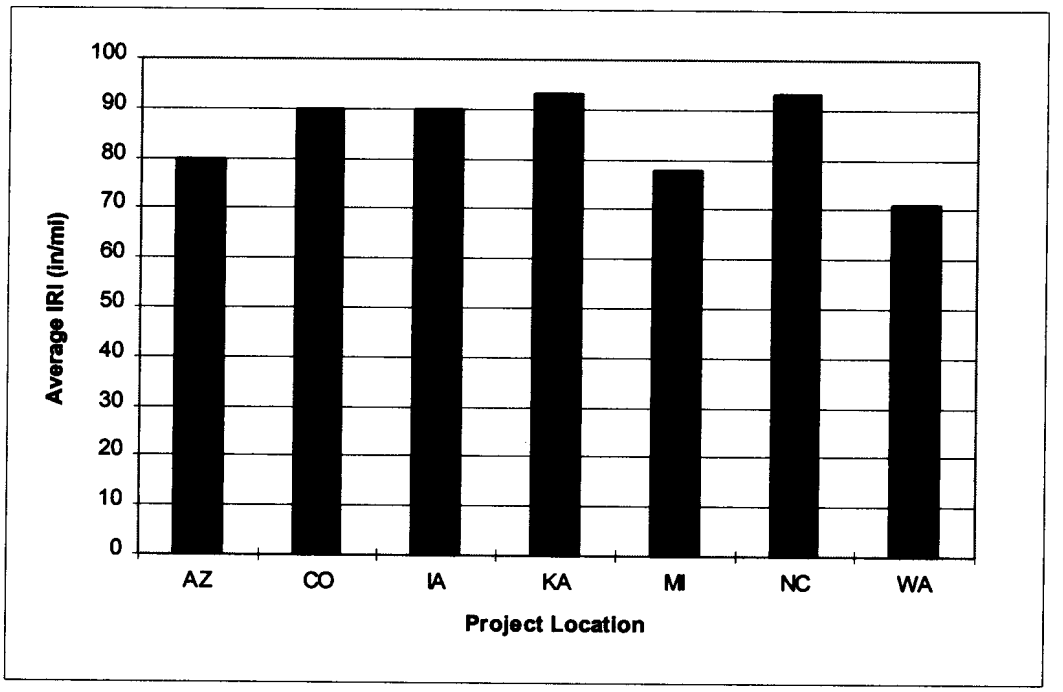

1 in/mi = 0.0158 m/km

Figure 6.2.1. Average IRI for SPS-2 projects.

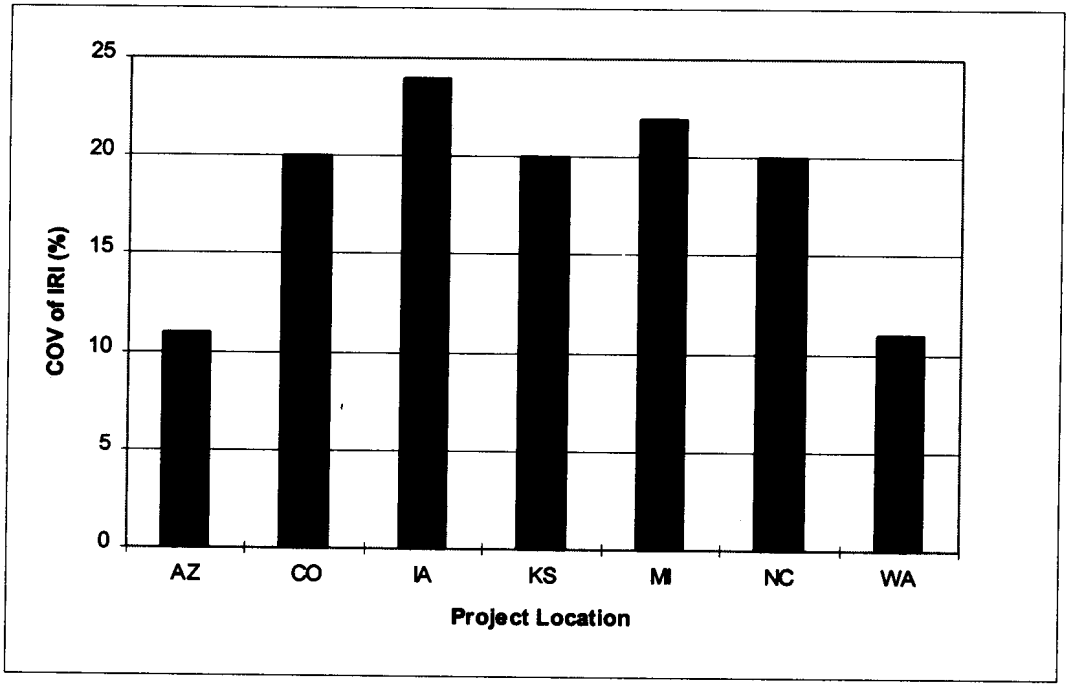

Figure 6.2.2. COV of IRI of test sections in SPS-2 projects.

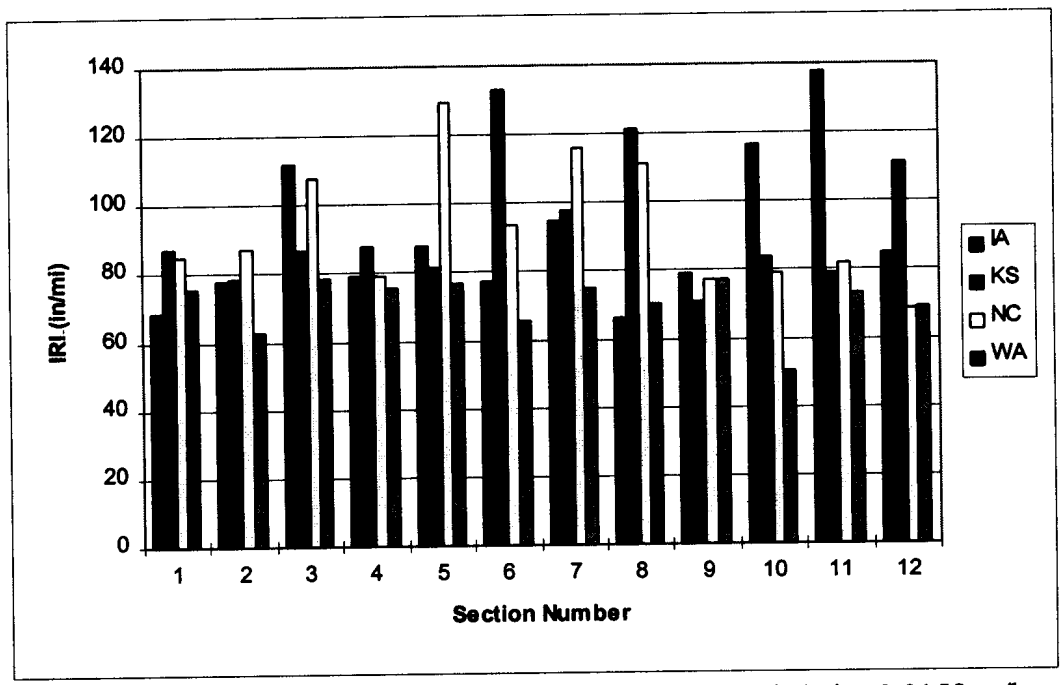

1 in/mi = 0.0158 m/km

Figure 6.2.3. IRI after construction for test sections 1-12 in SPS-2 projects.

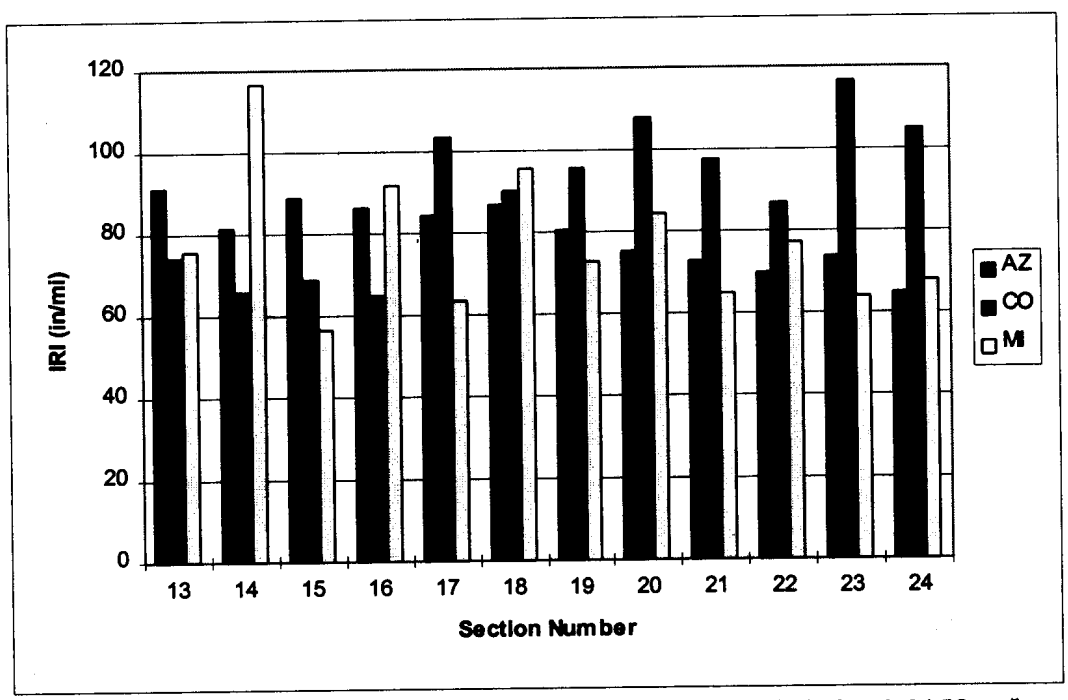

1 in/mi = 0.0158 m/km

Figure 6.2.4. IRI after construction for test sections 13-24 in SPS-2 projects.

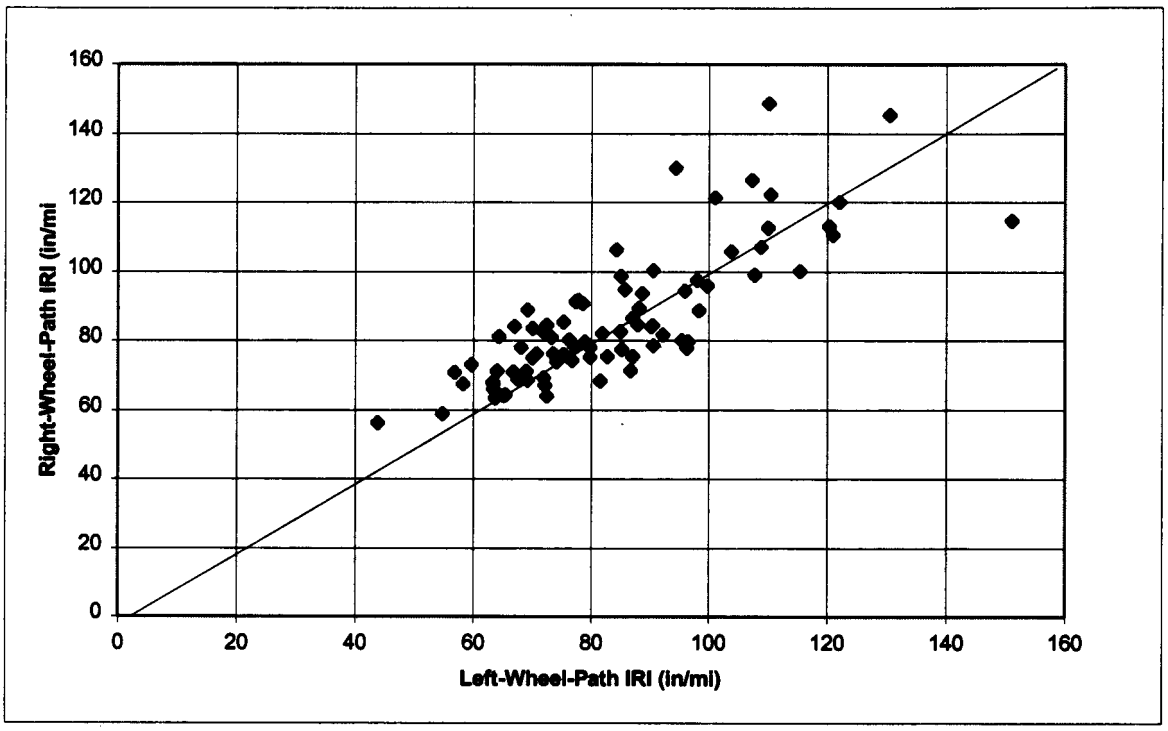

1 in/mi = 0.0158 m/km

Figure 6.2.5. Comparison between left- and right-wheel-path IRI for SPS-2 test sections.

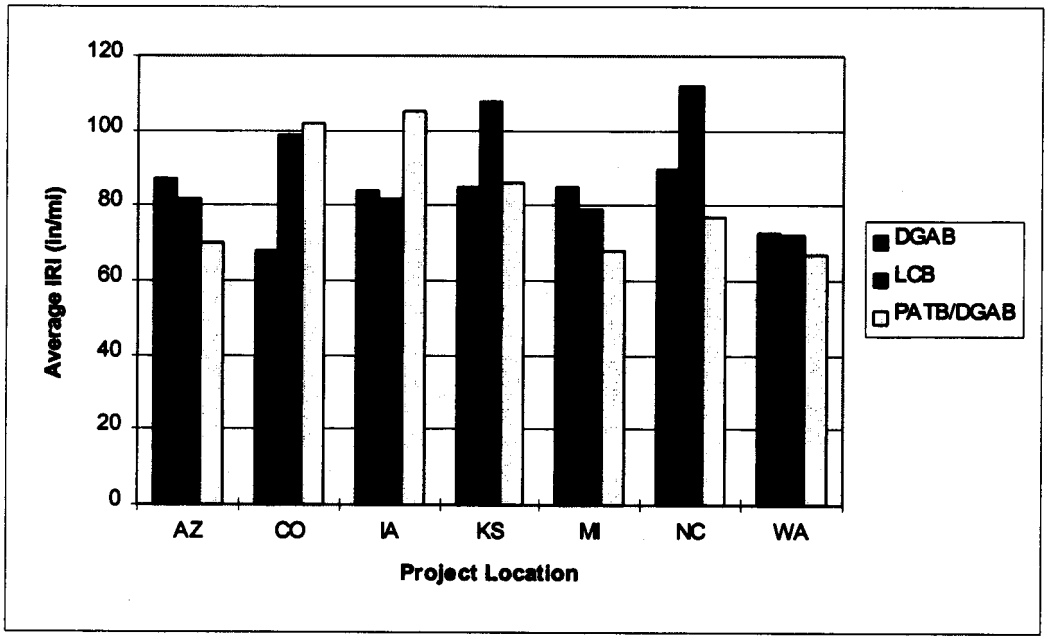

1 in/mi = 0.0158 m/km

Figure 6.2.6. Average IRI after construction for different base types.

Table 6.2.3. Average IRI for different base types in the SPS-2 projects.

Project Location	Average IRI (in/mi)			Coefficient of Variation of IRI (%)		
	Base Type			Base Type		
	DGAB	LCB	PATB/DGAB	DGAB	LCB	PATB/DGAB
Arizona	87	82	70	5	7	6
Colorado	68	99	102	6	8	12
Iowa	84	82	105	23	15	27
Kansas	85	108	86	5	21	20
Michigan	85	79	68	30	18	9
North Carolina	90	112	77	14	13	8
Washington	73	72	67	10	7	18

Note 1: DGAB - dense-graded aggregate base, LCB - lean concrete base, PATB - permeable asphalt-treated base.
Note 2: 1 in/mile = 0.0158 m/km.

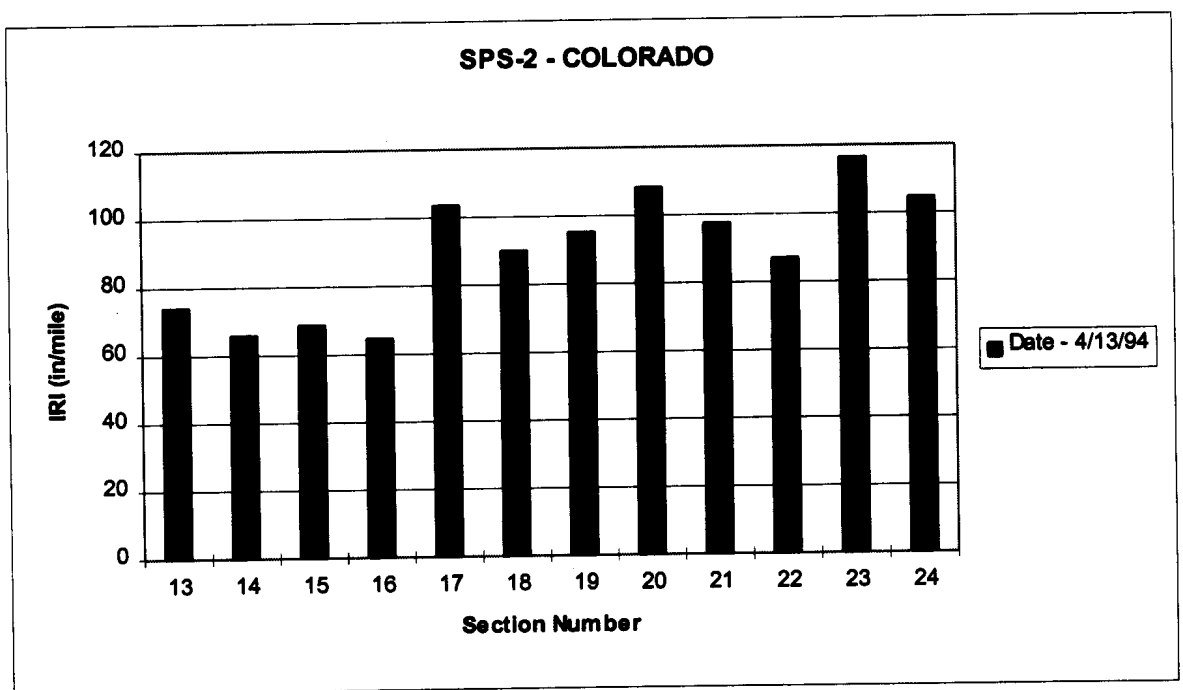

1 in/mi = 0.0158 m/km

Figure 6.2.7. IRI for SPS-2 project in Colorado.

lower IRI when compared with the other two base types. In the SPS-2 project in North Carolina test sections 5 through 8 which are on a lean concrete base have a higher IRI when compared with the other two base types. Similar observations on the differences in IRI were noted at other several other SPS-2 projects.

Table 6.2.4 presents the average IRI values of the test sections in each SPS-2 project that have PCC flexural strengths of 3.8 MPa (550 psi) and 6.2 MPa (900 psi). An overall trend in the differences in IRI value between the PCC sections that have different flexural strengths could not be observed for the SPS-2 projects. However, some specific trends related to the PCC flexural strength were noted at some SPS-2 projects.

As shown in table 6.2.5, in the SPS-2 project in Washington, all test sections that had a PCC flexural strength of 6.2 MPa (900 psi) had a lower IRI than the test sections that had a flexural strength of 3.8 MPa (550 psi). The test sections in the Michigan SPS-2 exhibited the reverse of this pattern (see table 6.2.5), with test sections having a PCC flexural strength of 6.2 MPa (900 psi) showing a higher IRI than the test sections that have PCC flexural strength of 3.8 MPa (550 psi).

6.2.4 Changes in IRI at SPS-2 Sections

Figures 6.2.8 through 6.2.12 show the IRI at the test sections in each SPS-2 project that has been profiled at least two times. The first profile date shown in these plots corresponds to the IRI obtained immediately after construction. Examination of these plots does not indicate clear trends in the change in IRI values. In some projects, large changes, either reductions or increases in IRI values, are observed between the profiling dates.

Figure 6.2.9 show the IRI values at the test sections in the SPS-2 project in Arizona for two different test dates. The first test date corresponds to testing performed after construction, and the second test date is approximately 1 year after the first profile date. At all test sections, the IRI value after approximately 1 year was less than the IRI values obtained after construction. The test sections were first profiled after construction on January 25, 1994, at approximately 6 a.m., when the air temperature was estimated to be 13 °C (45 °F). The sections were then profiled approximately 1 year later on March 5, 1995, at 11:20 a.m., when the air temperature was estimated to be 18 °C (65 °F). The reductions in IRI noted at all test sites in this project between

Table 6.2.4. Average IRI of SPS-2 projects for the two PCC flexural strengths.

Project Location	Average IRI (in/mi)	
	Flexural Strength of PCC (psi)	
	550	900
Arizona	82	77
Colorado	93	87
Iowa	97	84
Kansas	84	103
Michigan	66	89
North Carolina	99	86
Washington	76	65

Note 1: 1 in/mile = 0.0158 m/km.
Note 2: 1 psi = 6.89 kPa.

Table 6.2.5. Comparison of IRI values of SPS-2 projects in Michigan and Washington.

State	PCC Thickness (in)	Base Type	Average IRI	
			PCC Flexural Strength (psi)	
			550	900
Washington	8	DGAB	76	63
	11	DGAB	78	76
	8	LCB	77	66
	11	LCB	75	70
	8	PATB/DGAB	77	50
	11	PATB/DGAB	73	69
Michigan	8	DGAB	76	116
	11	DGAB	57	92
	8	LCB	64	95
	11	LCB	73	84
	8	PATB/DGAB	65	77
	11	PATB/DGAB	64	68

Note 1: DGAB - dense-graded aggregate base, LCB - lean concrete base, PATB - permeable asphalt-treated base.
Note 2: 1 in = 25.4 mm, 1 psi = 6.89 kPa.

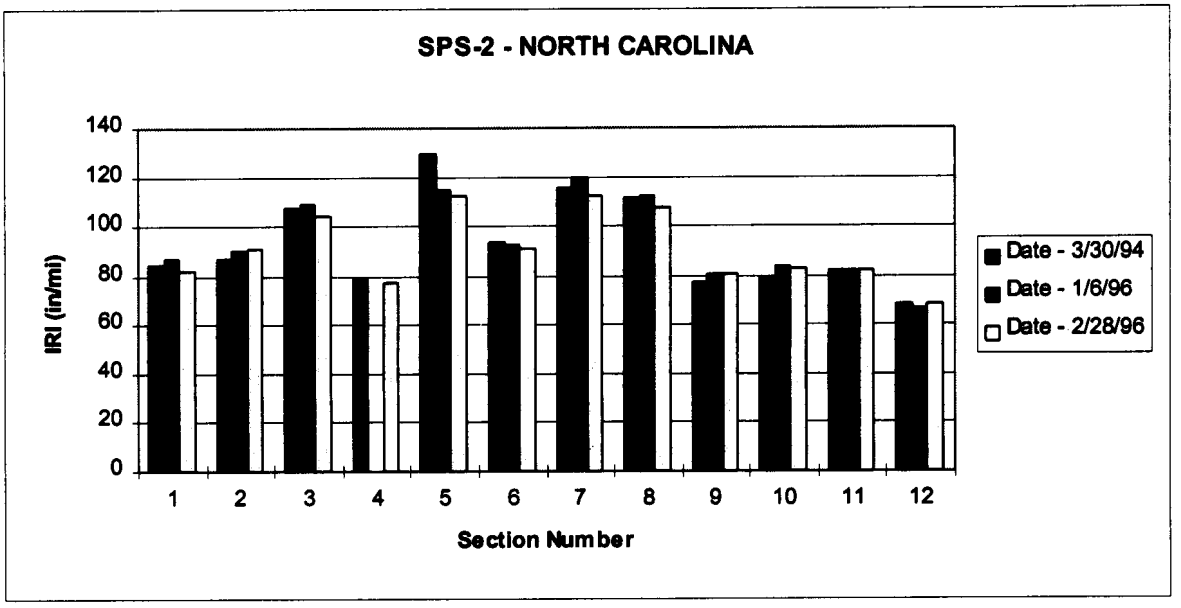

1 in/mi = 0.0158 m/km

Figure 6.2.8. IRI for SPS-2 project in North Carolina.

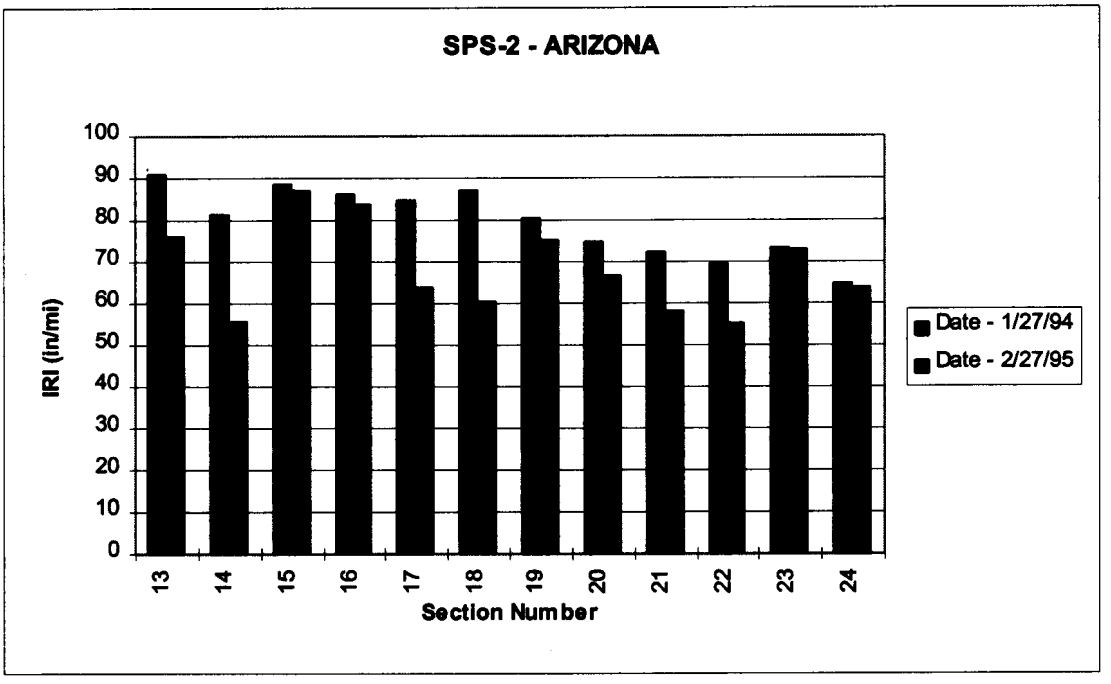

1 in/mi = 0.0158 m/km

Figure 6.2.9. IRI for SPS-2 project in Arizona.

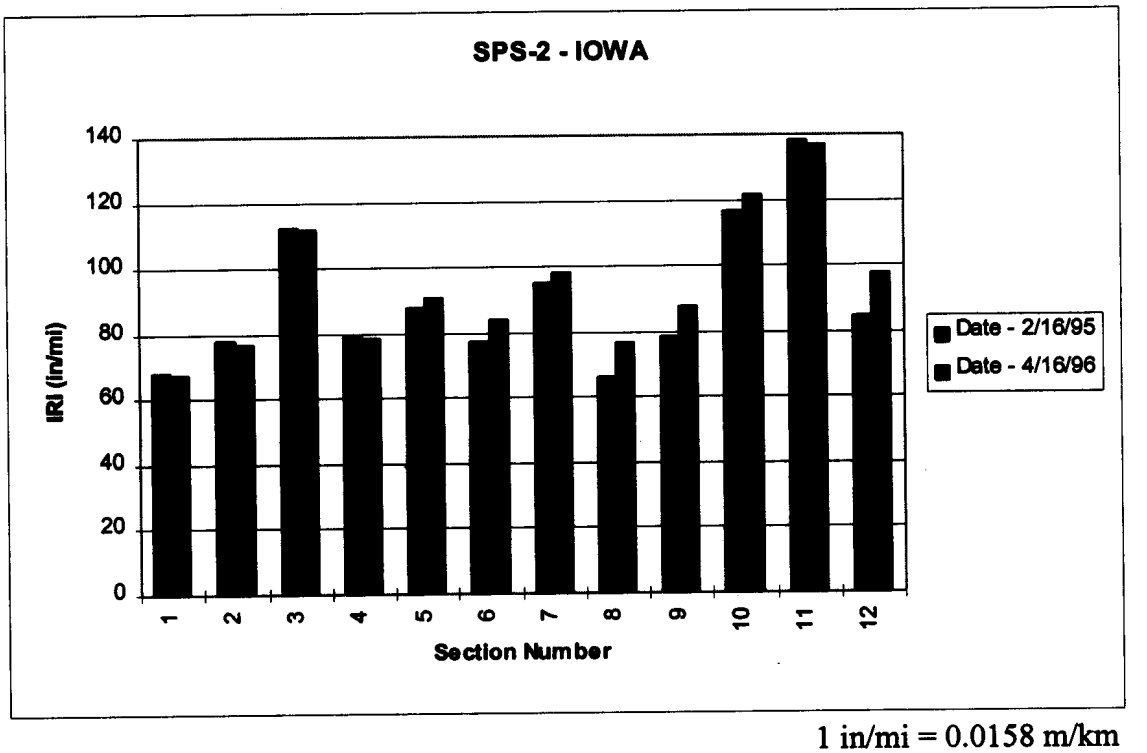

1 in/mi = 0.0158 m/km

Figure 6.2.10. IRI for SPS-2 project in Iowa.

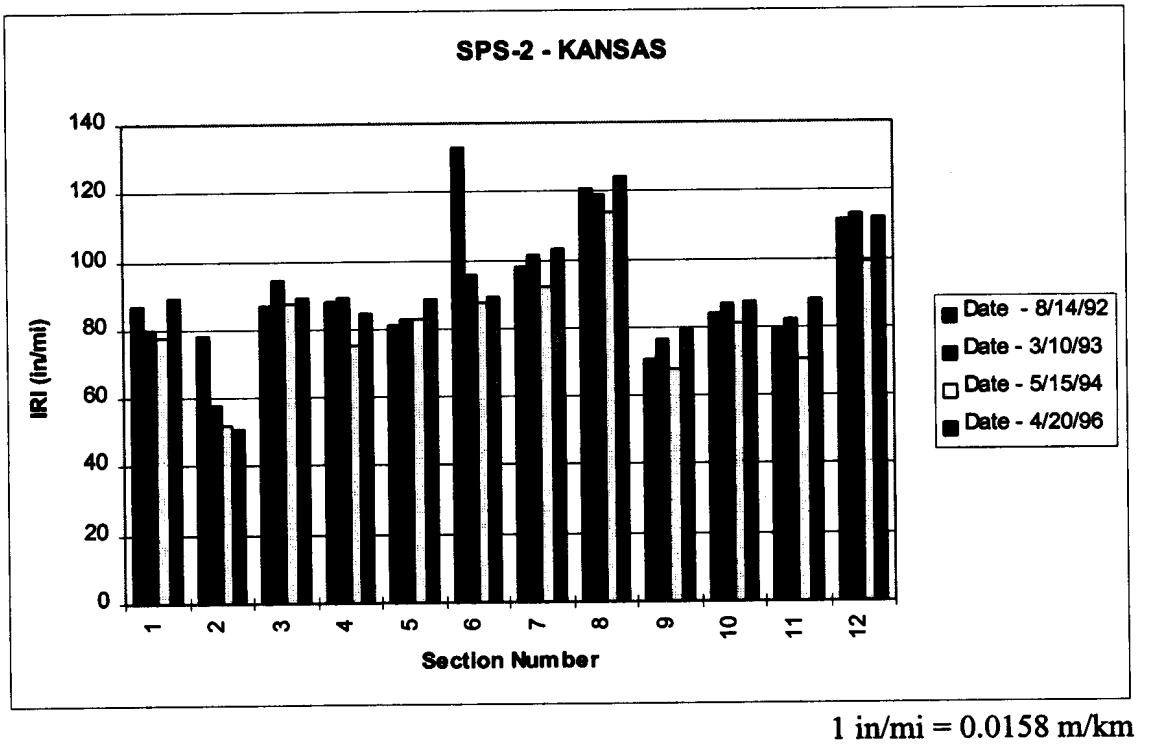

1 in/mi = 0.0158 m/km

Figure 6.2.11. IRI for SPS-2 project in Kansas.

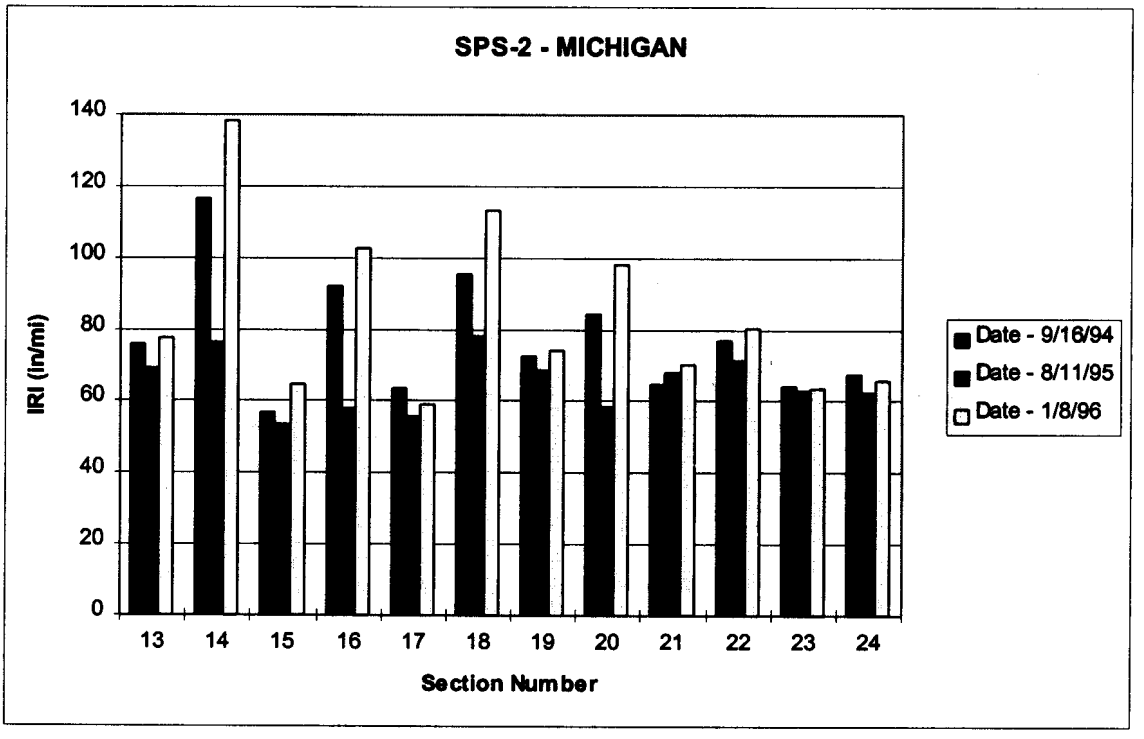

1 in/mi = 0.0158 m/km

Figure 6.2.12. IRI for SPS-2 project in Michigan.

the profile dates are tabulated in table 6.2.6. Large reductions in IRI were noted at all test sections that had 200-mm- (8-in-) thick slabs. The magnitude of the reduction in IRI at the sites that had 200-mm- (8-in-) thick slabs ranged from 0.25 to 0.49 (16 to 31 in/mi). The changes in IRI that were noted at the test sites are attributed to curling effects at the joints most likely caused by temperature variations. Thin slabs are more susceptible to curling effects when compared with thick slabs, and this effect is seen in the data presented in table 6.2.6. In the SPS-2 test sections the joints are at 4.5-m (15-ft) intervals, and movements at these joints can have a large influence in the IRI values as each joint has an influence on the IRI value. Vastly different interpretations in the IRI at the test sections in this project can be drawn depending on the test date that is used to compare the IRI between the test sections.

The IRI values of the test sections in the Michigan SPS-2 project are shown in figure 6.2.12. Test sections 13 through 16 have a dense-graded aggregate base, with test sections 17 through 20 having a lean concrete base, and test sections 21 through 24 having a permeable asphalt-treated base. All test sections except for section 21 show a reduction in IRI between the first and the second profiling date. All sections show an increase in IRI between the second and

Table 6.2.6. IRI values at the Arizona SPS-2 project.

Test Section	PCC Thickness (in)	Base Type	IRI at T1 (in/mil (Note 1)	IRI at T2 (in/mi) (Note 2)	Difference in IRI (in/mi)	Percentage Reduction in IRI (%)
13	8	DGAB	91	76	15	16
14	8	DGAB	81	56	26	31
15	11	DGAB	89	87	2	2
16	11	DGAB	86	84	3	3
17	8	LCB	85	64	21	25
18	8	LCB	87	61	26	30
19	11	LCB	80	75	5	7
20	11	LCB	75	67	8	11
21	8	PATB/DGAB	73	58	15	20
22	8	PATB/DGAB	70	55	14	21
23	11	PATB/DGAB	73	73	1	1
24	11	PATB/DGAB	65	64	1	1

Note 1:DGAB - dense-graded aggregate base, LCB - lean concrete base, PATB - permeable asphalt treated base.
Note 2: T1 - 1/25/94, T2 - 3/5/95.
Note 3: 1 in/mile = 0.0158 m/km, 1 in = 25.4 mm.

the third profiling dates. The magnitude of the change in IRI between the first and the second profiling dates, and the second and the third profiling dates vary between the test sections. Relatively small changes in IRI are observed at: (1) the four test sections located on the permeable asphalt-treated base (sections 21 through 24), (2) the two test sections that have a PCC flexural strength of 3.8 MPa (550 psi) located on dense-graded aggregate base (sections 13 and 15), and (3) the two test sections that have a PCC flexural strength of 3.8 MPa (550 psi) located on lean concrete base (sections 17 and 19). The test sections having a PCC flexural strength of 6.2 MPa (900 psi) located on dense-graded aggregate base (sections 14 and 16) and lean concrete base (sections 16 and 18) show large changes in IRI. Figure 6.2.13 show the filtered profile of the first 30 m (100 ft) of test section 14 for the first two profile dates. The peaks in this figure correspond to the joints. The figure shows that the two profiles are different, with the magnitudes of the peaks corresponding to the second test date being smaller. As described earlier, the SPS-2 test sections have joint spacings of 4.6 m (15 ft), and changes in the profile at joints can have a large influence on the IRI.

The SPS-2 projects in North Carolina and Kansas both have been profiled three times (see figures 6.2.8 and 6.2.11), while the SPS-2 project in Iowa has been profiled twice (see figure

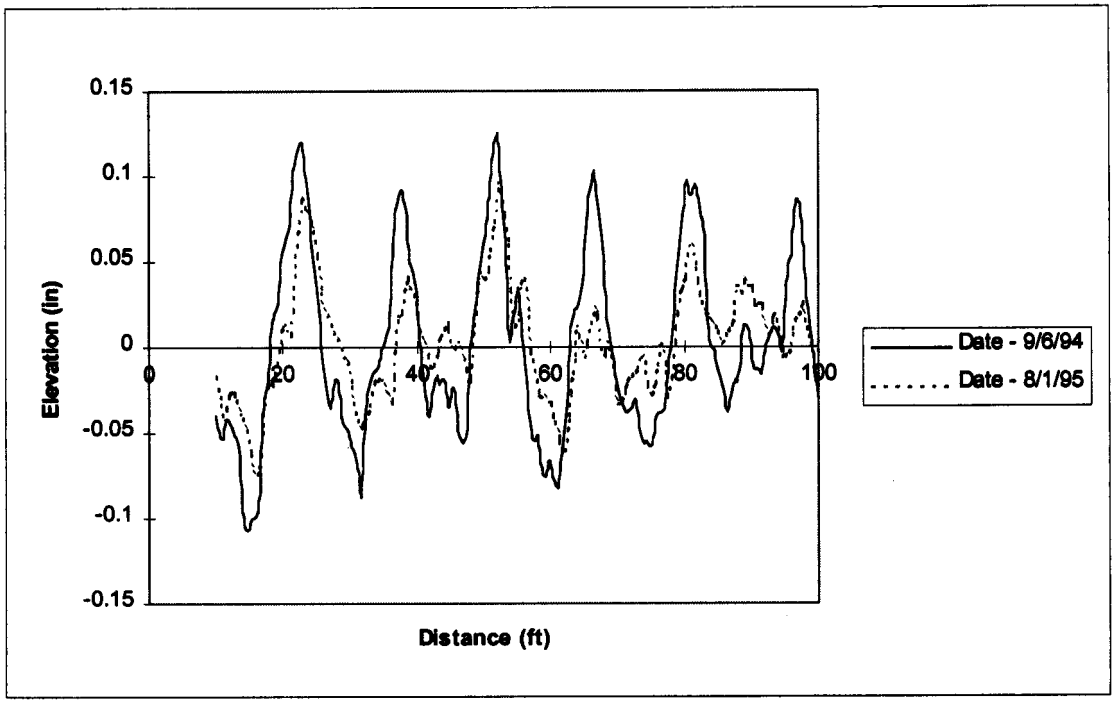

1 in = 25.4 mm, 1 ft = 0.305 m

Figure 6.2.13. Filtered right-wheel-path profile for two profile dates for section 14 in the Michigan SPS-2 project.

6.2.10). Large variations in IRI across all sites are not seen in these projects. However, large changes in IRI are noted at some test sections.

The analysis of changes in IRI at SPS-2 test sections indicated that movement at joints can have a large effect on the IRI value of the test sections. Joint movements are likely to be influenced by: temperature gradients in PCC slabs, variations in the moisture conditions in PCC, type of base, and mechanical properties of PCC. The analysis indicated that the changes in IRI of over 0.39 m/km (25 in/mi) can be caused by curling effects at joints. The limited time-sequence data and the lack of test data for the SPS-2 projects prevent an extensive analysis from being performed to explain the observations described in this chapter. The changes in IRI that were noted at the test sections are expected to be caused by environmental as well as PCC mix-related properties.

6.2.5 Summary for SPS-2 Projects

Profile data were available for seven SPS-2 projects. Of these, one project has been profiled four times, two projects have been profiled three times, two projects have been profiled twice, and two projects have been profiled once. Therefore, only a limited amount of profile data were available for analysis. The average IRI of the SPS-2 projects, which is the average of the 12 test sections in the project, ranged from 1.12 m/km (71 in/mi) to 1.47 m/km (93 in/mi). The COV of the IRI of the test sections within a project ranged from 11 percent to 24 percent. The left- and right-wheel-path IRI were generally close to each other for most test sections, with this difference typically being less than 0.16 m/km (10 in/mi). The IRI after construction at all test sections in the Washington SPS-2 project that had a PCC flexural strength of 6.2 MPa (900 psi) had an IRI that was less than the IRI at the test sections that had PCC flexural strength of 3.8 MPa (550 psi). A reversal of this trend was observed at the Michigan SPS-2, where all test sections that had PCC flexural strength of 6.2 MPa (900 psi) had an IRI that was greater than the IRI at the test sections with a PCC flexural strength of 3.8 MPa (550 psi). These observations indicate that the PCC mix properties affect the IRI after construction of PCC sections. There were large differences in the IRI values between the annual profiling dates at several sections. The analysis of data from the Arizona SPS-2 project indicated that the IRI values obtained approximately 1 year after construction were much less than the IRI values obtained after construction at some sections. The maximum difference that was observed at a test section in this project was 0.49 m/km (31 in/mi). Variability in IRI between profile dates was also noted at some sections in the Michigan SPS-2 project, and a filtered profile analysis at such a section indicated that the differences in IRI were caused by curling at the joints. Because of the short joint spacing of the slabs, joint curling can have a large effect on the IRI. Joint movements in the PCC slabs are likely to be influenced by PCC mix properties, temperature, and support conditions below the slab. Because of the confounding effect on IRI caused by these factors, an accurate estimate of the development of roughness at SPS-2 sections cannot be estimated.

CHAPTER 7: ROUGHNESS CHARACTERISTICS OF SPS-5 AND SPS-6 PROJECTS

7.1 ROUGHNESS CHARACTERISTICS OF SPS-5 PROJECTS

7.1.1 Description of SPS-5 Experiment

The Specific Pavement Studies SPS-5 experiment was developed to investigate the performance of selected AC rehabilitation treatment factors. The rehabilitation treatment factors include overlay mix type (recycled and virgin), overlay thickness, and surface preparation of the existing AC surface prior to overlay (minimal and intensive preparation). Nine test sections are included in each SPS-5 project, with eight sections being experimental sections and one section being a control section. The overlay thickness as well as the type of material used for the overlay (virgin or recycled AC) and the type of surface preparations that are carried out at the test sections prior to placing the AC overlay are described in table 7.1.1. Table 7.1.2 presents a description of the types of surface preparation activities that are carried out at the sections prior to placing the AC overlay. Section 1 is designated as a control section, which receives only limited routine-type maintenance. Repair activities on the control section are limited to those maintenance activities needed to keep the section in a safe and functional condition. Repair activities on this section are carried out according to the guidelines of the State highway agency. The minimal level of surface preparation applies to test sections 2 through 5, and consists primarily of patching of severely distressed areas and potholes and placement of a leveling course in ruts that are greater than 12 mm (1/2 in) deep. The intensive level of preparation applies to test sections 6 through 9, and includes milling of the existing AC surface, patching of distressed areas, and crack sealing after milling. Milling of the surface is the primary difference between the minimal and intensive preparation levels in this experiment. Milling is performed in the intensive surface preparation sections to a depth of 38 to 50 mm (1.5 to 2 in), and the depth of material removed by milling is replaced with an equal thickness of AC overlay material. This material will be virgin mix on test sections 6 and 7 and a recycled mix on test sections 8 and 9. The depth of replacement material is not counted as a part of the overlay thickness specified in the experiment. The recycled AC that is used consists of 30 percent recycled asphalt mix. The monitored portion of each test section is 152 m (500 ft).

Table 7.1.1. Treatments applied to SPS-5 test sections.

Section Number	Preparation	Type of AC	Overlay Thickness (in)
1	Routine Maintenance	-	0
2	Minimum Surface Preparation	Recycled	2
3	Minimum Surface Preparation	Recycled	5
4	Minimum Surface Preparation	Virgin	5
5	Minimum Surface Preparation	Virgin	2
6	Intensive Surface Preparation	Virgin	2
7	Intensive Surface Preparation	Virgin	5
8	Intensive Surface Preparation	Recycled	5
9	Intensive Surface Preparation	Recycled	2

Note : 1 in = 25.4 mm.

Table 7.1.2. Surface preparation activities for SPS-5 test sections.

TEST SECTION DETAILS	SURFACE PREPARATION								
Treatment Options		Minimal				Intense			
Section Number	1	2	3	4	5	6	7	8	9
Overlay Thickness (in)	0	2	5	5	2	2	5	5	2
Overlay Material		R	R	V	V	V	V	R	R
Patching	X	X	X	X	X	P	P	P	P
Crack Sealing	X					P	P	P	P
Leveling		A	A	A	A				
Milling		F	F	F	F	X	X	X	X
Seal Coat	B								

R - Recycled Hot Mixed Asphalt Concrete
V - Virgin Hot Mixed Asphalt Concrete
X - Peform
A - If ruts are >1/2 inch
B - Not permitted in first year of study
P - Peform after milling as required
F - Milling permitted only to remove open graded friction courses

Note: 1 in = 25.4 mm.

7.1.2 Data Availability for SPS-5 Projects

The IRI values for the SPS-5 test sections were obtained from the RIMS, through the regional contractors. Table 7.1.3 presents the SPS-5 projects for which IRI data were available before and after rehabilitation of the pavement. This table also indicates the number of times each project has been profiled after rehabilitation, the subgrade type, the environmental region, and the estimated ESALs/yr that will be applied to the test section As shown in table 7.1.3, profile data are available for eleven SPS-5 projects. The number of times each project has been profiled after pavement rehabilitation ranged from one to six. Table 7.1.4 presents the pavement structure existing at the SPS-5 project locations prior to pavement rehabilitation.

7.1.3 IRI Values of SPS-5 Sections Prior to Rehabilitation

For each SPS-5 project, the IRI was variable between the test sections. Figure 7.1.1 presents the IRI of the test sections prior to pavement rehabilitation for the projects located in Georgia, Maryland, Mississippi, and California. As seen in this figure, the IRI of the test sections for a given project was variable. The COV of the IRI of the test sections for each SPS-5 project are presented in figure 7.1.2. The COV of the IRI for the projects ranged from 10 to 33 percent.

The IRI values of each test section in each SPS-5 project before pavement rehabilitation is presented in table 7.1.5. The average IRI for each SPS-5 project, computed by averaging the IRI of the test sections, and the standard deviation of IRI of the test sections are also presented in table 7.1.5. The difference between maximum and minimum IRI of the test sections in each project is presented in table 7.1.6. As indicated in figure 7.1.2 and table 7.1.6, the IRI values at the test sections within each project were variable. Large variations between the test sections were noted at several SPS-5 projects. For example, in the SPS-5 project in California, section 1 had a IRI of 3.88 m/km (246 in/mi) while section 5 had a IRI of 1.56 m/km (99 in/mi). As indicated in table 7.6.1, the difference between the maximum and the minimum IRI values of test sections within a SPS-5 project ranged from 0.33 m/km (21 in/mi) for the project in Georgia to 2.32 m/km (147 in/mi) for the project in California.

Table 7.1.3. SPS-5 projects for which profile data are available.

State	State Code	Number of Times Profiled After Rehabilitation	Subgrade Type	Enviromnetal Zone	ESALs/yr
Alberta	AB	6	Coarse Grained	Dry Freeze	N.A.
Arizona	AZ	3	Coarse Grained	Dry-No freeze	210,000
California	CA	2	Fine Grained	Dry-No freeze	N.A.
Colorado	CO	5	Fine Grained	Dry Freeze	100,000
Georgia	GA	2	Fine Grained	Wet-No Freeze	600,000
Maine	ME	1	Coarse Grained	Wet Freeze	200,000
Maryland	MD	4	Fine Grained	Wet Freeze	127,000
Mississippi	MS	4	Fine Grained	Wet-No Freeze	204,000
Minnesota	MN	4	Fine Grained	Wet Freeze	85,000
Montana	MT	5	Coarse Grained	Dry Freeze	200,000
New Jersey	NJ	4	Coarse Grained	Wet Freeze	305,000

Table 7.1.4. Pavement structure prior to rehabilitation for SPS-5 projects.

State	Thickness of AC (in)	Base Type and Thickness
Alberta	6	2" Asphalt-Treated Base and 12" Coarse Soil Aggregate Mix
Arizona	4	15" Coarse Soil-Aggregate Mix
California	4	5" Cement-Treated Base and 19" Coarse Soil/Aggregate Mix
Colorado	5	3" Asphalt-Treated Base
Georgia	14	5" Base and 6" Subbase
Maine	9	4" Crushed Stone and 42" Uncrushed Gravel
Maryland	4.4	4.2" Cement-Treated Base and 5.9 Aggregate Base
Minnesota	7	18" Base
Mississippi	12.5	6" Lime-Treated Subgrade
Montana	4	17" Coarse Soil Aggregate Mix
New Jersey	9.2	10.2" Gravel Base and 54" Coarse Soil-Agggregate Mixture

Note: 1 in = 25.4 mm.

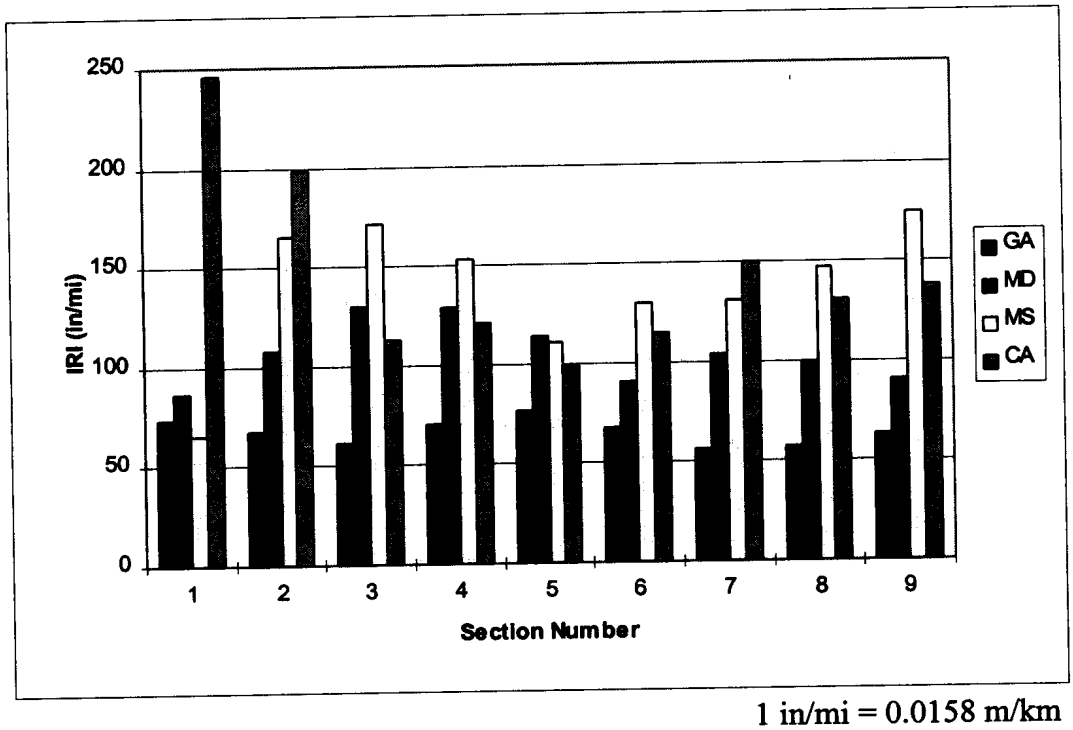

1 in/mi = 0.0158 m/km

Figure 7.1.1. IRI of test sections prior to pavement rehabilitation for selected SPS-5 projects.

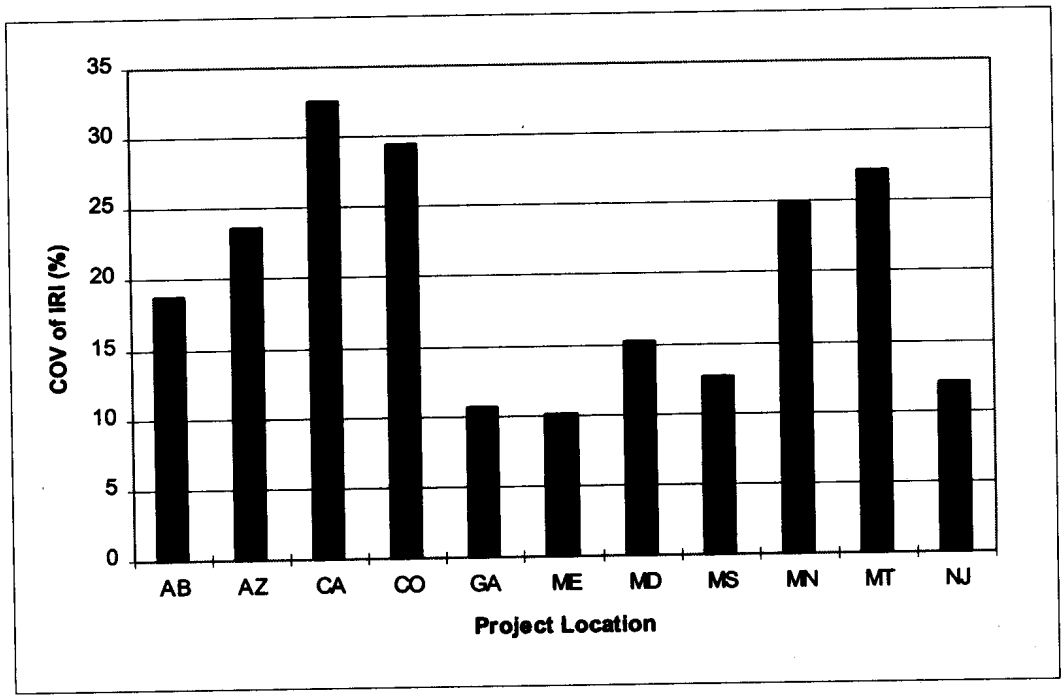

Figure 7.1.2. COV of IRI of test sections prior to rehabilitation for SPS-5 projects.

Table 7.1.5. IRI before rehabilitation for SPS-5 test sections.

State	Section Number									Average IRI of Sections (in/mi)	Standard Deviation of IRI of Sections IRI (in/mi)
	1	2	3	4	5	6	7	8	9		
Alberta	105	131	134	158	88	96	102	116	126	117	22
Arizona	75	130	107	99	164	111	116	98	151	117	28
California	246	199	113	121	99	115	150	131	138	146	47
Colorado	89	94	111	96	87	163	188	118	128	119	35
Georgia	74	68	61	70	77	68	56	58	63	66	7
Maine	77	65	77	87	81	73	91	78	72	78	8
Maryland	87	108	130	129	114	90	104	100	91	106	16
Minnesota	143	178	174	202	168	131	166	160	181	167	21
Mississippi	66	166	171	153	111	130	131	147	174	139	35
Montana	71	110	116	86	68	126	67	83	62	88	24
New Jersey	110	131	128	102	114	111	130	97	138	118	14

Note: 1 in/mi = 0.0158 m/km.

Table 7.1.6. Difference between maximum and minimum IRI of test sections in an SPS-5 project before pavement rehabilitation.

State	Difference Between Maximum and Minimum IRI of Test Sections in Project (in/mi)
Alberta	70
Arizona	89
California	147
Colorado	101
Georgia	21
Maine	26
Maryland	43
Minnesota	71
Mississippi	109
Montana	64
New Jersey	41

Note: 1 in/mi = 0.0158 m/km.

7.1.4 IRI Values of SPS-5 Sections After Rehabilitation

Figure 7.1.3. presents the IRI before and after rehabilitation for four SPS-5 projects. As seen in this figure, for a specific project, the IRI after overlay of the test sections fell within a relatively narrow band, irrespective of the IRI before overlay. Figure 7.1.4 and 7.1.5 present the IRI before and after pavement rehabilitation for test sections 2 and 9, respectively, for all SPS-5 projects. A 50-mm- (2-in-) thick recycled AC overlay is placed on both these sections. In section 2, minimum surface preparation is carried out prior to the overlay while in section 9 intensive surface preparation is carried out prior to the overlay. As indicated in these figures, a unique relationship between the IRI before and after an overlay does not exist. As described previously, the IRI after the overlay for a specific project fell within a relatively narrow range irrespective of the IRI before the overlay. However, the limits of this range varied from project to project. The factors that are expected to influence the IRI of the overlaid section are: profile of the pavement prior to overlay, the predominant wavelengths in the section that contribute to the IRI, and the capability of the contractor placing the overlay.

The IRI values before rehabilitation of each test section in a SPS-5 project was different. If all test sections in each SPS-5 project had the same IRI, a statistic such as the percentage reduction in IRI could be used to compare the effectiveness in reducing the IRI associated with each treatment. Because the IRI values of the test sections within a project were different, such a statistic cannot be used to compare the effectiveness of each treatment in reducing the roughness at a test section.

The IRI values at the test sections after the AC overlay are shown in table 7.1.7. The average IRI after overlay for each SPS-5 project, computed by averaging the IRI of each test section, is also shown in this table. The average IRI of the SPS-5 projects ranged from 0.50 m/km (32 in/mi) for the project in Georgia to 1.50 m/km (95 in/mi) for the project in Mississippi. The project in Georgia had the lowest IRI before pavement rehabilitation of all SPS-5 projects, with the average IRI being 1.04 m/km (66 in/mi). The average IRI values for each test section computed across the SPS-5 projects are also presented in table 7.1.7. The average values for all sections were generally close to each other, with the values ranging from 0.88 to 1.03 m/km (56 to 65 in/mi), and did not indicate a trend associated with a particular test section.

The average IRI values after overlay for the test sections receiving minimum surface preparation prior to overlay (sections 2 to 5) as well as for the test sections receiving intensive surface preparation prior to overlay (sections 6 to 9) are presented in figure 7.1.6. For each SPS-5

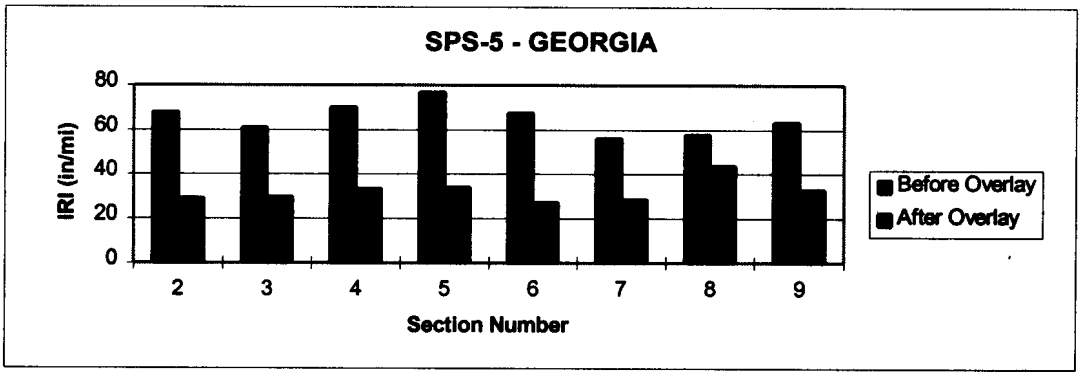

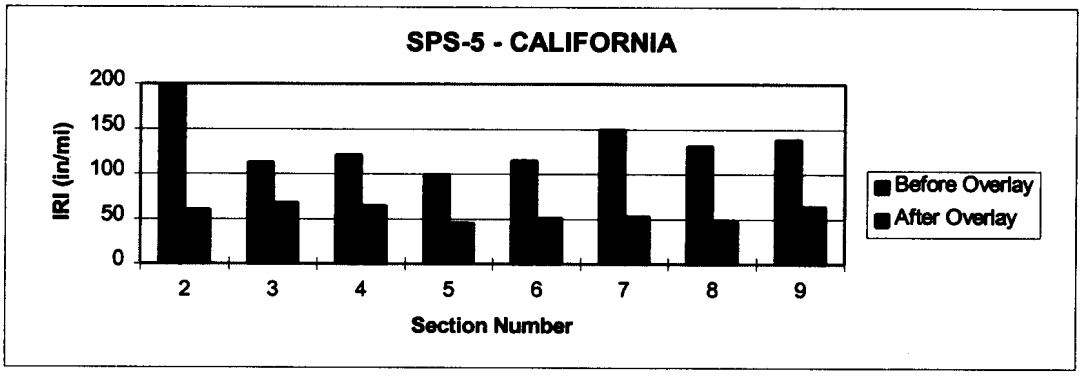

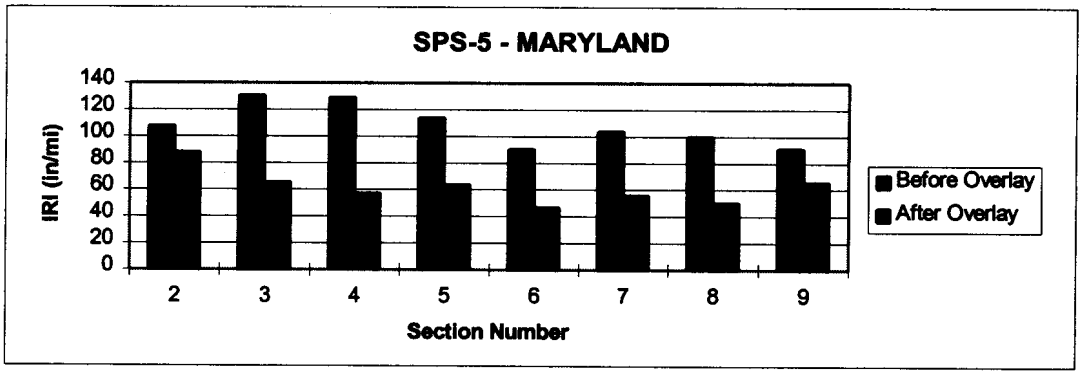

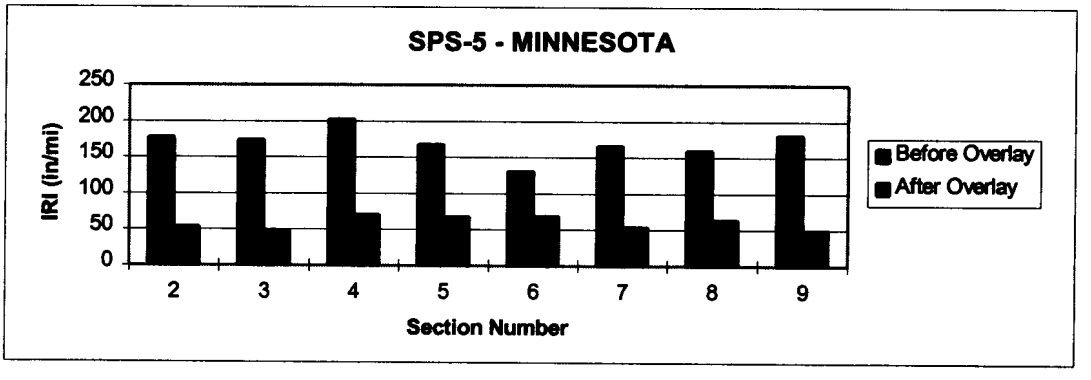

1 in/mi = 0.0158 m/km

Figure 7.1.3. IRI before and after AC overlay for four SPS-5 projects.

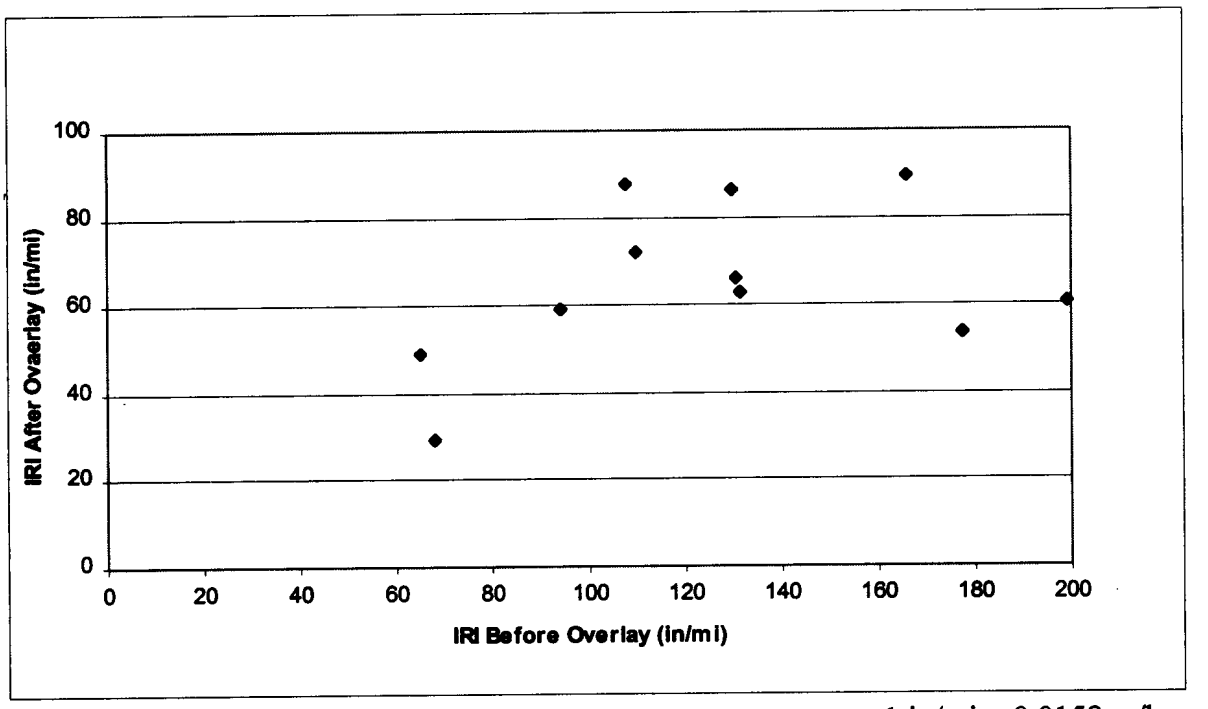

1 in/mi = 0.0158 m/km

Figure 7.1.4. IRI after overlay versus IRI before overlay for test section 2 in SPS-5 projects.

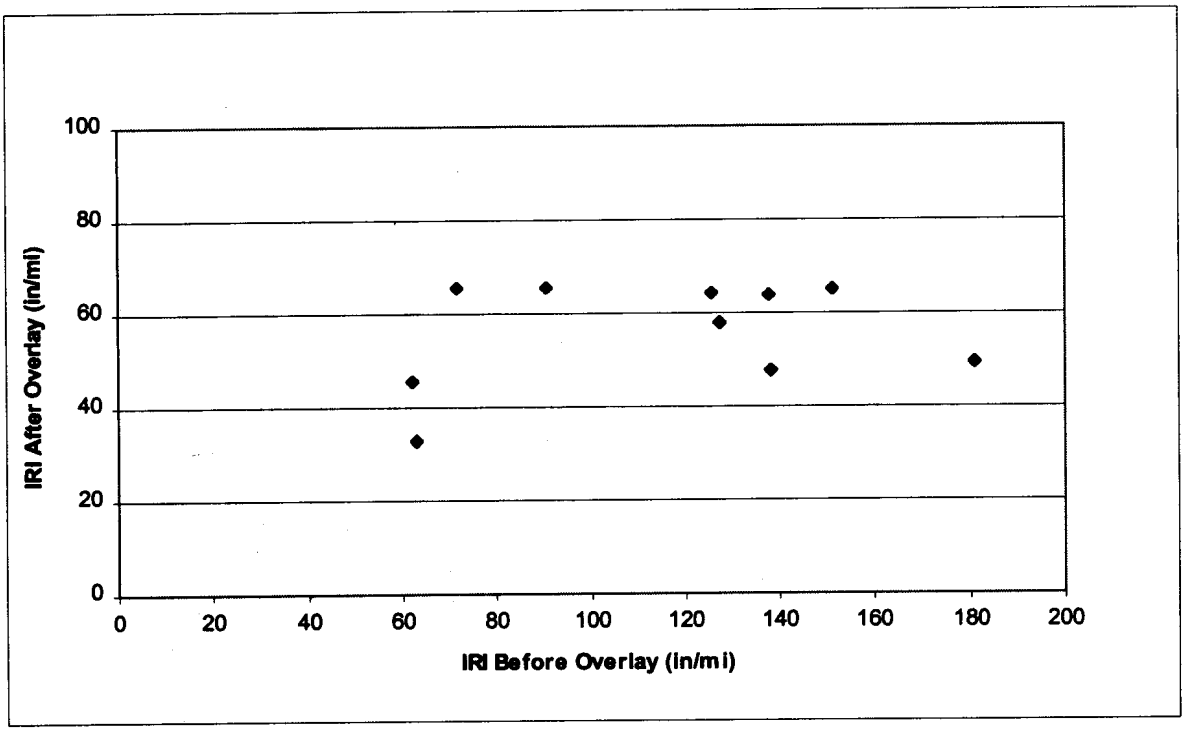

1 in/mi = 0.0158 m/km

Figure 7.1.5. IRI after overlay versus IRI before overlay for test section 9 in SPS-5 projects.

Table 7.1.7. IRI after overlay for test sections receiving an overlay in the SPS-5 experiment.

State	IRI After Overlay Section Number								Average IRI of Sections (in/mi)	Standard Deviation of IRI of Sections (in/mi)	COV of IRI of Test Sections (%)
	2	3	4	5	6	7	8	9			
Alberta	66	67	84	73	68	89	67	64	72	8	11
Arizona	86	60	76	81	65	82	60	65	72	11	16
California	60	68	65	45	51	53	47	64	57	10	18
Colorado	59	49	53	45	58	45	49	58	52	6	12
Georgia	29	30	33	34	27	28	44	33	32	2	8
Maine	49	60	55	45	48	54	52	66	53	7	13
Maryland	88	65	57	64	47	56	50	65	62	13	22
Minnesota	54	48	71	68	69	54	63	49	60	11	18
Mississippi	89	114	76	109	90	80	89	113	95	18	19
Montana	72	63	45	43	44	56	48	46	52	14	27
New Jersey	63	42	45	56	46	49	47	48	50	10	19
AVERAGE	65	61	60	60	56	59	56	61			

Note: 1 in/mi = 0.0158 m/km.

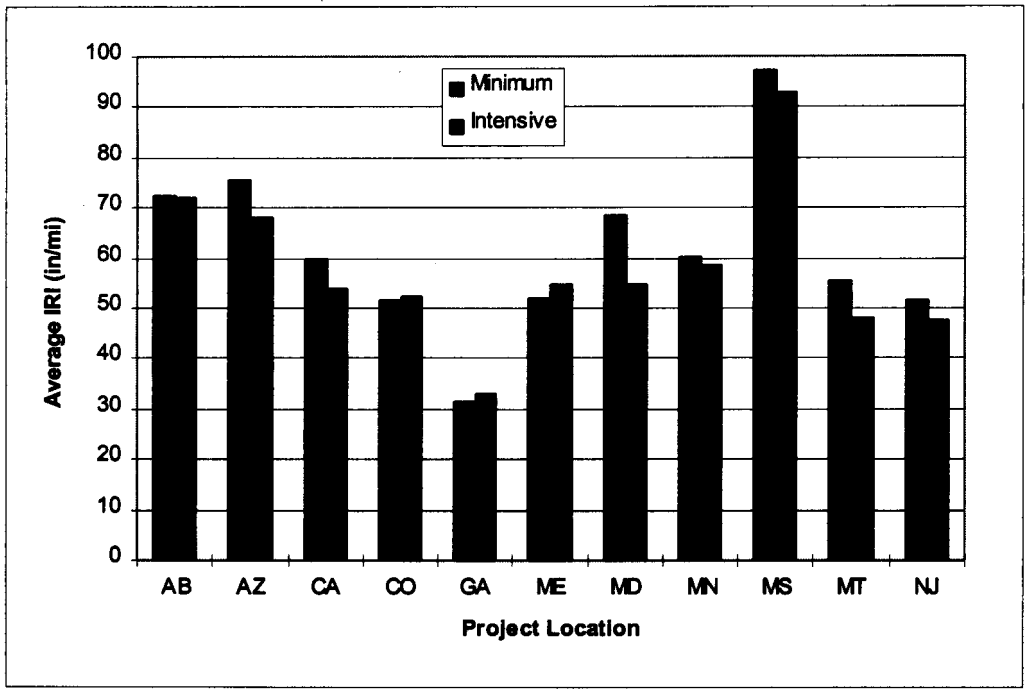

1 in/mi = 0.0158 m/km

Figure 7.1.6. Average IRI after overlay for sections receiving minimum and intensive surface preparation prior to overlay.

project, the average IRI values after overlay for both the minimum and intensive surface preparation sections were close to each other. For eight projects, the average IRI after overlay of the minimum surface preparation sections were higher than the intensive surface preparation sections, with the magnitude of the difference ranging from 0.02 to 0.22 m/km (1 to 14 in/mi), with an average of 0.09 m/km (5.8 in/mi). In three projects, the average IRI after overlay of the intensive surface preparation sections, was higher than the average IRI after overlay of the minimum surface preparation sections, with the difference ranging from 0.015 to 0.044 m/km (1 to 2.8 in/mi), with an average of 0.027 m/km (1.7 in/mi).

The control section in the SPS-5 experiment is only subjected to routine maintenance activities such as patching and crack sealing, carried out according to the standard maintenance activities of the State in which the project is located. The IRI values of the control section in each SPS-5 project before and after maintenance together with the change in IRI at the section, which is the IRI after repair subtracted from IRI before repair, are presented in table 7.1.8. A positive value for the change in IRI in table 7.1.8 indicates that the IRI of the section decreased after pavement repairs, while a negative value indicates that the IRI of the section increased after pavement repairs. The changes in IRI at the control sections, as indicated in table 7.1.8, were generally small except for the projects in Colorado and California where the IRI of the section decreased by 0.66 and 2.76 m/km (42 and 175 in/mi) respectively, after pavement repairs.

7.1.5 Rate of Increase of IRI at SPS-5 Sections

The number of times each SPS-5 project has been profiled after rehabilitation ranged from one to six as shown in table 7.1.3. The rate of increase of IRI at each test section that has been profiled two or more times was computed using the equation presented below:

$$\text{Rate of increase of IRI} = \frac{\text{IRI (t) - IRI (0)}}{\text{Time}}$$

where:

IRI (t) = IRI of section at last profile date,
IRI (0) = IRI of section immediately after pavement rehabilitation, and
Time = time in years between the two profile dates.

The rate of increase of IRI for the SPS-5 projects in Alberta, Mississippi, Maryland, and Colorado that are over 3.5 years old are presented in figure 7.1.7. This figure indicates different trends for the four projects, and conclusions about the effectiveness of each treatment on the rate

Table 7.1.8. IRI before and after pavement rehabilitation for control section in the SPS-5 projects.

State	IRI (in/mi)		
	Section Number and Treatment Type		
	Routine Maintenance Section 1		
	Before Repair	After Repair	Change in IRI
Alberta	105	102	3
Arizona	75	80	-5
California	246	71	175
Colorado	89	47	42
Georgia	74	74	0
Maine	77	81	-4
Maryland	87	83	4
Minnesota	143	130	13
Mississippi	66	68	-3
Montana	71	57	14
New Jersey	110	114	-4

Note 1: Change in IRI = IRI before rehabilitation - IRI after rehabilitation.
Note 2: 1in/mi = 0.0158 m/km.

of increase of IRI cannot be made yet. Most test sections are not yet showing much change in IRI after overlay and, as seen in figure 7.1.7, the rate of increase of IRI for most sections is very small. The IRI values at the test sections for the SPS-5 projects in Arizona and Colorado for the different profile dates are presented in figures 7.1.8 and 7.1.9, respectively. The first IRI value in each figure is the IRI of the section prior to pavement rehabilitation. As shown in these figures, changes in IRI at most sections after pavement rehabilitation are small.

The rate of increase of IRI for all test sections in each SPS-5 project is shown in table 7.1.9. The age of the projects ranges from 1.9 to 4.7 years. A negative value for the rate of change of IRI indicates that the IRI at the last profile date was lower than the IRI obtained after the overlay. The average rate of increase of IRI for each test section, computed by averaging the rate of increase of IRI across all SPS-5 projects, is also presented in table 7.1.9. The average rates of increase of IRI for all overlaid sections are close to each other and, in general, the sections with a 125-mm- (5-in-) thick AC overlay have a lower rate of increase of IRI than the sections with a 50-mm- (2-in-) thick overlay. The largest rate of change of IRI was noted for the control section in Georgia. However, this section has been profiled only twice after rehabilitation, immediately after the overlay and 1.9 years after the overlay. Therefore, the rate of increase of

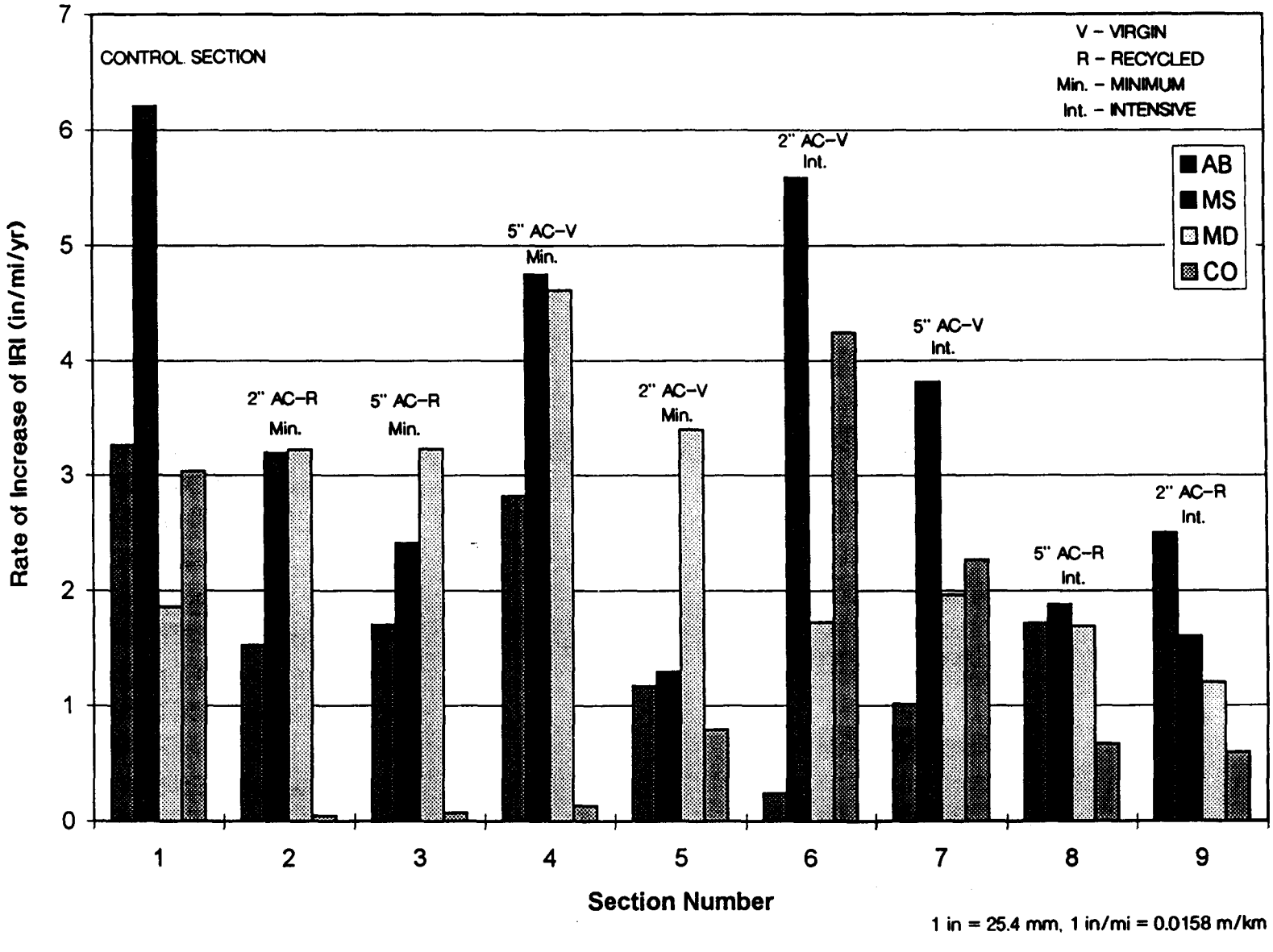

Figure 7.1.7. Rate of increase of IRI for selected SPS-5 projects.

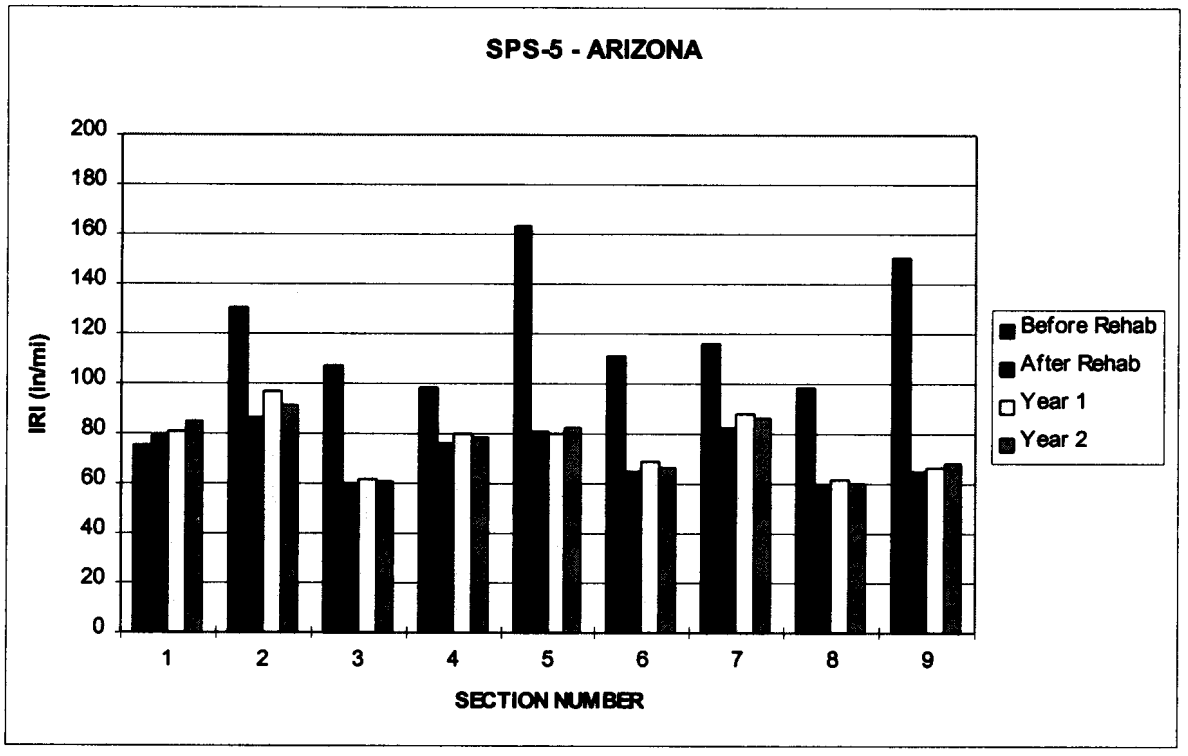

1 in/mi = 0.0158 m/km

Figure 7.1.8. IRI for SPS-5 project in Arizona.

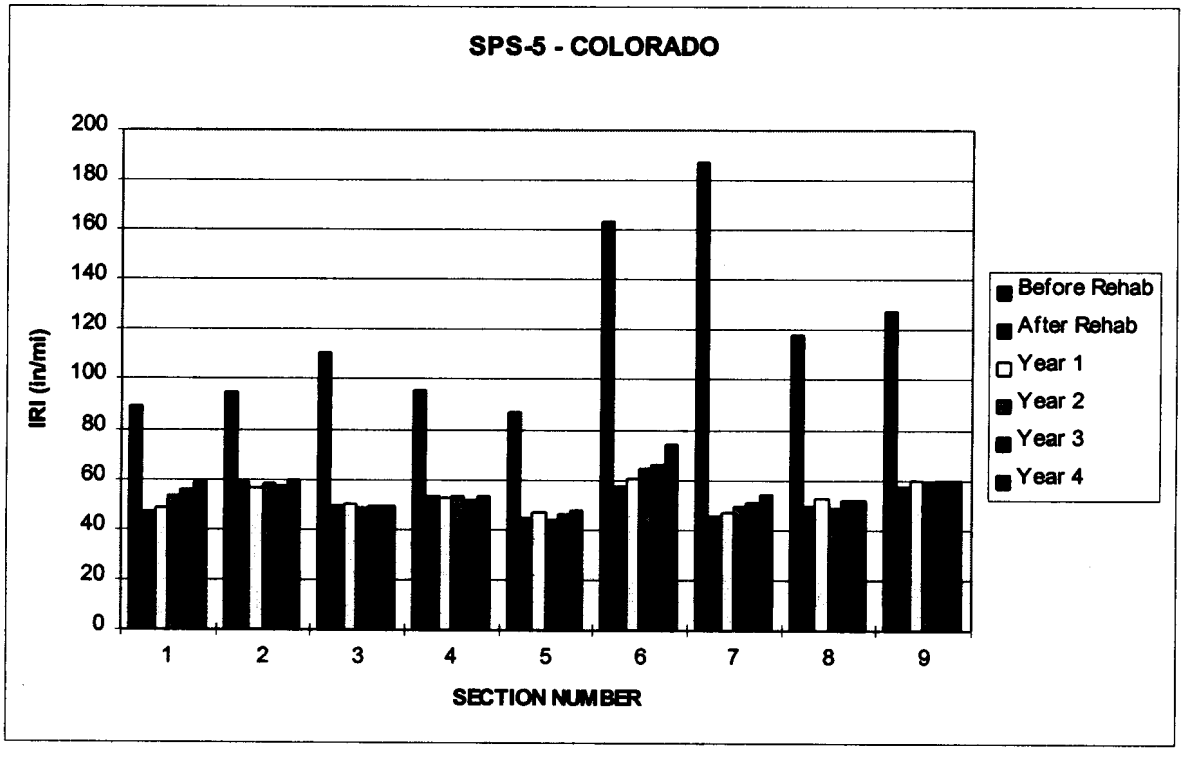

1 in/mi = 0.0158 m/km

Figure 7.1.9. IRI for SPS-5 project in Colorado.

IRI was based on these two points. IRI values at this section at future dates should be used to investigate the rate of increase of IRI at this section to see if this rate of increase of IRI is representative for the section.

Table 7.1.9. Rate of increase of IRI for SPS-5 test sections.

State	Average IRI of Project Before Rehabilitation (in/mi)	Age of Project (yr)	Rate of Change of IRI (in/mi/yr)								
			Surface Preparation								
			Control	Minimum Preparation				Intensive Preparation			
			Section Number								
			1	2	3	4	5	6	7	8	9
			Overlay Type and Thickness								
			0"	2" R	5" R	5" V	2" V	2" V	5" V	5" R	2" R
Alberta	117	4.7	3.3	1.5	1.7	2.8	1.2	0.2	1.0	1.7	2.5
Arizona	117	2.4	2.1	1.9	0.3	1.0	0.8	0.7	1.6	0.3	1.2
California	146	2.2	3.4	1.4	0.5	0.2	7.1	3.6	4.1	1.8	3.3
Colorado	119	3.9	3.0	0.0	0.1	0.1	0.8	4.2	2.3	0.7	0.6
Georgia	66	1.9	22.9	2.0	2.0	-1.7	0.5	1.1	0.8	-0.9	-0.2
Maryland	106	3.5	1.9	3.2	3.2	4.6	3.4	1.7	2.0	1.7	1.2
Minnesota	167	3.0	8.6	6.0	4.7	2.7	4.8	2.7	1.4	1.1	4.9
Mississippi	139	4.7	6.2	3.2	2.4	4.8	1.3	5.6	3.8	1.9	1.6
Montana	88	3.9	-	2.3	0.6	0.9	3.9	2.6	3.7	0.1	4.4
New Jersey	118	2.6	4.8	0.8	0.8	0.4	0.2	0.6	0.6	0.0	0.5
AVERAGE	118	3.3	6.2	2.2	1.6	1.6	2.4	2.3	2.1	0.8	2.0

Note 1: V - virgin AC, R - recycled AC.
Note 2: 1 in = 25.4 mm.
Note 3: 1 in/mi = 0.0158 m/km.

7.1.6 Summary for SPS-5 Projects

Profile data were available for 11 SPS-5 projects, and the number of times these sections have been profiled after rehabilitation ranged from one to six. The IRI values of the test sections within a SPS-5 project were variable, and the COV of the IRI between the test sections for the projects ranged from 10 to 33 percent. The data indicated that, irrespective of the IRI before overlay of the section, the IRI after overlay of the sections for a specific project would fall within a relatively narrow band. However, the limits of this range varied from project to project. For all projects, the average IRI after overlay of the sections that received minimal and intensive surface preparation were very close to each other. Most of the SPS-5 test sections have shown little change in IRI after pavement rehabilitation. A detailed analysis of the rate of increase of IRI carried out on four projects that were over 3.5 years old did not indicate any common trends in the increase of the IRI.

7.2 ROUGHNESS CHARACTERISTICS OF SPS-6 PROJECTS

7.2.1 Description of SPS-6 Experiment

The SPS-6 experiment was developed to investigate the effect of different rehabilitation techniques performed on jointed concrete pavements. In the experimental design, preparation and/or restoration of the existing pavement is classed into three levels: minimal, intensive, crack and seat or break and seat. These preparation treatments are applied with and without an AC overlay. The rehabilitation treatments applied to the test sections in the SPS-6 test sections are presented in table 7.2.1. A detailed description of the surface preparation that is applied to the test sections is presented in table 7.2.2. Each SPS-6 project consists of seven test sections and a control section. The control section designated as section 1 receives only maintenance activities that are needed to keep the section in a safe and functional condition in accordance with the standard procedure of the State agency where the project is located. The monitored portion of test sections 2 and 5 are 305 m (1000 ft), while that of the other sections is 152 m (500 ft).

Table 7.2.1. Treatments applied to SPS-6 test sections.

Section Number	Surface Preparation	AC Overlay Thickness (in)
1	Routine Maintenance	0
2	Minimum Restoration	0
3	Minimum Restoration	4
4	Minimum Restoration (saw and seal joints)	4
5	Intensive Restoration	0
6	Intensive Restoration	4
7	Crack/Break Seat	4
8	Crack/Break Seat	8

Note 1: In section 4, after the placement of the AC overlay, the AC surface is sawed and sealed over the joints and working cracks of the PCC.
Note 2: 1 in = 25.4 mm.

Table 7.2.2. Surface preparation activities for SPS-6 test sections.

TEST SECTION DETAILS & TREATMENT OPTIONS	SURFACE PREPARATION							
		Minimal			Intensive		Crack & Seat	
Section number	1	2	3	4	5	6	7	8
Section length (100 ft)	5	10	5	5	10	5	5	5
Overlay thickness (in)	0	0	4	4	0	4	4	8
Joint sealing	X	X	N	N	R&R	N	N	N
Crack sealing	X	X	N	N	R&R	N	N	N
Partial depth patch	N	X	X	X	R&R	R&R	N	N
Full depth patch/joint repair	N	X	X	X	R&R	R&R	N	N
Load transfer restoration	N	N	N	N	B	B	N	N
Full surface diamond grinding	N	X	N	N	A	N	N	N
Undersealing	N	N	N	N	X	X	N	N
Subdrainage	N	N	N	N	A	A	A	A
Crack/break and seat	N	N	N	N	N	N	A	A
Saw and seal	N	N	N	A	N	N	N	N

X - Apply treatment as warranted
R&R - Remove and replace existing and apply additional as warranted
N - Do not perform
B - Full depth doweled patch or retrofit dowels in slots.
A - Apply treatment regardless of condtion or need.

Note: 1 in = 25.4 mm and 1 ft = 0.3 m.

7.2.2 Data Availability for SPS-6 Projects

The IRI values for the SPS-6 test sections were obtained from the RIMS, through the regional contractors. Table 7.2.3 presents the SPS-6 projects for which IRI data were available before and after rehabilitation of the pavement. This table also indicates the number of profile runs available after rehabilitation, the subgrade type, environmental region, and the annual ESALs in the test lane for each SPS-6 project. As shown in table 7.2.3, profile data are available for nine SPS-6 projects. The number of times each project has been profiled after rehabilitation ranged from two to five. Table 7.2.4 presents the existing pavement structure prior to pavement rehabilitation for each SPS-6 project.

Table 7.2.3. SPS-6 projects for which profile data are available.

State	State Code	Number of Times Profiled After Rehabilitation	Subgrade Type	Environmental Zone	ESALs/yr for Project
Arizona	AZ	5	Coarse Grained	Dry Freeze	1,610,000
California	CA	2	Coarse Grained	Dry Freeze	1,700,000
Illinois	IL	5	Fine Grained	Wet Freeze	622,000
Indiana	IN	4	Fine Grained	Wet Freeze	N/A
Michigan	MI	5	Fine Grained	Wet Freeze	300,000
Missouri	MO	2	Fine Grained	Wet Freeze	426,000
Oklahoma	OK	2	Fine Grained	Dry-No Freeze	404,000
Pennsylvania	PA	4	Fine Grained	Wet Freeze	2,060,000
South Dakota	SD	2	Fine Grained	Dry Freeze	200,000

Table 7.2.4. Pavement structure prior to rehabilitation for SPS-6 projects.

State	Thickness of PCC (in)	Base Type and Thickness
Arizona	8	4" Cement-Treated Base and 9" Aggregate Base
California	8	4" Cement-Treated Base
Illinois	10	6" Aggregate Base
Indiana	10	4" Open-Graded Cold Mix AC
Michigan	9	4" Sand and Gravel Base and 9" of Sand subbase
Missouri	9	4" Aggregate Base
Oklahoma	9	12" Sand
Pennsylvania	10	11" Aggregate Base
South Dakota	8	4" Cement-Treated Base

Note: 1 in = 25.4 mm.

7.2.3 IRI Values at SPS-6 Sections Prior to Pavement Rehabilitation

For each SPS-6 project, the IRI was variable between the test sections. Figure 7.2.1 presents the IRI of the test sections prior to pavement rehabilitation for projects located in California, Indiana, Pennsylvania, and Oklahoma. As seen in this figure, the IRI of the test sections for each project was variable. The COV of the IRI of the test sections for each SPS-6 project is presented in figure 7.2.2. The COV of the IRI for the projects ranged from 10 to 24

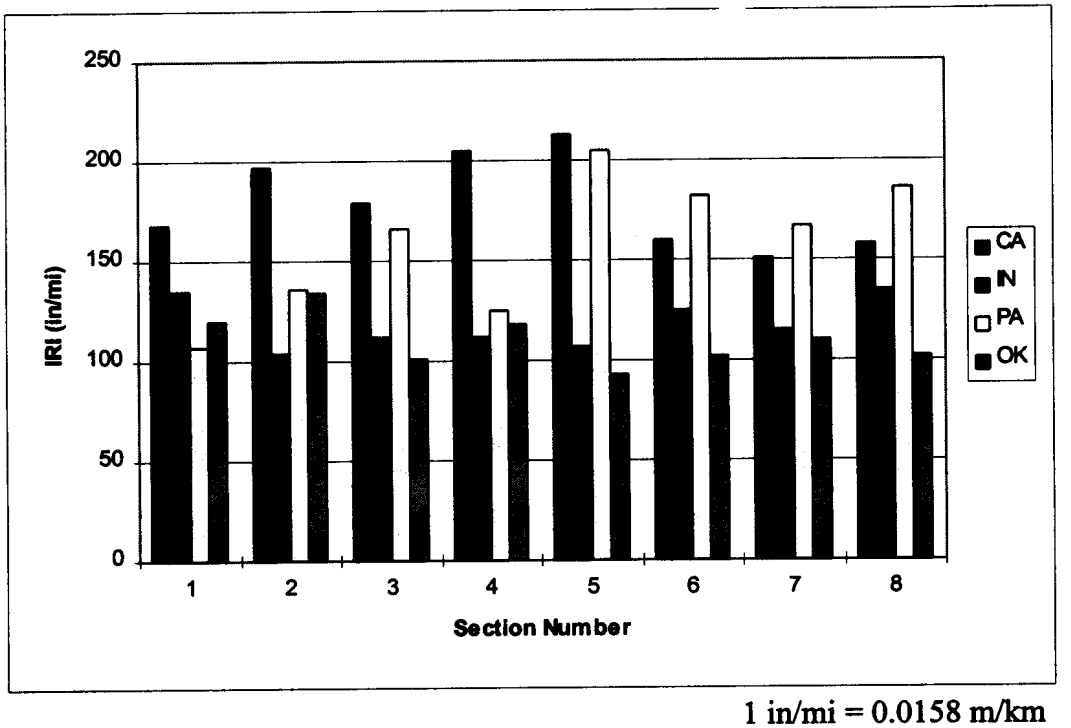

1 in/mi = 0.0158 m/km

Figure 7.2.1. IRI of test sections prior to pavement rehabilitation for selected SPS-6 projects.

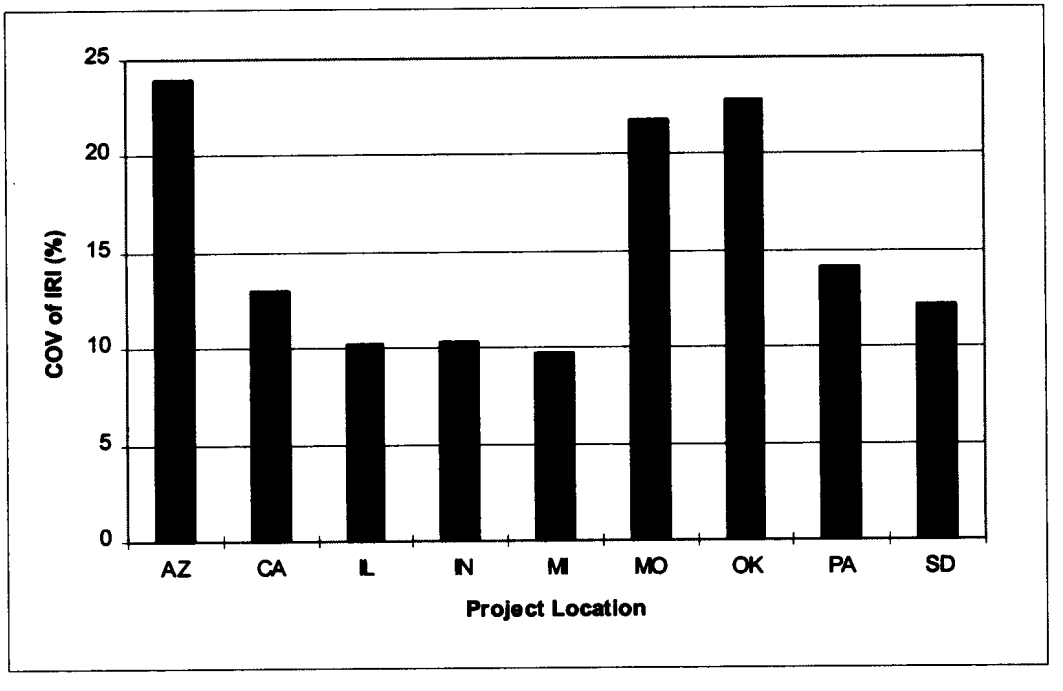

Figure 7.2.2. COV of IRI of test sections prior to rehabilitation for SPS-6 projects.

percent. The IRI values of the sections in each SPS-6 project before pavement rehabilitation is presented in table 7.2.5. The average IRI of the test sections in each project and the standard deviation of IRI for the test sections are also presented in table 7.2.5. Large variations in IRI between the test sections exist in many projects. The difference between the minimum IRI and the maximum IRI of test sections in a project is presented in table 7.2.6, and ranged from 0.49 to 1.55 m/km (31 to 98 in/mi).

Table 7.2.5. IRI before rehabilitation for SPS-6 test sections.

State	Section Number								Average IRI of Sections (in/mi)	Standard Deviation of IRI of Sections (in/mi)
	1	2	3	4	5	6	7	8		
Arizona	105	154	170	103	152	105	98	101	124	30
California	168	197	179	205	213	160	151	158	179	23
Illinois	162	136	150	173	143	177	135	155	154	16
Indiana	135	104	112	112	107	125	115	135	118	12
Michigan	136	131	157	144	129	139	138	111	136	13
Missouri	117	187	124	117	138	125	142	96	132	29
Pennsylvania	107	136	166	125	205	182	167	186	158	36
South Dakota	162	193	165	200	180	158	144	219	178	25
Oklahoma	120	134	101	118	93	102	110	102	111	14

Note: 1 in/mi = 0.0158 m/km.

Table 7.2.6. Difference between maximum and minimum IRI of test sections in an SPS-6 project prior to treatment.

State	Difference Between Maximum and Minimum IRI of Sections in Project (in/mi)
Arizona	72
California	61
Illinois	41
Indiana	31
Michigan	46
Missouri	91
Pennsylvania	98
South Dakota	75
Oklahoma	40

Note: 1 in/mile = 0.0158 m/km.

7.2.4 IRI Values at SPS-6 Sections After Pavement Rehabilitation

Figure 7.2.3 presents the IRI values before and after pavement rehabilitation for the test sections that receive a AC surface for four SPS-6 projects. Test sections 3, 4, and 6 receive an AC overlay, while test sections 7 and 8 are crack/break seated, and then an AC surface is placed. As seen in figure 7.2.3, for the three sections receiving an overlay on the existing PCC surface (sections 3, 4, and 6), the IRI values after the overlay for a specific project were close to each other irrespective of the IRI before the overlay. Except for the project in Oklahoma, the other three projects showed more uniformity of IRI after rehabilitation for all five sections. For each project, the IRI of the test sections after the placement of the AC surface was within a narrow band. However, the lower and upper limits of this band varied from project to project. Figures 7.2.4 and 7.2.5 present the IRI before and after the AC overlay for sections 3 and 6. Both sections received a 100-mm- (4-in-) thick AC overlay. Prior to placing the overlay, section 3 received minimum surface preparation while section 6 received intensive surface preparation. As seen from these figures, no unique relationship exists between IRI before and after overlay. The factors that are expected to influence the IRI of the overlaid section are: profile of the pavement prior to overlay, the predominant wavelengths in the section that contribute to the IRI, and the capability of the contractor placing the overlay.

The IRI values of the test sections in all SPS-6 projects after the placement of the AC surface are tabulated in table 7.2.7. The average IRI of the test sections in each project that received an AC surface ranged from 0.90 to 1.18 m/km (57 to 75 in/mi). The variability of the IRI (after the placement of the AC surface) between the test sections can be characterized by the standard deviation and COV that are presented in table 7.2.7. The COV of the IRI for the projects ranged from 4 to 22 percent, with an average of 11 percent. The average IRI for each test section averaged across the SPS-6 projects is also presented in table 7.2.7. These averages were close to each other, ranged from 0.99 to 1.07 m/km (63 to 68 in/mi), and did not show a specific trend associated with a particular treatment. The IRI before rehabilitation of each test section within a project was different. If all test sections had the same IRI, a statistic such as the percentage reduction in IRI could be used to compare the effectiveness in reducing the IRI associated with each treatment. However, because the IRI of the test sections within a project were different, such a statistic cannot be used to compare the effectiveness of each treatment in reducing the IRI.

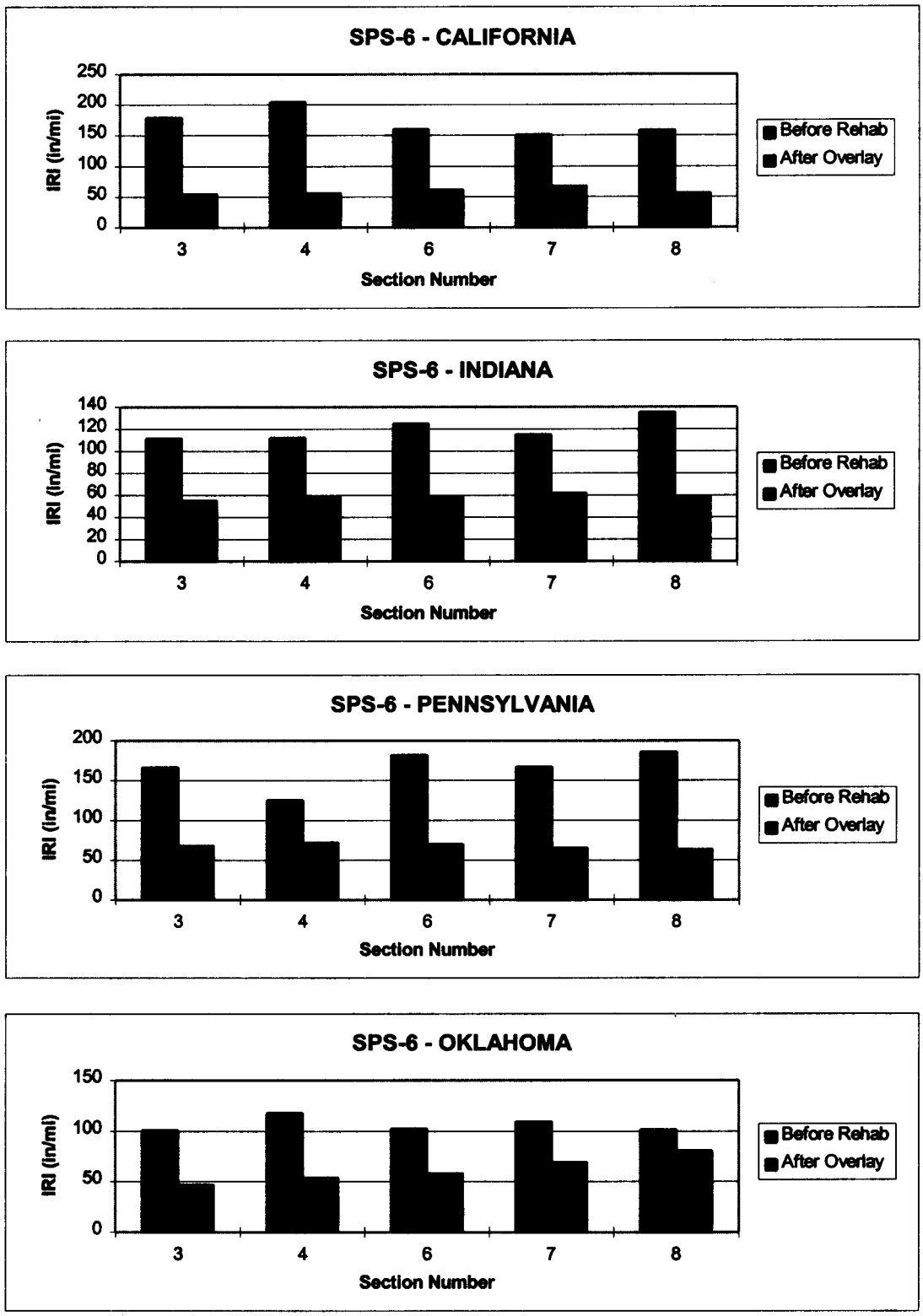

1 in/mi = 0.0158 m/km

Figure 7.2.3. IRI before and after placement of AC surface for four SPS-6 projects.

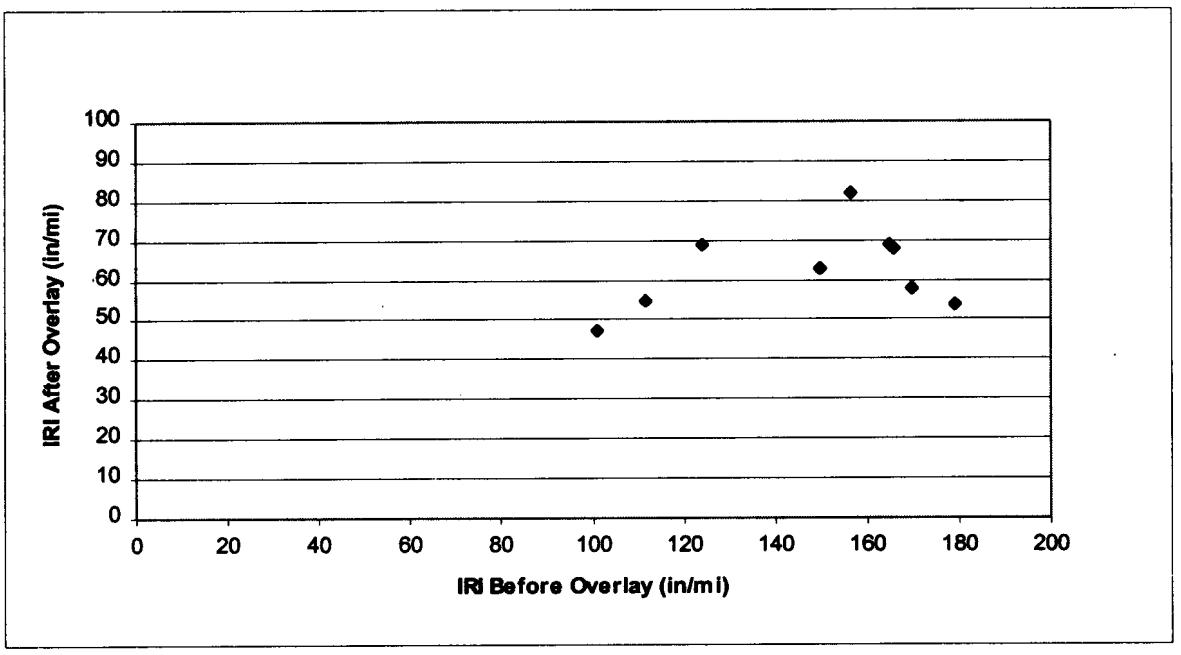

1 in/mi = 0.0158 m/km

Figure 7.2.4. IRI after overlay versus IRI before overlay for section 3 in SPS-6 projects.

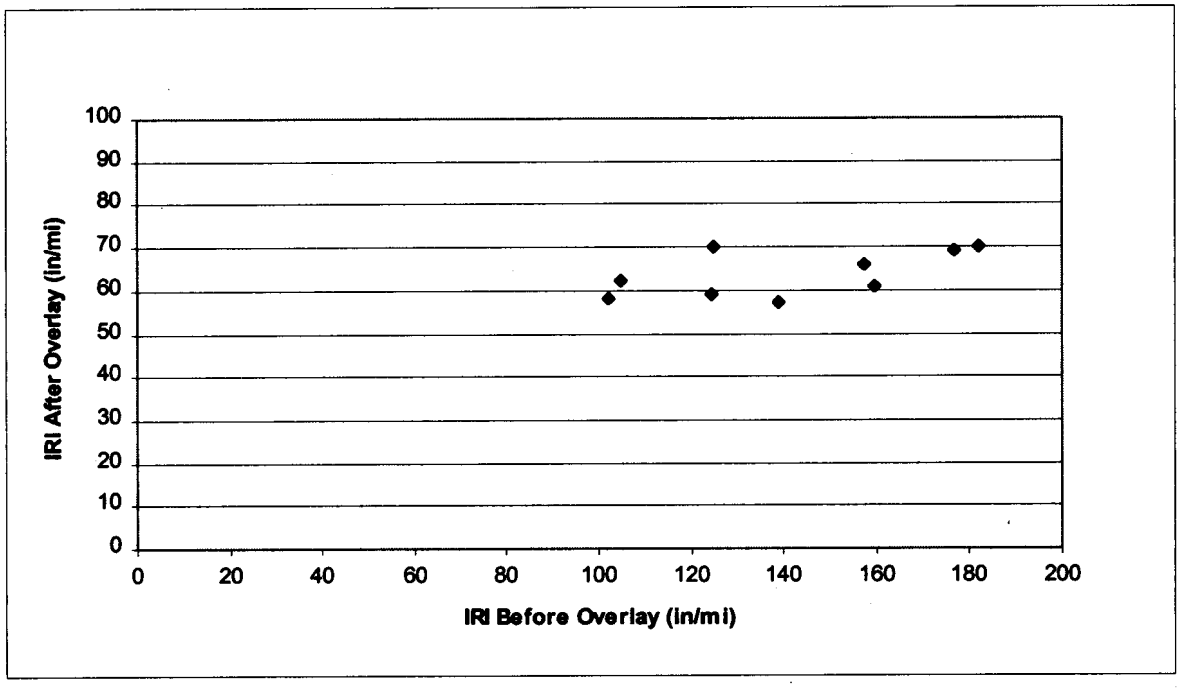

1 in/mi = 0.0158 m/km

Figure 7.2.5. IRI after overlay versus IRI before overlay for section 6 in SPS-6 projects.

Table 7.2.7. IRI after placement of AC surface for SPS-6 test sections.

State	IRI After Overlay (in/mi) Section Number					Average IRI of Sections (in/mi)	Standard Deviation of IRI of Sections (in/mi)	COV of IRI of Sections (%)
	3	4	6	7	8			
Arizona	58	55	62	51	57	57	4	7
California	54	56	61	67	56	59	5	9
Illinois	63	72	69	78	75	71	6	8
Indiana	55	59	59	62	59	59	2	4
Michigan	82	73	57	69	56	67	11	16
Missouri	69	69	70	83	82	75	7	10
Pennsylvania	68	72	70	65	63	68	4	5
South Dakota	69	80	66	65	53	67	10	15
Oklahoma	47	54	58	69	81	62	13	22
AVERAGE	63	66	64	68	65	65		

Note: 1 in/mile = 0.0158 m/km.

Table 7.2.8 presents the IRI values before rehabilitation and after rehabilitation for the three sections not receiving an overlay (Sections 1, 2, and 5). The change in IRI presented in this table for each treatment is the IRI after rehabilitation subtracted from the IRI before rehabilitation. Positive values for change in IRI indicate that the IRI of the section decreased after the treatment, while negative values indicate that the IRI of the sections increased after the treatment. Section 1 is subjected to routine maintenance according to agency practice, with section 2 being subjected to minimal surface preparation, and section 5 being subjected to intensive surface preparation (table 7.2.2 presented the activities associated with these treatments). In the SPS-6 projects, the following observations were noted for the section receiving routine maintenance: (1) the IRI of some sections decreased by a large amount, (2) the IRI of some sections remained at the relatively same level, and (3) the IRI of some sections increased. Similar observations were noted for the minimum restoration section (section 2). The guidelines for maintenance activities in these sections may have been interpreted differently by the different agencies, and the amount of maintenance activities carried out at the sections may have been different, resulting in these observations. Reductions in IRI observed at all sections receiving intensive surface restoration (section 5), except for the sections in Michigan and Indiana where the IRI increased after rehabilitation. The IRI of section 5 should have decreased for all SPS-6 projects as the surface should have been diamond ground after pavement rehabilitation. However, test section 5 in the SPS-6 project in Michigan and Indiana had not been diamond ground. Patching was performed on both these projects and the increase in IRI is likely due to roughness created at the interfaces

Table 7.2.8. IRI before and after maintenance for sections not receiving an AC surface in the SPS-6 experiment.

State	IRI (in/mi)								
	Section Number and Treatment Type								
	Routine Maintenance Section 1			Minimum Restoration Section 2			Intensive Restoration Section 6		
	Before Repair	After Repair	Change	Before Repair	After Repair	Change	Before Repair	After Repair	Change
Arizona	105	147	-42	154	184	-30	152	89	63
California	218	85	133	188	54	134	237	71	166
Illinois	162	163	-1	136	139	-3	143	52	91
Indiana	135	170	-35	104	231	-127	107	218	-111
Michigan	136	132	4	131	133	-2	129	169	-40
Missouri	117	140	-23	187	68	119	138	64	74
Pennsylvania	108	107	1	140	130	10	223	88	135
South Dakota	162	163	-1	193	65	128	180	58	122
Oklahoma	134	69	65	101	47	54	93	48	45

Note 1: Change = IRI before rehabilitation - IRI after rehabilitation.
Note 2: 1 in/mi = 0.0158 m/km.

between the patches and the original pavement. The rehabilitation files in the database do not contain this information yet, and an evaluation of the type of maintenance activities carried out at each section could not be studied in detail.

7.2.5 Rate of Increase of IRI at SPS-6 Sections

The number of times each SPS project has been profiled after rehabilitation, as shown in table 7.2.3, ranged from two to five. The rate of increase of IRI at each section was computed by subtracting the IRI obtained immediately after pavement rehabilitation from the latest available IRI, and dividing the value by the time period between the two observations (see section 7.1.5). This provides a rate of increase of IRI in terms of inches per mile for a section. The rate of increase of IRI is presented in figure 7.2.6 for four SPS-6 projects that are more than 3 years old. A negative rate of increase of IRI at a test section indicates that the IRI at the last profile date is less than the IRI after pavement rehabilitation. Most test sections are not yet showing much change in IRI after the overlay, and small changes in IRI can be masked by variability in profile measurements between the years. Trends in IRI development at the test sections cannot yet be seen across all sections because of this variability.

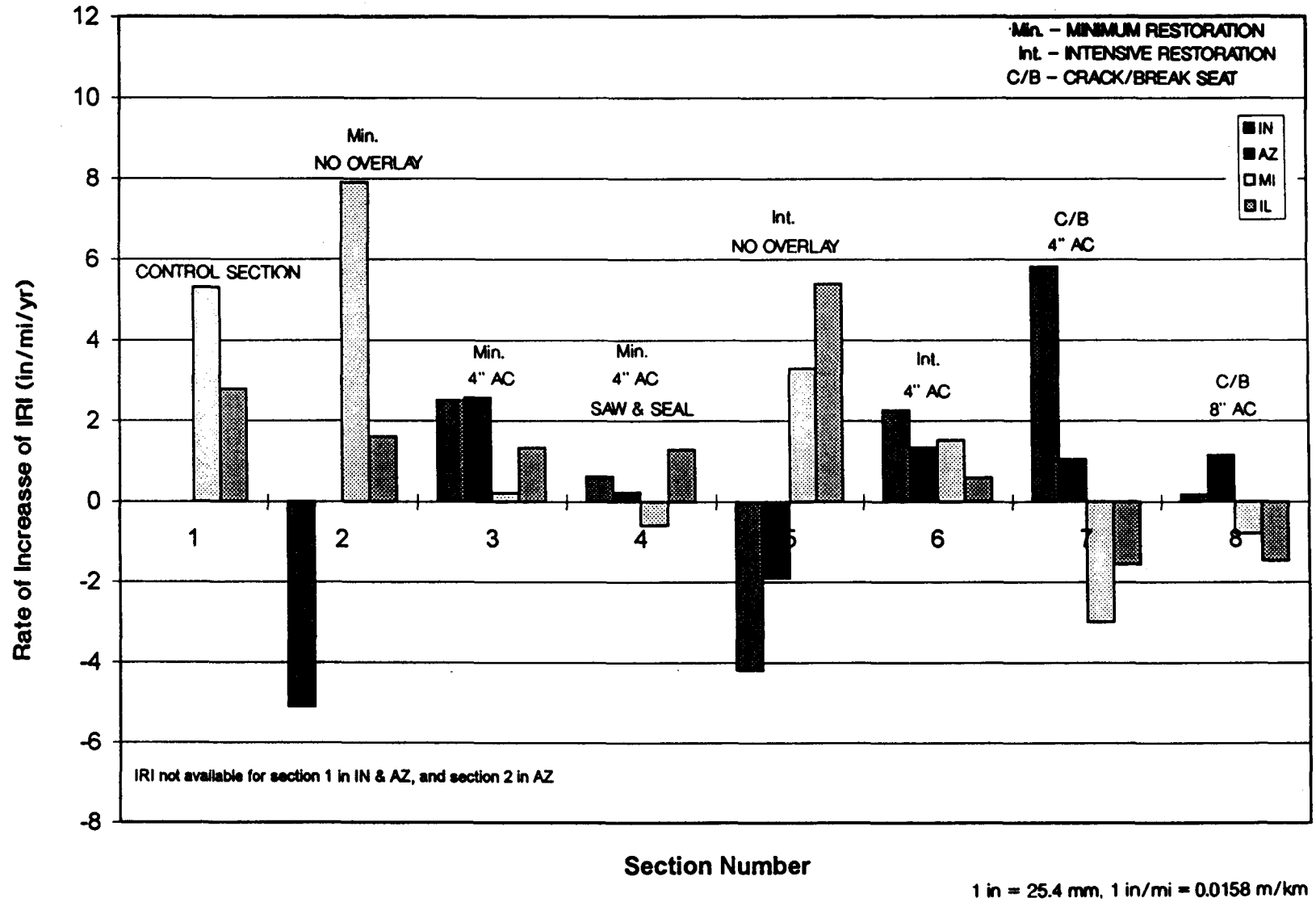

Figure 7.2.6. Rate of increase of IRI for selected SPS-6 projects.

Section 6 received a 100-mm (4-in) overlay after intensive restoration of the existing PCC surface, but its rate of IRI development was generally comparable to section 3, which received the same overlay thickness but with minimum restoration of the existing surface (see figure 7.2.6). Section 4 received a 100-mm- (4-in-) thick AC overlay after minimum restoration of the existing PCC surface, but the AC surface was sawed and sealed over joints and working cracks. As seen in figure 7.2.6, this section had a lower rate of increase in IRI when compared with sections 3 and 6.

Figures 7.2.7 and 7.2.8 present the IRI values for the SPS-6 projects in Illinois and Michigan for the different profile dates, respectively. As seen in these figures, most of the sections are not yet showing much change in IRI after pavement rehabilitation. This phenomenon was also noted for the other SPS-6 projects.

The computed rates of increase of IRI for the test sections at all SPS-6 projects are tabulated in table 7.2.9. The time period in years between the latest profile date and the profile date immediately after construction is presented as the age of the project in this table.

Four projects presented in table 7.2.9 that have the age of project listed as less than 2 years old have been profiled only twice after pavement rehabilitation. The rates of increase in IRI for these projects were computed from these two IRI values. As the profile data for the SPS-6 projects are available for only a limited time period, the rates of increase in IRI values presented in table 7.2.9 should be considered as preliminary values.

Table 7.2.9. Rate of increase of IRI for SPS-6 test sections.

State	Average IRI of Project Before Rehabilitation (in/mi)	Age of Project (yr)	Rate of Change of IRI (in/mi/yr) Section Number							
			1	2	3	4	5	6	7	8
South Dakota	178	0.8	20.1	4.0	-0.3	6.5	9.5	8.4	4.6	6.5
California	179	1.2	N/A	10.1	11.9	11.9	7.4	17.1	2.2	0.6
Missouri	132	1.2	-4.0	11.7	1.0	2.7	12.7	0.5	21.1	-9.1
Oklahoma	111	1.8	-0.4	3.0	0.9	2.1	6.2	4.3	8.0	0.0
Pennsylvania	158	2.9	11.6	4.2	6.3	5.5	7.9	6.9	5.1	2.7
Indiana	118	3.1	N/A	-5.1	2.5	0.6	-4.2	2.3	5.8	0.2
Arizona	124	3.6	N/A	N/A	2.6	0.2	-1.9	1.3	1.0	1.1
Michigan	136	3.7	5.3	7.9	0.2	-0.6	3.3	1.5	-3.0	-0.8
Illinois	154	4.2	2.8	1.6	1.3	1.3	5.4	0.6	-1.6	-1.5

Note: 1 in/mi = 0.0158 m/km.

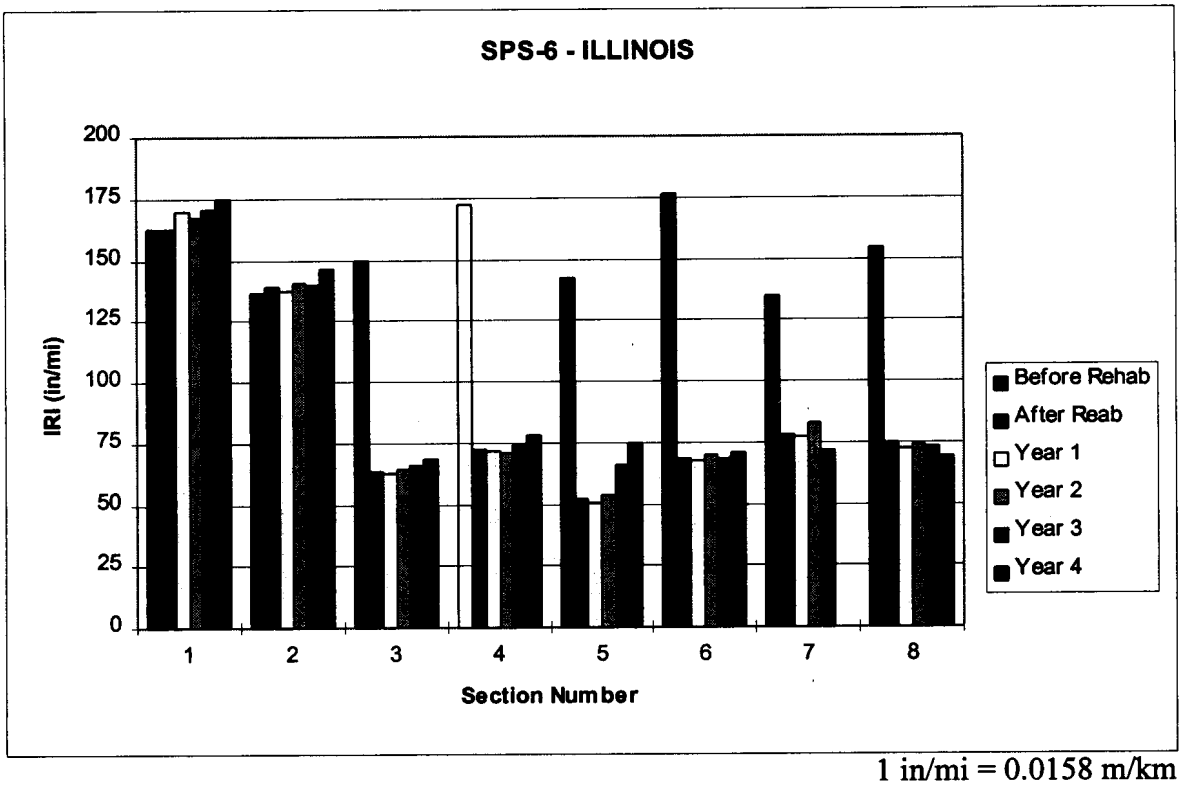

1 in/mi = 0.0158 m/km

Figure 7.2.7. IRI values for SPS-6 project in Illinois.

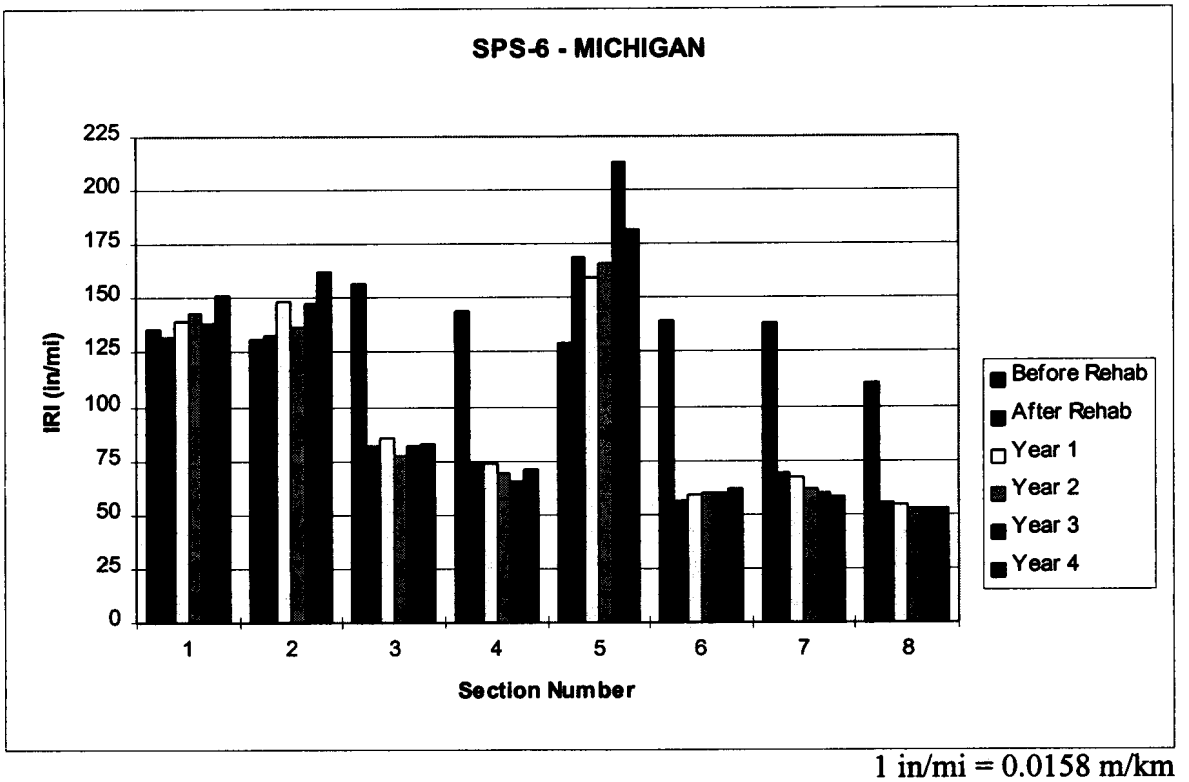

1 in/mi = 0.0158 m/km

Figure 7.2.8. IRI values for SPS-6 project in Michigan.

7.2.6 Summary for SPS-6 Projects

Profile data were available for nine SPS-6 projects, and the number of times these sections have been profiled after rehabilitation ranged from two to five. The IRI of the test sections within a SPS-6 project prior to pavement rehabilitation was variable, and the COV of the IRI between the test sections for the projects ranged from 10 to 24 percent. Three sections in an SPS-6 project received an AC overlay, while two sections received an AC surface after being crack/break seated. In general, for a specific project, the IRI values for all test sections that received an AC surface (overlaid and crack and seated sections) was within a relatively narrow band. The lower and upper limits of this band varied from project to project. The capability of the contractor and the wavelength content of the existing pavement are likely to be important factors in determining the IRI after the placement of the AC surface. Most of the test sections in the SPS-6 projects are showing little change in IRI after pavement rehabilitation, and overall trends across all sections cannot be seen. The variability of profile measurements between the years may be masking the small changes in IRI that occur at most of the sections. Three test sections in this experiment received an AC overlay of 100-mm (4-in) thickness. Prior to the overlay, two sections received minimal surface preparation while one section received intensive surface preparation. On one section that received minimal surface preparation, the AC overlay was sawed and sealed over joints and working cracks. The rate of increase of IRI of this section was lower than the rate of increase of IRI of the other two sections that received the AC overlay.

CHAPTER 8: RECOMMENDATIONS FOR QUALITY ASSURANCE AND PROFILING FREQUENCY

8.1 QUALITY ASSURANCE PROCEDURES

8.1.1 Current Profile Data Collection Procedure

The current profile data collection procedure at GPS sections requires the collection of five profiler runs that satisfy the following two criteria for the both-wheel-path IRI (average of left- and right-wheel-path IRI):

1. The IRI of three profiler runs should be within 1 percent of the mean IRI computed from the five runs.
2. The standard deviation of IRI of the five profiler runs should be within 2 percent of the mean IRI.

If the first five profiler runs that are obtained do not satisfy the above criteria, additional profiler runs, up to a maximum of nine runs, are performed at the section in order to obtain five profiler runs that satisfy the two criteria. After performing nine profiler runs, if five runs that satisfy the criteria cannot be obtained, the five best profiler runs are selected.

The criterion that the IRI of the five profiler runs should be less than 2 percent of the mean IRI is similar to stating that the COV of the five runs should be less than 2 percent. At the beginning of the LTPP program this criterion was at 3 percent, and later it was reduced to 2 percent. The COV of the IRI values obtained from the five profiler runs at a section were analyzed previously (see section 3.4 of this report). These COV values had the cumulative frequency distribution that is shown in table 8.1.1. The data for which the COV were analyzed were all collected during or prior to 1993, and most of the data would have been collected when the COV criterion was 3 percent. At an average of 94 percent of the test sections, the COV of IRI was less than 3 percent. The values shown in table 8.1.1 indicate that for each profile date at a GPS section, the profile data that are collected are extremely repeatable with respect to IRI.

Table 8.1.1. Cumulative frequency distribution of COV of IRI obtained from five replicate runs.

COV of IRI (%)	Percent Cases				
	GPS Experiment				
	GPS-1	GPS-2	GPS-3	GPS-4	GPS-5
<=1	40	36	47	56	47
<=2	79	81	88	88	87
<=3	91	92	97	95	95
<=4	97	96	98	98	98
<=5	98	98	99	100	99
<=6	99	99	100	100	100
<=7	99	100	100	100	100
<=8	99	100	100	100	100

8.1.2 Recommendations for Quality Assurance

The examination of time-sequence IRI data at the GPS sections was described in chapter 2. At some GPS sections inconsistent IRI values were observed for some profile dates, and the cause of the inconsistency was attributed to one of the following factors:

1. Temperature or seasonal effects
2. Maintenance activities at the section
3. Variations in the profiled path
4. Data collection errors

Inconsistent IRI values that are caused by the first two factors cannot be avoided. However, inconsistencies in IRI caused by data collection errors can be avoided, and it may be possible to minimize inconsistencies caused by variations in the profiled path. The current profile data collection criteria at GPS sections ensure that five repeatable runs are collected when each section is profiled. However, it is possible to collect five repeatable runs at a section when the equipment is not working properly. For example, even if the sensors are incorrectly calibrated, five repeatable runs can be obtained at the section. At sections where transverse variability exists, it is possible to obtain five profile runs that satisfy the data collection criteria, and yet obtain an IRI value that is substantially different from the IRI value that was obtained when the section was profiled previously because a different wheel path was followed.

We recommend that the following procedures be adopted during profiler operations to minimize the variability in profile data caused by transverse variability at test sections and to eliminate data collection errors.

Follow a Consistent Wheel Path

A consistent wheel path should be profiled at each section in order to identify changes in roughness at a section over the years. At sections that have a transverse variability in profile, or at sections where distresses are located close to the wheel paths, variations in the profiled path can have a large influence on the IRI value. A regional contractor may utilize different drivers for profiling within a year, and also between the years. The interpretation of the wheel path could be different between the drivers. All profiler drivers in each LTPP region should be trained to follow a consistent path when the sections are being profiled, in order to ensure that the interpretation of the wheel path is consistent between the drivers. The training of the drivers could include videotaping the wheel path followed by the driver to ensure all drivers in each region interpret a consistent wheel path.

Eliminate Data Collection Errors

After the profile data are collected at the test site, the IRI that is reported at 30-m (100-ft) intervals for the different runs should be compared to see that they are comparable between the runs. Then the IRI values for the left and the right wheel paths should be compared with the IRI values that were obtained during the previous profile date. If the change in IRI that is noted for a wheel path is greater than the limits presented in table 8.1.2, the operator should verify that these differences are not caused by equipment errors. If the cause of the discrepancy is attributed to equipment error, the problem should be corrected and additional profiler runs should be obtained at the test section.

Table 8.1.2 IRI ranges to check for data collection errors.

IRI of a Wheel Path (in/mi)	Change in IRI (in/mi)
< 100	±5
100 - 200	±10
>200	±15

Note: 1 in/mi = 0.0158 m/km.

8.2 PROFILING FREQUENCY

8.2.1 Analysis Procedure

Two analysis methods were used to identify GPS sections that showed variations in IRI over time. A linear regression analysis (described in section 5.1) was used to identify GPS sections that showed a statistically significant linear relationship between IRI and pavement age (determined from profile dates). At some GPS sections, the IRI showed variability between the profile dates, and the COV of IRI between the years was used to identify the sections that showed variable IRI patterns.

Linear Regression Analysis

The percentage of sections that showed a statistically significant positive or negative linear relationship between IRI and pavement age for each GPS experiment are presented in table 8.2.1. Appendix B presents the following information obtained from the linear regression analysis for each GPS section: the intercept, slope (which is the rate of increase of IRI), the coefficient of determination (R^2), and if the t-test determined that a linear relationship existed between IRI and pavement age. The IRI values for each GPS section are also presented in appendix B.

Table 8.2.1. Percentage of GPS sections showing statistically significant linear relationship between IRI and pavement age.

GPS Experiment	Percentage of Sections (%)	
	Positive Linear Relationship	Negative Linear Relationship
GPS-1	38	3
GPS-2	30	0
GPS-3	18	2
GPS-4	17	0
GPS-5	4	4
GPS-6A	42	0
GPS-6B	22	0
GPS-7A	13	6
GPS-7B	18	12
GPS-9	16	4

Coefficient of Variation

At some GPS sections the IRI showed an inconsistent pattern. For example, for a specific year the IRI value would be higher or lower than the IRI observed for the previous and the subsequent year, or the IRI was variable across the years. At each GPS section, the variability of the time-sequence IRI values was examined by computing the COV of the IRI. High COV values would be obtained at the sections where high variability in IRI exists between the profile dates. The COV values computed for each GPS section are presented in appendix B. The percent distribution of COV of the test sections that did not show a statistically significant linear relationship between IRI and pavement age, which fall into the different ranges of IRI, are presented in table 8.2.2. These values indicate there are sections that show very high variability in IRI across the years, as well as sections that show very low variability in IRI across the years.

Table 8.2.2. Distribution of COV of GPS sections not exhibiting a statistically significant linear relationship according to ranges of COV.

Range of COV (%)	Percentage of Sections (%)
0 - 2	14
2 - 4	31
4 - 6	21
6 - 8	10
8 - 10	8
>10	16

8.2.2 Recommendations for Profiling Frequency

Table 8.2.3 presents the recommended profiling frequency for the GPS sections. The first priority for profiling should be given to the test sections that show a statistically significant linear increase or decrease in IRI with time, and for the sections that show high variability in IRI between the years. We recommend that the sections that show a statistically significant linear behavior and the sections that have a COV greater than 6 percent be profiled annually. The 6 percent value was selected on the basis of the distribution of COV values presented in table 8.2.2 and the COV values presented in appendix B. For each GPS section, the regression analysis computes a slope, which indicates the rate of increase of IRI at that section. If a section does not show a statistically significant linear relationship and if the COV is not greater than 6 percent, but the slope is greater than 0.05 m/km/yr (3 in/mi/yr), these sections should also be

Table 8.2.3. Recommended profiling frequency for GPS sections

Priority	Frequency	Description of IRI Pattern
1	Once a Year	1. Test sections that show a statistically significant linear relationship between time and IRI 2. Test sections that have a COV greater than 6 percent for time-sequence IRI values 3. Test sections that do not satisfy criteria 1 or 2, but have a a rate of increase of IRI greater than 3 in/mi/yr from linear regression analysis of time-sequence IRI 4. Test sections that have been profiled less than three times
2	Once a Year	Test sections that have a COV between 4 and 6 percent for time-sequence IRI values
3	Once in 2 years	Test sections that have a COV of 4 percent for time-sequence IRI values
Note 1: Closely monitor the IRI history of the section. If a sudden increase in IRI is noted at a section, this may indicate that the section is starting to deteriorate rapidly and these sections should be monitored annually. The following guidelines are offered to define a sudden increase in IRI when compared with the previous IRI value: (a) IRI < 100 in/mi: 5 in/mi (b) IRI between 100 and 200 in/mi: 10 in/mi (c) IRI > 200 in/mi: 15 in/mi. Note 2: 1 in/mi = 0.0158 m/km.		

profiled annually. As indicated in appendix B, most of the sections that have a slope greater than 0.05 m/km/yr (3 in/mi/yr) show a statistically significant linear relationship, or have a COV that is greater than 6 percent. The test sections that have been profiled less than three times should be profiled annually until their IRI behavior pattern can be identified.

The second priority for profiling should be given to the sections that have a COV between 4 and 6 percent; these sections may be profiled annually. The last priority should be given to the sections that have a COV less than 4 percent; these sections may be profiled once in 2 years. The IRI history of the sections should be monitored closely to see if a sudden increase in IRI is noted at a section. This may indicate that the section is starting to deteriorate rapidly, and such sections

should be monitored annually. The following guidelines are presented to define a sudden increase in IRI when compared with the previous IRI value for different IRI ranges: (1) IRI < 1.58 m/km (100 in/mi) - 0.08 m/km (5 in/mi), (2) IRI between 1.58 and 3.15 m/km (100 and 200 in/mi) - 0.16 m/km (10 in/mi), and (3) IRI > 3.15 m/km - 0.24 m/km (15 in/mi).

The time-sequence IRI values available at the GPS sections ranged from 3 to 7. The statistical tests as well as the COV analysis could be affected by the number of data points that were available for each test section. Therefore, the more recent IRI values that are available for the test sections should be used to update the information presented in appendix B.

In the SPS experiments that were evaluated in this study (1, 2, 5, and 6) the time-sequence IRI data were variable at some projects. This variability is attributed to seasonal variations, and for the SPS-2 projects, temperature appears to be a key factor that affects the IRI. A better understanding of the IRI behavior of new pavements could be obtained by profiling the SPS-1 and SPS-2 projects twice a year. This will provide an understanding of how seasonal variability affects changes in IRI of new pavements, and the collected profile data can also be analyzed to determine the changes in wavelengths that occur in these sections. Extensive laboratory and field testing was performed for SPS-1 and SPS-2 projects, and this information can be used with the profile data to understand the behavior of new pavements.

8.3 SUMMARY

On the basis of analysis of time-sequence IRI data, recommendations for data collection were presented in this chapter. One recommendation is to train the profiler drivers to ensure that the interpretation of wheel path at a test section is consistent between the different profiler drivers in each LTPP region. This will ensure that consistent data are collected at the test sections over the years. In addition, guidelines are provided to ensure that the collected data are free of equipment errors. On the basis of information obtained from a statistical analysis, recommendations for profiling frequency at GPS sections were developed, and these were presented in table 8.2.3. Given the variability in IRI values that were noted at SPS-1 and SPS-2 projects, we recommend that these projects be profiled twice a year.

CHAPTER 9: SUMMARY OF KEY FINDINGS

The six main tasks that were addressed in this study were:

1. Investigate development of roughness at GPS sections
2. Compare International Roughness Index and Ride Number for GPS sections
3. Develop roughness models for GPS sections
4. Investigate roughness characteristics of SPS-1 and SPS-2 projects
5. Investigate roughness characteristics of SPS-5 and SPS-6 projects
6. Provide recommendations for quality assurance and profiling frequency

A brief summary of the key findings for each task is presented in this chapter.

9.1 DEVELOPMENT OF ROUGHNESS AT GPS SECTIONS

The collection of profile data at the GPS sections commenced on or after 1990. The profile along the left and right wheel paths at the GPS sections are collected by a K.J. Law profiler that is equipped with optical sensors. The GPS sections are generally profiled annually. Although the time difference between two consequent dates when a section is profiled is close to a year, differences of several months can be present. This results in data being collected during different seasons of the year, and therefore the profile collected between the years can include seasonal variability effects.

The development of roughness at GPS sections was studied using the IRI as the roughness index and the time-sequence IRI data that are available for each GPS section. For each profile date at a GPS section, the IRI of five profiler runs are available. The IRI of the five profiler runs for a given profile date were averaged to obtain the average IRI for each wheel path. For each GPS section, these data were used to prepare plots showing the variation of IRI along the left and the right wheel paths with pavement age. The IRI patterns that were observed for the sections were: (1) IRI along both the left and the right wheel path or along one wheel path increases with time, (2) IRI remains relatively stable over time with minor variations between the profile dates, (3) IRI of both the left and the right wheel path or one of the wheel paths for a given profiling date is higher than the IRI obtained for the profiling dates before and after this date, (4) IRI of both the left and the right wheel paths or one of the wheel paths was lower than the IRI obtained for the profiling dates before and after this date, (5) IRI of both the left and the right wheel paths for different profiling dates were variable, and (6) an abrupt decrease in IRI was observed for both wheel paths, and the IRI at the subsequent dates remained close to this value. The sections that

showed a IRI pattern similar to cases 3 through 6 above were classified as sections that showed inconsistent IRI values; 27 percent of GPS sections showed such behavior.

For cases 3 through 5, the variability of the IRI may have been caused by variations in the profiled paths between the years or by temperature or seasonal effects. In jointed PCC pavements, variations in the profile of the pavement can occur due to temperature effects. The profile of the pavement can also change because of frost heave and changes in moisture content of the subgrade that cause the subgrade to swell or shrink. For pavements that have transverse variability or that have distress adjacent to or along the wheel paths, the IRI will be affected by the path that is profiled. For case 6 where the IRI of the section drops and remains at that level at subsequent profile dates, the change in IRI can be caused by maintenance activities at a section. However, it should also be noted that maintenance activities at a section could also cause the IRI of the pavement to increase (e.g., a patch that introduces a bump).

9.2 COMPARISON BETWEEN IRI AND RN

In this study, a comparison between the IRI and RN computed by the method developed by Spangler and Kelly[1] was performed for the GPS sections. The IRI was developed from the data obtained from the International Road Roughness experiment that was sponsored by the World Bank.[3] The IRI is sensitive to wavelengths between 1 and 30 m (4 and 100 ft). The RN is a roughness index that is correlated with the subjective opinion of the road users, and procedures for computing the RN are presented by Spangler and Kelly.[1] The RN assigns a score between 0 and 5 for a pavement, and is computed by an algorithm that provides a method to predict mean panel ratings from measured profiles. The data from two studies that were sponsored by the NCHRP and two studies funded by the Ohio Department of Transportation were used in developing RN.[1,7,8,9] Only wavelengths in the range of 0.48 and 2.4 m (1.6 and 8 ft) are considered in the computation of RN. The RN computation method requires road profile data measured in two wheel paths at 25-mm (1-in) intervals, averaged over a 305-mm (12-in) distance, and stored at 152-mm (6-in) intervals. The data collected by the K.J. Law profilers at GPS sections satisfy these requirements.

The IRI computed from the profile data is available in the NIMS database. However, the RN is not available in the NIMS. Profile data obtained from NIMS were used to compute the RN of the profiles. For each GPS section five profile runs are available for each profile date. In the comparison between IRI and RN, the average value obtained for each parameter for the five runs was used.

Separate comparisons between IRI and RN were performed for experiments GPS-1 through GPS-5. These comparisons indicated that a unique relationship between the IRI and RN does not exist. The IRI is sensitive to wavelengths between 1.2 and 30 m (4 and 100 ft), while the RN is sensitive to wavelengths between 0.48 and 2.4 m (1.6 and 8 ft). There could be a range of IRI values that correspond to a specific value of an RN. For example, consider two profiles that have similar short wavelength contents, but different long wavelength contents. As the RN is sensitive to the short wavelength content, the two profiles can have the same RN, but because the long wavelength contents are different, they can have different IRI values. For GPS-1 and GPS-2 sections, the spread in IRI values associated with a given RN increased with decreasing RN values, with this effect being more pronounced for RNs less than 3. For the PCC pavements (GPS experiments 3 through 5), the band of IRI values associated with a specific RN was much narrower.

The study of trends in IRI and RN at selected sections indicated that these two parameters generally have similar trends. As the IRI has a maximum sensitivity at wavelengths of 2.1 m (7 ft) and 15.2 m (50 ft), short wavelength content also has a significant contribution to the IRI. Therefore, short wavelength contents that are between 0.48 and 2.4 m (1.6 to 8 ft) that reduce the RN will cause an increase in the IRI.

The algorithm presented by Spangler and Kelly[1] for computing the RN is only valid for profiles obtained from profilers that obtain data at 25-mm (1-in) intervals, and then apply a 305-mm (12-in) moving average and record data at 152-mm (6-in) intervals. Currently, only K.J. Law profilers satisfy this data collection criterion, and this limitation prevents the RN from being computed for profiles collected by other profiling devices. The UMTRI developed a new ride index called the Rideability Index in a research project that was sponsored by the FHWA.[10] The UMTRI final report documenting the research was published in June 1996, after the analysis for this study had been completed. The Rideability Index developed by UMTRI is not restricted to a specific profiling sample interval and can be computed for any data sampling interval. The Rideability Index is influenced by wavelengths ranging from 0.6 to 9.1 m (2 to 30 ft). For a profile, the RN computed from the Spangler and Kelly algorithm is not equal to the Rideability Index developed by UMTRI. This is because the wavelengths and the gain factors that are used by the two indices are different. However, there is a very good correlation between these two indices. As there was a very good correlation between the RN and the Rideability Index, relationships between the Rideability Index and the IRI are expected to be similar to the relationships that were observed for the RN. Currently, an ASTM standard for computing the

RN, which uses the algorithm for Rideability Index developed by UMTRI, has been proposed and is going through the balloting process of ASTM.

9.3 ROUGHNESS MODELS FOR GPS SECTIONS

This section will present the overall trends in development of IRI that were observed for each GPS experiment, describe models that were developed to predict IRI, and describe general observations on factors that related to IRI for each GPS experiment.

9.3.1 General Trends in Roughness Development

The first step in investigating the general trends in IRI was to study plots of IRI versus pavement age for each GPS experiment. Four time-sequence IRI values that had been obtained over a 4-year period were on average available for the GPS sections. The IRI versus age of pavement plots indicated that most pavement sections showed little change in IRI over the monitored period. A linear regression analysis was performed between the time-sequence IRI values and the pavement age at each GPS section to identify the sections for which a linear relationship exists between the two parameters. The percentage of sections for which a positive or negative linear relationship existed between IRI and pavement age are presented in table 9.3.1. All GPS sections that had 3 or more years of data were used in this analysis. The frequency distribution of GPS sections according to the slope obtained from linear regression analysis is presented in table 9.3.2.

Table 9.3.2 shows that for each GPS experiment a large number of sections had either a negative rate for the increase of IRI or a low rate that was between zero and 0.03 m/km/yr (2 in/mi/yr). The available IRI data indicated that the GPS sections have been profiled an average of four times, and a rate of increase of IRI of 0.03 m/km/yr (2 in/mile/yr) corresponds to a change of 0.13 m/km (8 in/mi). This change represents a small value when considering the changes in IRI that can occur between the years resulting from environmental effects and variability in the profiled path. For nonoverlaid PCC pavements (GPS-3 to GPS-5), the percentage of sections that had a rate of increase of IRI less than 0.03 m/km/yr (2 in/mi/yr) or a negative rate were: GPS-3: 72 percent, GPS-4: 73 percent, and GPS-5: 91 percent. For nonoverlaid AC pavements (GPS-1 and GPS-2 sections), the percentage of sections exhibiting a similar behavior were

Table 9.3.1. Percentage of GPS sections showing statistically significant linear relationship between IRI and pavement age.

GPS Experiment	Number of Sites With 3 or More Years of Profile Data	Percentage of Sections	
		Positive Linear Relationship	Negative Linear Relationship
GPS-1	188	38	3
GPS-2	124	30	0
GPS-3	120	18	2
GPS-4	56	17	0
GPS-5	73	4	4
GPS-6A	57	42	0
GPS-6B	27	22	0
GPS-7A	30	13	6
GPS-7B	16	18	12
GPS-9	24	16	4

Table 9.3.2. Distribution of sections according to rate of increase of IRI obtained from linear regression.

Rate of Change of IRI (in/mi/yr)	Percentage of Sections (%) GPS Experiment									
	1	2	3	4	5	6A	6B	7A	7B	9
<0	17	20	42	30	47	12	41	23	50	29
0 - 2	31	35	30	43	44	33	30	37	31	38
2 - 4	21	19	15	14	7	21	15	10	6	4
4 - 6	7	12	5	5	1	9	7	13	6	8
6 - 8	12	5	3	5	0	9	7	7	6	13
8 - 10	4	3	2	2	0	9	0	3	0	4
>10	7	7	4	0	1	7	0	7	0	4
Total	100	100	100	100	100	100	100	100	100	100

Note:1 in/mi = 0.0158 m/km.

48 percent and 55 percent, respectively. GPS-6B and GPS-7B are overlaid pavements, and virtually all of these are less than 5 years old: 71 percent of GPS-6B and 81 percent of GPS-7B sections exhibited a growth rate that was negative or less than 0.03 m/km/yr (2 in/mi/yr).

9.3.2 Models for Predicting IRI

The IRI data that were available in the database when this study commenced indicated that the GPS sections have on average been profiled four times over a 4-year period. For a majority of the sections, changes in IRI were minimal over this period. The pavements in the LTPP program should see increase in roughness over time resulting from traffic and environmental effects. However, the trend in roughness development cannot be observed for most of the sections from the data that are available for such a short period. In the short-term data, variability caused by seasonal effects and profile measurements can mask the increase in IRI that occurs at the section. Long-term monitoring data are needed to observe the true trend in development of roughness.

The roughness models that were developed in this study were based on a data set that, on average, had four time-sequence IRI values over a 4-year period. The models reflect the behavior pattern observed for the analyzed data set, and could reflect the biases that were present in the data set. The developed models have not been verified using an independent data set. For the GPS sections that were used in the analysis, the applicability of the models in predicting the IRI can be evaluated when more time-sequence data become available. However, these models can be used to gain an insight into the factors that affect the IRI development at the analyzed sections. The GPS sections in the LTPP program were established on in-service pavements, and the IRI of the test section after construction is not known. The time-sequence IRI values at the test sections are available starting from some point within its service life.

Models for GPS 1 Through GPS-4

In this study, an optimization technique was used to develop models to predict IRI of GPS experiments 1 through 4. The models predict the initial IRI of the pavements with the use of subgrade and structural properties of the pavement, and then predict a growth rate for the section that is a function of time, traffic, subgrade properties, climatic properties, and pavement structure. In the modeling process, the aim was to predict a model that would fit the time-sequence IRI data that were available for a site. The developed models are sensitive to input parameters, and care should be taken not to use input parameters that are unrealistic or beyond the range of data from which the model was developed.

For GPS-1 pavements (AC pavements on granular base), eight models were developed. Four environmental zones, which correspond to the LTPP environmental zones, were used in the analysis. These environmental zones are: wet freeze, wet-no freeze, dry freeze, and dry-no freeze. In the analysis, the dry zone was defined to be an area that received less than 508 mm (20 in) of annual precipitation, and areas receiving a higher precipitation were in the wet zone. The no freeze zone was defined to be areas that had an annual freezing index less than 89°C days (160°F days), and areas higher than this were in the freeze zone. For the GPS-1 sections in the wet zones, separate models were developed based on the percentage of material passing the number 75-μm (No. 200) sieve (P200). For GPS-1 sections separate models were developed for the following cases: (1) dry freeze, (2) dry-no freeze, (3) wet freeze, P200 greater than 50 percent, (4) wet freeze, P200 between 20 and 50 percent, (5) wet freeze, P200 less than 20 percent, (6) wet-no freeze, P200 greater than 50 percent, (7) wet-no freeze, P200 between 20 and 50 percent, and (8) wet-no freeze, P200 less than 20 percent.

For GPS-2 pavements (AC pavements on stabilized base), five base types were available. These base types are: cement-aggregate mixtures, hot mix AC, asphalt-treated mixtures, soil cement, and lean concrete. Models were developed for the different base types except for lean concrete, which did not have sufficient sections for building a model.

Three models were developed for GPS-3 pavements (JPCP). For the wet regions, separate models were developed for doweled and undoweled pavements. For the dry regions, one model was developed as sufficient sections were not available to build separate models. One model was developed for all GPS-4 pavements (JRCP) .

Model for GPS-5 Pavement

The GPS-5 sections showed a relatively constant IRI over time, and multiple linear regression was used to develop a model to predict IRI. However, this model has a very low coefficient of determination ($R^2 = 0.14$).

Models for Overlaid Pavements

GPS-6B and GPS-7B sections are generally less than 5 years old. Very little change in IRI has occurred at most of these sections after the overlay. Therefore, a statistical analysis on the data cannot be performed yet. For GPS-6A, -7A, and -9 sections, a linear regression analysis

was performed on the time-sequence IRI data to determine the rate of increase of IRI. Correlation analyses were performed separately for each experiment to relate the rate of increase of IRI with parameters that could affect the increase of IRI. For GPS-7A and GPS-9 experiments, strong and logical correlations were not observed, and models to predict IRI development could not be developed. For GPS-6A sections, a relationship between the rate of increase of IRI and the minimum surface modulus was developed by considering all sections, while a relationship between the rate of increase of IRI and SN was developed for the sections that had a rate of increase of IRI that was greater than 0.03 m/km/yr (2 in/mi/yr). However, both these relationships had low R^2 values and high standard errors of estimates.

9.3.3 General Observations on IRI Patterns

Flexible Pavements on Granular Base (GPS-1)

The analysis of IRI data indicated that flexible pavements generally start off with lower roughness but develop roughness more quickly and at lower traffic volumes than rigid pavements. Climatic conditions and subgrade conditions showed a strong relationship with IRI for GPS-1 sections. Performance of GPS-1 sections over fine-grained soils was strongly related to Atterberg limits and the percentage of subgrade passing the 75-μm (No. 200) sieve (P200). Good performance was indicated for sections that rested on subgrade that were clayey sand with 10 to 30 percent P200 content and lower moisture contents. Generally higher roughness is indicated in sections that are located in areas of higher precipitation. In freezing environments, pavements in areas that have a high freeze index or high freeze-thaw cycles had higher IRI values. In freezing environments, the data indicated that adequate frost protection is an important factor for good performance. In hot climates, the IRI value of the pavements was strongly related to days above 32°C (90°F). Sections in very hot environments generally had higher IRI values, but better performance was indicated for sections that are subjected to higher precipitation. This may be related to the cooling effect on AC from precipitation. For the analyzed data set, traffic effects on IRI development were mostly seen for sections that had lower SNs.

Flexible Pavements on Stabilized Base (GPS-2)

The IRI behavior trends observed for the GPS-2 data set were generally similar to that observed for GPS-1 sections. It was noted that some GPS-2 sections located in freeze regions did not perform well. The use of a stabilized base results in a lower total pavement thickness. This has a significant effect on the frost heave potential for pavements located in freezing zones.

Poor performance was also noted for GPS-2 sections that were located on high-moisture-content clay subgrades. Analysis of GPS-2 sections that contain cement stabilized bases indicated that the best environment for these types of bases from an IRI point of view is the wet-no freeze environment.

Rigid Pavements

The overall analysis of all rigid pavements in the LTPP database shows that JPC pavements with short slab lengths (GPS-3) have the highest IRI, while CRC pavements have the lowest IRI, with the JRC pavements falling within these two limits. This observation indicates that transverse joints and cracks have a large influence on the IRI.

GPS-3 Sections: Subgrade and climatic properties were seen to have a strong influence in the performance of the GPS-3 sections. It was noted that the IRI of undoweled jointed pavements was closely related to the amount of faulting at a given site. Better performance can be achieved for these pavements by designing them to minimize faulting. For PCC pavements located on subgrades that are susceptible to pumping, an adequate base and subbase should be provided to prevent pumping. A strong relationship between IRI and faulting was not seen for doweled pavements. Lower water to cement ratios and higher cement content appear to indicate higher initial IRI values, but the rate of development of IRI of these pavements seems to be low. It appears that some sections that had a higher PCC split tensile strength while having a relatively low PCC modulus provided good performance.

GPS-4 Sections: Subgrade and climatic properties were seen to have a major influence on the performance of these pavements. Sections that had thicker PCC slabs had higher IRI, and this factor is likely to be related to construction of the pavement Higher precipitation as well as higher subgrade moisture contents indicated higher IRI values. This may be related to erosion and faulting potential of the pavements. Increased joint spacing also indicated higher IRI values. Longer joint spacing would likely result in a greater proportion of transverse discontinuities (cracks and joints) that could increase the potential for faulting. The IRI value was related to the water to cement ratio of the PCC mix, with higher water to cement ratios resulting in smoother pavements. This can be explained in terms of workability because a mix with a low water to cement ratio would be less workable. However, such a mix is expected to be more durable over the long term. It appears that sections that had a higher PCC split tensile strength while having a relatively low PCC modulus provided good performance.

GPS-5 Sections: The GPS-5 sections showed a nearly constant IRI over the monitored period. This behavior was observed for young pavements (less than 5 years old) as well as for old pavements (greater than 20 years). For all climatic regions, a higher percentage of longitudinal steel and higher water to cement ratios indicated lower IRI values, while higher values of PCC elastic modulus indicated higher IRI values.

AC-Overlaid Pavements

The analysis of GPS-6B and GPS-7B pavements for which IRI before and after the overlay were available indicated that relatively thin overlays can reduce the IRI of a pavement by a large amount. For example, a 100-mm- (2.5-in-) thick AC overlay reduced the IRI of a flexible pavement from 3.15 to 0.63 m/km (200 to 40 in/mi). Similarly, a 84-mm- (3.3-in-) thick overlay reduced the IRI of a PCC pavement from 2.68 to 0.87 m/km (170 to 55 in/mi). A review of the IRI data at these sites indicated there is little effect of the roughness prior to overlay on the roughness immediately after the overlay. Generally, for most cases, the IRI after the AC overlay of the pavement fell within a relatively narrow band, irrespective of the IRI value of the pavement before the overlay. The IRI after overlay of the GPS-6B sections ranged from 0.42 to 1.80 m/km (27 to 114 in/mi) with 73 percent of the sections having an IRI less than 1.10 m/km (70 in/mi). For GPS-7B sections, the IRI after the overlay ranged from 0.73 to 1.58 m/km (46 to 100 in/mi), with 76 percent of the IRI values being less than 1.10 m/km (70 in/mi). However, sufficient time-sequence IRI data are not available for the GPS-6B and GPS-7B experiments to see how the rate of IRI development is affected by the IRI before the overlay.

The trend in the data of the GPS-6A versus GPS-6B experiments indicates on a qualitative basis that roughness starts to develop after about 10 years of service. The continued monitoring of these sections is considered important. It could be seen that the trend in increase in IRI after overlaid pavements after 10 years is a larger rate of increase than the GPS-1 or GPS-2 pavements.

PCC Overlay of PCC Pavements

There are six different combinations of original pavement type and overlay type for the GPS-9 experiment (e.g., CRCP overlay of JRCP, JPCP overlay of JPCP, etc.). Because there were few GPS-9 sections (28 sections) and six combination of pavement types, specific trends in IRI development could not be observed for this experiment.

9.4 ROUGHNESS CHARACTERISTICS OF SPS-1 AND SPS-2 PROJECTS

The SPS-1 and SPS-2 experiments are designed to study the effect of specific design features on pavement performance. Each SPS experiment consists of multiple test sections. An SPS-1 project consists of AC-surfaced test sections that have different layer types and thicknesses. An SPS-2 project consists of jointed PCC test sections that have different slab thicknesses, PCC strengths, and base types. The investigation of roughness characteristics at SPS-1 and SPS-2 projects provided information on roughness characteristics in newly constructed pavements.

SPS-1 Projects

The SPS-1 experiment was developed to investigate the effect of selected structural factors on long-term performance of flexible pavements constructed on different subgrade types in different environmental regions. The subgrade types considered in this experiment are classified as fine grained and coarse grained. The environmental regions considered are wet freeze, wet-no freeze, dry freeze, and dry-no freeze. There are 24 test sections in an SPS-1 experiment. These 24 test sections are to be constructed for each combination of subgrade type and environmental region, with test sections 1 through 12 being constructed at one site, and test sections 13 through 24 being constructed at a different site. The structural factors considered in this experiment are: surface layer thickness, base type, base course thickness, and drainability. Two different surface course thicknesses of AC, 100 mm (4 in) and 175 mm (7 in), and five different base types are used in the experiment. The base types are: dense-graded aggregate base, asphalt-treated base, asphalt-treated base over dense-graded aggregate base, permeable asphalt-treated base over dense-graded aggregate base, and asphalt-treated base over permeable asphalt-treated base.

Profile data were available for six SPS-1 projects. Of these, one project has been profiled three times, three projects had been profiled twice, and two projects had been profiled only once. As only a limited amount of profile data were available, a detailed analysis to quantify the changes in IRI at the SPS-1 sites could not be carried out. The average IRI of the SPS-1 projects, which is the average of the 12 test sections in the project, ranged from 0.74 m/km (47 in/mi) for the SPS-1 project in Arizona to 1.13 m/km (72 in/mi) for the SPS-1 project in Nebraska. The COV of the IRI of the test sections within a project ranged from 8 percent for the project in Alabama to 19 percent for the project in Kansas. There were large differences between the right- and the left-wheel-path IRI for the SPS-1 projects in Alabama and Arizona, where the right-wheel-path IRI was higher than the left-wheel-path IRI. The average difference between the IRI of the wheel

paths for the SPS-1 projects in Alabama and Arizona were 0.32 and 0.30 m/km (20 and 19 in/mi), respectively. This average difference for the other four projects ranged from 0.02 to 0.08 m/km (1 to 5 in/mi).

The test sections in the SPS-1 project in Arizona, which are located on a coarse-grained subgrade in a dry-no freeze environment, showed little change in IRI when they were profiled approximately 1 year after construction. The test sections in the Kansas project that have estimated SNs less than four, showed a large increase in IRI when they were profiled approximately 1 year after construction. The test sections in Kansas are located on a fine-grained subgrade and are subjected to an estimated 469 KESAL/yr. Apart from the SPS-1 project in Arizona, all other SPS-1 projects generally indicated that the sections that had low SNs had a higher rate of increase of IRI when compared with the sections that had high SNs.

SPS-2 Projects

The SPS-2 experiment was developed to investigate the effect of selected structural factors on the long-term performance of rigid pavements constructed on different subgrade types in different environmental regions. All rigid pavement test sections are doweled, jointed PCC with a joint spacing of 4.6 m (15 ft). The subgrade types considered in this experiment are classified as fine grained and coarse grained. The environmental regions considered in this experiment correspond to the four LTPP environmental regions: wet freeze, wet-no freeze, dry-freeze and dry-no freeze. The SPS-2 experiment consists of 24 tests sections. These 24 sections are to be constructed for each combination of subgrade type and environmental region, with half of the test sections (sections 1 through 12) being constructed at one site, and the other half (sections 13 through 24) being constructed at a different site. The structural factors considered in this experiment are: thickness of PCC layer, flexural strength of the PCC, base type, drainability, and lane width. The two PCC slab thicknesses considered in this experiment are 200 mm (8 in) and 275 mm (11 in), while the two PCC flexural strengths that are used are 3.8 MPa (550 psi) and 6.2 MPa (900 psi). The three base types used are: lean concrete base of 150-mm (6-in) thickness, dense-graded aggregate base of 150-mm (6-in) thickness, and a 100-mm- (4-in-) thick permeable asphalt-treated base over a 100-mm (4-in) thick dense-graded aggregate base. Underdrains are provided in the test sections that have a permeable asphalt-treated base. The lane widths considered in this experiment are 12 ft (3.66 m) and 14 ft (4.27 m).

Profile data were available for seven SPS-2 projects. Of these, one project has been profiled four times, two projects had been profiled three times, two projects have been profiled

twice, and two projects have been profiled once. Therefore, a detailed study to quantify roughness development at SPS-2 sections could not be performed because of the limited amount of data that were available for analysis. The average IRI of the SPS-2 projects, which is the average of the 12 test sections in the project, ranged from 1.12 m/km (71 in/mi) to 1.47 m/km (93 in/mi). The COV of the IRI of the test sections within a project ranged from 11 percent to 24 percent. The left- and right-wheel-path IRI were generally close to each other for most test sections, with this difference typically being less than 0.16 m/km (10 in/mi). The IRI after construction at all test sections in the Washington SPS-2 project that had a PCC flexural strength of 6.2 MPa (900 psi) had an IRI that was less than the IRI at the test sections that had PCC flexural strength of 3.8 MPa (550 psi). A reversal of this trend was observed at the Michigan SPS-2, where all test sections that had PCC flexural strength of 6.2 MPa (900 psi) had an IRI that was greater than the IRI at the test sections with a PCC flexural strength of 3.8 MPa (550 psi). These observations indicate that the PCC mix properties affect the IRI after construction of PCC sections. There were large differences in the IRI values between the annual profiling dates at several sections. The analysis of data from the Arizona SPS-2 project indicated that the IRI values obtained approximately 1 year after construction were much less than the IRI values obtained after construction at some sections. The maximum difference that was observed at a test section in this project was 0.49 m/km (31 in/mi). Variability in IRI between profile dates was also noted at some sections in the Michigan SPS-2 project, and a filtered profile analysis at such a section indicated that the differences in IRI were caused by curling at the joints. Because of the short joint spacing of the slabs, joint curling can have a large effect on the IRI. Joint movements in the PCC slabs are likely to be influenced by PCC mix properties, temperature, and support conditions below the slab. Because of the confounding effect on IRI caused by these factors, an accurate estimate of the development of roughness at SPS-2 sections cannot be estimated from the limited profile data that were available.

9.5 ROUGHNESS CHARACTERISTICS FOR SPS-5 AND SPS-6 PROJECTS

In the SPS-5 and SPS-6 experiments, different rehabilitation techniques are used in the rehabilitation of existing AC and PCC pavements, respectively. The reduction in roughness resulting from different rehabilitation techniques for SPS-5 and SPS-6 experiments, as well as the development of roughness at the test sections, was studied.

SPS-5 Sections

The Specific Pavement Studies SPS-5 experiment was developed to investigate the performance of selected AC rehabilitation treatment factors. The rehabilitation treatment factors include overlay mix type (recycled and virgin), overlay thickness, and surface preparation of the existing AC surface prior to overlay (minimal and intensive preparation). Nine test sections are included in each SPS-5 project, with eight sections being experimental sections and one section being a control section. Table 9.5.1 presents the treatments that are applied to SPS-5 sections.

Table 9.5.1. Treatments applied to SPS-5 test sections.

Section Number	Preparation	Type of AC	Overlay Thickness (in)
1	Routine Maintenance	-	0
2	Minimum Surface Preparation	Recycled	2
3	Minimum Surface Preparation	Recycled	5
4	Minimum Surface Preparation	Virgin	5
5	Minimum Surface Preparation	Virgin	2
6	Intensive Surface Preparation	Virgin	2
7	Intensive Surface Preparation	Virgin	5
8	Intensive Surface Preparation	Recycled	5
9	Intensive Surface Preparation	Recycled	2

Note : 1 in = 25.4 mm.

Each SPS-5 project is profiled prior to rehabilitation and then immediately after rehabilitation. Thereafter, they are profiled annually. Profile data were available for 11 SPS-5 projects, and the number of times these sections have been profiled after rehabilitation ranged from one to six. The profile data obtained prior to pavement rehabilitation indicated that the IRI values of the test sections within a SPS-5 project were variable, with the COV of the IRI between the test sections for the projects ranging from 10 to 33 percent. The difference between the maximum and minimum IRI values of test sections within an SPS-5 project prior to rehabilitation ranged from 0.33 m/km (33 in/mi) for the project in Georgia to 2.32 m/km (147 in/mi) for the project in California.

The IRI values after pavement rehabilitation indicated that, for a specific SPS-5 project, the IRI after overlay of the different sections fell within a relatively narrow band irrespective of the IRI before the overlay of the sections. However, the limits of this band varied from project to project. For example, the IRI values of the overlaid test sections (sections 2 through 9) for the

project in Minnesota before the overlay ranged from 2.07 to 2.85 m/km (131 to 181 in/mi) with the standard deviation of the IRI between the sections being 0.32 m/km (20 in/mi) The IRI of the test sections after the overlay ranged from 0.76 to 1.12 m/km (48 to 71 in/mi), with the standard deviation in IRI between the sections being 0.17 m/km (11 in/mi). For the project in California, the IRI before the overlay of the test sections (2 through 9) ranged from 1.56 to 3.13 m/km (99 to 199 in/mi) with the standard deviation of the test sections being 0.49 m/km (31 in/mi). The IRI of the test sections after the overlay ranged from 0.70 to 1.07 m/km (45 to 68 in/mi) with the standard deviation of IRI between the test sections being 0.16 m/km (10 in/mi). For each SPS-5 project, the average IRI after overlay of the sections that received minimal and intensive surface preparation were very close to each other.

Of the 11 projects for which profile data were available, four projects were more than 3.5 years old, with the other projects being less than 3.5 years old. Most of the SPS-5 test sections have shown little change in IRI after pavement rehabilitation. A detailed analysis of the rate of increase of IRI carried out on four projects that were more than 3.5 years old did not indicate any common trends in the increase of IRI.

SPS-6 Sections

The SPS-6 experiment was developed to investigate the effect of different rehabilitation techniques performed on jointed concrete pavements. The rehabilitation treatments applied to the test sections in the SPS-6 test sections are presented in table 9.5.2. The SPS-6 sections are profiled before and immediately after pavement rehabilitation, and thereafter they are profiled annually.

Table 9.5.2. Treatments applied to SPS-6 test sections.

Section Number	Surface Preparation	AC Overlay Thickness (in)
1	Routine Maintenance	0
2	Minimum Restoration	0
3	Minimum Restoration	4
4	Minimum Restoration (saw and seal joints)	4
5	Intensive Restoration	0
6	Intensive Restoration	4
7	Crack/Break Seat	4
8	Crack/Break Seat	8

Note 1: In section 4, after the placement of the AC overlay, the AC surface is sawed and sealed over the joints and working cracks of the PCC.
Note 2: 1 in = 25.4 mm.

The IRI prior to rehabilitation of the test sections within a SPS-6 project was variable, and the COV of the IRI between the test sections for the projects ranged from 10 to 24 percent. Profile data were available for nine SPS-6 projects, and the number of times these sections have been profiled after rehabilitation ranged from two to five. In general, for a specific project, the IRI values for all test sections that received an AC surface (overlaid and crack and seated sections) was within a relatively narrow band. The lower and upper limits of this band varied from project to project. For example, the range of IRI for these five sections (sections 3, 4, 6, 7, and 8) for the project in California prior to pavement rehabilitation was between 2.38 and 3.23 m/km (151 and 205 in/mi) with the standard deviation in IRI between the test sections being 0.34 m/km (22 in/mi). The IRI after the placement of the AC surface at the test sections ranged from 0.85 to 1.05 m/km (54 to 67 in/mi) with the standard deviation of IRI between the test sections being 0.08 m/km (5 in/mi). For the project in Pennsylvania, the IRI of the sections receiving a AC surface ranged from 1.97 to 2.93 m/km (125 to 186 in/mi) with the IRI after the overlay for these sections ranging from 1 to 1.13 m/km (63 to 72 in/mi). The standard deviations of IRI between the test sections prior to the overlay and after the overlay were 0.44 m/km (28 in/mi) and 0.06 m/km (4 in/mi), respectively.

Of the nine SPS-6 projects, four projects are between 3 and 4.5 years old, with the other five projects being less than 3 years old. Most of the test sections in the SPS-6 projects are showing little change in IRI after pavement rehabilitation, and overall trends across all sections cannot be seen. The variability of profile measurements between the years may be masking the small changes in IRI that occur at most of the sections. An analysis was performed to determine the rate of development of IRI at the four projects that were between 3 and 4.5 years old. Three test sections in each project received an AC overlay of 100-mm (4-in) thickness. Prior to the overlay, two sections received minimal surface preparation while one section received intensive surface preparation. On one section that received minimal surface preparation, the AC overlay was sawed and sealed over joints and working cracks. The rate of increase of IRI of the saw and seal section was lower than the rate of increase of IRI of the other two sections that received the AC overlay at three projects. Apart from this trend, other trends in IRI development were not noted between the tests sections.

9.6. RECOMMENDATIONS FOR QUALITY ASSURANCE AND PROFILING FREQUENCY

On the basis of analysis of the time-sequence IRI values at GPS sections, recommendations for quality assurance during profiling were developed. The recommendations included following a consistent wheel path between the years, and comparing the IRI values at the section with the previous year's IRI value. If the change in IRI was greater than a specified limit, it was recommended that the operator ensure that the differences were not caused by equipment errors.

The trends in change of IRI observed at the test sections were used to develop guidelines for profiling frequency at the GPS sections. The recommendations for profiling frequency were developed on the basis of analysis of time-sequence IRI data.

CHAPTER 10: CONCLUSIONS AND RECOMMENDATIONS

10.1 CONCLUSIONS

Variability in Profile Data

The examination of time-sequence IRI data collected at GPS sections indicated that variability in IRI values can occur between the test dates. For example, there were cases where the IRI value for a specific test date would be higher than the IRI values prior to and subsequent to this date. The reverse of this case, where the IRI value for a specific date was lower than the IRI values prior to and subsequent to this date, was also noted. At some sections, the IRI values were variable across all test dates. These variations in IRI values are attributed to the following factors: variations in the profiled path, temperature or seasonal effects, and maintenance activities at test sections.

Comparison Between IRI and RN

A comparison between the IRI and RN computed from the algorithm developed by Spangler and Kelly[1] indicated that a unique relationship between the IRI and RN does not exist. The IRI is sensitive to wavelengths between 1.2 and 30 m (4 and 100 ft), while the RN is sensitive to wavelengths between 0.48 and 2.4 m (1.6 and 8 ft). For a specific value of RN, there could be a range of IRI values that correspond to that RN. For example, consider two profiles that have similar short wavelength contents, but different long wavelength contents. As the RN is sensitive to the short wavelength content, the two profiles can have the same RN, but because the long wavelength contents are different, they can have different IRI values. The study of trends in IRI and RN at selected sections indicated that these two parameters generally have similar trends. As the IRI has a maximum sensitivity at wavelengths of 2.1 m (7 ft) and 15.2 m (50 ft), short wavelength content also has a significant contribution to the IRI. Therefore, short wavelength contents that are between 0.48 and 2.4 m (1.6 and 8 ft) that reduce the RN will cause an increase in the IRI.

Models for Predicting IRI

The IRI data that were available in the database when this study commenced indicated that, on average, four time-sequence IRI values obtained over a 4-year period were available for

a GPS section. For a majority of the sections, changes in IRI were minimal over this period. The pavements in the LTPP program should see increase in roughness over time resulting from traffic and environmental effects. However, a trend in roughness development cannot be observed for most of the sections from data available for a such short period. In the short-term data, variability caused by seasonal effects and profile measurements can mask the increase in IRI that occurs at the section. Long-term monitoring data are needed to observe the true trend in development of roughness.

In this study, an optimization technique was used to develop models to predict IRI of GPS experiments 1 through 4. The models predict the initial IRI of the pavements with the use of subgrade properties and structural properties of the pavement. The models reflect the behavior pattern observed for the analyzed data set. For the analyzed GPS sections, the applicability of the model can be evaluated when more time-sequence IRI data become available. The models predict the initial IRI of the pavement with the use of subgrade properties and structural properties of the pavement, and then predict a growth rate for the section that is a function of time, traffic, subgrade properties, climatic properties, and pavement structure. In the modeling process, the aim was to predict a model that would fit the time-sequence IRI data that were available for a site. The developed models are sensitive to input parameters, and care should be taken not to use input parameters that are unrealistic or beyond the range of data from which the model was developed.

The GPS-5 sections showed a relatively constant IRI over time, and multiple linear regression was used to develop a model to predict IRI. However, this model has a very low coefficient of determination ($R^2 = 0.14$). For the GPS experiments that include overlaid pavements (GPS-6A, GPS-7A, and GPS-9), a rate of development of IRI for each section was obtained using linear regression analysis. This rate was then related to possible factors that could affect the development of IRI that are available in the database. This effort was unsuccessful for the GPS-7A and GPS-9 experiments, and models could not be developed. For the GPS-6A experiments, two models to predict the rate of increase of IRI were developed.

Behavior of Flexible Pavements

The analysis of IRI data indicated that flexible pavements generally start off with lower roughness but develop roughness more quickly and at lower traffic volumes than rigid pavements. Climatic conditions and subgrade conditions showed a strong relationship with IRI for GPS-1 sections. Performance of GPS-1 sections over fine-grained soils was strongly related

to Atterberg limits and the percentage of subgrade passing the 75-μm (No. 200) sieve (P200). Generally higher roughness is found where sections are located in areas of higher precipitation. In freezing environments, pavements in areas that have a high freeze index or a high number of freeze-thaw cycles had higher IRI values. In the freezing environments, the data indicated that adequate frost protection is an important factor for good performance. In hot climates, the IRI value of the pavements was strongly related to days above 32°C (90°F). Sections in very hot environments generally had higher IRI values, but better performance was indicated for sections that are subjected to higher precipitation. This may be related to the cooling effect on AC from precipitation. For the analyzed data set, traffic effects on IRI development were mostly seen for sections that had lower SNs.

The IRI behavior trends observed for the GPS-2 data set were generally similar to that observed for GPS-1 sections. It was noted that some GPS-2 sections located in freeze regions did not perform well. The use of a stabilized base results in a lower total pavement thickness. This has a significant effect on the frost heave potential for pavements located in freezing zones. Poor performance was also noted for GPS-2 sections that were located on high-moisture-content clay subgrades. Analysis of GPS-2 sections that contain cement stabilized bases indicated that the best environment for these types of bases from an IRI point of view is the wet-no freeze environment.

Behavior of Overlaid Pavements

The analysis of GPS-6B and GPS-7B pavements for which IRI before and after the overlay were available indicated that a relatively thin overlay can reduce the IRI of a pavement by a large amount. For example, a 100-mm- (2.5-in-) thick AC overlay reduced the IRI of a flexible pavement from 3.15 to 0.63 m/km (200 to 40 in/mi). Similarly, a 84-mm- (3.3-in-) thick overlay reduced the IRI of a PCC pavement from 2.68 to 0.87 m/km (170 to 55 in/mi). Generally, for most cases, the IRI after the AC overlay of the pavement fell within a relatively narrow band, irrespective of the IRI value of the pavement before the overlay. However, sufficient time-sequence IRI data are not available for the GPS-6B and GPS-7B experiments to see how the rate of IRI development is affected by the IRI before the overlay. There are six different combinations of original pavement type and overlay type for the GPS-9 experiment (e.g., CRCP overlay of JRCP, JPCP overlay of JPCP, etc.). Because there were few GPS-9 sections (28 sections) and six combination of pavement types, specific trends in IRI development could not be observed for this experiment.

General Observations for Rigid Pavements

The overall analysis of all rigid pavements in the LTPP database shows that JPC pavements (GPS-3) have the highest IRI, while CRC pavements (GPS-5) have the lowest IRI, with the JRC pavements (GPS-4) falling within these two limits. Generally, for PCC pavements higher PCC modulus was associated with higher IRI, and a lower water to cement ratio was associated with a higher IRI. There are some indications that PCC pavements that have higher strength (split tensile) while maintaining a relatively low modulus may provide better performance. Subgrade and climatic factors were seen to have a strong influence on IRI for GPS-3 and GPS-4 pavements. It was noted that the IRI of undoweled, jointed pavements is closely related to the amount of faulting at a given site. For GPS-4 sections it was noted that sections in higher precipitation areas had higher IRI values. Higher PCC thickness for GPS-4 pavements also indicated higher IRI values, and this factor is likely to be related to construction of the pavement. The GPS-5 sections showed a nearly constant IRI over the monitored period. This behavior was observed for young pavements (less than 5 years old) as well as for old pavements (more than 20 years old). For CRC pavements, sections that had higher percentage of longitudinal steel had lower IRI values.

SPS-1 and SPS-2 Experiments

Most of the SPS-1 and SPS-2 projects have been profiled fewer than three times, and clear trends in IRI development cannot yet be established for the test sections in these projects. At the SPS-1 projects in Arizona and Alabama, large differences were observed between the left- and the right-wheel-path IRI, with the right-wheel-path IRI being higher. Differences as much as 0.6 m/km (37 in/mi) were noted at some sections. In SPS-1 projects, sections that had lower SNs had a higher rate of increase of IRI when compared with sections that had higher SNs.

At several SPS-2 projects, large variations in IRI between profile dates occurred at some test sections, with differences as much as 0.41 m/km (26 in/mi) being noted. These variations are attributed to curling and warping effects of slabs. The variations in IRI were seen to be related to PCC mix properties and support conditions below the PCC slab. Because of the confounding effect of climatic factors on IRI, estimates for development of IRI cannot be made yet for the SPS-2 experiments. As more time-sequence IRI data are available, trends in IRI development will be seen more clearly.

SPS-5 and SPS-6 Experiments

The IRI values of the test sections prior to pavement rehabilitation in an SPS-5 as well as an SPS-6 project were variable. The COV of the IRI prior to rehabilitation for a project ranged from 10 to 33 percent for SPS-5 experiments and 10 to 24 percent for the SPS-6 experiments. Most of the test sections in the SPS-5 and SPS-6 projects are currently showing little change in IRI after pavement rehabilitation, and overall trends in the development of IRI across all sections cannot be seen. The variability of profile measurements between the years may be masking the small changes in IRI that occur at most of the sections.

For the SPS-5 projects the data indicated that, irrespective of the IRI before the overlay of the sections, the IRI after overlay of the sections for a specific project would fall within a relatively narrow band. However, the lower and upper limits of this range varied from project to project. The average IRI after overlay of the sections that received minimum and intensive surface preparation prior to overlay were close to each other for a specific project. Most of the SPS-5 sections have shown little change in IRI after pavement rehabilitation, and common trends in the increase of IRI for this experiment cannot be determined yet.

Three sections in the SPS-6 project received an AC overlay, while two sections received an AC surface after being crack/break seated. In general, for a specific project, the IRI values for all test sections that received an AC surface (overlaid and crack and seated sections) were within a narrow band. The lower and upper limits of this band varied from project to project. Four SPS-6 projects were between 3 and 4.5 years old, and the rate of increase of IRI of the test sections in these projects were computed. Clear trends in IRI development could not be seen between the test sections except at the three test sections that received an AC overlay of 100-mm (4-in) thickness. Prior to the overlay, two sections received minimal surface preparation while one section received intensive surface preparation. On one section that received minimal surface preparation, the AC overlay was sawed and sealed over joints and working cracks. The section that was sawed and sealed had a lower rate of increase of IRI than the other two sections for three of the analyzed projects.

Profiling Frequency

A statistical analysis was performed on the time-sequence IRI data to identify sections that showed an increase in IRI over time and to identify sections that showed a variable IRI

behavior over time. On the basis of the information obtained from the statistical analysis, recommendations for profiling frequency at GPS sections were developed.

10.2 RECOMMENDATIONS

1. At the time of this study, four time-sequence IRI values obtained over a 4-year period were on average available for a GPS section. These limited data are not sufficient to characterize the roughness growth at each section. The roughness of the pavement sections will increase over time resulting from traffic and climatic effects. The roughness is also expected to vary because of seasonal and environmental effects, and these effects can mask the true roughness behavior of the section when looking at roughness data for a limited period. Both the GPS and SPS sections should be profiled in the future to establish the roughness growth characteristics of the sections. It is recommended that SPS-1 and SPS-2 projects be profiled twice a year to characterize the seasonal variability in IRI.

2. The analysis of time-sequence IRI data available for the GPS sections indicated that variability in IRI values was present at some GPS sections. For example, there were cases where the IRI value for a specific test date would be higher than the IRI values prior to and subsequent to this date. The reverse of this case, where the IRI value for a specific date was lower than the IRI values prior to and subsequent to this date, was also noted. At some sections the IRI values were variable across all test dates. We recommend that the cause of these inconsistencies be analyzed, as it could provide valuable insight into variability of roughness at sections. This analysis should consist of examining the filtered profile that shows an inconsistency, and then comparing it with the profiles prior to and subsequent to this date to identify the cause of the inconsistency.

3. The mix design parameters of PCC appear to have a large effect on the performance of PCC pavements. Regions that are very hot have evolved low strength (split tensile) mixes that generally result in low modulus PCC, while regions that are cool and wet but have little freezing have evolved high strength (split tensile) mixes. The fact that such different mix types have evolved in different climates indicates the importance of climate on performance. There are indications that performance of PCC pavements may be influenced by the relative values of the split tensile strength and the modulus for a specific PCC mix. Further research should be performed to investigate these observations.

4. Variations in IRI values were observed between the profile dates at several SPS-2 projects. The changes in IRI that were observed at the SPS-2 projects were seen to be related to temperature, PCC mix parameters, and the support conditions below the PCC slab. For example, in the SPS-2 project in Arizona, the IRI value at some sections 1 year after construction was lower than the IRI immediately after construction by as much as 0.41 m/km (26 in/mi). Further research is recommended to investigate these observations.

APPENDIX A
GPS SECTIONS WITH INCONSISTENT IRI VALUES

REGION	GPS EXPERIMENT	STATE	SECTION ID	COMMENT
North Atlantic	1	23	1001	Note 1
North Atlantic	1	23	1009	Note 1
North Atlantic	1	23	1012	Note 1
North Atlantic	1	23	1026	Note 2
North Atlantic	1	23	1028	Note 1
North Atlantic	1	33	1001	Note 1
North Atlantic	1	34	1003	Note 1
North Atlantic	1	34	1030	Note 2
North Atlantic	1	36	1011	Note 1
North Atlantic	1	37	1006	Note 2
North Atlantic	1	37	1024	Note 1
North Atlantic	1	37	1030	Note 1
North Atlantic	1	37	1817	Note 1
North Atlantic	1	42	1597	Note 1
North Atlantic	1	50	1002	Note 1
North Atlantic	1	50	1004	Note 1
North Atlantic	1	51	1002	Note 1
North Atlantic	1	89	1021	Note 1
North Atlantic	2	24	1632	Note 1
North Atlantic	2	34	1033	Note 1
North Atlantic	2	36	1644	Note 1
North Atlantic	2	37	2819	Note 1
North Atlantic	2	37	2824	Note 1
North Atlantic	2	50	1681	Note 1
North Atlantic	2	51	1417	Note 1
North Atlantic	2	84	1802	Note 2
North Atlantic	2	88	1646	Note 1
North Atlantic	2	89	2011	Note 1
North Atlantic	3	23	3013	Note 2
North Atlantic	3	23	3014	Note 1
North Atlantic	3	37	3011	Note 1
North Atlantic	3	37	3807	Note 1
North Atlantic	3	37	3816	Note 1
North Atlantic	3	42	3044	Note 1
North Atlantic	4	10	1201	Note 1
North Atlantic	4	34	4042	Note 1
North Atlantic	4	36	4017	Note 1
North Atlantic	4	54	4003	Note 1
North Atlantic	4	54	4004	Note 1
North Atlantic	5	9	5001	Note 1
North Atlantic	5	37	5827	Note 2
North Atlantic	5	42	1598	Note 2
North Atlantic	5	51	5008	Note 1
North Atlantic	6A	84	6804	Note 1
North Atlantic	6B	36	1005	Note 1
North Atlantic	6B	37	1803	Note 1

REGION	GPS EXPERIMENT	STATE	SECTION ID	COMMENT
North Atlantic	6B	51	1423	Note 2
North Atlantic	7A	23	7023	Note 2
North Atlantic	7A	42	1610	Note 2
North Atlantic	7A	42	7037	Note 1
North Atlantic	7A	54	7008	Note 1
North Atlantic	7A	42	1613	Note 1
North Atlantic	9	42	1627	Note 1
North Atlantic	9	42	9027	Note 1
North Central	1	18	1028	Note 1
North Central	1	19	1044	Note 1
North Central	1	21	1010	Note 1
North Central	1	26	1001	Note 1
North Central	1	26	1010	Note 1
North Central	1	26	1013	Note 1
North Central	1	27	1016	Note 1
North Central	1	27	1023	Note 1
North Central	1	27	1029	Note 1
North Central	1	29	1005	Note 1
North Central	1	90	6405	Note 1
North Central	2	18	2008	Note 2
North Central	2	38	2001	Note 2
North Central	2	83	6454	Note 2
North Central	3	18	3003	Note 1
North Central	3	18	3030	Note 2
North Central	3	20	3013	Note 2
North Central	3	20	3060	Note 1
North Central	3	26	3068	Note 1
North Central	3	27	3003	Note 1
North Central	3	31	3033	Note 1
North Central	3	38	3005	Note 1
North Central	3	38	3006	Note 1
North Central	3	39	3801	Note 1
North Central	3	46	3009	Note 1
North Central	3	46	3010	Note 1
North Central	3	46	3013	Note 1
North Central	3	46	3052	Note 1
North Central	3	55	3014	Note 1
North Central	3	55	6351	Note 2
North Central	3	55	6355	Note 1
North Central	4	17	4082	Note 1
North Central	4	18	4021	Note 1
North Central	4	18	4042	Note 1
North Central	4	20	4052	Note 1
North Central	4	27	4033	Note 2
North Central	4	27	4037	Note 2
North Central	4	27	4040	Note 1
North Central	4	27	4050	Note 1
North Central	4	27	4055	Note 2
North Central	4	27	4082	Note 1

REGION	GPS EXPERIMENT	STATE	SECTION ID	COMMENT
North Central	4	29	4036	Note 2
North Central	4	29	5503	Note 1
North Central	5	17	5843	Note 1
North Central	5	17	5849	Note 1
North Central	5	18	5043	Note 1
North Central	5	18	5518	Note 2
North Central	5	29	5047	Note 1
North Central	5	46	5020	Note 2
North Central	6A	18	6012	Note 1
North Central	6A	19	6049	Note 2
North Central	6A	26	6016	Note 1
North Central	6A	39	6019	Note 1
North Central	6A	90	6400	Note 1
North Central	6B	29	5403	Note 2
North Central	6B	29	5413	Note 2
North Central	6B	83	6451	Note 2
North Central	6B	90	6410	Note 1
North Central	6B	90	6412	Note 1
North Central	7A	20	7085	Note 2
North Central	7A	27	7090	Note 2
North Central	7A	31	7017	Note 2
North Central	7A	39	7021	Note 1
North Central	7B	29	4069	Note 1
North Central	7B	29	5493	Note 2
North Central	7B	31	6702	Note 1
North Central	7B	39	5010	Note 1
North Central	9	18	9020	Note 2
North Central	9	26	9029	Note 1
North Central	9	39	9022	Note 1
Southern	1	1	1001	Note 1
Southern	1	1	4129	Note 2
Southern	1	12	1370	Note 2
Southern	1	12	4154	Note 1
Southern	1	47	3075	Note 2
Southern	1	48	1047	Note 1
Southern	1	48	1068	Note 1
Southern	1	48	1076	Note 1
Southern	1	48	1077	Note 1
Southern	1	48	1096	Note 2
Southern	1	48	1169	Note 2
Southern	1	48	1181	Note 1
Southern	1	48	3739	Note 1
Southern	2	13	4112	Note 1
Southern	2	13	4113	Note 2
Southern	2	28	3085	Note 2
Southern	2	28	3087	Note 2
Southern	2	35	2006	Note 1
Southern	2	40	4088	Note 1
Southern	2	40	4165	Note 1

REGION	GPS EXPERIMENT	STATE	SECTION ID	COMMENT
Southern	2	47	1023	Note 2
Southern	2	47	1029	Note 2
Southern	2	47	2001	Note 1
Southern	2	47	3101	Note 1
Southern	2	48	2172	Note 1
Southern	2	48	3559	Note 1
Southern	3	1	3028	Note 2
Southern	3	12	4000	Note 1
Southern	3	12	4138	Note 2
Southern	3	48	3003	Note 2
Southern	4	1	4007	Note 2
Southern	4	5	4023	Note 2
Southern	4	48	4146	Note 2
Southern	4	48	4152	Note 1
Southern	5	1	3998	Note 1
Southern	5	28	5805	Note 1
Southern	5	48	5035	Note 1
Southern	5	48	5284	Note 1
Southern	5	48	5310	Note 1
Southern	6A	1	6019	Note 1
Southern	6A	48	6079	Note 1
Southern	7A	28	3097	Note 1
Southern	9	28	7012	Note 1
Southern	9	28	9030	Note 1
Western	1	4	1002	Note 1
Western	1	4	1003	Note 1
Western	1	4	1007	Note 2
Western	1	4	1015	Note 1
Western	1	4	1024	Note 1
Western	1	4	1025	Note 2
Western	1	4	1034	Note 1
Western	1	6	7454	Note 1
Western	1	1	8156	Note 1
Western	1	8	1029	Note 2
Western	1	6	8535	Note 1
Western	1	8	7780	Note 1
Western	1	16	1005	Note 1
Western	1	16	1009	Note 1
Western	1	16	9032	Note 2
Western	1	49	1008	Note 1
Western	1	53	1007	Note 1
Western	1	56	7775	Note 1
Western	2	4	1065	Note 1
Western	2	6	2002	Note 1
Western	2	6	2040	Note 1
Western	2	6	2053	Note 1
Western	2	6	2647	Note 1
Western	2	6	7452	Note 1
Western	2	6	8149	Note 1

REGION	GPS EXPERIMENT	STATE	SECTION ID	COMMENT
Western	2	6	8151	Note 1
Western	2	6	8202	Note 2
Western	2	8	2008	Note 1
Western	2	32	2027	Note 1
Western	2	56	2015	Note 2
Western	3	6	3013	Note 1
Western	3	6	3017	Note 2
Western	3	6	3019	Note 1
Western	3	6	3024	Note 1
Western	3	6	3042	Note 1
Western	3	6	7456	Note 2
Western	3	32	3010	Note 1
Western	3	49	3011	Note 1
Western	3	49	7082	Note 1
Western	3	53	3013	Note 1
Western	3	53	3014	Note 1
Western	3	53	3019	Note 1
Western	3	53	7409	Note 2
Western	5	6	7455	Note 1
Western	6A	6	6044	Note 1
Western	6A	8	6002	Note 2
Western	6A	16	6027	Note 1
Western	6A	30	6004	Note 1
Western	6A	41	6012	Note 2
Western	6A	53	6048	Note 1
Western	6A	56	6029	Note 1
Western	7A	8	7035	Note 2
Western	7A	8	7036	Note 1
Western	7A	41	7018	Note 1
Western	7A	41	7019	Note 1
Western	7A	41	7025	Note 1
Western	9	6	9048	Note 2
Western	9	6	9049	Note 1

Note 1: The time-sequence data for both-wheel-path IRI show inconsistencies.

Note 2: The time-sequence data for both-wheel-path IRI do not show a clear inconsistency, but the IRI of a wheel path shows inconsistencies.

APPENDIX B
OUTPUT FROM LINEAR REGRESSION ANALYSIS

State	GPS ID	GPS Expt	Number Profile Runs	Both-Wheel-Path IRI (in/mi) Profile Sequence							COV of IRI (%)	Linear Regression Results			Linear Relationship Significant?	COV > 6% ?	Slope > 3
				1st	2nd	3rd	4th	5th	6th	7th		Intercept	Slope	R2			
1	1001	1	6	54	62	59	58	57	40		14.1	96.0	-3.46	0.26		Yes	
1	1019	1	4	87	90	89	96				4.1	79.8	1.93	0.89	Positive		
1	4125	1	4	60	61	59	70				7.9	22.6	2.01	0.60		Yes	
1	4126	1	3	52	53	53					1.6	50.7	0.47	0.83			
1	4129	1	3	64	64	68					3.4	61.4	1.28	0.85			
1	4155	1	4	60	60	61	68				6.4	32.9	1.87	0.79		Yes	
4	1001	1	4	68	68	68	70				1.5	61.3	0.52	0.46			
4	1002	1	3	99	191	201					34.1	-283.4	37.99	0.95		Yes	Yes
4	1006	1	3	49	59	68					16.8	-29.5	6.70	0.99	Positive	Yes	Yes
4	1007	1	3	85	116	115					16.5	-37.5	10.83	0.84		Yes	Yes
4	1015	1	3	71	62	69					7.1	79.5	-0.96	0.09		Yes	
4	1016	1	3	51	56	60					7.7	20.5	2.93	1.00	Positive	Yes	
4	1018	1	3	62	65	68					4.6	35.2	1.96	0.99	Positive		
4	1021	1	3	80	72	80					5.7	83.6	-0.50	0.03			
4	1022	1	3	42	42	47					6.8	23.6	1.63	0.66		Yes	
4	1024	1	3	64	59	75					11.9	33.2	2.65	0.24		Yes	
4	1025	1	3	70	54	71					14.4	77.1	-0.92	0.02		Yes	
4	1034	1	5	73	67	69	83	76			8.6	35.6	2.29	0.31		Yes	
4	1036	1	4	45	49	109	122				49.0	-108.2	24.14	0.97	Positive	Yes	Yes
4	1037	1	3	112	126	143					12.1	61.8	10.22	0.95		Yes	Yes
6	1253	1	7	110	110	109	111	112	113	117	2.2	82.5	1.36	0.75	Positive		
6	7454	1	5	110	109	106	117	123			5.8	54.5	2.96	0.61			
6	8153	1	4	86	79	96	98				10.0	16.1	5.23	0.61		Yes	Yes
6	8156	1	4	109	98	108	112				5.8	77.0	1.74	0.15			
8	1029	1	4	144	146	151	155				3.5	81.9	3.39	0.94	Positive		Yes
8	1047	1	4	104	115	76	86				18.3	157.4	-7.36	0.42		Yes	
8	1053	1	7	76	74	77	78	77	78	79	2.2	70.6	0.76	0.51	Positive		
8	1057	1	4	70	71	73	77				4.1	62.5	1.77	0.82	Positive		
8	7780	1	3	104	86	79					14.6	267.8	-9.90	0.99	Negative	Yes	
9	1803	1	6	95	104	101	96	98	99		3.3	98.7	-0.01	0.00			

1 in/mile = 0.0158 m/km

State	GPS ID	GPS Expt	Number Profile Runs	Both-Wheel-Path IRI (in/mi) Profile Sequence							COV of IRI (%)	Linear Regression Results			Linear Relationship Significant?	COV > 6% ?	Slope > 3
				1st	2nd	3rd	4th	5th	6th	7th		Intercept	Slope	R2			
12	1030	1	3	70	74	69					3.6	77.1	-0.29	0.05			
12	1060	1	3	41	42	40					3.4	46.6	-0.43	0.36			
12	1370	1	3	85	87	78					5.9	119.9	-1.92	0.58			
12	3995	1	3	64	64	61					2.9	77.4	-0.88	0.89			
12	3996	1	3	68	71	68					2.3	67.5	0.09	0.01			
12	3997	1	4	70	72	70	80				6.6	27.5	2.56	0.74		Yes	
12	4103	1	3	41	41	39					2.7	45.8	-0.51	0.83			
12	4106	1	3	38	39	39					1.8	37.3	0.34	0.90			
12	4107	1	3	73	76	73					2.5	73.8	0.04	0.00			
12	4153	1	3	138	153	159					7.3	124.5	4.97	0.92		Yes	Yes
12	4154	1	4	101	118	127	120				9.6	28.1	4.02	0.43		Yes	Yes
12	9054	1	4	61	63	62	66				3.6	42.1	1.19	0.89	Positive		
13	1001	1	3	51	52	54					2.7	47.9	0.73	0.99	Positive		
13	1005	1	6	60	62	63	62	66	64		3.0	56.3	1.04	0.47			
13	1031	1	6	49	55	55	53	56	63		8.0	16.2	3.48	0.88	Positive	Yes	Yes
16	1001	1	5	59	59	60	62	60			1.9	49.0	0.61	0.56			
16	1005	1	7	93	85	81	112	114	126	111	16.4	-18.0	7.30	0.48	Positive	Yes	Yes
16	1007	1	7	73	69	73	78	80	84	83	7.4	21.7	2.75	0.87	Positive	Yes	
16	1010	1	7	83	85	89	96	94	93	95	5.8	28.1	2.76	0.87	Positive		
16	1020	1	6	44	44	45	46	44	44		2.1	44.6	0.01	0.00			
16	1021	1	5	81	78	80	81	79			1.6	80.6	-0.14	0.03			
16	9032	1	6	112	99	108	115	116	120		6.6	99.1	2.84	0.45		Yes	
16	9034	1	6	99	97	100	105	106	106		4.1	95.1	2.11	0.79	Positive		
17	1002	1	5	78	73	77	74	86			6.5	65.6	2.28	0.45		Yes	
17	1003	1	6	60	63	59	60	62	59		3.0	62.0	-0.35	0.08			
18	1028	1	5	71	85	83	78	87			8.0	39.2	2.51	0.40		Yes	
18	1037	1	4	119	126	127	131				4.0	101.2	2.74	0.93	Positive		
19	1044	1	5	106	125	110	117	118			6.5	84.9	1.47	0.11		Yes	
20	1005	1	4	180	189	181	184				2.2	180.0	0.19	0.00			
20	1009	1	5	120	124	127	124	125			1.9	117.2	0.94	0.40			
20	1010	1	4	83	88	84	85				2.7	87.9	-0.28	0.03			
21	1010	1	6	78	69	69	71	72	74		4.9	70.9	0.21	0.01			
21	1014	1	5	91	100	103	103	128			13.0	57.6	7.19	0.80	Positive	Yes	Yes

1 in/mile = 0.0158 m/km

State	GPS ID	GPS Expt	Number Profile Runs	Both-Wheel-Path IRI (in/mi) Profile Sequence							COV of IRI (%)	Linear Regression Results			Linear Relationship Significant?	COV > 6% ?	Slope > 3
				1st	2nd	3rd	4th	5th	6th	7th		Intercept	Slope	R2			
21	1034	1	5	69	72	65	69	71			3.9	66.1	0.17	0.01			
23	1001	1	6	118	139	116	110	153	125		12.7	85.3	2.14	0.06		Yes	
23	1009	1	7	61	67	61	62	60	49	51	11.4	121.8	-2.90	0.57	Negative	Yes	
23	1012	1	6	46	56	48	45	52	51		8.4	47.5	0.36	0.03		Yes	
23	1026	1	6	90	95	86	86	92	88		4.1	100.0	-0.57	0.08			
23	1028	1	7	103	108	98	95	98	95	85	7.3	159.2	-3.14	0.67	Negative	Yes	
25	1002	1	6	74	76	75	72	76	80		3.8	67.3	0.85	0.29			
25	1004	1	6	68	71	66	69	64	69		3.5	74.9	-0.40	0.10			
26	1001	1	4	48	48	47	47				1.6	57.5	-0.49	0.91	Negative		
26	1004	1	5	86	93	90	87	82			4.8	95.8	-1.37	0.22			
26	1010	1	5	75	76	86	81	91			8.6	23.3	3.61	0.72	Positive	Yes	Yes
26	1012	1	5	60	66	69	72	92			16.7	-13.9	7.52	1.00	Positive	Yes	Yes
26	1013	1	6	77	80	75	95	87	103		12.9	23.0	5.92	0.69	Positive	Yes	Yes
27	1016	1	5	126	121	115	140	140			8.6	77.5	3.14	0.36		Yes	Yes
27	1018	1	3	159	172	180					6.2	96.6	5.67	0.86		Yes	Yes
27	1019	1	3	100	96	94					2.9	114.0	-1.44	0.82			
27	1023	1	6	101	112	112	122	126	142		12.0	47.4	7.05	0.88	Positive	Yes	Yes
27	1028	1	5	144	129	143	146	142			4.7	111.3	1.51	0.15			
27	1029	1	4	107	112	118	122				5.8	13.4	4.58	0.99	Positive		Yes
27	1085	1	4	175	183	181	196				4.9	138.7	5.53	0.78			Yes
27	1087	1	4	88	101	102	116				11.2	1.3	7.63	0.94	Positive	Yes	Yes
27	6251	1	5	77	91	105	108	120			16.4	-1.5	9.57	0.97	Positive	Yes	Yes
29	1002	1	5	79	85	76	82	87			5.6	72.2	1.99	0.31			
29	1005	1	4	50	50	51	46				4.1	59.9	-0.58	0.24			
29	1008	1	5	101	102	104	101	103			1.3	99.9	0.34	0.17			
29	1010	1	5	78	81	89	97	111			14.5	0.7	7.85	0.96	Positive	Yes	Yes
30	1001	1	5	65	65	65	68	68			2.7	57.8	0.93	0.69	Positive		
30	7066	1	3	48	49	61					13.7	-14.3	7.90	0.89		Yes	Yes
30	7088	1	3	56	65	69					10.7	-6.5	7.68	0.93		Yes	Yes
30	8129	1	7	53	47	55	64	66	62	65	12.2	44.8	3.53	0.71	Positive	Yes	Yes
31	1030	1	6	69	71	68	87	101	107		20.7	-23.8	11.69	0.85	Positive	Yes	Yes
32	1020	1	5	44	46	59	60	69			18.7	15.0	5.24	0.96	Positive	Yes	Yes
32	1021	1	5	97	99	99	100	126			11.7	34.0	7.53	0.60		Yes	Yes

1 in/mile = 0.0158 m/km

State	GPS ID	GPS Expt	Number Profile Runs	Both-Wheel-Path IRI (in/mi) Profile Sequence							COV of IRI (%)	Linear Regression Results			Linear Relationship Significant?	COV > 6% ?	Slope > 3
				1st	2nd	3rd	4th	5th	6th	7th		Intercept	Slope	R2			
33	1001	1	6	37	47	39	39	41	46		10.2	31.7	0.93	0.16		Yes	
34	1003	1	5	127	117	103	96	104			11.3	238.5	-7.50	0.72	Negative	Yes	
34	1011	1	6	102	103	109	103	109	116		5.1	53.2	2.66	0.69	Positive		
34	1030	1	6	225	253	302	285	304	364		16.5	-301.2	27.14	0.88	Positive	Yes	Yes
34	1031	1	6	111	115	122	115	127	155		13.1	-16.8	7.68	0.67	Positive	Yes	Yes
35	1003	1	3	56	62	66					8.6	33.4	3.12	0.87		Yes	Yes
35	1005	1	3	34	39	42					11.4	17.8	2.65	0.92		Yes	
35	1022	1	3	43	47	48					5.8	38.0	1.51	0.84			
35	1112	1	7	49	48	50	52	54	54	53	5.3	39.3	1.35	0.90	Positive		
36	1011	1	7	83	69	74	71	73	69	75	6.7	88.0	-2.07	0.23		Yes	
37	1006	1	7	44	49	49	47	46	47	66	14.9	27.0	2.28	0.34		Yes	
37	1024	1	7	61	78	75	65	85	88	88	13.9	15.7	5.30	0.64	Positive	Yes	Yes
37	1028	1	7	61	53	54	56	59	58	58	5.4	53.1	0.41	0.06			
37	1030	1	7	66	69	71	70	63	67	70	3.9	67.8	0.04	0.00			
37	1040	1	6	76	80	79	79	83	83		3.3	61.8	1.32	0.80	Positive		
37	1352	1	7	75	74	73	72	70	71	71	2.4	81.7	-0.81	0.59	Negative		
37	1801	1	6	66	66	68	61	69	63		4.5	71.3	-0.31	0.04			
37	1802	1	7	52	55	57	55	67	72	89	20.7	17.5	6.93	0.83	Positive	Yes	Yes
37	1814	1	6	54	48	49	51	57	56		6.9	27.0	1.17	0.33		Yes	
37	1817	1	7	65	74	57	56	57	62	64	10.3	68.5	-0.79	0.03		Yes	
37	1992	1	5	72	73	71	77	82			5.9	69.5	2.20	0.67	Positive		
42	1597	1	7	108	126	110	114	125	129	146	11.0	52.2	6.23	0.67	Positive	Yes	Yes
42	1599	1	6	87	89	89	92	94	103		6.2	79.5	2.73	0.84	Positive	Yes	
42	1605	1	7	123	122	119	121	123	123	134	3.9	85.8	1.87	0.47	Positive		
45	1011	1	3	86	98	96					7.2	74.4	2.72	0.55		Yes	
45	1024	1	6	88	96	90	88	87	90		3.4	87.7	0.31	0.01			
47	3075	1	4	117	118	113	130				6.0	59.4	2.89	0.47		Yes	
47	3104	1	3	133	153	156					8.4	111.8	6.03	0.90		Yes	Yes
48	1	1	3	43	45	46					3.5	42.0	0.90	0.97			
48	1039	1	3	66	86	145					41.6	-139.4	25.44	0.92		Yes	Yes
48	1047	1	3	132	133	137					2.1	90.7	2.11	0.93			
48	1050	1	4	77	86	88	110				15.7	44.0	6.81	0.93	Positive	Yes	Yes
48	1056	1	3	82	89	131					26.4	-314.9	19.48	1.00	Positive	Yes	Yes

1 in/mile = 0.0158 m/km

State	GPS ID	GPS Expt	Number Profile Runs	Both-Wheel-Path IRI (in/mi) Profile Sequence							COV of IRI (%)	Linear Regression Results			Linear Relationship Significant?	COV > 6% ?	Slope > 3
				1st	2nd	3rd	4th	5th	6th	7th		Intercept	Slope	R2			
48	1060	1	7	88	80	84	86	87	86	89	3.3	81.5	0.57	0.13			
48	1065	1	4	132	135	154	168				11.6	-48.0	8.79	1.00	Positive	Yes	Yes
48	1068	1	7	70	72	77	78	89	77	76	8.1	62.4	2.46	0.43		Yes	
48	1076	1	4	117	117	121	105				5.9	148.0	-2.24	0.41			
48	1077	1	7	76	79	79	68	76	80	84	6.2	71.2	0.55	0.03		Yes	
48	1094	1	4	55	58	56	61				4.4	42.1	0.98	0.56			
48	1096	1	4	135	146	146	147				4.0	114.4	2.61	0.72			
48	1111	1	4	98	102	107	132				14.0	-37.9	7.41	0.84	Positive	Yes	Yes
48	1122	1	7	69	67	64	70	64	70	72	4.4	61.1	0.37	0.04			
48	1123	1	4	48	51	58	50				8.6	36.2	0.99	0.10		Yes	
48	1168	1	3	65	71	75					7.2	52.3	3.03	0.89		Yes	Yes
48	1169	1	4	84	85	89	111				14.0	-20.4	5.67	0.80		Yes	Yes
48	1174	1	4	75	75	84	90				9.1	1.7	4.80	0.87	Positive	Yes	Yes
48	1178	1	3	112	156	198					27.9	84.7	27.48	0.99	Positive	Yes	Yes
48	1181	1	5	107	105	126	120	148			14.6	18.1	8.51	0.79	Positive	Yes	Yes
48	1183	1	4	145	153	152	205				17.1	-85.9	14.54	0.73		Yes	Yes
48	3579	1	4	83	87	89	87				3.1	83.0	0.82	0.34			
48	3729	1	4	97	98	103	106				4.1	77.8	2.76	0.93	Positive		
48	3739	1	7	127	138	141	161	160	163	149	9.2	69.2	7.51	0.82	Positive	Yes	Yes
48	3739	1	4	154	173	161	160				4.9	155.3	0.52	0.00			
48	3749	1	5	79	78	83	102	117			18.7	-7.5	8.79	0.91	Positive	Yes	Yes
48	3769	1	4	91	101	109	128				14.7	-24.1	8.22	0.96	Positive	Yes	Yes
48	3835	1	3	95	110	116					10.0	91.9	9.12	0.95		Yes	Yes
48	3855	1	3	83	81	86					3.0	75.4	0.68	0.19			
48	3865	1	3	75	79	88					8.0	-22.6	4.65	0.99	Positive	Yes	Yes
48	9005	1	4	76	90	94	114				16.8	50.0	7.69	0.94	Positive	Yes	Yes
49	1001	1	7	63	59	66	68	69	70	71	6.2	42.9	2.05	0.88	Positive	Yes	
49	1008	1	5	98	82	90	96	96			7.2	77.3	0.99	0.07		Yes	
49	1017	1	5	87	85	87	96	94			5.3	30.5	2.36	0.71	Positive		
50	1002	1	6	78	77	68	71	83	83		8.1	66.1	1.42	0.18		Yes	
50	1004	1	6	105	107	93	104	131	132		14.3	62.9	6.65	0.59	Positive	Yes	Yes
51	1002	1	6	176	160	149	146	152	154		6.9	199.1	-3.42	0.33		Yes	
51	1023	1	7	96	97	98	107	100	113	113	7.2	57.5	4.13	0.73	Positive	Yes	Yes

1 in/mile = 0.0158 m/km

State	GPS ID	GPS Expt	Number Profile Runs	Both-Wheel-Path IRI (in/mi) Profile Sequence							COV of IRI (%)	Linear Regression Results			Linear Relationship Significant?	COV > 6% ?	Slope > 3
				1st	2nd	3rd	4th	5th	6th	7th		Intercept	Slope	R2			
51	1464	1	7	75	78	74	80	77	75	74	3.2	82.5	-0.51	0.15			
53	1002	1	5	103	97	104	105	105			3.3	93.2	1.31	0.29			
53	1006	1	7	54	53	55	56	58	63	64	7.7	35.6	2.62	0.87	Positive	Yes	
53	1007	1	6	69	63	107	99	97	97		20.1	31.9	6.74	0.44		Yes	Yes
53	1008	1	5	65	72	83	87	99			16.2	-41.1	9.58	0.97	Positive	Yes	Yes
53	1501	1	5	56	63	68	73	80			13.3	8.2	6.57	1.00	Positive	Yes	Yes
53	1801	1	4	59	59	62	71				9.0	3.8	3.30	0.75		Yes	Yes
56	1007	1	7	56	54	54	57	58	58	59	3.2	47.4	0.77	0.56	Positive		
56	7775	1	6	64	42	52	63	63	80		20.8	43.2	3.80	0.33		Yes	Yes
81	1803	1	5	79	79	82	81	80			1.8	75.6	0.56	0.44			
81	1804	1	4	157	183	207	214				13.7	-33.2	24.62	1.00	Positive	Yes	Yes
81	1805	1	5	149	158	177	179	176			8.1	81.2	7.14	0.83	Positive	Yes	Yes
82	1005	1	4	41	42	45	47				6.4	32.4	2.09	0.94	Positive	Yes	
83	1801	1	5	89	90	92	90	96			2.9	81.3	1.29	0.68	Positive		
84	1684	1	6	92	91	89	98	95	93		3.3	80.7	0.90	0.29			
85	1801	1	6	112	128	136	136	156	160		13.0	68.4	9.28	0.93	Positive	Yes	Yes
85	1803	1	6	77	78	79	78	80	85		3.5	65.5	1.21	0.65	Positive		
85	1808	1	6	54	61	60	57	55	57		4.5	58.9	-0.20	0.02			
87	1620	1	5	98	110	107	108	106			4.4	82.5	2.44	0.25			
87	1622	1	7	88	91	94	97	96	102	104	6.0	48.3	3.09	0.91	Positive		Yes
87	1806	1	6	56	55	53	57	61	60		5.3	48.8	1.26	0.59	Positive		
88	1645	1	6	55	58	61	62	63	60		4.5	54.8	1.07	0.54	Positive		
89	1021	1	7	90	91	94	125	99	111	116	13.2	47.0	7.06	0.46		Yes	Yes
89	1125	1	6	129	137	162	180	213	218		21.7	-95.7	20.12	0.98	Positive	Yes	Yes
89	1127	1	7	163	168	168	177	178	188	237	13.9	24.2	12.19	0.71	Positive	Yes	Yes
90	6405	1	6	72	86	72	92	104	89		14.5	-5.7	4.03	0.38		Yes	Yes
1	1011	2	3	57	53	50					6.2	67.8	-2.04	0.97		Yes	
1	1021	2	3	61	60	63					2.1	58.1	0.46	0.44			
1	4073	2	3	56	56	56					0.6	55.8	0.09	0.27			
4	1065	2	3	74	68	59					10.8	125.9	-4.74	0.92		Yes	
5	2042	2	3	182	189	222					10.8	-86.6	14.74	0.96		Yes	Yes
5	3048	2	4	104	105	107	106				1.2	99.9	0.62	0.68			
5	3058	2	4	50	53	53	57				5.5	50.0	1.41	0.72			

1 in/mile = 0.0158 m/km

State	GPS ID	GPS Expt	Number Profile Runs	Both-Wheel-Path IRI (in/mi) Profile Sequence							COV of IRI (%)	Linear Regression Results			Linear Relationship Significant?	COV > 6% ?	Slope > 3
				1st	2nd	3rd	4th	5th	6th	7th		Intercept	Slope	R2			
5	3071	2	4	38	38	41	45				8.4	32.7	1.74	0.98	Positive	Yes	
6	2002	2	5	96	84	88	89	92			4.9	94.4	-0.42	0.03			
6	2004	2	4	93	105	116	134				15.4	-74.8	12.56	0.99	Positive	Yes	Yes
6	2038	2	5	72	67	73	72	74			3.5	59.5	0.62	0.18			
6	2040	2	5	66	68	75	91	82			13.7	14.3	4.98	0.70	Positive	Yes	Yes
6	2041	2	5	81	82	89	91	107			11.8	-28.3	5.72	0.87	Positive	Yes	Yes
6	2051	2	5	58	65	63	66	65			4.9	48.1	1.37	0.55			
6	2053	2	5	84	88	64	98	89			15.0	46.2	2.04	0.07		Yes	
6	2647	2	5	57	60	92	60	57			23.3	68.1	-0.18	0.00		Yes	
6	7452	2	5	87	89	73	93	93			9.5	59.3	1.41	0.09		Yes	
6	7491	2	4	100	113	126	145				15.6	-227.3	14.48	0.98	Positive	Yes	Yes
6	8149	2	4	55	58	69	46				16.6	79.5	-1.12	0.02		Yes	
6	8150	2	4	43	39	42	47				8.1	32.8	1.41	0.31		Yes	
6	8201	2	4	84	83	88	90				3.8	43.7	2.11	0.76			
6	8202	2	4	126	118	130	132				5.0	63.8	2.97	0.40			
8	2008	2	4	131	147	164	159				9.9	-27.6	9.14	0.84	Positive	Yes	Yes
10	1450	2	6	71	76	78	73	78	81		4.7	48.7	1.75	0.61	Positive		
12	4096	2	3	38	39	38					1.8	37.6	0.04	0.02			
12	4097	2	3	44	45	55					12.1	31.2	2.56	0.84		Yes	
12	4100	2	3	44	43	53					11.7	10.7	2.25	0.76		Yes	
12	4108	2	3	45	47	52					7.8	37.7	1.71	0.91		Yes	
13	4092	2	3	44	44	44					0.6						
13	4093	2	3	44	47	47					3.2	42.4	0.58	0.62			
13	4096	2	3	58	57	57					1.2	60.0	-0.34	0.90			
13	4112	2	3	80	92	89					7.7	52.2	2.31	0.46		Yes	
13	4113	2	3	54	57	65					10.1	13.9	2.99	0.96		Yes	
13	4119	2	3	62	62	60					1.9	68.7	-0.53	0.75			
18	2008	2	5	115	143	168	174	177			16.9	-18.9	14.65	0.82	Positive	Yes	Yes
18	2009	2	4	97	108	110	122				9.6	54.7	4.87	0.97	Positive	Yes	Yes
19	6150	2	4	80	77	86	83				4.6	40.6	1.57	0.35			
22	3056	2	3	47	54	52					7.1	45.1	1.31	0.44		Yes	
24	1632	2	6	66	49	55	55	54	57		10.1	59.5	-0.73	0.04		Yes	
24	1634	2	7	60	63	65	65	65	59	60	4.3	70.4	-0.51	0.08			

1 in/mile = 0.0158 m/km

State	GPS ID	GPS Expt	Number Profile Runs	Both-Wheel-Path IRI (in/mi) Profile Sequence							COV of IRI (%)	Linear Regression Results			Linear Relationship Significant?	COV > 6% ?	Slope > 3
				1st	2nd	3rd	4th	5th	6th	7th		Intercept	Slope	R2			
24	2401	2	6	53	55	55	55	57	61		5.3	49.3	1.56	0.78	Positive		
24	2805	2	4	80	83	93	100				10.1	48.2	9.35	0.93	Positive	Yes	Yes
28	1001	2	3	50	55	59					8.4	39.8	2.81	0.97		Yes	
28	1016	2	7	66	69	68	68	67	67	68	1.5	65.6	0.35	0.11			
28	1802	2	6	57	64	72	74	75	79		11.8	-15.9	8.88	0.98	Positive	Yes	Yes
28	2807	2	4	93	98	98	98				2.3	84.4	1.25	0.65			
28	3081	2	3	48	49	55					7.6	33.7	2.29	0.91		Yes	
28	3082	2	3	67	70	73					4.6	64.7	1.96	0.97			
28	3083	2	3	93	93	88					2.8	110.7	-1.44	0.86			
28	3085	2	3	94	111	109					8.5	51.6	3.91	0.50		Yes	Yes
28	3087	2	3	64	80	85					14.6	13.5	6.49	0.83		Yes	Yes
28	3089	2	3	69	74	80					7.8	40.2	3.57	0.99	Positive	Yes	Yes
28	3090	2	3	77	79	74					2.8	92.7	-0.86	0.38			
28	3091	2	3	83	95	111					14.7	-6.8	7.64	1.00	Positive	Yes	Yes
28	3094	2	3	53	57	55					3.8	47.8	0.66	0.32			
30	7076	2	4	45	47	50	63				15.7	13.3	7.11	0.70		Yes	Yes
32	1030	2	3	59	56	59					3.1	52.6	0.34	0.06			
32	7000	2	5	75	70	74	65	71			5.3	86.5	-1.13	0.25			
34	1033	2	6	202	174	177	185	182	184		5.3	216.8	-1.89	0.10			
34	1034	2	7	85	86	85	88	88	89	92	2.6	79.1	1.37	0.91	Positive		
34	1638	2	6	57	60	63	58	58	61		4.0	57.3	0.35	0.06			
35	2006	2	3	89	91	81					6.4	124.3	-2.97	0.74		Yes	
35	2118	2	3	72	74	79					5.0	40.6	2.36	1.00	Positive		
36	1643	2	7	84	93	82	96	114	134	165	27.9	-102.3	16.61	0.91	Positive	Yes	Yes
36	1644	2	7	60	61	60	77	63	67	68	9.5	49.2	1.42	0.16		Yes	
37	1645	2	6	50	49	51	52	59	56		7.3	43.1	1.79	0.67	Positive	Yes	
37	2819	2	6	60	62	69	74	51	52		14.8	89.3	-2.66	0.27		Yes	
37	2824	2	7	49	45	49	51	67	60	62	14.9	11.0	5.54	0.60	Positive	Yes	Yes
37	2825	2	7	103	102	105	102	101	106	107	2.2	100.0	0.69	0.28			
38	2001	2	4	126	126	136	131				3.6	95.0	3.00	0.54			
40	1015	2	3	96	100	101					2.7	82.1	1.26	0.44			
40	1017	2	3	86	95	100					7.2	49.7	4.22	0.78		Yes	Yes
40	4087	2	4	67	71	70	71				2.7	67.1	0.46	0.24			

1 in/mile = 0.0158 m/km

State	GPS ID	GPS Expt	Number Profile Runs	Both-Wheel-Path IRI (in/mi) Profile Sequence							COV of IRI (%)	Linear Regression Results			Linear Relationship Significant?	COV > 6% ?	Slope > 3
				1st	2nd	3rd	4th	5th	6th	7th		Intercept	Slope	R2			
40	4088	2	3	189	169	214					11.6	-27.6	13.43	0.67		Yes	Yes
40	4154	2	3	78	81	81					2.3	76.9	0.93	0.55			
40	4163	2	3	48	51	65					16.4	23.7	6.28	1.00	Positive	Yes	Yes
40	4164	2	3	60	80	84					17.3	-22.9	7.12	0.72		Yes	Yes
40	4165	2	7	128	132	127	130	129	126	124	2.0	134.2	-0.68	0.20			
41	2002	2	4	82	84	86	96				7.1	10.2	3.79	0.78		Yes	Yes
47	1023	2	4	50	53	49	50				3.6	55.7	-0.26	0.06			
47	1028	2	3	77	89	86					7.6	61.2	2.63	0.62		Yes	
47	1029	2	3	45	55	48					10.4	42.0	0.74	0.08		Yes	
47	2001	2	3	52	38	44					15.7	71.1	-2.07	0.32		Yes	
47	2008	2	3	75	77	72					3.7	90.9	-0.86	0.34			
47	3101	2	4	67	73	69	93				15.7	3.0	5.92	0.73		Yes	Yes
47	3108	2	4	34	36	36	37				3.8	23.3	0.63	0.66			
47	3109	2	3	73	74	74					0.5	72.6	0.09	0.20			
47	3110	2	3	41	45	45					5.4	32.3	1.07	0.79			
47	9024	2	3	92	91	84					4.8	120.5	-2.13	0.84			
47	9025	2	3	95	100	117					10.8	34.9	5.63	0.90		Yes	Yes
48	1048	2	4	104	115	113	127				8.1	27.8	4.84	0.85	Positive	Yes	Yes
48	1049	2	3	70	80	86					9.9	41.4	4.99	0.99	Positive	Yes	Yes
48	1069	2	4	84	95	91	94				5.3	68.1	1.55	0.38			
48	1070	2	4	64	68	73	66				5.3	59.7	0.55	0.08			
48	1109	2	3	88	101	107					9.6	55.2	5.86	0.98	Positive	Yes	Yes
48	2108	2	3	94	97	98					2.6	88.5	1.29	0.73			
48	2133	2	3	52	54	53					2.3	49.3	0.58	0.52			
48	2172	2	4	46	48	47	64				16.9	11.5	4.07	0.79		Yes	Yes
48	2176	2	4	80	78	84	85				3.9	47.0	1.58	0.90	Positive		
48	3559	2	4	56	55	54	72				14.7	-15.9	3.43	0.63		Yes	Yes
48	3669	2	3	77	84	91					8.5	44.2	4.62	1.00	Positive	Yes	Yes
48	3679	2	3	114	148	173					20.4	79.2	18.99	0.99	Positive	Yes	Yes
48	3689	2	3	89	107	120					14.6	60.9	9.58	0.99	Positive	Yes	Yes
50	1681	2	7	76	76	84	68	54	51	66	18.1	232.3	-6.12	0.42		Yes	
50	1683	2	4	134	140	146	141				3.4	0.0	5.21	0.47			Yes
51	2004	2	6	83	85	89	94	100	102		8.6	46.8	4.34	0.99	Positive	Yes	Yes

1 in/mile = 0.0158 m/km

State	GPS ID	GPS Expt	Number Profile Runs	Both-Wheel-Path IRI (in/mi) Profile Sequence							COV of IRI (%)	Linear Regression Results			Linear Relationship Significant?	COV > 6% ?	Slope > 3
				1st	2nd	3rd	4th	5th	6th	7th		Intercept	Slope	R2			
51	2021	2	6	93	94	96	93	102	112		7.6	74.0	3.44	0.69	Positive	Yes	Yes
56	2015	2	7	108	104	110	116	121	117	121	5.7	74.1	2.88	0.84	Positive		
56	2017	2	7	77	76	80	79	90	91	92	8.4	53.1	3.25	0.87	Positive	Yes	Yes
56	2018	2	5	59	57	64	67	67			6.6	44.1	2.31	0.78	Positive	Yes	
56	2019	2	6	84	89	95	98	103	106		8.5	67.4	4.18	0.98	Positive	Yes	Yes
56	2020	2	7	61	70	73	84	105	115	130	28.4	-3.8	14.57	0.98	Positive	Yes	Yes
56	2037	2	6	86	87	85	87	84	83		1.9	88.7	-0.49	0.35			
56	7772	2	6	111	105	105	109	109	112		2.7	105.1	0.59	0.14			
56	7773	2	6	70	71	73	73	73	74		2.1	68.6	0.73	0.86	Positive		
81	2812	2	5	82	86	87	94	93			5.8	68.6	2.75	0.87	Positive		
81	8529	2	5	49	51	50	49	52			2.3	45.1	0.24	0.12			
82	9017	2	3	67	68	69					1.4	65.5	0.73	0.91			
84	1802	2	6	95	99	94	86	91	101		5.8	95.5	-0.10	0.00			
87	1680	2	6	82	80	83	79	81	81		1.7	82.3	-0.20	0.07			
87	2811	2	6	71	74	76	75	80	75		4.2	57.8	1.18	0.49			
87	2812	2	6	58	66	65	72	82	101		21.0	-7.6	7.67	0.86	Positive	Yes	Yes
88	1647	2	6	79	89	95	98	100	98		8.5	72.9	3.76	0.78	Positive	Yes	Yes
89	2011	2	6	72	72	74	75	95	74		11.7	46.8	2.44	0.25		Yes	
1	3028	3	3	202	217	214					3.8	144.0	3.22	0.58			Yes
5	3011	3	4	72	70	74	77				4.5	57.4	1.68	0.83	Positive		
6	3005	3	5	149	164	177	196	210			13.6	-69.2	14.03	0.99	Positive	Yes	Yes
6	3010	3	4	86	78	81	80				4.5	100.5	-1.42	0.29			
6	3013	3	4	116	105	93	95				10.4	169.4	-7.34	0.86	Negative	Yes	
6	3017	3	4	95	91	98	95				3.0	85.5	0.69	0.11			
6	3019	3	4	93	91	60	94				19.7	116.6	-2.74	0.05		Yes	
6	3021	3	4	89	87	89	90				1.4	83.9	0.27	0.09			
6	3024	3	4	96	96	74	102				13.3	97.3	-0.47	0.00		Yes	
6	3030	3	5	81	81	81	82	83			1.0	74.7	0.36	0.55			
6	3042	3	5	62	60	109	61	59			31.1	79.7	-0.74	0.00		Yes	
6	7456	3	5	140	146	132	140	133			4.1	172.1	-1.67	0.25			
6	7493	3	4	89	91	87	88				1.9	95.5	-0.83	0.45			
8	3032	3	4	94	94	94	89				2.9	113.8	-1.44	0.64			
8	7776	3	4	88	95	97	93				4.1	87.4	1.62	0.42			

1 in/mile = 0.0158 m/km

State	GPS ID	GPS Expt	Number Profile Runs	Both-Wheel-Path IRI (in/mi) Profile Sequence							COV of IRI (%)	Linear Regression Results			Linear Relationship Significant?	COV > 6% ?	Slope > 3
				1st	2nd	3rd	4th	5th	6th	7th		Intercept	Slope	R2			
12	3804	3	3	97	112	125					13.0	64.2	6.88	0.99	Positive	Yes	Yes
12	3811	3	4	106	117	112	118				5.0	77.8	2.24	0.52			
12	4000	3	4	104	105	98	87				8.4	181.7	-4.78	0.93	Negative	Yes	
12	4057	3	3	48	48	53					5.7	43.5	1.10	0.67			
12	4059	3	3	63	65	63					2.5	63.8	-0.06	0.01			
12	4109	3	3	120	125	117					3.3	123.9	-0.98	0.22			
12	4138	3	3	169	175	182					3.7	116.8	3.31	1.00	Positive		Yes
13	3007	3	3	112	115	113					1.6	108.9	0.44	0.20			
13	3011	3	3	72	72	67					4.2	91.7	-1.31	0.76			
13	3015	3	3	77	80	78					2.1	73.0	0.37	0.18			
13	3016	3	3	88	83	84					2.9	100.1	-1.05	0.46			
13	3017	3	3	79	81	76					3.4	93.7	-0.82	0.34			
13	3018	3	3	62	63	64					1.8	52.2	0.58	0.93			
13	3019	3	6	92	97	93	95	100	92		3.5	92.3	0.26	0.01			
13	3020	3	3	87	83	88					3.3	83.8	0.34	0.05			
16	3017	3	6	100	94	101	102	100	106		3.6	94.3	1.16	0.37			
16	3023	3	7	96	98	98	96	103	94	94	3.0	99.8	-0.34	0.03			
18	3002	3	5	111	113	116	111	110			2.3	119.9	-0.50	0.11			
18	3003	3	4	107	107	105	113				3.4	75.4	2.02	0.50			
18	3030	3	6	98	95	94	97	97	109		5.6	72.4	2.38	0.59	Positive		
18	3031	3	5	98	99	96	98	96			1.5	106.1	-0.57	0.49			
19	3006	3	5	176	180	201	200	207			7.1	75.4	7.02	0.82	Positive	Yes	Yes
19	3009	3	4	144	147	143	145				1.3	146.9	-0.14	0.01			
19	3028	3	5	107	108	105	107	110			1.7	104.6	0.41	0.15			
19	3033	3	5	107	110	106	103	106			2.3	113.6	-0.85	0.35			
19	3055	3	4	108	112	117	114				3.1	61.7	2.29	0.62			
20	3013	3	5	101	96	100	101	96			3.0	103.1	-0.52	0.08			
20	3015	3	5	70	71	69	69	70			1.2	70.2	-0.05	0.01			
20	3060	3	5	70	76	79	83	84			7.0	54.3	3.26	0.91	Positive	Yes	Yes
21	3016	3	5	97	88	98	94	99			4.4	91.3	0.60	0.06			
23	3013	3	6	129	130	141	133	135	138		3.4	107.7	1.46	0.34			
23	3014	3	6	91	91	102	93	99	97		4.8	71.0	1.33	0.28			
26	3068	3	5	141	134	129	139	127			4.6	171.4	-2.17	0.26			

1 in/mile = 0.0158 m/km

State	GPS ID	GPS Expt	Number Profile Runs	Both-Wheel-Path IRI (in/mi) Profile Sequence							COV of IRI (%)	Linear Regression Results			Linear Relationship Significant?	COV > 6% ?	Slope > 3
				1st	2nd	3rd	4th	5th	6th	7th		Intercept	Slope	R2			
26	3069	3	6	86	84	86	82	83	83		2.2	97.4	-0.75	0.48			
27	3003	3	4	123	131	132	99				12.4	163.4	-6.58	0.42		Yes	
27	3013	3	4	81	82	78	84				3.2	78.1	0.54	0.09			
28	3018	3	3	107	113	108					3.0	108.8	0.06	0.00			
28	3019	3	3	100	110	107					4.9	92.9	1.72	0.29			
31	3018	3	4	82	98	94	104				9.7	58.0	5.49	0.82	Positive	Yes	Yes
31	3023	3	5	72	73	73	73	73			0.8	70.6	0.32	0.49			
31	3024	3	5	92	91	91	91	95			2.1	87.7	0.61	0.30			
31	3028	3	4	76	68	72	68				5.3	91.6	-1.89	0.57			
31	3033	3	5	53	60	56	71	63			11.4	43.7	2.83	0.60		Yes	
32	3010	3	5	141	144	150	165	151			6.0	115.1	3.76	0.48		Yes	Yes
32	3013	3	5	111	112	115	123	124			5.3	80.7	3.55	0.90	Positive		Yes
35	3010	3	3	88	90	81					5.3	116.9	-3.75	0.86			
37	3008	3	7	113	108	105	104	103	111	112	3.9	108.0	0.00	0.00			
37	3011	3	6	105	111	112	100	108	106		4.2	115.4	-0.59	0.06			
37	3044	3	6	117	121	126	122	125	128		3.0	83.3	1.56	0.59	Positive		
37	3807	3	7	115	124	114	113	113	114	113	3.5	128.8	-1.14	0.24			
37	3816	3	7	137	137	136	146	144	129	139	4.0	134.2	0.22	0.00			
38	3005	3	5	85	86	50	71	69			20.2	102.3	-4.83	0.23		Yes	
38	3006	3	5	62	83	64	59	60			15.0	80.4	-2.34	0.21		Yes	
39	3013	3	4	228	251	252	251				4.7	128.6	5.62	0.49			Yes
39	3801	3	5	120	141	124	122	139			7.7	119.0	1.29	0.06		Yes	
40	3018	3	3	122	131	133					4.4	80.0	3.14	0.73			Yes
40	4157	3	3	68	78	70					7.4	74.8	-0.43	0.01		Yes	
40	4160	3	3	111	107	111					2.2	101.6	0.62	0.09			
40	4162	3	3	106	113	108					3.5	109.9	-0.15	0.00			
42	1623	3	6	84	82	80	79	81	84		2.4	83.2	-0.19	0.03			
42	3044	3	6	151	146	144	144	142	147		2.0	151.0	-0.85	0.30			
45	3012	3	3	71	77	75					3.9	63.2	1.08	0.48			
46	3009	3	4	183	179	190	195				3.8	137.0	3.27	0.61			Yes
46	3010	3	4	131	117	138	144				8.8	98.6	4.12	0.34		Yes	Yes
46	3012	3	5	180	185	187	179	180			2.0	186.7	-0.56	0.05			
46	3013	3	5	107	109	92	93	105			8.2	134.3	-2.20	0.14		Yes	

1 in/mile = 0.0158 m/km

State	GPS ID	GPS Expt	Number Profile Runs	Both-Wheel-Path IRI (in/mi) Profile Sequence							COV of IRI (%)	Linear Regression Results			Linear Relationship Significant?	COV > 6% ?	Slope > 3
				1st	2nd	3rd	4th	5th	6th	7th		Intercept	Slope	R2			
46	3014	3	4	128	123	127	137				4.4	113.3	2.10	0.38			
46	3052	3	4	80	60	61	60				15.3	82.9	-5.11	0.72		Yes	
46	3053	3	5	73	76	71	71	79			4.7	69.0	0.84	0.11			
48	3003	3	4	133	135	128	139				3.5	122.2	0.72	0.09			
48	3010	3	3	138	146	139					3.1	141.7	-0.16	0.00			
48	3589	3	5	157	150	146	145	148			3.2	210.7	-1.99	0.48			
49	3010	3	5	88	94	114	110	108			11.1	32.3	5.40	0.63		Yes	Yes
49	3011	3	7	85	103	103	113	125	121	107	12.2	33.2	6.10	0.71	Positive	Yes	Yes
49	3015	3	6	125	125	125	128	125	130		1.6	121.2	0.77	0.55	Positive		
49	7082	3	4	58	69	64	58				8.9	62.7	-0.19	0.00		Yes	
49	7083	3	3	80	71	74					6.2	84.8	-2.89	0.42		Yes	
50	1682	3	4	146	158	158	154				3.7	16.7	5.10	0.30			Yes
53	3011	3	5	91	98	99	100	100			3.7	73.5	1.62	0.74	Positive		
53	3013	3	6	118	110	98	103	97	97		8.0	187.9	-4.00	0.72	Negative	Yes	
53	3014	3	6	62	72	57	66	58	63		9.0	66.9	-0.79	0.06		Yes	
53	3019	3	7	75	76	57	63	67	58	68	11.4	78.2	-2.10	0.20		Yes	
53	3812	3	6	75	78	77	77	79	82		3.0	47.1	1.14	0.69	Positive		
53	3813	3	4	114	110	116	125				5.4	37.4	3.15	0.55			Yes
53	7409	3	6	76	65	61	77	68	75		9.8	67.5	0.72	0.03		Yes	
55	3008	3	5	217	240	236	241	240			4.2	157.2	4.67	0.58			Yes
55	3009	3	5	159	207	223	220	259			17.0	53.1	20.62	0.86	Positive	Yes	Yes
55	3010	3	5	119	129	143	148	155			10.5	18.4	8.73	0.96	Positive	Yes	Yes
55	3012	3	4	107	104	102	110				3.1	97.9	0.55	0.07			
55	3014	3	4	206	221	238	208				6.9	175.1	2.84	0.06		Yes	
55	3015	3	5	124	135	128	134	144			5.6	104.3	3.71	0.65	Positive		Yes
55	3016	3	5	79	84	79	82	87			4.0	74.7	1.27	0.39			
55	3019	3	5	69	77	78	79	72			5.6	59.6	0.97	0.19			
55	6351	3	4	126	122	120	126				2.6	123.4	-0.01	0.00			
55	6352	3	4	78	78	79	79				0.9	77.5	0.25	0.28			
55	6353	3	4	95	91	92	103				5.7	85.5	2.38	0.46			
55	6354	3	4	78	79	78	77				1.1	79.9	-0.37	0.49			
55	6355	3	4	107	105	94	104				5.8	107.3	-1.19	0.09			
56	3027	3	6	143	164	163	191	197	192		12.2	59.2	10.74	0.90	Positive	Yes	Yes

1 in/mile = 0.0158 m/km

State	GPS ID	GPS Expt	Number Profile Runs	Both-Wheel-Path IRI (in/mi) Profile Sequence							COV of IRI (%)	Linear Regression Results			Linear Relationship Significant?	COV > 6% ?	Slope > 3
				1st	2nd	3rd	4th	5th	6th	7th		Intercept	Slope	R2			
83	3802	3	5	117	109	123	142	176			19.9	46.2	14.84	0.87	Positive	Yes	Yes
84	3803	3	6	152	151	177	179	180	191		9.5	74.9	8.24	0.87	Positive	Yes	Yes
89	3001	3	7	153	161	153	160	151	152	157	2.6	160.8	-0.42	0.03			
89	3002	3	6	221	226	243	233	242	241		3.9	184.3	3.95	0.63	Positive		Yes
89	3015	3	6	74	95	96	106	105	141		21.6	34.8	10.71	0.80	Positive	Yes	Yes
89	3016	3	7	191	184	187	187	182	187	183	1.7	193.2	-0.97	0.29			
1	4007	4	3	94	103	98					4.7	77.3	0.97	0.16			
1	4084	4	3	187	209	213					7.0	52.5	6.91	0.86		Yes	Yes
5	3059	4	4	105	104	110	115				4.9	72.2	2.72	0.97	Positive		
5	3073	4	4	120	129	127	124				3.0	114.8	0.37	0.03			
5	3074	4	4	120	134	146	156				11.1	-62.3	7.76	0.98	Positive	Yes	Yes
5	4019	4	4	108	111	103	106				3.2	129.6	-1.18	0.35			
5	4021	4	4	116	121	118	119				1.7	114.2	0.20	0.03			
5	4023	4	4	163	168	163	158				2.6	193.3	-1.76	0.56			
5	4046	4	4	101	108	109	105				3.8	95.5	0.78	0.12			
9	4008	4	6	99	94	92	84	87	96		6.0	100.1	-1.22	0.16		Yes	
10	1201	4	6	127	116	116	110	119	118		4.8	148.2	-1.18	0.11			
10	4002	4	6	135	130	131	119	120	136		5.6	164.2	-2.44	0.19			
17	4074	4	4	108	109	105	112				2.7	105.2	0.60	0.11			
17	4082	4	5	90	90	87	103	81			9.2	95.4	-0.97	0.03		Yes	
18	4021	4	5	140	135	156	127	138			7.9	166.0	-1.59	0.06		Yes	
18	4042	4	4	141	152	138	147				4.5	138.4	0.34	0.01			
18	5518	4	3	84	85	86					1.0	65.2	0.98	0.55			
20	4016	4	4	89	89	91	90				1.1	82.3	0.61	0.64			
20	4052	4	5	94	120	102	104	105			8.8	100.4	0.52	0.01		Yes	
20	4053	4	5	87	88	91	100	101			6.9	75.2	3.73	0.87	Positive	Yes	Yes
20	4054	4	4	100	112	106	114				5.7	88.6	3.31	0.48			Yes
20	4063	4	5	123	129	131	125	130			2.7	117.8	0.92	0.18			
21	4025	4	4	160	167	170	177				4.2	73.5	5.14	0.99	Positive		Yes
22	4001	4	3	111	122	126					6.5	37.6	3.96	0.84		Yes	Yes
26	4015	4	7	102	103	103	104	103	102	103	0.8	102.5	0.06	0.02			
27	4033	4	4	79	89	82	95				8.2	45.4	3.66	0.56		Yes	Yes
27	4034	4	4	106	113	112	111				2.6	86.5	1.25	0.41			

1 in/mile = 0.0158 m/km

State	GPS ID	GPS Expt	Number Profile Runs	Both-Wheel-Path IRI (in/mi) Profile Sequence							COV of IRI (%)	Linear Regression Results			Linear Relationship Significant?	COV > 6% ?	Slope > 3
				1st	2nd	3rd	4th	5th	6th	7th		Intercept	Slope	R2			
27	4037	4	4	87	97	89	99				6.3	65.8	2.62	0.44		Yes	
27	4040	4	4	109	120	111	114				4.4	104.3	0.76	0.07			
27	4050	4	4	86	82	87	94				5.7	49.7	1.87	0.44			
27	4054	4	4	111	116	123	122				4.8	56.1	3.18	0.81			Yes
27	4055	4	4	74	75	68	76				5.1	74.8	-0.10	0.00			
27	4082	4	3	113	125	130					7.2	-76.5	9.15	0.99	Positive	Yes	Yes
28	4024	4	3	96	97	93					2.4	127.3	-1.73	0.47			
29	4036	4	5	83	82	83	87	86			2.7	75.3	1.04	0.57			
29	5000	4	5	128	126	128	132	133			2.0	108.8	1.44	0.81	Positive		
29	5058	4	5	101	100	102	103	100			1.3	100.5	0.06	0.01			
29	5081	4	5	115	113	118	127	131			6.6	56.0	4.53	0.88	Positive	Yes	Yes
29	5091	4	5	99	97	98	100	104			2.7	82.6	1.19	0.54			
29	5473	4	5	100	68	70	68	69			18.6	256.8	-5.77	0.46		Yes	
29	5503	4	4	80	90	86	77				6.8	97.7	-1.55	0.14		Yes	
31	4019	4	4	108	124	119	131				8.0	39.3	5.38	0.86	Positive	Yes	Yes
34	4042	4	6	117	161	121	109	126	121		14.4	187.3	-2.50	0.06		Yes	
36	4017	4	6	129	123	136	120	131	127		4.4	128.0	-0.02	0.00			
36	4018	4	6	113	109	110	106	117	109		3.6	110.3	0.01	0.00			
39	4018	4	5	107	108	114	106	105			3.2	116.9	-0.52	0.08			
39	4031	4	4	123	126	126	128				1.6	103.9	0.98	0.94	Positive		
42	1606	4	7	90	93	93	87	93	97	94	3.4	81.5	0.89	0.26			
42	1690	4	7	112	114	105	114	111	109	112	2.8	112.0	-0.06	0.00			
48	3699	4	3	99	105	107					4.0	60.0	2.37	0.86			
48	4142	4	7	121	123	125	123	126	133	124	2.9	105.5	1.24	0.36			
48	4143	4	7	141	146	140	141	142	149	149	2.6	122.7	0.96	0.20			
48	4146	4	3	136	137	135					0.8	141.6	-0.55	0.66			
48	4152	4	4	164	176	166	172				3.4	160.5	0.86	0.08			
54	4003	4	6	100	110	100	96	105	101		4.7	105.9	-0.40	0.02			
54	4004	4	6	185	171	182	182	196	219		8.8	133.3	7.04	0.63	Positive	Yes	Yes
1	5008	5	3	60	59	59					1.4	64.6	-0.38	0.53			
5	5803	5	4	95	97	94	92				2.1	110.7	-0.84	0.54			
5	5805	5	4	79	86	81	83				3.8	75.5	0.39	0.06			
6	7455	5	5	79	76	61	75	74			9.5	91.6	-0.91	0.05		Yes	

1 in/mile = 0.0158 m/km

State	GPS ID	GPS Expt	Number Profile Runs	Both-Wheel-Path IRI (in/mi) Profile Sequence							COV of IRI (%)	Linear Regression Results			Linear Relationship Significant?	COV > 6% ?	Slope > 3
				1st	2nd	3rd	4th	5th	6th	7th		Intercept	Slope	R2			
9	5001	5	6	118	127	118	112	118	118		4.0	128.3	-0.94	0.12			
10	5004	5	7	79	68	76	72	77	76	85	7.0	51.6	1.64	0.23		Yes	
10	5005	5	7	69	67	68	68	64	70	74	4.5	43.6	1.21	0.35			
13	5023	5	3	90	89	80					6.0	130.9	-2.46	0.84		Yes	
16	5025	5	6	140	137	140	143	137	150		3.5	114.5	1.36	0.28			
17	5020	5	4	76	78	75	74				2.3	79.8	-0.79	0.58			
17	5843	5	4	77	82	93	86				8.1	56.2	2.98	0.48		Yes	
17	5849	5	4	96	87	86	86				5.5	140.2	-2.53	0.72			
17	5854	5	4	133	140	146	147				4.6	105.8	3.43	0.98	Positive		Yes
17	5869	5	4	110	104	105	105				2.6	117.5	-0.92	0.38			
17	5908	5	4	127	128	128	128				0.4	122.9	0.24	0.48			
17	9267	5	4	70	70	75	72				3.1	51.6	0.78	0.40			
18	5022	5	3	136	133	138					1.8	133.0	0.14	0.00			
18	5043	5	4	136	151	150	138				5.4	126.6	0.74	0.03			
19	5042	5	5	108	106	107	107	110			1.4	99.2	0.49	0.28			
19	5046	5	5	97	99	100	99	98			0.9	97.6	0.06	0.01			
26	5363	5	5	111	114	116	114	116			1.8	99.4	1.02	0.53			
28	5006	5	3	92	93	89					2.2	102.9	-0.87	0.44			
28	5803	5	3	100	103	98					2.7	113.2	-1.02	0.35			
28	5805	5	3	83	88	79					5.7	103.8	-1.23	0.22			
29	5047	5	5	99	96	98	97	98			1.3	99.7	-0.11	0.02			
31	5052	5	5	68	68	70	68	68			1.2	66.3	0.10	0.06			
37	5037	5	6	74	76	71	65	71	67		5.9	104.2	-1.71	0.52			
37	5826	5	7	84	75	77	73	74	80	79	5.0	85.3	-0.52	0.06			
37	5827	5	6	61	65	60	57	60	62		4.4	68.4	-0.40	0.07			
38	5002	5	4	80	82	79	77				2.5	91.9	-0.68	0.33			
39	5003	5	5	69	66	65	72	71			4.6	65.4	0.95	0.29			
40	4158	5	3	57	65	68					9.0	54.0	3.44	0.73		Yes	Yes
40	5021	5	3	58	61	59					2.4	59.4	-0.07	0.01			
41	5005	5	4	84	82	79	79				2.9	89.4	-1.46	0.87	Negative		
41	5006	5	6	86	83	87	87	86	85		1.7	86.2	-0.02	0.00			
41	5008	5	6	59	58	59	60	61	60		1.7	52.2	0.36	0.38			
41	5021	5	4	71	64	66	68				4.7	70.7	-0.72	0.11			

1 in/mile = 0.0158 m/km

State	GPS ID	GPS Expt	Number Profile Runs	Both-Wheel-Path IRI (in/mi) Profile Sequence							COV of IRI (%)	Linear Regression Results			Linear Relationship Significant?	COV > 6% ?	Slope > 3
				1st	2nd	3rd	4th	5th	6th	7th		Intercept	Slope	R2			
41	5022	5	4	64	59	64	64				3.7	61.1	0.24	0.02			
41	7081	5	7	48	50	53	47	48	49	47	4.2	50.1	-0.36	0.11			
42	1598	5	6	106	107	103	99	108	109		3.3	101.2	0.23	0.02			
42	5020	5	7	119	119	116	114	115	117	120	2.0	116.1	0.08	0.00			
45	5017	5	3	125	130	129					2.0	113.7	1.08	0.62			
45	5034	5	3	96	90	91					3.5	114.2	-1.29	0.55			
45	5035	5	3	81	80	78					1.9	92.5	-0.77	0.92			
46	5020	5	5	60	62	62	61	62			1.2	57.0	0.25	0.22			
46	5025	5	5	82	79	82	80	81			1.8	80.9	0.01	0.00			
46	5040	5	4	126	135	135	132				3.2	89.1	1.51	0.35			
48	3719	5	3	154	152	151					1.0	177.6	-0.93	1.00	Negative		
48	3779	5	4	152	136	134	139				5.6	166.2	-1.86	0.19			
48	5024	5	3	156	163	162					2.3	147.2	1.35	0.33			
48	5026	5	3	108	106	106					0.9	108.6	-0.54	0.73			
48	5035	5	4	112	116	109	118				3.6	108.8	0.40	0.04			
48	5154	5	3	103	98	98					2.7	122.6	-1.15	0.49			
48	5274	5	4	101	109	103	105				3.2	96.9	0.39	0.06			
48	5278	5	4	108	105	105	106				1.2	114.7	-0.50	0.50			
48	5283	5	4	72	74	73	75				1.6	71.6	0.43	0.58			
48	5284	5	4	124	139	125	153				10.3	114.1	4.80	0.50		Yes	Yes
48	5287	5	4	118	123	119	128				3.9	88.3	1.78	0.60			
48	5301	5	4	102	107	103	106				2.4	98.6	0.55	0.19			
48	5310	5	4	123	133	122	127				3.9	127.3	-0.22	0.01			
48	5317	5	4	138	143	144	149				3.0	122.2	2.06	0.96	Positive		
48	5323	5	4	113	113	110	115				1.8	110.3	0.20	0.03			
48	5328	5	4	106	104	101	103				2.0	113.2	-0.59	0.28			
48	5334	5	3	70	74	68					4.1	97.9	-1.26	0.30			
48	5335	5	4	129	132	127	128				1.8	137.9	-0.68	0.27			
48	5336	5	4	89	93	92	91				1.9	90.0	0.14	0.03			
51	2564	5	6	61	61	62	57	62	64		3.9	53.0	0.35	0.07			
51	5008	5	6	138	150	132	128	122	127		7.6	192.4	-4.04	0.54	Negative	Yes	
51	5009	5	6	143	138	141	140	142	144		1.7	134.7	0.57	0.17			
51	5010	5	6	98	93	101	99	102	106		4.4	93.3	2.03	0.61	Positive		

1 in/mile = 0.0158 m/km

State	GPS ID	GPS Expt	Number Profile Runs	Both-Wheel-Path IRI (in/mi) Profile Sequence							COV of IRI (%)	Linear Regression Results			Linear Relationship Significant?	COV > 6% ?	Slope > 3
				1st	2nd	3rd	4th	5th	6th	7th		Intercept	Slope	R2			
54	5007	5	3	144	155	160					5.4	18.1	10.14	0.95			Yes
55	5037	5	4	73	77	71	71				3.7	86.8	-0.76	0.31			
55	5040	5	5	147	150	148	149	151			1.2	140.6	0.72	0.43			
1	4127	6B	3	57	59	55					3.2	59.5	-0.70	0.36			
1	6012	6A	3	76	102	121					23.0	0.6	12.02	1.00	Positive	Yes	Yes
1	6019	6A	3	42	50	45					8.8	38.0	0.65	0.12		Yes	
4	6053	6A	3	77	86	88					6.8	71.6	3.70	0.96		Yes	Yes
4	6054	6A	4	48	51	59	63				12.4	43.6	3.34	0.93	Positive	Yes	Yes
4	6055	6A	3	40	43	45					5.8	37.0	1.66	0.99	Positive		
6	6044	6A	5	54	56	87	56	58			22.6	59.6	0.66	0.01		Yes	
8	6002	6A	4	154	165	169	190				9.0	134.7	9.37	0.86	Positive	Yes	Yes
8	6013	6A	4	115	121	147	139				11.7	98.9	8.51	0.69		Yes	Yes
8	7781	6B	5	71	76	80	82	84			6.7	70.0	5.94	0.91	Positive	Yes	Yes
8	7783	6A	4	63	70	72	75				7.3	60.8	3.15	0.97	Positive	Yes	Yes
11	1400	6B	6	199	185	195	184	194	197		3.3	192.3	-0.01	0.00			
16	6027	6A	6	82	83	87	87	104	84		9.3	79.6	2.17	0.26		Yes	
17	6050	6A	3	47	53	53					6.5	27.3	1.67	0.95		Yes	
18	6012	6A	3	80	103	93					12.1	66.0	2.40	0.20		Yes	
19	6049	6A	5	95	103	89	109	108			8.6	49.3	3.10	0.38		Yes	Yes
20	1006	6A	5	93	94	95	102	98			3.7	62.8	1.59	0.50			
21	6040	6A	4	96	94	98	106				5.4	68.7	3.12	0.63			Yes
21	6043	6A	5	63	67	63	66	66			2.7	58.6	0.48	0.22			
26	6016	6A	5	75	54	56	56	66			14.5	68.8	-1.08	0.04		Yes	
28	3093	6B	3	62	63	60					2.4	63.6	-0.58	0.49			
29	5403	6B	5	66	65	65	78	70			7.8	63.6	2.02	0.35		Yes	
29	5413	6B	5	59	62	60	73	60			9.3	59.5	1.34	0.13		Yes	
29	6067	6A	5	91	92	95	95	103			5.1	64.3	2.77	0.80	Positive		
30	6004	6A	6	104	99	105	126	116	120		9.5	95.4	4.37	0.57	Positive	Yes	Yes
30	7066	6B	3	51	54	56					4.5	51.1	2.59	0.94			
30	7075	6A	6	57	57	56	62	62	64		5.9	54.3	1.72	0.79	Positive		
30	7076	6B	3	63	62	59					3.3	64.4	-2.08	0.94			
30	7088	6B	4	40	43	44	44				4.7	40.7	1.46	0.75			
31	6700	6B	4	82	92	88	100				8.2	75.6	4.55	0.85	Positive	Yes	Yes

1 in/mile = 0.0158 m/km

State	GPS ID	GPS Expt	Number Profile Runs	Both-Wheel-Path IRI (in/mi) Profile Sequence							COV of IRI (%)	Linear Regression Results			Linear Relationship Significant?	COV > 6% ?	Slope > 3
				1st	2nd	3rd	4th	5th	6th	7th		Intercept	Slope	R2			
34	6057	6A	5	96	95	96	96	96			0.5	94.6	0.09	0.09			
35	1002	6A	3	43	52	67					21.9	-0.2	7.49	1.00	Positive	Yes	Yes
35	2007	6A	3	30	33	35					8.0	14.5	1.59	0.93		Yes	
35	6033	6A	3	80	83	93					7.6	39.6	4.08	0.98	Positive	Yes	Yes
35	6035	6A	3	71	74	91					13.4	31.7	6.56	0.95		Yes	Yes
35	6401	6A	3	37	45	68					32.0	-33.2	10.17	0.99	Positive	Yes	Yes
36	1008	6B	5	78	75	62	74	66			9.5	79.2	-2.74	0.45		Yes	
37	1803	6B	5	68	52	53	53	51			12.3	62.5	-3.13	0.58		Yes	
38	6004	6A	3	166	182	204					10.4	-59.0	20.65	0.96		Yes	Yes
39	6019	6A	3	97	63	64					25.4	105.0	-13.57	0.62		Yes	
40	4086	6B	3	50	64	71					17.4	43.8	6.89	0.77		Yes	Yes
40	4161	6B	3	80	90	104					13.4	70.9	7.76	0.99	Positive	Yes	Yes
40	6010	6A	3	94	105	103					5.7	86.0	2.04	0.33			
41	6011	6A	4	61	54	58	75				14.8	49.6	3.95	0.38		Yes	Yes
41	6012	6A	3	56	51	58					6.7	55.5	-0.26	0.00		Yes	
42	1608	6A	6	102	103	105	104	110	110		3.4	99.4	1.70	0.82	Positive		
42	1618	6B	6	105	108	105	104	110	110		2.6	106.2	0.73	0.32			
46	9106	6B	4	58	61	54	59				5.1	59.6	-0.64	0.06			
46	9197	6B	4	52	59	58	66				9.4	50.9	3.15	0.89	Positive	Yes	Yes
47	6015	6A	3	56	50	54					5.7	56.6	-0.47	0.09			
47	6022	6A	3	64	79	77					11.5	3.7	5.36	0.83		Yes	Yes
48	1046	6A	4	84	91	95	95				5.5	37.8	2.46	0.78			
48	1093	6B	3	45	48	49					5.1	43.5	1.29	0.86			
48	1119	6B	4	64	64	65	64				1.0	64.4	0.07	0.04			
48	6079	6A	4	155	164	188	184				9.2	110.8	7.98	0.81	Positive	Yes	Yes
48	6086	6A	3	49	46	48					3.2	49.3	-0.22	0.06			
48	6160	6A	3	112	121	136					10.0	19.3	9.39	0.99	Positive	Yes	Yes
48	6179	6A	4	61	66	69	90				17.9	-44.9	6.55	0.84	Positive	Yes	Yes
49	1004	6A	5	132	146	170	174	194			14.9	117.4	14.03	0.97	Positive	Yes	Yes
49	1005	6A	6	41	42	39	59	59	56		19.6	33.8	4.15	0.67	Positive	Yes	Yes
49	1006	6A	5	45	51	51	51	52			6.0	45.5	1.38	0.61		Yes	
49	1007	6A	5	66	67	67	69	74			5.0	62.6	1.83	0.82	Positive		
51	1417	6B	5	69	73	71	74	77			4.2	69.0	1.88	0.81	Positive		

1 in/mile = 0.0158 m/km

State	GPS ID	GPS Expt	Number Profile Runs	Both-Wheel-Path IRI (in/mi) Profile Sequence							COV of IRI (%)	Linear Regression Results			Linear Relationship Significant?	COV > 6% ?	Slope > 3
				1st	2nd	3rd	4th	5th	6th	7th		Intercept	Slope	R2			
51	1419	6B	6	85	88	86	86	87	89		1.8	85.9	0.46	0.28			
51	1423	6B	6	115	117	114	116	124	131		5.7	112.0	2.90	0.66	Positive		
53	1005	6B	5	46	41	45	53	48			9.6	40.5	1.97	0.39		Yes	
53	6020	6A	6	43	42	43	43	43	41		1.9	43.3	-0.23	0.25			
53	6048	6A	6	79	76	86	62	63	62		14.5	86.4	-3.99	0.44		Yes	
53	6049	6A	5	73	82	77	78	85			5.8	73.0	1.61	0.43			
53	6056	6A	5	62	59	62	63	67			4.7	57.2	1.76	0.66	Positive		
53	7322	6A	5	47	43	47	48	51			6.0	44.5	1.36	0.42			
56	6029	6A	6	74	76	75	83	79	78		3.9	73.5	1.04	0.41			
56	6031	6A	6	96	106	117	115	121	127		9.8	92.2	5.73	0.90	Positive	Yes	Yes
56	6032	6A	6	70	71	74	79	77	86		7.7	65.5	2.85	0.82	Positive	Yes	
82	6006	6A	4	80	82	84	82				1.8	79.0	0.89	0.59			
82	6007	6A	3	112	119	117					2.9	110.0	1.94	0.45			
83	6450	6B	6	52	51	52	51	52	51		1.2	51.5	-0.06	0.04			
83	6451	6B	6	69	67	63	70	64	64		4.5	67.9	-0.73	0.22			
84	6804	6A	6	60	61	60	52	61	65		7.0	53.2	0.51	0.05		Yes	
86	6802	6A	6	85	92	108	116	129	122		15.9	-36.5	8.97	0.90	Positive	Yes	Yes
90	6400	6A	6	76	80	91	94	98	111		13.6	18.5	6.60	0.96	Positive	Yes	Yes
90	6410	6B	5	90	66	52	76	70			19.5	80.5	-3.51	0.16		Yes	
90	6412	6B	5	66	54	70	62	56			11.0	64.5	-1.16	0.08		Yes	
90	6801	6A	5	93	107	111	114	132			12.5	22.8	8.35	0.86	Positive	Yes	Yes
8	7035	7A	5	89	87	98	95	93			5.2	85.1	1.76	0.35			
8	7036	7A	4	100	96	117	106				8.8	92.5	3.34	0.29		Yes	Yes
9	4020	7B	4	97	98	97	102				2.5	95.3	1.36	0.55			
13	7028	7A	3	64	64	70					5.5	55.2	1.70	0.78			
17	5151	7B	3	55	77	75					18.0	53.6	7.01	0.96		Yes	Yes
17	5453	7A	4	78	75	75	73				2.7	84.9	-1.19	0.96	Negative		
17	7937	7A	3	104	110	129					11.6	57.1	7.09	1.00	Positive	Yes	Yes
18	5528	7B	3	57	58	69					10.5	51.1	5.02	0.80		Yes	Yes
18	5538	7B	3	53	52	52					1.2	52.8	-0.42	0.64			
19	9116	7B	4	53	51	56	53				3.8	52.5	0.21	0.04			
19	9126	7B	5	76	78	79	81	83			3.3	75.2	1.36	0.92	Positive		
20	7073	7A	3	75	79	106					19.4	-88.7	15.50	0.85		Yes	Yes

1 in/mile = 0.0158 m/km

State	GPS ID	GPS Expt	Number Profile Runs	Both-Wheel-Path IRI (in/mi) Profile Sequence							COV of IRI (%)	Linear Regression Results			Linear Relationship Significant?	COV > 6% ?	Slope > 3
				1st	2nd	3rd	4th	5th	6th	7th		Intercept	Slope	R2			
20	7085	7A	3	104	99	104					2.8	100.1	0.32	0.01			
23	7023	7A	6	56	63	57	53	53	63		7.7	56.9	0.06	0.00		Yes	
26	7072	7A	5	48	52	59	56	68			13.7	29.5	3.96	0.87	Positive	Yes	Yes
27	5076	7B	3	60	52	56					7.4	59.4	-1.68	0.22		Yes	
27	7090	7A	4	105	114	107	113				4.2	93.5	1.76	0.31			
28	3097	7A	3	60	64	63					3.4	57.5	0.58	0.19			
29	4069	7B	3	86	80	77					5.7	87.0	-3.99	0.99	Negative		
29	5393	7B	4	84	86	86	84				1.4	85.7	-0.26	0.09			
29	5483	7B	3	57	58	54					3.3	57.9	-1.01	0.38			
29	7054	7A	4	61	60	63	64				3.1	38.8	1.24	0.67			
29	7073	7A	5	72	73	75	76	82			5.1	50.2	2.25	0.94	Positive		
31	6702	7B	4	44	56	45	44				12.6	48.8	-0.51	0.02		Yes	
31	7005	7A	4	105	111	109	113				3.1	92.4	1.91	0.73			
31	7017	7A	4	109	133	132	133				9.7	64.6	6.27	0.69		Yes	Yes
31	7050	7A	4	85	91	86	85				3.2	88.5	-0.27	0.02			
39	5010	7B	4	62	59	52	48				11.2	63.0	-3.97	0.97	Negative	Yes	
39	7021	7A	5	90	99	115	105	118			10.9	68.0	5.38	0.74	Positive	Yes	Yes
40	7024	7A	3	93	109	112					9.9	52.1	5.82	0.69		Yes	Yes
41	7018	7A	5	77	77	63	44	54			22.6	91.2	-9.16	0.65		Yes	
41	7019	7A	5	99	87	97	97	96			5.1	94.1	0.32	0.01			
41	7025	7A	4	100	96	114	165				27.1	60.8	18.38	0.71		Yes	Yes
42	1610	7A	6	71	66	66	61	64	64		4.8	72.0	-1.27	0.59	Negative		
42	1613	7B	5	67	76	67	65	63			7.4	72.2	-1.97	0.37		Yes	
42	1614	7B	6	64	65	69	68	69	74		5.3	63.6	1.77	0.88	Positive		
42	1617	7B	4	52	51	54	54				2.8	51.5	0.86	0.52			
42	7025	7A	6	95	94	89	95	93	97		2.9	92.0	0.46	0.09			
42	7037	7A	6	59	60	65	66	54	56		8.4	65.9	-0.82	0.09		Yes	
44	7401	7A	6	71	73	70	70	71	71		1.5	71.4	-0.11	0.04			
45	7019	7A	3	86	96	89					5.5	85.9	0.62	0.05			
46	7049	7A	4	86	108	105	107				10.2	83.7	5.10	0.66		Yes	Yes
48	3629	7A	3	56	50	48					7.6	70.5	-2.22	0.81		Yes	
54	7008	7A	4	122	132	142	128				6.4	103.6	4.37	0.33		Yes	Yes
55	7030	7A	3	145	163	165					6.9	26.3	9.76	0.88		Yes	Yes

1 in/mile = 0.0158 m/km

State	GPS ID	GPS Expt	Number Profile Runs	Both-Wheel-Path IRI (in/mi) Profile Sequence							COV of IRI (%)	Linear Regression Results			Linear Relationship Significant?	COV > 6% ?	Slope > 3
				1st	2nd	3rd	4th	5th	6th	7th		Intercept	Slope	R2			
83	6452	7B	6	73	79	81	85	83	91		7.0	75.5	2.69	0.79	Positive	Yes	
6	9048	9	4	112	103	114	109				4.6	109.1	0.08	0.00			
6	9049	9	5	71	69	67	88	71			11.4	67.3	1.62	0.11		Yes	
6	9107	9	5	75	81	87	91	110			14.8	62.0	7.20	0.90	Positive	Yes	Yes
8	9019	9	4	87	93	115	106				12.4	75.3	6.77	0.66		Yes	Yes
8	9020	9	4	65	80	110	88				21.8	52.8	8.83	0.50		Yes	Yes
13	4118	9	3	36	38	38					2.2	29.7	0.36	0.67			
18	9020	9	4	96	99	97	97				1.3	96.3	0.16	0.09			
20	9037	9	5	113	121	130	128	131			6.1	63.8	4.26	0.80	Positive	Yes	Yes
26	9029	9	5	116	119	118	83	117			14.2	141.5	-4.05	0.15		Yes	
26	9030	9	6	115	122	121	120	115	115		2.8	126.2	-1.11	0.21			
27	6300	9	3	85	94	104					9.8	62.1	5.43	0.97		Yes	Yes
27	9075	9	3	122	125	121					1.8	128.2	-0.36	0.08			
28	9030	9	3	65	69	60					7.3	70.2	-1.38	0.31		Yes	
31	6701	9	5	122	133	136	150	153			9.2	105.8	7.23	0.99	Positive	Yes	Yes
39	5569	9	3	141	144	144					1.3	114.5	1.31	0.70			
39	9006	9	4	94	95	99	97				2.1	90.3	0.95	0.47			
39	9022	9	5	86	87	97	96	90			5.8	85.2	1.55	0.29			
40	4155	9	3	64	63	61					2.6	65.5	-1.18	1.00	Negative		
42	1627	9	6	118	121	116	124	109	116		4.5	122.2	-1.18	0.17			
42	9027	9	6	181	175	171	172	169	174		2.3	183.6	-1.36	0.40			
48	3569	9	3	76	84	83					5.2	70.7	2.17	0.62			
48	3845	9	3	106	114	109					3.7	108.1	0.77	0.06			
48	9167	9	3	111	116	112					2.3	112.6	0.14	0.01			
89	9018	9	5	125	122	144	146	164			12.4	92.4	10.36	0.89	Positive	Yes	Yes

1 in/mile = 0.0158 m/km

REFERENCES

1. Spangler, E. B. and Kelly, W. J., *Long-Term Time Stability of Pavement Ride Quality Data.* Federal Highway Administration Report FHWA/OH-91/001, 1990, 99p.

2. *Manual for Profile Measurement: Operational Field Guidelines*, SHRP-P-378, Strategic Highway Research Program, National Research Council, Washington, D.C., 1994, 130p.

3. Sayers, M. W., Gillespie, T. D., Queiroz, A.V., *The International Road Roughness Experiment*, World Bank Technical Paper Number 45, World Bank, 1986, 453 p.

4. Gillespie, T. D., Sayers, M. W., and Segel, L., *Calibration of Response Type Road Roughness Measuring Systems*, National Cooperative Highway Research Program Report 228, 1980, 81p.

5. Sayers, M. W., Gillespie, T. D., and Paterson, D. O., *Guidelines for Conducting and Calibrating Road Roughness Measurements*, World Bank Technical Paper Number 46, World Bank, 1986, 87p.

6. Sayers, M. W. and Karamihas, S. M., *The Little Book of Profiling, Basic Information About Measuring and Interpreting Road Profiles*, University of Michigan Transportation Research Institute, 1996, 101p.

7. Spangler, E. B., and Kelly, W. J., *Integration of the Inertial Profilometer in the Ohio DOT Pavement Management System*, Ohio Department of Transportation Report FHWA/OH-87/005, 1987, 122p.

8. Janoff, M. S., *Pavement Roughness and Rideability*, National Cooperative Highway Research Program Report 275, 1985, 69p.

9. Janoff, M. S. *Pavement Roughness and Rideability Field Evaluation.* National Cooperative Highway Research Program Report 308, 1988, 54p.

10. Sayers, M. W. and Karamihas, S. M., *Interpretation of Road Roughness Profile Data*, Federal Highway Administration, Report No. FHWA-RD-96-101, University of Michigan Transportation Research Institute, June 1996, 166p.

11. *Long Term Pavement Performance Information Management System, Data User's Guide*, Report No. FHWA-RD-93-094, 41p.

12. Simpson, A. L., Rauhut, J. B., Jordhal, P. R., Owusu-Antwi, E., Darter, M. I., Ahamad, R., Pendleton, O. J., and Lee, Y. *Sensitivity Analysis for Selected Pavement Distresses*, SHRP-P-393, Strategic Highway Research Program, National Research Council, Washington, D.C., 1994, 341p.

13. Paterson, W.D.O., *Road Deterioration and Maintenance Effects, Models for Planning and Management*, World Bank, 1987, 453p.

14. Chaparral Systems Corporation, *Monitored Traffic Data Status Report*, October 1995, 95p.

15. Lasdon, L. S., Waren, A., Jain, A., and Ratner, M., *Design and Testing of a Generalized Reduced Gradient Code for Nonlinear Programming*, ACM Transactions on Mathematical Software 4:1, 1978, pp. 34-50.